
Doctoral Dissertations

Student Theses and Dissertations

Summer 2019

Hydrodynamics of trickle bed reactors (TBRS) packed with industrial catalyst using advanced measurement techniques

Mohammed Jaber Al-Ani

Follow this and additional works at: https://scholarsmine.mst.edu/doctoral_dissertations



Part of the [Chemical Engineering Commons](#)

Department: Chemical and Biochemical Engineering

Recommended Citation

Al-Ani, Mohammed Jaber, "Hydrodynamics of trickle bed reactors (TBRS) packed with industrial catalyst using advanced measurement techniques" (2019). *Doctoral Dissertations*. 2819.

https://scholarsmine.mst.edu/doctoral_dissertations/2819

This thesis is brought to you by Scholars' Mine, a service of the Missouri S&T Library and Learning Resources. This work is protected by U. S. Copyright Law. Unauthorized use including reproduction for redistribution requires the permission of the copyright holder. For more information, please contact scholarsmine@mst.edu.

HYDRODYNAMICS OF TRICKLE BED REACTORS (TBRS) PACKED WITH
INDUSTRIAL CATALYST USING ADVANCED MEASUREMENT TECHNIQUES

by

MOHAMMED JABER YAS AL-ANI

A DISSERTATION

Presented to the Faculty of the Graduate School of the
MISSOURI UNIVERSITY OF SCIENCE AND TECHNOLOGY

In Partial Fulfillment of the Requirements for the Degree

DOCTOR OF PHILOSOPHY

in

CHEMICAL ENGINEERING

2019

Approved

Dr. Muthanna Al-Dahhan, Advisor

Dr. Douglas Ludlow

Dr. Xinhua Liang

Dr. Joontaek Park

Dr. Fatih Dogan

© 2019

MOHAMMED JABER YAS AL-ANI

All Rights Reserved

PUBLICATION DISSERTATION OPTION

This dissertation consists of following seven articles that may be submitted for publishing in the future:

Paper I, pages 15-57. Flow Regimes Identification of Trickle Bed Reactor (TBR) Packed with Different Shape of industrial Using Non-Invasive Gamma-ray Densitometry (GRD).

Paper II, pages 58-102. Effect of Catalyst Shape on Pressure Drop and Overall Liquid Holdup in a Pilot Plant Trickle Bed Reactor.

Paper III, pages 103-149. Phase Distribution Investigations in a Mimicked Bench Scale Hydrotreater Reactor using Gamma-ray Densitometry (GRD).

Paper IV, pages 150-176. Non-Invasive Catalyst Utilization Measurement in a Mimicked Bench Scale Hydrotreater Reactor.

Paper V, pages 177-189. Local Gas and Liquid Saturations and Velocities Study of Various Hydrotreating Catalyst Shapes using Advanced Optical Fiber Probe in A Pilot Plant Trickle Bed Reactor.

ABSTRACT

The impacts of the packing characteristics on the hydrodynamics of a trickle bed reactor (TBR) have been investigated using advanced measurements techniques of Gamma-ray densitometry (GRD) and Optical fiber probe and conventional measurement techniques of high-frequency differential pressure transducer and load cell. Two different reactor sizes of bench and pilot plant scale were used. Bench-scale TBR carried out the experiments to assess phase distribution and catalyst utilization with 1.18 cm inside diameter and 72 cm length at ambient pressure and temperature. The mixture of catalyst and fine particles displayed considerable improvements in the phase distribution, liquid holdup profile, and catalyst utilization efficiency. In the pilot plant scale reactor, the catalyst shape showed a significant impact on the hydrodynamics, pressure drop, local gas and liquid velocities, and flow regime transition. The currently used trilobe and quadrilobe in hydrotreating processes showed lower pressure drop, increased liquid holdup, enhanced local gas and liquid saturation and velocities, and lower flow regime transition compared with spherical and cylindrical shapes of catalysts. Meanwhile, mechanistic model named slit model predicted the pressure drop and liquid holdup better than selected correlations where equivalent diameter is used and the bed characteristic is quantitated properly by measured Ergun constants.

ACKNOWLEDGMENT

First of all, praise belongs to God (ALLAH) for his kindness and so many blessings in my life. Completion of this doctoral dissertation was possible with the support of several people. I would like to express my sincere gratitude to all of them. I am extremely grateful to my research guide, Professor Muthanna Al-Dahhan, for his valuable guidance, scholarly inputs and consistent encouragement I received throughout the research work. I consider it as a great opportunity to do my doctoral program under his guidance and to learn from his research expertise. Thank you, for all your help and support. I would also like to acknowledge the members of my committee, namely, Prof. Douglas Ludlow, Prof. Xinhua Liang, Prof. Joontaek Park, and Prof. Fatih Dogan, for taking interest in my work and examining my dissertation. I want to express my gratitude to my sponsor, The Ministry of Higher Education and Scientific Research in Iraq, for awarding me a fully funded scholarship. I appreciatively would like to thank my research group members. My sincere thanks go to my colleagues (Mr. Kasim Alwan, Bushraa Ismael, Suham Mohammed, Zainab Hasan, and Haider Jasem) at Research and Industrial development center, Iraq for their help and support. I wish to thank all my relatives and friends in Iraq and the United States who have encouraged and supported me during my Ph.D. journey. I am gratitude also (Dr. Ryad Khalil) and (Dr. Hamed Mahmoud) for their support which they were as a source of inspiration and motivation. I would like to give special thanks to my dear parents and siblings for their encouragement and support. Finally, great indebted to my wife (Marwah) and kids (Hamsa, Ayoob, Baha) for their patience and support. She was the one who suffered from the hard work that I went through this accomplishment.

TABLE OF CONTENTS

	Page
PUBLICATION DISSERTATION OPTION	iii
ABSTRACT.....	iv
ACKNOWLEDGMENT.....	v
LIST OF ILLUSTRATIONS.....	xi
LIST OF TABLES.....	xvii
 SECTION	
1. INTRODUCTION	1
1.1. RESEARCH MOTIVATION	7
1.2. RESEARCH OBJECTIVES	13
 PAPER	
I. FLOW REGIMES IDENTIFICATION OF TRICKLE BED REACTOR (TBR) PACKED WITH TRILOBE AND QUADRILOBE INDUSTRIAL CATALYST USING NON-INVASIVE GAMMA-RAY DENSITOMETRY (GRD)	15
ABSTRACT.....	15
1. INTRODUCTION	17
2. EXPERIMENTAL WORK.....	20
2.1. EXPERIMENTAL SETUP	20
2.2. GAMMA-RAY DENSITOMETRY (GRD) TECHNIQUE	21
3. GRD SIGNALS PROCESSING AND DATA ANALYSIS METHODS.....	24
3.1. TIME SERIES OF PHOTON COUNTS	24
3.2. VARIATION OF POISSON DISTRIBUTION.....	27
3.3. STATISTICAL ANALYSIS (STANDARD DEVIATION)	29
3.4. KOLMOGOROV ENTROPY (KE) ANALYSIS METHOD.....	30

4. RESULTS AND DISCUSSION	31
4.1. STATISTICAL ANALYSIS (STANDARD DEVIATION)	31
4.2. KOLMOGOROV ENTROPY ANALYSIS (KE).....	33
4.3. VARIATION FROM POISSON DISTRIBUTION	40
5. REMARKS	52
ACKNOWLEDGMENT.....	53
REFERENCES	53
II. EFFECT OF CATALYST SHAPE ON PRESSURE DROP AND OVERALL LIQUID HOLDUP IN A PILOT PLANT TRICKLE BED REACTOR.....	58
ABSTRACT.....	58
1. INTRODUCTION	59
2. PHENOMENOLOGICAL MODEL.....	63
3. EXPERIMENTAL WORK.....	69
3.1. APPARATUS	69
3.2. OPERATION CONDITION.....	72
4. RESULTS AND DISCUSSION.....	74
4.1. ERGUN’S COEFFICIENTS CALCULATION	74
4.2. LOW TO HIGH INTERACTION TRANSITION BOUNDARY	79
4.3. PRESSURE DROP	79
4.4. LIQUID HOLDUP.....	82
4.5. MODELS COMPARISON	88
4.5.1. Pressure Drop	88
4.5.2. Liquid Holdup	94
5. REMARKS	97
ACKNOWLEDGMENT.....	99

REFERENCES	99
III. PHASE DISTRIBUTION INVESTIGATIONS IN A MIMICKED BENCH SCALE HYDROTREATER REACTOR USING GAMMA-RAY DENSITOMETRY (GRD)	103
ABSTRACT	103
1. INTRODUCTION	104
2. EXPERIMENTAL WORK.....	109
2.1. EXPERIMENTAL SETUP	109
2.2. GAMMA-RAY DENSITOMETRY (GRD) TECHNIQUE	112
2.3. PRINCIPAL OF MEASUREMENTS	116
2.4. VALIDATION OF THE GRD MEASUREMENTS	119
2.5. METHODOLOGY OF MEASUREMENTS	123
2.6. DYNAMIC LIQUID HOLDUP CALCULATIONS	130
2.7. GAS HOLDUP CALCULATIONS	131
2.8. EXTERNAL VOID SPACE CALCULATIONS	132
3. RESULTS AND DISCUSSIONS.....	133
3.1. EFFECT OF THE DISTRIBUTOR REGION ON THE LINE AVERAGED LIQUID HOLDUP DIAMETRICAL PROFILE IN BOTH DILUTED AND NON-DILUTED BEDS AT TWO DIFFERENT CONFIGURATIONS (SIDE AND TOP).....	133
3.2. EFFECTS OF THE BED DILUTION ON THE LINE AVERAGED DIAMETRICAL PROFILES OF THE DYNAMIC LIQUID HOLDUP ALONG BED HEIGHT	134
3.3. EFFECTS OF THE BED DILUTION ON THE LINE AVERAGED DIAMETRICAL PROFILES OF THE VOID FRACTION OF THE BED.....	135
3.4. EFFECTS OF INLET CONFIGURATION FOR THE MIXED GAS AND LIQUID ON THE LINE AVERAGED DIAMETRICAL PROFILES OF THE DYNAMIC LIQUID HOLDUP ALONG THE BED HEIGHT	139

3.5. EFFECTS OF GAS AND LIQUID FLOW RATES ON THE LINE AVERAGED DIAMETRICAL PROFILES OF THE DYNAMIC LIQUID HOLDUP ALONG THE BED HEIGHT	141
4. REMARKS	141
ACKNOWLEDGMENT.....	144
REFERENCES	144
IV. NON-INVASIVE CATALYST UTILIZATION MEASUREMENT IN A MIMICKED BENCH SCALE HYDROTREATER REACTOR	150
ABSTRACT.....	150
1. INTRODUCTION	151
2. EXPERIMENTAL WORK.....	155
2.1. EXPERIMENTAL SETUP.....	155
2.2. MEASUREMENT TECHNIQUE	156
2.3. CATALYST UTILIZATION.....	159
3. RESULTS AN DISCUSSION.....	164
4. MODELING SIMULATION TO IDENTIFY CATALYST UNDER UTILIZATION USING EXPERIMENTAL DATA.....	169
5. REMARKS	173
ACKNOWLEDGMENT.....	174
REFERENCES	174
V. LOCAL GAS AND LIQUID SATURATIONS AND VELOCITIES STUDY OF VARIOUS HYDROTREATING CATALYST SHAPES USING ADVANCED OPTICAL FIBER PROBE IN A PILOT PLANT TRICKLE BED REACTOR.....	177
ABSTRACT.....	177
1. INTRODUCTION	177
2. EXPERIMENTAL WORK.....	179
2.1. SETUP	179

2.2. OPERATION CONDITIONS.....	179
2.3. ADVANCED TWO TIP OPTICAL PROBES (TTOP) TECHNIQUE.....	180
2.3.1. Measurement Technique Two-Tip Optical Probe (TTOP).....	180
2.3.2. Raw Signal of Two Tip Optical Fiber Probes.....	181
2.3.3. Local Phase Saturations Measurements.....	183
2.3.4. Local Phase Velocities Measurement	183
3. SAMPLE OF RESULTS	184
4. REMARKS	188
ACKNOWLEDGMENT.....	188
REFERENCE.....	189
SECTION	
2. CONCLUSION.....	190
3. RECOMMENDATIONS.....	192
REFERENCES	194
VITA.....	197

LIST OF ILLUSTRATIONS

SECTION	Page
Figure 1.1. BP primary energy consumption by major sources [1]	2
Figure 1.2. Show the percentages of commercial processes that include the use of heterogeneous, homogeneous and bio-catalysis [1].....	2
Figure 1.3. Schematic diagram of a TBR	4
 PAPER I	
Figure 1. Schematic Diagram for Trickle Bed Reactor.....	22
Figure 2. (a) Photo for source (b) Schematic diagram for source.....	23
Figure 3. (a) Photo of NaI scintillating detector (b) schematic diagram for NaI scintillating detector collimated and sited in shield house	25
Figure 4. Time series of photon counts fluctuations in 14 cm diameter column at superficial liquid velocity (a) 4, (b) 8, and (c) 14 mm/s.....	26
Figure 5. Time series of photon counts fluctuations in 14 cm diameter column in dry solid case.	26
Figure 6. Time series of photon counts fluctuation in 14 cm diameter column in air only case.....	28
Figure 7. Time series of photon counts fluctuation in 14 cm diameter column in water only case.	28
Figure 8. Time series of photon counts fluctuation in 14 cm diameter column in solid only case.	28
Figure 9. Standard deviation versus superficial liquid velocity at the middle ($Z/D= 6.6$) and center ($r/R=0$) of reactor within spherical catalyst shape.....	34
Figure 10. Standard deviation versus superficial liquid velocity at the middle ($Z/D= 6.6$) and center ($r/R=0$) of reactor within cylindrical catalyst shape.....	35
Figure 11. Standard deviation versus superficial liquid velocity at the middle ($Z/D= 6.6$) and center ($r/R=0$) of reactor within trilobe catalyst shape.....	36

Figure 12. Standard deviation versus superficial liquid velocity at the middle ($Z/D= 6.6$) and center ($r/R=0$) of reactor within quadrilobe catalyst shape.....	37
Figure 13. Standard deviation versus superficial liquid velocity within trilobe catalyst at the middle and bottom positions ($Z/D= 6.6$ and $Z/D= 12.5$) and at the center of reactor.	38
Figure 14. Kolmogorov Entropy (KE) of photon counts vs. superficial liquid velocity at the middle ($Z/D= 6.6$) and center of pilot plant reactor within spherical catalyst shape	41
Figure 15. Kolmogorov Entropy (KE) of photon counts vs. superficial liquid velocity at the middle ($Z/D= 6.6$) and center of pilot plant reactor within cylindrical catalyst shape	42
Figure 16. Kolmogorov Entropy (KE) of photon counts vs. superficial liquid velocity at the middle ($Z/D= 6.6$) and center of pilot plant reactor within trilobe catalyst shape	43
Figure 17. Kolmogorov Entropy (KE) of photon counts vs. superficial liquid velocity at the middle ($Z/D= 6.6$) and center of pilot plant reactor within quadrilobe catalyst shape	44
Figure 18. Kolmogorov Entropy of photon counts vs. superficial liquid velocity within quadrilobe catalyst shape at center and different axial locations of pilot plant reactor.	45
Figure 19. Variation coefficient from Poisson distribution vs. superficial liquid velocity at the middle ($Z/D= 6.6$) and center of pilot plant reactor within spherical catalyst shape	48
Figure 20. Variation coefficient from Poisson distribution vs. superficial liquid velocity at the middle ($Z/D= 6.6$) and center of pilot plant reactor within cylindrical catalyst shape	49
Figure 21. Variation coefficient from Poisson distribution vs. superficial liquid velocity at the middle ($Z/D= 6.6$) and center of pilot plant reactor within trilobe catalyst shape	50
Figure 22. Variation coefficient from Poisson distribution vs. superficial liquid velocity at the middle ($Z/D= 6.6$) and center of pilot plant reactor within quadrilobe catalyst shape	51
 PAPER II	
Figure1. Schematic diagram for single slit model.	64

Figure 2. Schematic diagram of TBR.	71
Figure 3. Physical picture for (a) differential pressure transducer (b) data acquisition.	74
Figure 4. Physical picture for (a) digital load cell (b) sensor connected to load cell.	74
Figure 5. Pressure drop versus superficial gas velocity with single phase flow through (a) spherical (b) cylindrical (c) trilobe (d) quadrilobe catalyst bed.	77
Figure 6. Parity plot for (a) using universal Ergun coefficients (b) using universal non-spherical coefficients (c) using modified coefficients by comparing the experimental observations with the predicted single phase pressure drop by original Ergun correlation.	78
Figure 7. Transition boundary at different catalyst shape.	80
Figure 8. The effects of catalyst shape on the dimensionless pressure drop at different commercial beds.	81
Figure 9. Dimensionless pressure drop vs superficial liquid velocity at different superficial gas velocity (a) spherical (b) cylindrical (c) trilobe (d) quadrilobe.	83
Figure 10. Dimensionless pressure drop vs superficial gas velocity at different superficial liquid velocity (a) spherical (b) cylindrical (c) trilobe (d) quadrilobe.	84
Figure 11. The effects of catalyst shape on the liquid holdup at different commercial catalyst particles (spherical, cylindrical, trilobe, and quadrilobe).	86
Figure 12. The effect of superficial gas and liquid velocities on the liquid holdup at different beds (a) spherical (b) cylindrical (c) trilobe (d) quadrilobe.	87
Figure 13. Comparison of predicted dimensionless pressure drop to experimental with 70% of total data at high interaction flow regime (a) slit model (by Holub) (b) empirical model (by Larachi) (c) extended model (by Al-Dahhan).	92
Figure 14. Comparison of dimensionless pressure drop data versus superficial liquid velocity for different model approaches, with (a) spherical (b) cylindrical (c) trilobe (d) quadrilobe catalyst particles.	93

Figure 15. Comparison of predicted liquid holdup to experimental with 30% of total data at low interaction flow regime (a) slit model (by Holub) (b) empirical model (by Larachi) (c) extended model (by Al-Dahhan).....	95
Figure 16. Comparison of liquid holdup data versus superficial liquid velocity for different model approaches, with (a) spherical (b) cylindrical (c) trilobe (d) quadrilobe catalyst particles.	96
 PAPER III	
Figure 1. Physical picture for mimicked industrial hot bench-scale TBR hydrotreater unit.	110
Figure 2. Bench-scale TBR design	111
Figure 3. Schematic diagram for trickle bed reactor.....	112
Figure 4. Online Single Beam of GRD at axial and radial positions.....	114
Figure 5. (a) Photo for Gamma-ray source (b) schematic diagram for Gamma-ray Source.....	115
Figure 6. (a) Photo of NaI scintillating detector (b) Schematic diagram for NaI scintillating detector collimated and sited in shield house.	115
Figure 7. (a) Schematic diagram of GRD technique (b) GRD technique photo with TBR system.....	116
Figure 8. Picture and schematic diagram for phantom structure.	120
Figure 9. Photon counts profile at (a) case I (air-air) (b) case II (air-water) (c) case III (dry solid-water) (d) case IV (flooded solid-water).	121
Figure 10. Comparison of photon counts profile for each case.	122
Figure 11. Liquid holdup diametrical profile at 5cm height above both diluted and non-diluted packed bed surface at two different inlet configuration (Side and Top configuration).....	136
Figure 12. Dynamic liquid holdup profile with and without dilution particles at $UG=1796.5$, and $UL=0.39$ cc/min along the height bed.	137
Figure 13. External void fraction diametrical profile within diluted and non-diluted at different axial levels along the bed height (A) at $Z/D=4.23$, (B) at $Z/D= 12.29$, (C) at $Z/D =21.18$, (D) at $Z/D =29.66$, (E) at $Z/D =38.13$, (F) at $Z/D =46.61$	138

Figure 14. Line averaged dynamic liquid holdup diametrical profile within bed dilution at different inlet configuration of mixed gas and liquid with $U_G=269.5$, and $U_L=0.39$ cc/min along bed height (a) at $Z/D=4.23$, (b) at $Z/D=12.71$, (c) at $Z/D=21.18$, (d) at $Z/D=29.6$.	140
Figure 15. Line averaged dynamic liquid holdup Vs dimensionless radius r/R within diluted bed with side inlet configuration of mixed gas and liquid,	143
 PAPER IV	
Figure 1. Schematic diagram of bench scale hydrotreater reactor	158
Figure 2. Photo and schematic diagram for Gamma-ray densitometry	160
Figure 3. Histogram for wettability factor frequency distribution within $U_G=1796.5$, $U_L=2.64$ cc/min at axial level ($Z/D=12.71$)	162
Figure 4. Volume of catalyst utilization vs bed height at $U_G= 1796.5$ and $U_L= 0.39$ cc/min from top direction (a) non-diluted bed (b) diluted bed	166
Figure 5. Volume of catalyst utilization vs bed height at $U_G= 269.5$ and $U_L= 2.46$ cc/min within non-diluted bed (a) top inlet direction (b) side inlet direction	167
Figure 6. Volume of catalyst utilization vs bed height at $U_G= 269.5$ and $U_L= 0.39$ cc/min within diluted bed (a) top inlet direction (b) side inlet direction	168
Figure 7. Reactor Performance Comparison of the experimental and model accounting for the catalyst under-utilization. ($T= 370^{\circ}C$, LHSV 2 hr ⁻¹ , Feed S = 4.644 wt%)	171
Figure 8. Reactor Performance Comparison of the experimental and model accounting for the catalyst under-utilization. ($T= 370^{\circ}C$, LHSV 2 hr ⁻¹ , Feed S = 4.644 wt%)	172
 PAPER V	
Figure 1. Schematic Diagram for Trickle Bed Reactor	182
Figure 2. Time series of two tip optical fiber probe technique	184
Figure 3. Schematic of matched bubble signals used for velocity measurement	185
Figure 4. Local liquid saturation diametrical profiles Vs dimensionless radius (r/R) within different industrial catalyst shapes at the top level of the bed.	186

Figure 5. Local liquid saturation diametrical profiles Vs dimensionless radius (r/R) within different industrial catalyst shapes at the bottom level of the bed.	187
---	-----

LIST OF TABLES

SECTION	Page
PAPER II	
Table 1. Slit Model (Phenomenological approach) of Holub et al., 1992, 1993 with single Phase Modified Ergun Coefficients.	65
Table 2. Extended Slit Model (Phenomenological Approach) Equations for Pressure Drop and Liquid Holdup	68
Table 3. Packed beds characteristics.....	70
Table 4. Modified Ergun Coefficients at Different industrial catalyst particles.....	75
Table 5. Average Mean Relative Error (MRE) with Different Catalyst Shapes and Total Data.....	76
Table 6. Correlations for pressure drop and liquid holdup	89
Table 7. Comparison of Models to Individual Beds in Terms of MRE.....	90
PAPER III	
Table 1. Characteristics of packed catalyst particles used in the reactor.....	110
PAPER IV	
Table 1. Packed bed characteristics	157
PAPER V	
Table 1. Operation conditions characteristics.....	180
Table 2. Packed beds characteristics.....	181

SECTION

1. INTRODUCTION

The interdependence and mutual necessity of people, environmental, and energy poses formidable technical difficulties. The effects of the world population growth are increasing the demand on the energy consumption that caused a significant influence and excessive stress on the environmental. According to, the BP Energy outlook 2018 reported that over 40% of the increase in world energy is providing between 2018 and 2040 as it is seen in Figure 1.1. In addition to, the essential source for energy providing was fossil fuels (petroleum coal, and natural gas) combined approximately 75% of world energy production (Figure 1.1.). Thereby, the environment would be exposed to high stress by rising up world energy demand.

However, fossil fuels have been considered one of the best sources for energy, but many attempts to develop alternative energy that is still in progress due to fossil fuels energy is expensive and has a significant impact on the environmental. Therefore, improve the efficiency and enhance the performance for energy production by fossil fuels can be considerably reduced the cost and decreased the emissions and pollutants to the environment.

Commercially, the operation processes for energy production by fossil fuels were classified into two processes: catalytic and non-catalytic processes. The catalytic processes are representing 85% of all industrial processes due to high performance and less cost to the products. Moreover, 80% of all catalytic processes are heterogeneous catalysts as displayed in Figure 1.2.

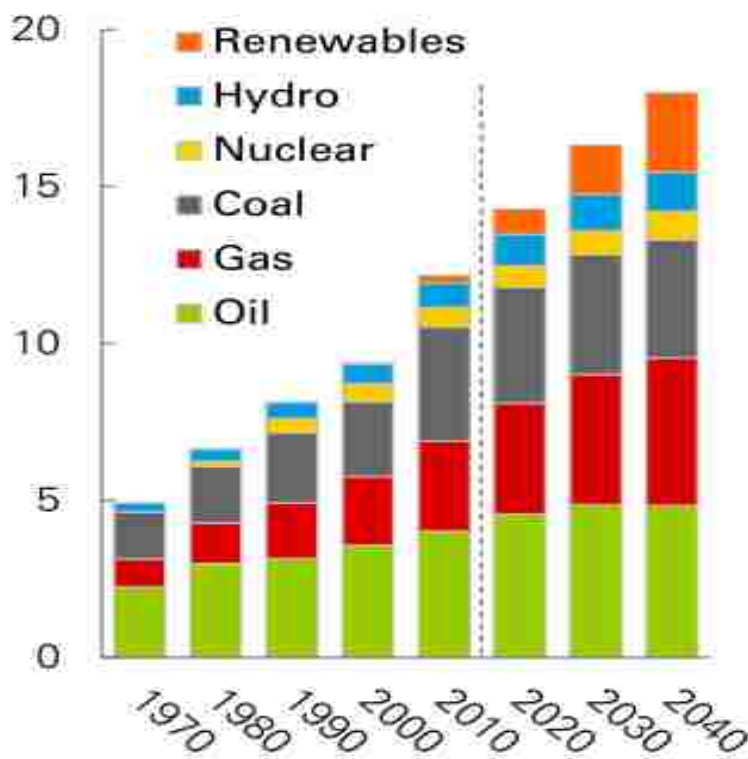


Figure 1.1. BP primary energy consumption by major sources [1]

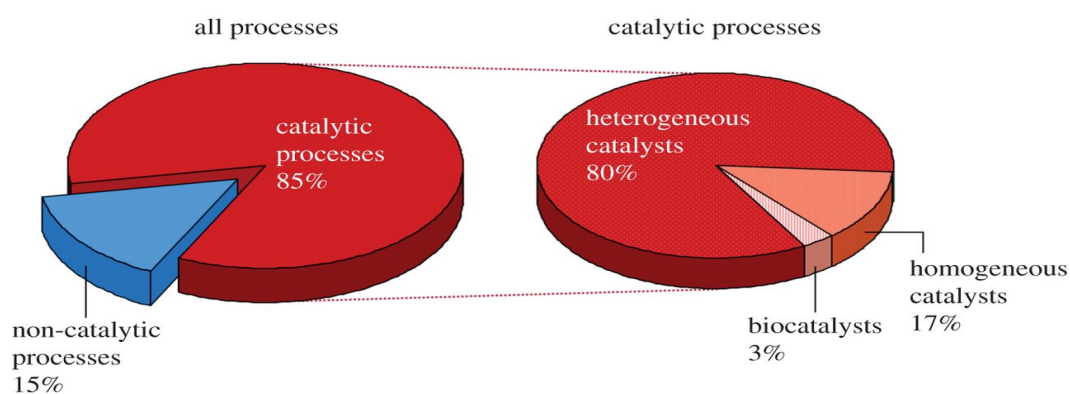


Figure 1.2. Show the percentages of commercial processes that include the use of heterogeneous, homogeneous and bio-catalysis [1]

For catalytic processes different types of multiphase reactors have been applied such as trickle beds, fluidized beds, slurry bubble reactors, and others. In the current work, trickle bed reactor packed with new shapes of catalysts such as trilobe and quadrilobe that lack hydrodynamics knowledge was selected for this study because it offers numerous merits compare to other reactors. The most important advantages are:

- Simplicity in operation conditions under high temperature and high pressure.
- Low catalyst attrition due to no need for catalyst separation.
- A wide range of particle size can be used (0.5-12 mm).
- Low energy consumption because the solids are not suspended.
- High conversion & selectivity because near plug flow conditions are more favorable in trickle bed reactors (TBRs).
- Reduce homogeneous reaction due to small liquid phase holdup.
- High throughput can be attained since the two phases move downward.

TBRs are fixed bed that gas and liquid flow concurrently downflow to contact the fixed solid particles which act as catalysts. The typical TBR is showed in Figure 1.3. The packing characteristics (shape, size, and angle) for catalyst particles have a significant impact on the hydrodynamic parameters and kinetic reaction in TBRs. A different sizes of catalyst particles have been widely investigated as porous and non-porous catalyst particles [3]–[5].

TBRs have been used extensively in industry such as petroleum or refining [6], petrochemicals [7], and chemicals [8], biochemical, pharmaceutical [9], and water and waste water treatment [10].

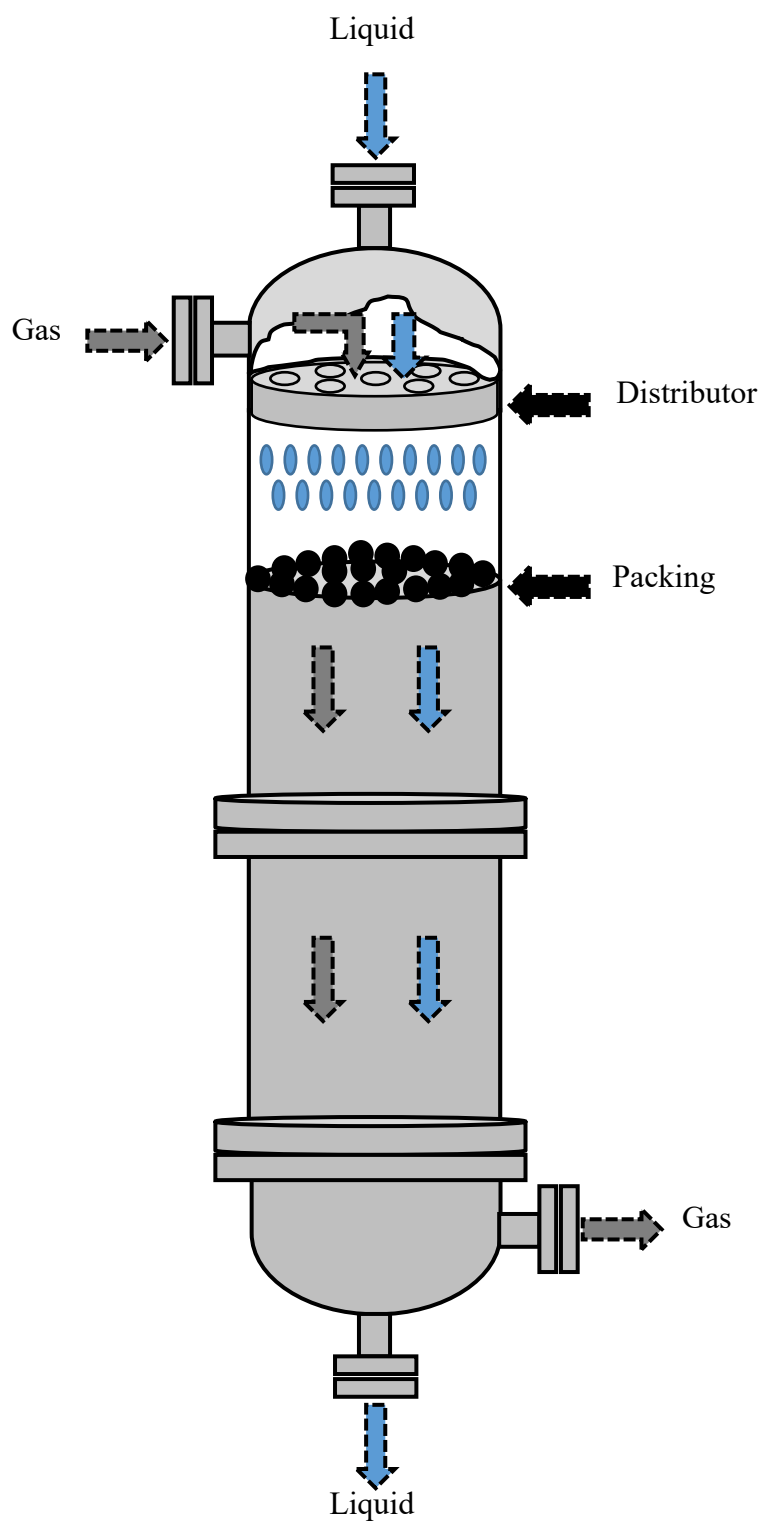


Figure 1.3. Schematic diagram of a TBR

The most applied reactions in TBRs are exothermic reactions that are generating excess heat in the reactor. The generated heat become uncontrolled in the non-wetted area due to creation hot spots that significantly affect the catalyst efficiency, kinetic reaction, and thus the performance and efficiency of the reactor and perhaps worse by temperature run away. The hot spots in the packed bed reactors represent a serious problem that leads to posing safety and design issues. The liquid maldistribution is a major reason for overheating materials (hot spots) that noticeably impact the catalyst particles efficiency by coking, sintering, and consequently catalyst particles agglomeration and blocking (channeling or bypassing) liquid flow in the bed.

Accordingly, the TBRs performance depends not only on the temperature and pressure but also on hydrodynamic parameters [11]. Furthermore, the hydrodynamics considerably affect the heat and mass transfer in the packed bed reactors. The essential parameters that effectively impact the hydrodynamics are gas and liquid flow rates [12], [13], distributor design [14], packing characteristics (shape and size) [15], gas and liquid properties [16], [17], and reactor design (bed diameter or bed height) [18]. Numerous studies have tackled different hydrodynamics such as phase distribution [19], gas and liquid holdup [20], gas and liquid interaction (flow regime) [21], pressure drop [22], heat and mass dispersion [23], local gas and liquid velocities [24], and many others.

The liquid distribution mainly depends on various parameters (gas and liquid flow rates, distributor design, and packing characteristics etc.) [25], [26]. However, Mohammed, Iman [26] reported that the distributor design has a practical impact only on the entrance surface area for the bed and the liquid flow rate has a noticeable influence on the liquid

distribution in the bed. Remarkably, the liquid maldistribution was observed in different axial surface area along the height bed.

The catalyst shape is playing a vital role in improving the liquid distribution in the axial surface area and other hydrodynamics as well (pressure drop, gas and liquid holdup, flow regime, local gas and liquid velocities, axial dispersion, and residence time distribution) due to the catalyst shape can provide effective surface area, contacting efficiency, and void distribution. Therefore, the catalyst shape is capable of overcoming some of the shortcoming by enhancing solid-solid contact and supply uniform void distribution along the axial surface area that consequence for improving liquid holdup and wetting efficiency in the bed.

Additionally, bench scale reactors have been used to test catalyst, obtain the kinetics, and to design and develop the industrial reactors to decrease the construction and operation expense, define the required chemical, identifying safety issues, and to recognize the proper flow patterns that provide a reliable data to being applicable for the industry. These reactors have been applied to investigate also the hydrodynamics by loading a commercial size of catalyst particles in small scale reactor was a big challenge which generating liquid maldistribution due to wall effects and the ratio of column diameter (D_c) to particle diameter (d_p) is less than 20. Meanwhile, low fluid flow rate when convert it from large scale to small scale that was also a major reason for creating a deviation in the results that cause no matching between the bench scale and large commercial reactors.

Therefore, adding fine particles to the catalyst particles as a diluent in approach that called dilution technique was used as a solution to decouple hydrodynamics from kinetics and have the catalysts performance match that of the industrial reactor. Consequently,

investigating the effects of fine particles on the hydrodynamics is significantly important to achieve the matching and reliability in fundamental understanding. Furthermore, the complexity for these reactors requires reliable and advanced measurement techniques to visualize the phenomena inside the reactor, and to quantify the parameters with a high degree of accuracy.

1.1. RESEARCH MOTIVATION

As mentioned earlier hydrodynamics in TBRs represents one of the crucial parameters that significantly affect the performance of the reactor. Over the past years, there has been a dramatic increase in hydrodynamics investigation of TBRs to enhance their performance due to their extensive use especially in the petroleum processes. Hydrodynamics are classified to various parameters such as phase distribution, gas and liquid holdup, flow regime, pressure drop, and local gas and liquid velocities, which can effectively impact the fluid interaction quality, wetting efficiency, catalyst utilization, due to liquid distribution and wetting, and others. Various correlations and models have been developed to predict these hydrodynamic parameters at different operation conditions (range of gas and liquid velocities, distributor design, reactor design, fluid's properties, and packing characteristics).

However, a significant limitation of the knowledge in the literature is related to particle shape effects, and no attention have been given to the theoretical efforts to predict the hydrodynamics in packed bed reactors packed with various catalyst shapes such as trilobe and quadrilobe that because widely used for hydrotreating processes. Also there is still limitation in benchmarking local data to validate computational fluid dynamics (CFD)

models and simulations. Moreover, most of the experimental and theoretical studies are confined to spherical and cylindrical particle shapes. Commercially, in the refining fields (hydrotreating), in the early of 1970s, American Cyanamid the pioneer of catalyst manufacturing introduced trilobe as new particle shape for hydrodesulfurization process. Then most of the providers have changed to manufacture shaped catalyst for hydrotreating operations. Although, in the past years, Polylobes (Trilobe and Quadrilobe) particle shapes extensively employed in the hydrotreating processes, a very few studies have investigated the effects of trilobe and quadrilobe particle shapes on hydrodynamics and transport of TBRs that are required to enrich the industrial and literature with fundamental engineering knowledge to improve performance of the TBRs. Theoretically, no attention is paid to predict the effects of particle shape on the hydrodynamics in the trickle bed reactors. Typically, The phenomenological models developed to predict the hydrodynamics in TBRs are based on spherical shapes [27]–[31]. Furthermore, concerns has been stated on the impacts of packing characteristics which Saroha et al. [17] and Lakota et al. [32] expressed that there is a catalyst shape influence on the relative permeability implemented in the models [17], [32].

In the literature [33] trilobe and spherical catalyst shapes were applied to investigate the hydrodynamics in the pilot plant TBR of 14 cm inside diameter and 100 cm height of column to conduct the experimental work. 1mm particle diameter for spherical and trilobe particles were packed with two various ways: sock and dense loading. A digital pressure drop measurement was used to measure pressure drop, while the drainage methods was used to estimate the average liquid holdup. Nitrogen and water flows at mass flux range 0-0.12 kg m⁻² s⁻¹ for nitrogen and 0-5.4 kg m⁻² s⁻¹ for liquid. Although, the effects of the

catalyst shape and Polylobes particle shape on the hydrodynamics have studied in the reactor, obviously, the limitation in the applied mass flux range of nitrogen and water is obvious as the flow range that is not sufficient to cover the two interested flow regime for industry trickling and pulsing flow regimes [33].

Kundu et al. 2001 [25] studied the impacts of shapes and sizes of catalyst particles and liquid physical properties on the liquid distribution in a pilot plant TBR of 0.152 m inside diameter and 62 cm bed height using air and different physical properties of the liquid. A wide range of gas and liquid mass flux were implemented to the study that is enough to cover the required industrial flow regimes of trickle and pulse flow regimes. Averaged liquid distribution was investigated with five different catalyst shapes using six annular collectors in the bottom. The effects of catalyst shapes on the liquid distribution in the wall have studied using a uniform distributor in the top. The evidence from this study points out that the liquid distribution depends not only on the liquid distributor but also on the catalyst shapes. In their work, the authors quantified averaged liquid distribution that is not sufficient to provide a clear picture for the whole bed in the reactor, indicating that measuring the liquid distribution at different axial positions along the bed height is highly recommended to improve the fundamental understanding of the impact of the liquid distribution on the studies parameters. Furthermore, using advanced measurements techniques to carry out the experimental work represents one of the most essential points recommended to enable to tracking the phenomena in the multiphase reactors [25].

Moreover, the impacts of the particle shapes on the hydrodynamics (liquid holdup, pressure drop, and flow regime transition) were studied by Trivizadakis et al. [15] in the pilot plant TBR. A cylindrical column with 14 cm inside diameter and 1.24 m bed height

was used at standard temperature and pressure. Air-water system was used in their [14] research within a range of gas and liquid mass flux 2.4-6.13 kg/m².s for liquid and 0-3.7 kg/m².s for gas. The reactor packed with 6 mm glass and 3 mm alumina spheres, and 1.5 mm cylindrical-extrudate. The results of their study found that the particle shapes significantly affect the hydrodynamics. In the previous years, in the industry, Polylobes particle shapes are broadly applied in the industrial field particularly in the petroleum industries (hydrotreating processes). These results therefore need to be expanded to indicate the impacts of Polylobes catalyst shapes compare to the spherical and cylindrical catalyst shapes on the hydrodynamics in the TBRs. Hence, there is a need to use different catalyst shapes (spherical, cylindrical, and Polylobes) at similar size and all porous to detect extent of catalyst shapes on the hydrodynamics in the multiphase reactors [15].

In addition to, experimental studies were performed and empirical correlations were suggested on flow regime transition in TBR [34]. Different liquid physical properties were used to study influence viscosity and surface tension of the liquid on the flow regime transition where Newtonian and non-Newtonian liquids were utilized. Furthermore, the effects of sphericity and void fraction on the flow regime transition were studied by packing different catalyst shape and size to the reactor. Porous (5.3 mm catalyst pellets) and non-porous (3.337 mm and 14.84 mm glass spheres, and 3.69 mm glass Raschig rings) particles have used to study the impacts of catalyst shape and size on the flow regime transition. Cylindrical column at 7.4 cm diameter and 40-50 cm height carried out the experiments using a liquid distributor with 16 holes in the top of the reactor. The research [34] produced results which revealed considerable impacts of catalyst shapes on the flow regime transition. The flow regime transition was measured using manometer by

observation of the onset of pulsing fluctuations. Unfortunately, authors [34] in the introduced work declared that they did not take wall effect into their accounts, and hence, must take the ratio of D_c/d_p must be taken in the consideration to use the results in identifying flow regime transition. Industrially, this study has been unable to demonstrate the impacts of commercial catalyst shapes due to implementing porous and non-porous catalyst particles. Meanwhile, the limitation in the measurement techniques using visual observation which is inapplicable in industry generated the need to implementing reliable and applicable techniques using robust tools to diagnose the flow regime transition in the multiphase reactors in general due to high demand in the industry [34].

Al-Dahhan et al. investigated the effects of catalyst bed dilution on the wetting efficiency, pressure drop, and liquid holdup in the bench scale TBR. The catalyst bed dilution technique has been performed for useful scale up and scale down due to using a commercial size of catalyst particles and low linear liquid velocities that lead to partial catalyst utilization because of incomplete wetting, liquid maldistribution, and wall effects. Al-Dahhan et al. [35] also developed new reproducible methodology for diluted beds by filling the void of the original packed bed with fines. Two columns have been designed which one of them with transparent window to visualize gas and liquid flows with 2.2 cm inside diameter and the second column with 2.19 cm at 57.15 cm length for both columns. High accuracy differential pressure transducer was mounted in the top and the bottom to measure the pressure drop in the reactor. Moreover, wetting efficiency have been assessed based on the results acquired by applying tracer. Simultaneously, load cell have been implemented to indicate the impacts of catalyst bed dilution on the liquid holdup by drainage method. Two different catalyst shapes (Spherical and extrudate) were packed to

the reactor. The results of their work revealed that the catalyst wetting efficiency, pressure drop, and liquid holdup were increased in the catalyst bed with fine due to improve contacting efficiency (solid-solid). Additionally, the authors recommended to investigate and predict the effects of bed dilution on the catalyst wetting at different particle shapes and sizes and develop model due to high demand in the industry [35].

The effects of particle shape on the hydrodynamics are still not at a mature level of technological development. Due to the complexity of multiphase flow, the geometry of tortuous space, and gas-liquid and liquid-solid interaction have not been yet solved. Meanwhile, in recent years the catalyst manufacturers developed catalyst shapes such as trilobe and quadrilobe which increased the needs to new knowledge and understanding of the packed bed reactors with different particle shapes. Therefore, a significant limitation in the open literature to investigate and evaluate the effects of the catalyst shape on the hydrodynamics, thus on the reactor performance in the pilot plant and bench scale trickle bed reactors. In the bench scale reactors, quite limited or rare studies reported in the literature to indicate the effects of adding fine particles to the industrial size of catalyst particles at different particle shape due to high lack in the measurement techniques.

Meanwhile, most of the phenomenological models that predicted hydrodynamics were not considered the effects of particle shape on the dynamic fluids phenomena and implemented as a uniform spherical shape. Therefore, high necessity to assess these models and modify if necessary the best phenomenological models to apply the effects of catalyst shape to improve the model precision that considerably impacts the calculation accuracy. This will strengthen the fundamental understanding, and supply ensured information for the industry.

Additionally, due to the complexity in the multiphase phenomena, the quality and capability of measurement techniques are a challenge. Obviously, Most of the studies used techniques with limited capabilities. The limitations made the measurements global for parameters (macro-scale data) for all bed which represent incomplete understanding of the reactor, for which a significant deviation in the data due to wall effect which is inapplicable to industry. Accordingly, there is an extreme need to develop and/or implement advanced techniques that are reliable and can be applicable for industry with high flexibility in measurements. Furthermore, the data can be considered as local benchmarking data to validate computed fluid dynamic (CFD) simulations and models which are also needed.

There is an urgent need to integrate the understanding and improve the knowledge that leads to enhancing the performance of the TBRs. Furthermore, obtain mesoscale data using advanced techniques can be benefited for developing models and improving the quality of measurements. Therefore, the concentrate of this work is to address these needs.

1.2. RESEARCH OBJECTIVES

The overall objectives of this study are to advancing the knowledge of the effects of catalyst shape, bed height, and wide range of gas and liquid velocities on the hydrodynamics of pressure drop, gas and liquid holdup, flow regime transition, local gas and liquid velocities, and gas and liquid saturation in the pilot plant scale TBR using advanced techniques (Gamma-ray densitometry, Optical fiber probe, and high frequency pressure transducer). The radial profiles of the mesoscale data at a wide range of gas and liquid velocities and different axial locations along the bed height will be illustrated. Additionally, for the first time the impacts of the present fine particles with a commercial

size of trilobe catalyst shape, gas and liquid inlet direction, a range of gas and liquid velocities, and bed height on the hydrodynamics have been studied to assess the liquid distribution and catalyst utilization in the bench scale TBR using advanced Gamma-ray densitometry. The detailed objectives are:

1. Identifying the trickling to pulsing flow regime transition and assessing extent the impacts of various catalyst shape, and gas and liquid velocities on the flow regime transition.
2. Studying the effects of different industrial catalyst shape, and gas and liquid flow rates on the pressure drop and liquid holdup in the pilot plant scale TBR.
3. Studying the impacts of adding fine particles to the commercial size of trilobe catalyst particles, gas, and liquid velocities, gas and liquid inlet direction, and bed height on the phase distribution and liquid holdup in a Mimicked Bench Scale Hydrotreater Reactor
4. Developing a methodology for catalyst utilization measurement and investigating the effects of adding fine particles to the commercial size of trilobe catalyst particles bed, gas and liquid velocities, and gas and liquid inlet direction on the catalyst utilization in a mimicked bench scale hydrotreater reactor.
5. Quantifying the effects of different shapes of commercial catalyst particles, gas and liquid velocities, and bed height on the local gas and liquid saturation, and local gas and liquid velocities.

PAPER**I. FLOW REGIMES IDENTIFICATION OF TRICKLE BED REACTOR (TBR) PACKED WITH TRILOBE AND QUADRILOBE INDUSTRIAL CATALYST USING NON-INVASIVE GAMMA-RAY DENSITOMETRY (GRD)****Mohammed Al-Ani, Muthanna Al-Dahhan***

Multiphase Reactors Engineering and Applications Bench (mReal), Department of Chemical and Biochemical Engineering, Missouri University of Science and Technology, Rolla, MO 65409-1230. USA

ABSTRACT

The influence of industrial catalyst shapes on the flow regimes and transition velocity has been investigated in pilot plant scale Plexiglas transparent column with 14 cm inside diameter and 185 cm height bed and air-water system using non-invasive radioactive Gamma-ray densitometry (GRD) technique. Moreover, four various industrial catalyst shapes (spherical, cylindrical, trilobe, and quadrilobe) have been randomly packed with wide range of superficial gas velocity from 30 to 270 mm/s and range of superficial liquid velocity from 4 to 14 mm/s in the TBRs. The high flexibility for GRD technique allowed to scan the reactor at different axial locations along the height bed. Time domain (Standard Deviation) and chaotic methods (Kolmogorov Entropy) are employed on time series of photon counts of GRD to diagnose trickle to pulse flow regimes and transition velocity in TBRs. A new flow regime identifier was implemented and validated with time domain and chaotic analysis methods which the new identifier revealed a similar trend compared to time domain and chaotic analysis methods and can be applicable for online flow regime tracking for GRD data. A comparison with results of analysis methods were implemented

on each catalyst shape which the comparison showed a significant effect for catalyst shapes on the flow regimes and transition velocity in the TBRs.

Keywords: Flow regime, trickle Bed Reactor, catalyst shapes (Trilobe and Quadrilobe), non-invasive Gamma-ray densitometry, Kolmogorov Entropy (KE)

Highlights

- Flow regime identification in TBRs
- Commercial catalyst shapes effects on the flow regimes and transition velocity
- Non-invasive GRD scanning at different axial positions along the height bed
- Conventional and chaotic analysis methods on time series of photon counts of GRD
- Variation from Poisson distribution identifier for flow regime diagnose on GRD data
- Trickle and pulse flow regime and their transition velocity

Nomenclature

TBR	trickle bed reactor
GRD	gamma-ray densitometry
V_c	variation coefficient from Poisson distribution
KE	Kolmogorov Entropy
STD	standard deviation
ID	inside diameter
r/R	radius dimensionless
Z/D	height bed dimensionless
mReal	multiphase engineering and applications bench

1. INTRODUCTION

Trickle bed reactors (TBRs) have been widely used in multiple commercial processes with different design and operation conditions such as chemical industries (e.g. Petroleum petrochemical, chemical processes, etc...). Several advantages for TBRs encouraged the industry to broadly use it in different industrial fields. The most important advantages for TBRs are simplicity in operation under high temperature and high-pressure conditions require for most industrial processes, low energy consumption due to the solids are not suspended, and plug flow conditions more favorable, hence higher conversion and selectivity. The effectiveness in TBRs is highly depended on gas and liquid interaction [1]–[9].

The flow regime represents the gas-liquid contacting which is related to many parameters such as pressure drop, liquid holdup, liquid distribution, and heat and mass transfer. The flow regimes in TBRs can be categorized according to gas and liquid interaction into four different flow regimes: trickle (low interaction regime), pulse, bubbly, and spray flow regimes (high interaction regime). The flow regime identification precisely is even important due to the flow regime considerably can cause variation in the activity of TBRs. The determination of flow transition plays a central role in the design and scale-up purposes. The flow transition between flows regimes in TBRs are depending on superficial gas and liquid velocities, fluid properties, and bed characteristics (catalyst shape, size, and surface properties). Various flow regimes can be diagnosed (trickle, pulse, spray, and bubble regimes) in TBRs in which two flow regimes (trickle and pulse regimes) are applicable in industry [7], [9]–[14].

However, flow regimes in packed bed have been investigated over the latest few decades, nonetheless many parameters that incompletely understood yet. The void distribution can impact by several hydrodynamic parameters such as flow regime, gas and liquid holdup, pressure drop, and liquid distribution, and catalyst utilization. The main factor that significantly affects the void distribution in the packed bed reactor is packing characteristics (catalyst shape, catalyst size, column height, and column diameter). Although, a considerable amount of literature has been published on flow regime identification, there has been limited studies that engaged with catalyst shape impacts [15], [16]. The criteria for selecting an optimum shape for particles based on surface area, voidage, and transfer coefficient. The optimum structure of packed bed reactors with uniform voids distribution are quite complex [17], [18]. Nemeč & Levec and Trivizadakis [15], [18] highlight the need to systematic study to investigating effects of catalyst shape on the flow regime and hydrodynamic parameters in TBRs to develop the models and correlations for improving predicting the hydrodynamic parameters in the TBRs.

Different measurement techniques to identify the flow regimes were used in the previous work. Helwick [19] reported the observation is one of more applicable methods to identify the flow regimes in TBRs. Although, the observation method is a simple and low-cost method, nonetheless it is not sufficient to providing complement understanding of gas and liquid interaction in the reactor due to the flow within the bed is different than near the wall. In addition to sophisticated techniques have been used to diagnose the flow regime boundary that classified into two types of invasive and non-invasive techniques.

The invasive techniques that applied in previous work are conductance [2], [15], cross-sectional distributed local capacitances [20], magnetic emulation of micro and macro

gravity [21], conductmeter [22], and microelectrode [9]. Although, most of these investigations were supplied with reliable data, still these techniques have issues due to these probes have access for a column during the measurements. Whitemarsh [23] noted that there is a significant impact of a probe on measured data. As well as, the non-invasive techniques include high-speed cameras [13], [24], [25] and pressure transducer at the wall [2], [26]. However, it is effective and applicable techniques, but according to Humair and Honda [13], [16] they noted that the void and particles distribution near to the wall in a considerable variation than the bed. Thereby, there is a significant difference in obtained data in two-phase flow reactors. Accordingly, there is an extreme need to a non-invasive technique that can be capable to do external measurements without any disturbance for flow and with high flexibility in measurements. Extensively, flow regime has been determined in TBRs using several measurement techniques and different types of data analysis methods. Time series of various measurement techniques have been analyzed by multiple approaches such as time domain, frequency domain, and state-space analysis methods [27]. Time series analysis by time domain methods that implemented to identify flow regimes in various reactors which expressed via standard deviation and /or variance [2], [9], [22]. However, the time domain method is simple and no need for programming, but it is considered an insufficient method to indicate the flow regime boundary [22], [28]. In addition to, frequency domain method that includes power spectral density distribution and wavelets. The frequency domain is a common method for examining pressure fluctuation signals. Moreover, state space approach which is a way for non-invasive systems investigations. State space approach expressed by (Kolmogorov Entropy, Correlation dimension, Lyapunov exponent). Kolmogorov Entropy analysis considered as

a one of a powerful method that used Schouten [29] approach based on maximum likelihood calculation for flow regimes identification in non-linear invariant systems [30], [31]. In spite of, Kolmogorov Entropy is a robust instrument to identify flow regime in nonlinear systems, but it is still hard to do complicated programming to implement this method. Therefore, it is necessary to find a simple approach with high accuracy to simplify flow regime determination in the multiphase reactors. To the best of author knowledge, nobody in previous studies published work in the literature that identified trickle to pulse flow regime and their transition velocity within commercial trilobe and quadrilobe catalyst shapes using advanced non-invasive radioactive technique by applying several analysis methods (standard deviation, Kolmogorov Entropy, and new flow regime identifier coefficient) as we can see in section 3. Thus, this study aims to experimentally investigate the effects of different commercial catalyst shapes on the flow regime and transition velocity using advanced non-invasive radioactive measurement. The acquired time series have been analyzed by using new analysis method and validate it by two different data analysis methods which are time domain analysis method (Standard Deviation) and state space analysis method (Kolmogorov Entropy).

2. EXPERIMENTAL WORK

2.1. EXPERIMENTAL SETUP

A cylindrical of transparent acrylic column with 14 cm inside diameter and 185 cm height bed was employed to conduct the experiments in the current work as it shown in the schematic diagram of Figure 1. Air was used as a gas phase with range of superficial gas

velocity from 30 to 270 mm/s which the gas have been controlled by two flowmeters with different range of flow rate. While, water was represented the liquid phase by pumping the water to the reactor by using water pump from circulating tank. Also, the liquid phase fed through two different range of flowmeters with range of liquid velocity from 4 to 14 mm/s through shower distributor and then distribute the gas and liquid by perforated plate. Four beds of catalyst shapes implemented to investigating effects of catalyst shape on gas- liquid interaction in the TBR. Furthermore, the TBR was installed in the middle between the source of gamma-ray of GRD technique and the detector that equipped and aligned to receive gamma-ray of photon counts as displayed in Figure 1.

2.2. GAMMA-RAY DENSITOMETRY (GRD) TECHNIQUE

Advanced GRD technique has been implemented to identify flow regime boundaries that evolved in multiphase reactors engineering and applications bench (mReal) at Missouri University of Science and Technology. Commercially, GRD was used widely at various applications as a reliable industrial measuring tool due to provide a reliable data with high integrity through the measurements that can be done with no contact for the process inside the reactors (non-invasive measurements with no interruption for operation condition).

In addition to, GRD considered as a cheap technique which no need to shut down the process to install GRD and offer long term performance as well. Moreover, GRD is offering a high flexibility and simplicity in measurements use through scanning the radial/diameter profile along the height of the reactor axially.

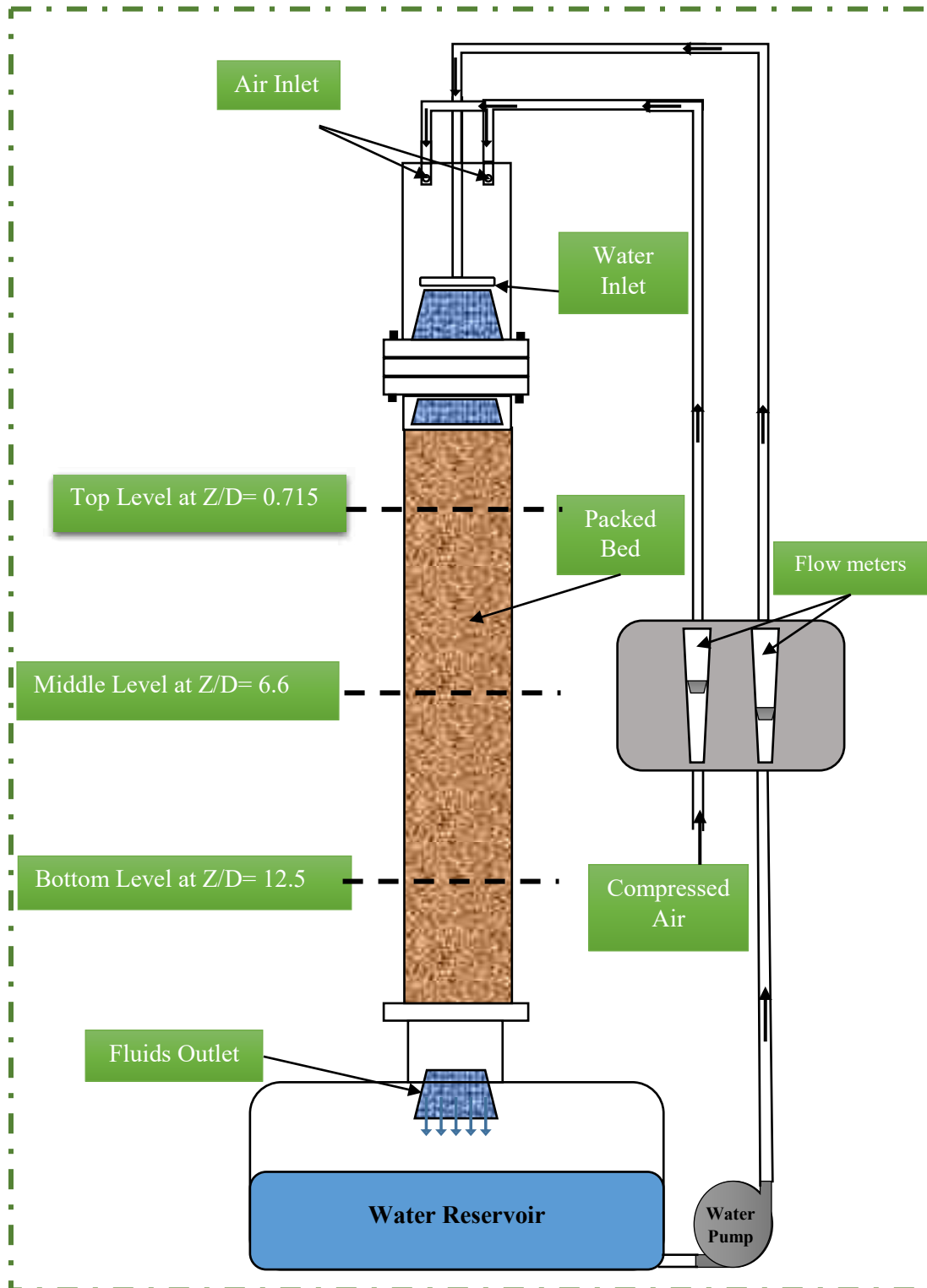


Figure 1. Schematic Diagram for Trickle Bed Reactor

In the current work, GRD measurements are applied at different positions along the length and at the center ($r/R=0$) of the reactor through different catalyst shapes. The concept of measuring for the GRD technique depend on the attenuation of beam of gamma-ray relying on density of examined substances. The time series of photon counts for GRD have been used to identify the flow pattern in multiphase reactors. The source Cs-137 with initial activity approximately 250 mCi housed inside sealed chamber of lead with suitable energy of 660 keV as displayed in the picture and schematic in Figures 2(a) and (b).

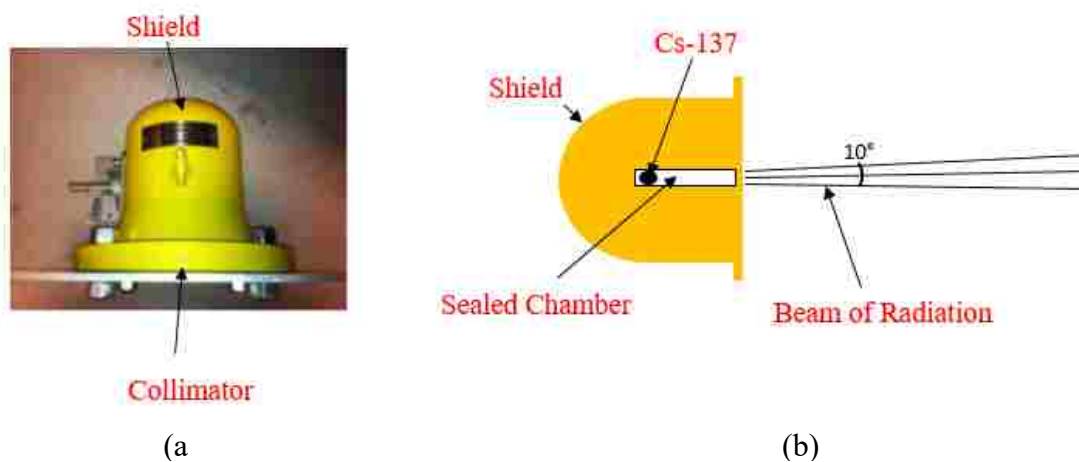


Figure 2. (a) Photo for source (b) Schematic diagram for source

NaI scintillating detector was linked to receive beam of radiation of gamma-ray. The detector connected to data acquisition system that consist of osprey unit (digital MCA

tube base for gamma-ray spectrometry), also has a USB interface, and the unit connected to computer with software to show and analysis of gamma-ray spectrometry data from detector as we can see in Figure 3a. The detector collimated and fixed inside shielded chamber to be ensured there is no detection for any scattering as shown in Figure 3b. the photon counts that indicated by the detector as a time series of photon counts have been treated by statistical and chaotic analysis methods to diagnose the flow regimes and their transition velocities.

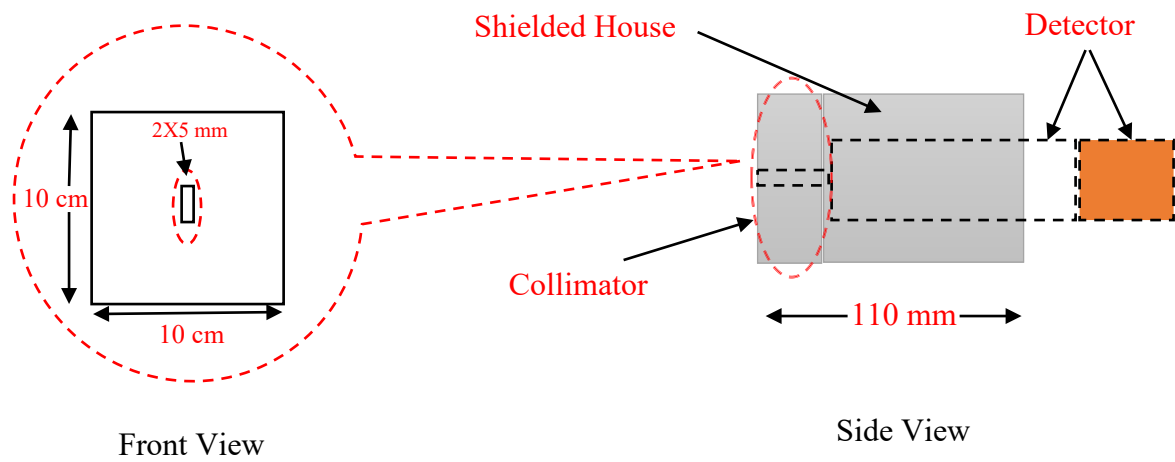
3. GRD SIGNALS PROCESSING AND DATA ANALYSIS METHODS

3.1. TIME SERIES OF PHOTON COUNTS

The time series of photon intensity fluctuation is illustrated in Figure 4 at constant superficial gas velocity and different superficial liquid velocity. Remarkably, the time series of photon counts signals show a noticeable decrease in the photon counts amplitude with increase the superficial liquid velocity due to increasing the attenuation for gamma-ray by increase the liquid flow rate. Moreover, the counts amplitude in Figures 4 and 5 indicate clearly the difference in counts amplitude between different superficial liquid velocities and dry solid (catalyst particles) with no fluids flow which the attenuation for gamma-ray in this case by the catalyst particles and the reactor wall. Therefore, the amplitude of counts signal were considerably increased from (380-480) at fluids flow rate conditions to (600-680) at dry solid case, since gamma-ray attenuation was decreased in case no liquid flow rate.



(a)



(b)

Figure 3. (a) Photo of NaI scintillating detector (b) schematic diagram for NaI scintillating detector collimated and sited in shield house

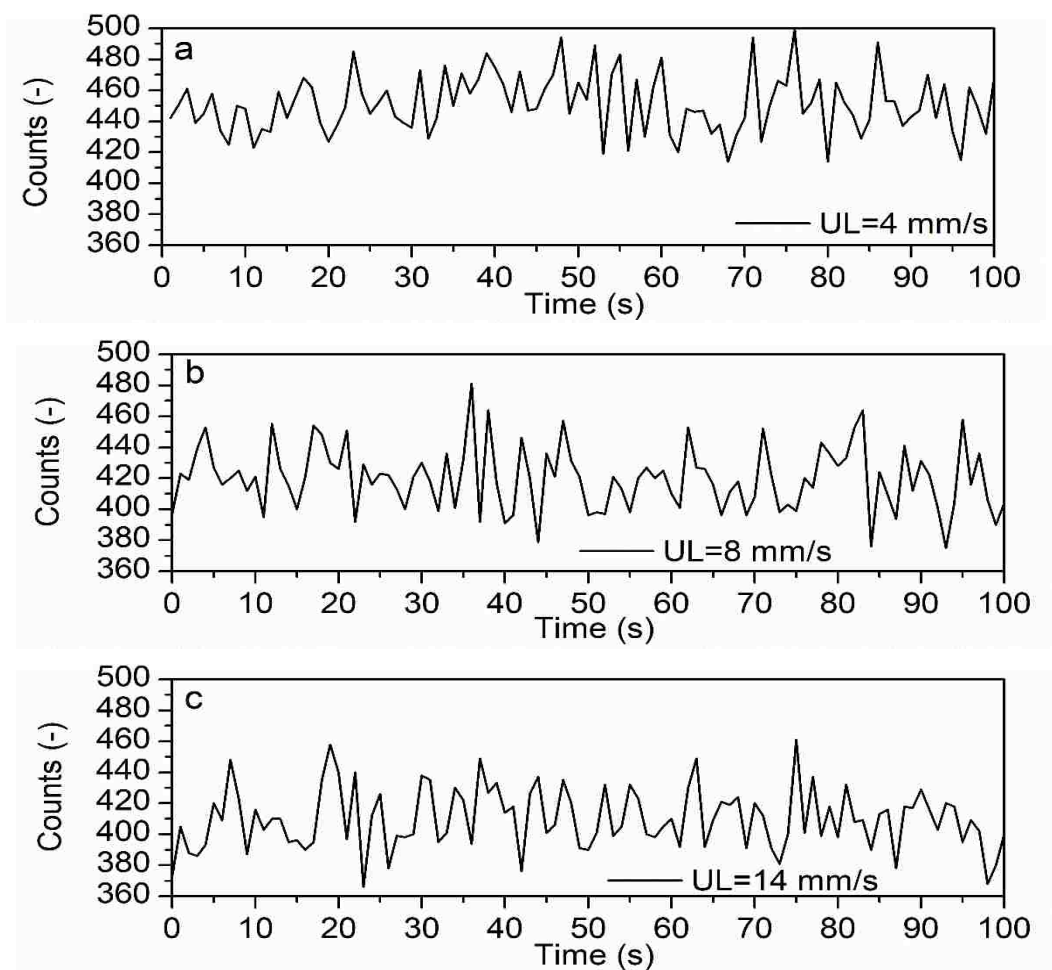


Figure 4. Time series of photon counts fluctuations in 14 cm diameter column at superficial liquid velocity (a) 4, (b) 8, and (c) 14 mm/s

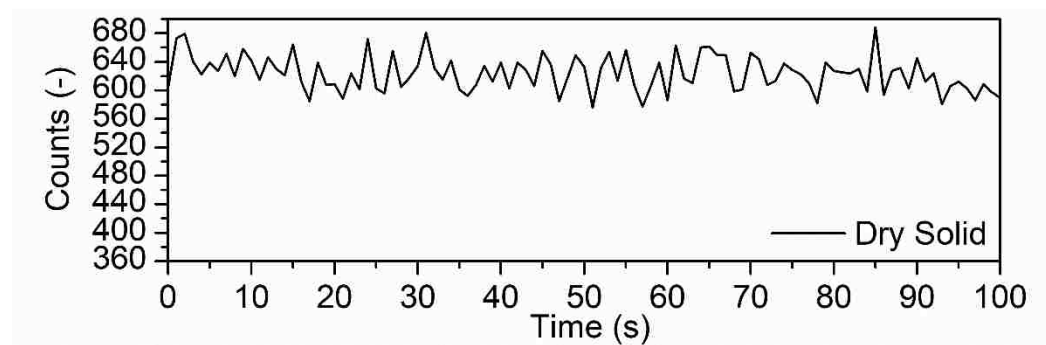


Figure 5. Time series of photon counts fluctuations in 14 cm diameter column in dry solid case.

Accordingly, the photon counts signals have been verified at high sensitivity for GRD technique to distinguish the change in liquid flow rate through catalyst bed in TBRs. The fluctuation of counts signals in Figure 4 display complex oscillation at different superficial liquid velocity conditions which is in good agreement with several gamma-ray counts signals [36], [37]. The complexity for counts frequency for GRD signals due to non-uniform void distribution that significantly affected on gas and liquid distribution in the void space region. Meanwhile, the characteristic geometrical parameters can be one of essential factor for bed void maldistribution [14]. However, a number of studies show that the behavior for the pressure fluctuation signal at different superficial liquid velocities can be indicated the flow regime boundary in TBRs. Albeit findings are somewhat contradictory [38]. Hence, the behavior of counts fluctuation for gamma-ray signals is quite different than the pressure fluctuation signals.

The quality differences that observed in the signal behavior revealed how it is difficult to identify the flow transition based on signal fluctuation. Consequently, further research to develop new numerical methods that capable to provide numerical value to determine the flow transition with high accuracy and simplicity in multiphase reactors.

3.2. VARIATION OF POISSON DISTRIBUTION

Over 120 s the time series of photon counts for empty column (air), only water, and melted catalyst (solid only) are displayed in Figures 6,7, and 8. The photon counts acquired in each case show Poisson distribution. In Poisson distribution, the mean is equal to the variance for the time series of photon counts. In cases of the empty column (air), only water, and melted solid the mean = variance = unity.

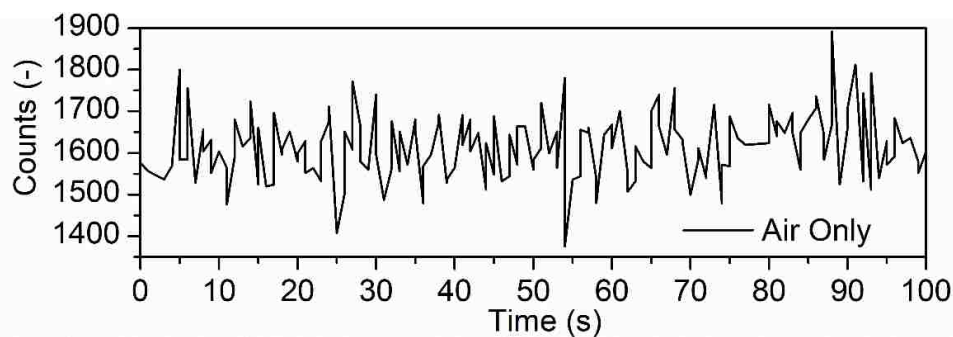


Figure 6. Time series of photon counts fluctuation in 14 cm diameter column in air only case.

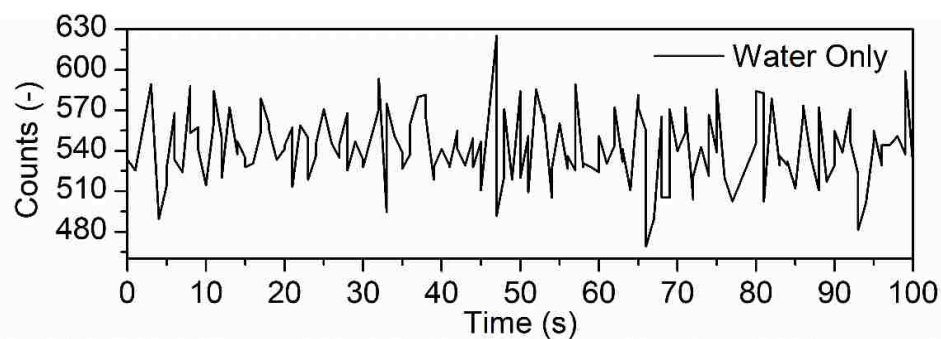


Figure 7. Time series of photon counts fluctuation in 14 cm diameter column in water only case.

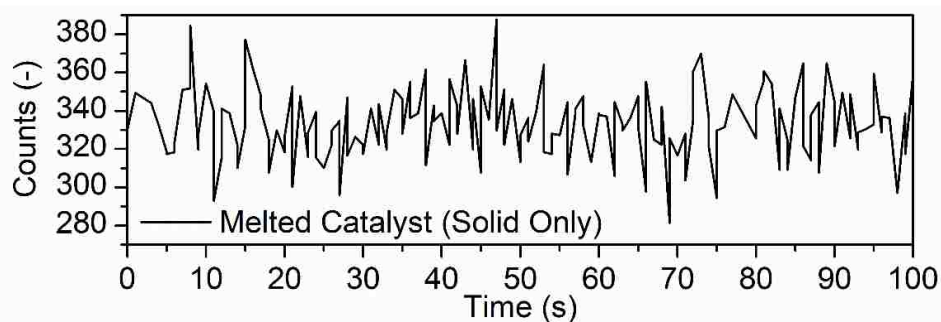


Figure 8. Time series of photon counts fluctuation in 14 cm diameter column in solid only case.

Figures 4 (a) and (c) indicate the photon counts that detected at range of superficial liquid velocities. It is obviously displays an increase in amplitude and oscillation of photon counts with increasing superficial liquid velocity. The fluctuation of time series of photon counts for low superficial liquid velocity are relatively low amplitude and low oscillation as it is seen in Figure 4a, while in Figure 4c at a higher superficial liquid velocity high amplitude and oscillation can be observed due to drop size distribution. Based on the deviation value from Poisson distribution for photon counts at range of gas and liquid flow rate conditions the flow regimes will be diagnosed. New coefficient identifier can be used for flow regime and transition velocity identification from time series of photon counts using gamma-ray in TBRs.

3.3. STATISTICAL ANALYSIS (STANDARD DEVIATION)

Standard deviation is one of conventional analysis method for time series in the turbulent systems to identify the flow regime. Statistical approach depend on calculating standard deviation (STD) as follows on in Eq. (1):

$$\text{STD} = \sqrt{\frac{\sum_{i=1}^N (\chi_i - \mu)^2}{N-1}} \quad (1)$$

Where χ_i the data is point and μ is the mean and N is the number of data points. The flow regime identification has been specified by the rate of change in the amplitude with range of operation conditions.

3.4. KOLMOGOROV ENTROPY (KE) ANALYSIS METHOD

State space analysis or chaos analysis is corresponding analysis in frequency and time domain. The dynamics of turbulent systems has been considered non-linear and chaotic characteristics. One of the powerful chaotic analysis to identify chaos is called Kolmogorov Entropy (KE). KE is one of deterministic methods to characterize chaos and non-linear hydrodynamic behavior of TBRs. KE is quantification approach that considered as robust and useful instrument to specify the chaos. This method is more appropriate method to quantify the level of disorder in dynamic or chaotic systems of time series analysis [39]–[41]. Intrinsically, multiphase flow in TBRs represent one of the chaotic and non-linear systems due to the complex interaction between gas and liquid through a solid phase. KE method used to analyze time series of pressure fluctuation, conductance fluctuation, and photon counts to identify the flow regime and transition velocity at different reactors [36], [39], [42], [43]. KE approach has been treated by Schouten approach [44]: maximum likelihood estimation of entropy and a Matlab program was developed to facilitate this approach at multiphase reactor engineering and applications bench (mReal). The maximum likelihood estimator of KE can be estimated in Eq. (2):

$$KE = -f_s \ln \left(1 - \frac{1}{\bar{b}} \right) \quad (2)$$

Where

f_s is the sample frequency and the \bar{b} is the average number of sequential pairs of points which can be expressed as follow:

$$\bar{b} = \frac{1}{M} \sum_{i=1}^M b_i \quad (3)$$

Whereas, b_i is the number of sequential pair of points on the attractors which are initially at distance within the cutoff length (L_0) and for the b_i^{th} step the distance between pair of points on the attractors is more than L_0 . These attractors are reconstructed based on the embedding dimension and delay time [44]. In most of the cases embedding dimension is to 50 and delay time is unity [45], and same is followed here. The maximum length or cut-off distance (L_0) was estimated from the time's average absolute deviation (AAD).

$$L_0 = 3 * AAD \quad (4)$$

$$AAD = \frac{1}{N} \sum_{i=1}^N |x_i - \bar{x}| \quad (5)$$

\bar{x} Is defined as follow

$$\bar{x} = \frac{1}{N} \sum_{i=1}^N x_i \quad (6)$$

Whereas x_i is the data points in time series and N is the total number of data points.

4. RESULTS AND DISCUSSION

4.1. STATISTICAL ANALYSIS (STANDARD DEVIATION)

STD widely applied to determine the amplitude of the pressure fluctuation signals, expressed in the form of standard deviation [42], [46]. Successful, time series of photon counts via GRD have been examined by time domain methods like a STD to identify the

flow regimes in multiphase system reactors [36], [37]. STD of photon counts at two different axial positions ($Z/D=6.6$ and $Z/D=12.5$) in the center of column ($r/R=0$) (Figure 1) and different superficial liquid velocities range from 4 to 14 mm/s for various commercial catalyst shapes (spherical, cylindrical, trilobe, quadrilobe) are plotted in Figures 9-12. The point of inflection in standard deviation plot refers to the change in flow regimes, and these points can be represented as flow regime indicator. Figure 13 verifies that the flow regime in TBR can be identified by GRD technique through analyzing the time series of the photon counts at different levels along the bed height successfully. In Figures 9-12 show the STD plot of GRD signals at different catalyst shapes. It appears from Figures 9-12 that the capability of STD analysis method to specify flow regimes via analyzing photon counts in TBRs. Two distinct flow regimes (trickle to pulse) have been identified for each catalyst shape.

Figure 9 exhibit clearly the change in the slope to indicate the change in the flow regime at spherical bed. What is interesting in this data is that the change in photon counts with superficial liquid velocity. It appears from the Figure 9 decrease in STD of photon counts with increase superficial liquid velocity until around superficial liquid velocity (8-10 mm/s) a noticeable increase in STD with increase liquid velocity was noticed. Hence, the slope change of STD of photon counts can be performed to identify flow regime transition. Meanwhile, Figure 10 present obviously the change in the slope for STD between superficial liquid velocity 10 to 12 mm/s through a cylindrical catalyst shape. While, in the Polylobes catalyst shapes (trilobe and quadrilobe) the change in slopes were observed in Figures 11 and 12 which STD of photon counts was specified the transition velocity between 8-10 mm/s for both Polylobes shapes.

The results revealed that the catalyst shape played role to change the flow regime transition due to geometry of catalyst significantly affected on void distribution in the bed that represent an essential factor to shift the flow transition. However, STD method commonly applied to identify flow regime transition. Nonetheless the STD method is not enough to objectively diagnose the flow regime because the sole information of statistical analysis method unable to distinguish clearly the transition point precisely.

4.2. KOLMOGOROV ENTROPY ANALYSIS (KE)

KE represents one of the most useful tools to identify the flow transition in non-linear systems due to developed based on deterministic chaos theory. Remarkably, the KE has been classified to be a robust and powerful instrument to objectively detect conditions that conduct to transition in dynamic regime for different types of reactors [39], [47]. It is important to notice that most reported literature that specified the transition is based on invasive and/or at the wall techniques, or by observation [48], [49].

In addition to, a few studies used a powerful analysis method like a chaotic analysis to identify the flow transition. chaotic analysis has been applied in flow transition identification for various multiphase systems like bubble columns, fluidized beds, and non-conventional TBR (with structure) [37], [39], [50]. The best of author's knowledge, no report has been found so far used KE analysis method to identify flow regimes and transition velocity within different commercial catalyst shapes (Trilobe and quadrilobe) in conventional TBRs.

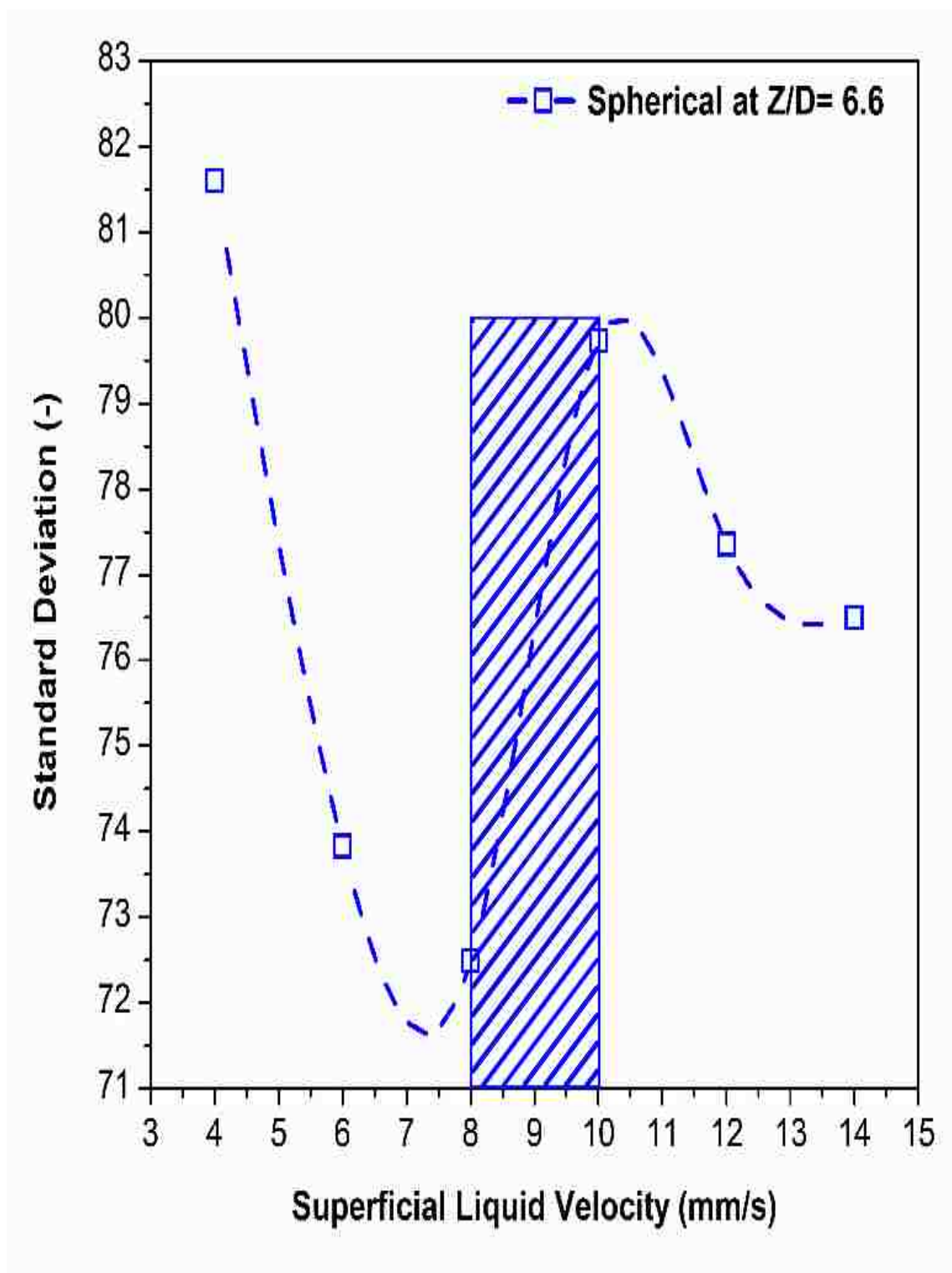


Figure 9. Standard deviation versus superficial liquid velocity at the middle ($Z/D = 6.6$) and center ($r/R = 0$) of reactor within spherical catalyst shape

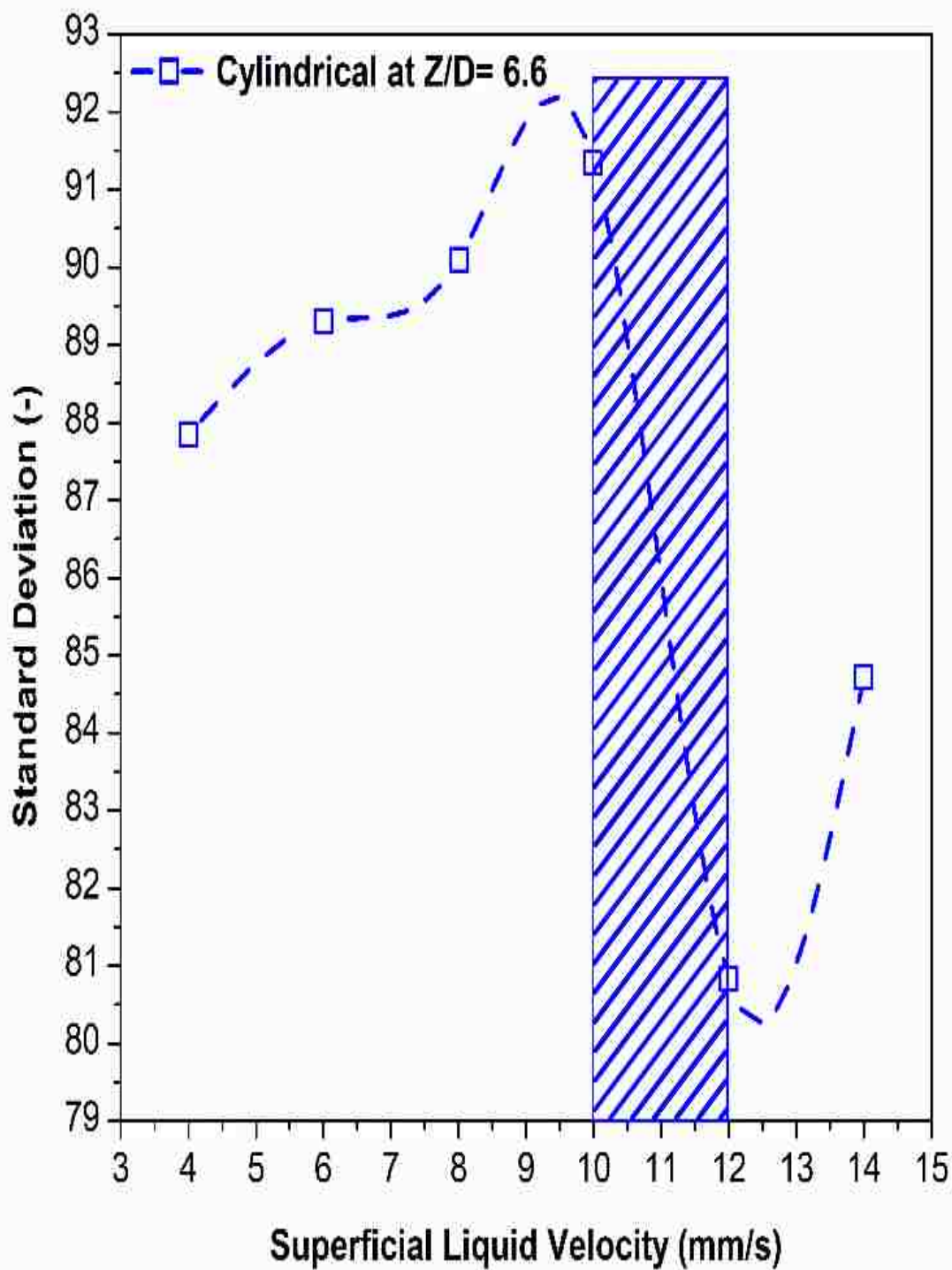


Figure 10. Standard deviation versus superficial liquid velocity at the middle ($Z/D=6.6$) and center ($r/R=0$) of reactor within cylindrical catalyst shape

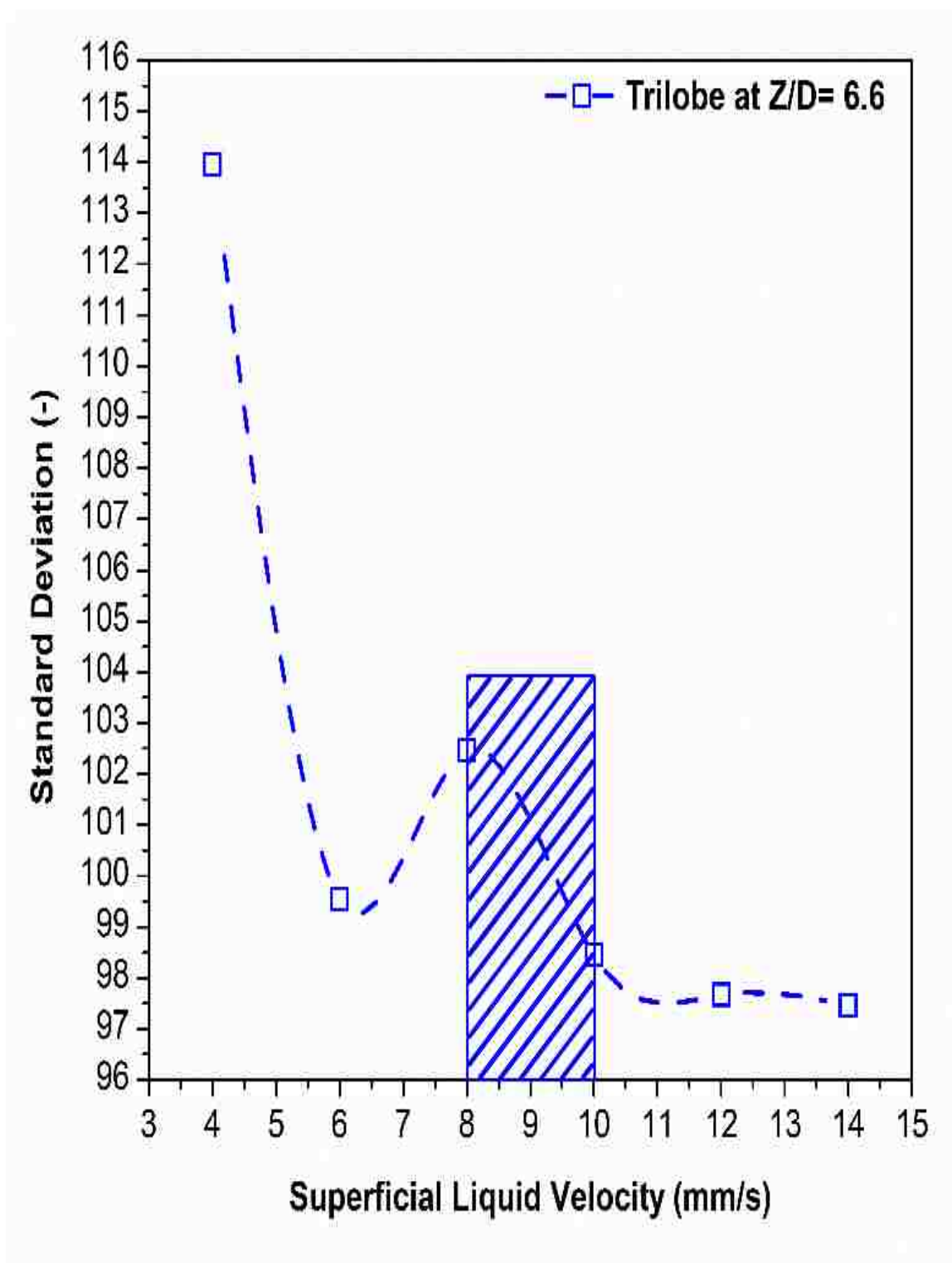


Figure 11. Standard deviation versus superficial liquid velocity at the middle ($Z/D= 6.6$) and center ($r/R=0$) of reactor within trilobe catalyst shape.

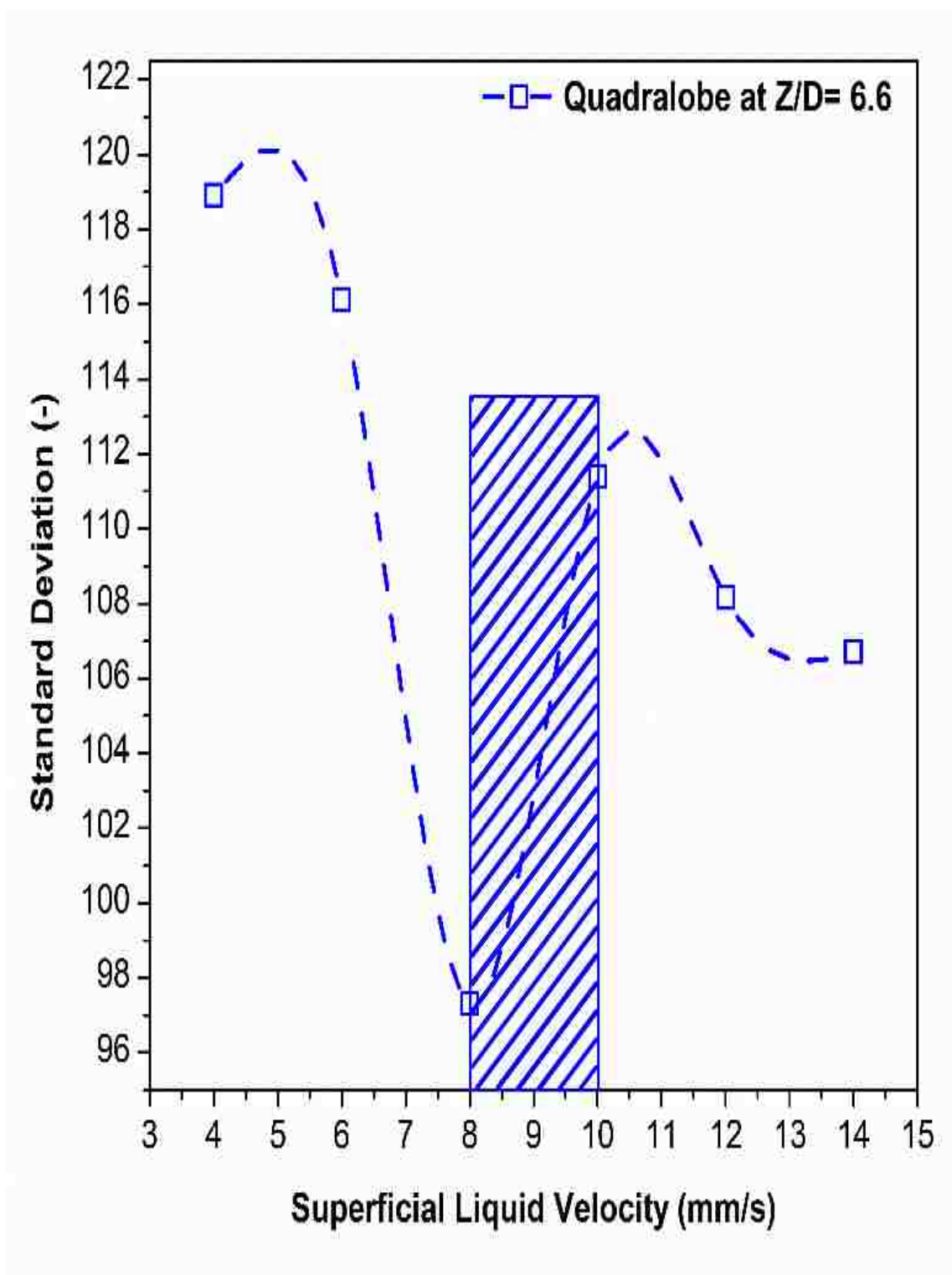


Figure 12. Standard deviation versus superficial liquid velocity at the middle ($Z/D=6.6$) and center ($r/R=0$) of reactor within quadrilobe catalyst shape.

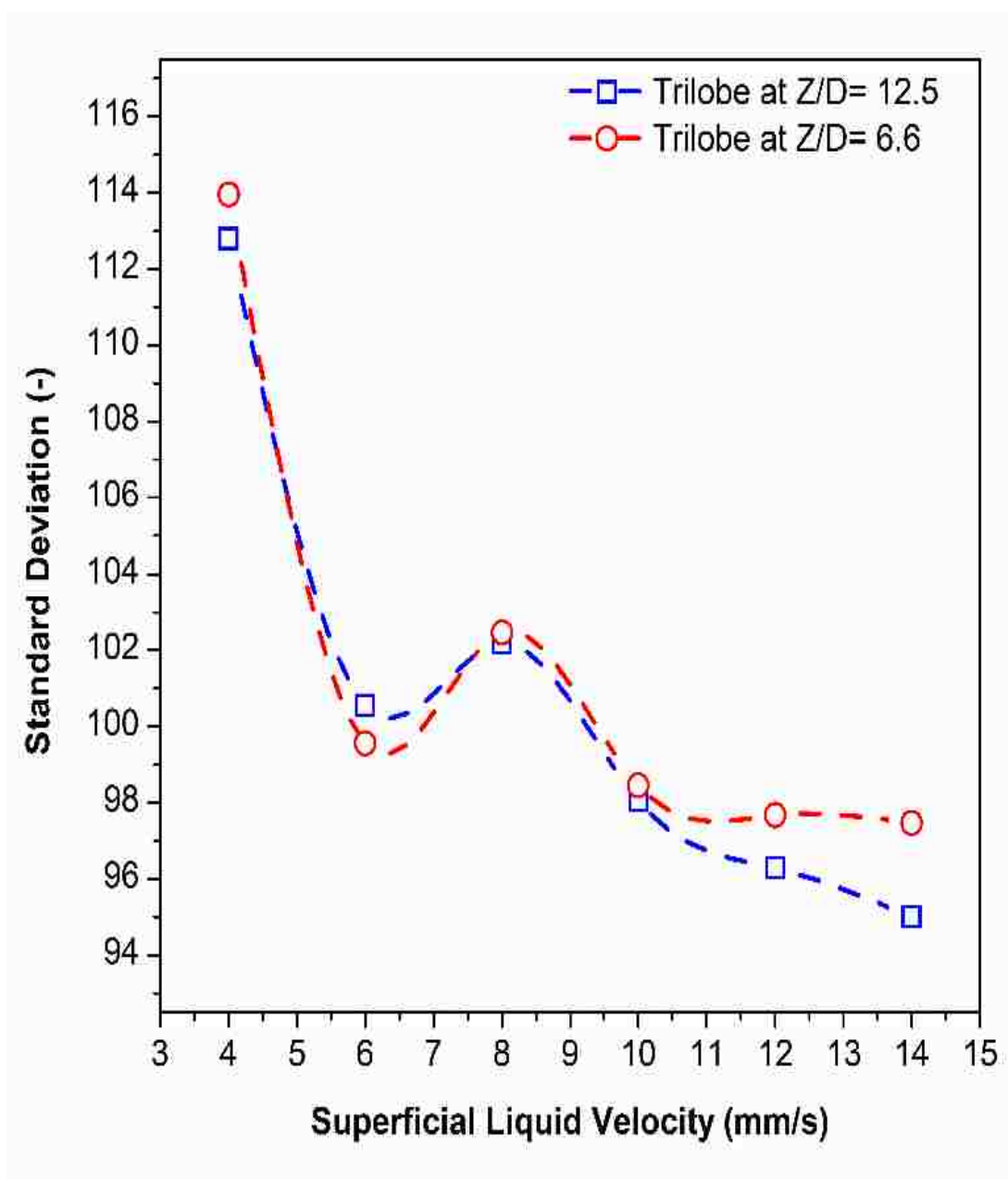


Figure 13. Standard deviation versus superficial liquid velocity within trilobe catalyst at the middle and bottom positions ($Z/D= 6.6$ and $Z/D= 12.5$) and at the center of reactor.

Figures 14-17 show the KE plot of photon counts at the middle and center of reactor within different industrial catalyst shapes. The curve of KE values follow the local maxima

and local minima values. The local maxima values represent the unstable part in a flow regime which refers to the transition velocity. While the local minima represents the stability part in flow regime or where reorganizing in flow regime occurs [36], [41], [51]. Thereby, the sudden fluctuation in the KE values for photon counts with intermediate superficial liquid velocities it was enabled to identify the boundaries of the flow regimes in TBR. Figure 18 confirms the high capability for KE method to identify clearly the flow regimes and their transition velocity by time series of GRD photon counts at different axial levels along the bed height. Apparently, Figures 14-17 reveals the oscillation path for KE values with superficial liquid velocities. KE is a quantitative method that has been postulated to be a powerful instrument to identify the prevailing flow transition. On other hand, STD method identified the flow transition based on the change in the slope that is not sufficient to determine the prevailing flow transition precisely. KE results as it is seen in Figures 14-17 display the capability of KE method to diagnose clearly the transition flow within different catalyst shapes. In order to show the capability for KE analysis method to specify the flow regimes and transition velocity, Figures 14-17 show the effects of the catalyst shape on trickle to pulse flow regime and transition velocity. It is seen in Figure 14 the transition velocity for spherical catalyst shape is 8 mm/s. while, the transition velocity for cylindrical catalyst shape is fallen in 12 mm/s of superficial liquid velocity as indicated in Figure 15. The transition velocities between trickle and pulse regimes for two Polylobes catalyst shapes have been identified by time series analysis of photon counts which transition velocity for trilobe catalyst shape equal to 8 mm/s and for quadrilobe catalyst shape equal to 10 mm/s as shown in Figures 16 and 17. The differences in the transition velocity between the uniform catalyst shape (spherical) and non-uniform catalyst

shapes is related to non-uniform void distribution, the contact lines between adjacent particles for non-uniform catalyst shapes, geometrical shape, and configuration of particles that lead to change in transition velocity within different catalyst shapes. Obviously, trilobe transition velocity is similar to spherical catalyst shape due to the geometrical merits with three regular lobes that attributed beneficially with more uniform void distribution and contact lines as displayed in Figures 14 and 16. Moreover, the transition velocity for quadrilobe catalyst particles with four irregular lobes is closer to the transition velocity for cylindrical catalyst shape as it is shown in Figure 17.

4.3. VARIATION FROM POISSON DISTRIBUTION

Photon counts of gamma-ray intrinsically present Poisson distribution (mean=variance) in case no gas flow such as empty column (only air) and column filled with water (only water). The variation from Poisson distribution used successfully to identify the flow regimes and transition velocities in bubble column reactor (gas-liquid system) [37]. In the current study, the photon counts of column empty (only air), column filled with water (only water), and melted catalyst (only solid) indicated to be Poisson distribution. Thus, the deviation from Poisson distribution is capable to identify the trickle to pulse regimes and their transition velocity in packed bed reactors (gas-liquid-solid systems). It was detected that the mean and variance values deviated from Poisson distribution with two phase flow within flow rate conditions in TBR. As well as, the deviation value between the mean and variance was escalated with increase the superficial gas and liquid velocities

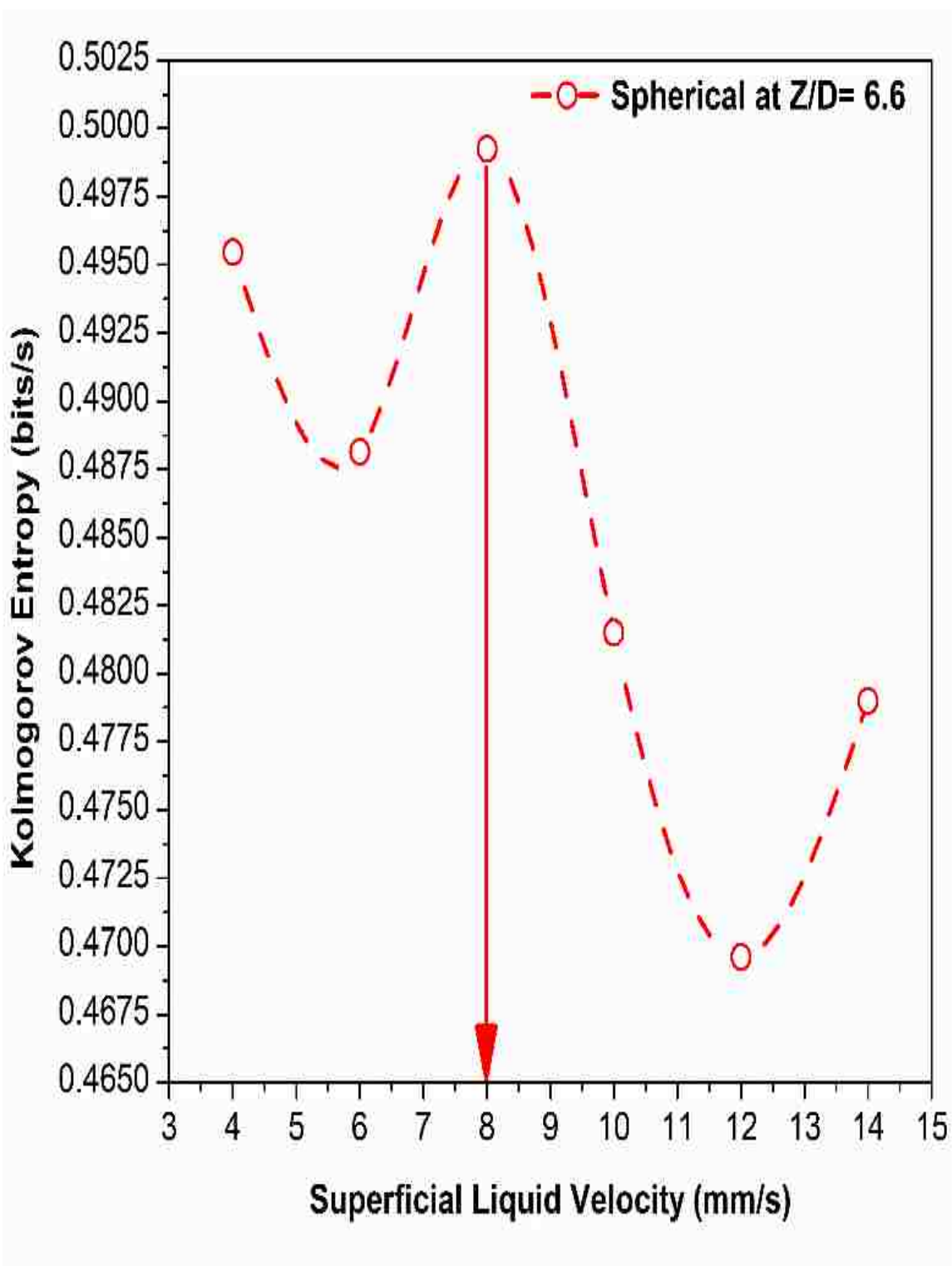


Figure 14. Kolmogorov Entropy (KE) of photon counts vs. superficial liquid velocity at the middle ($Z/D= 6.6$) and center of pilot plant reactor within spherical catalyst shape

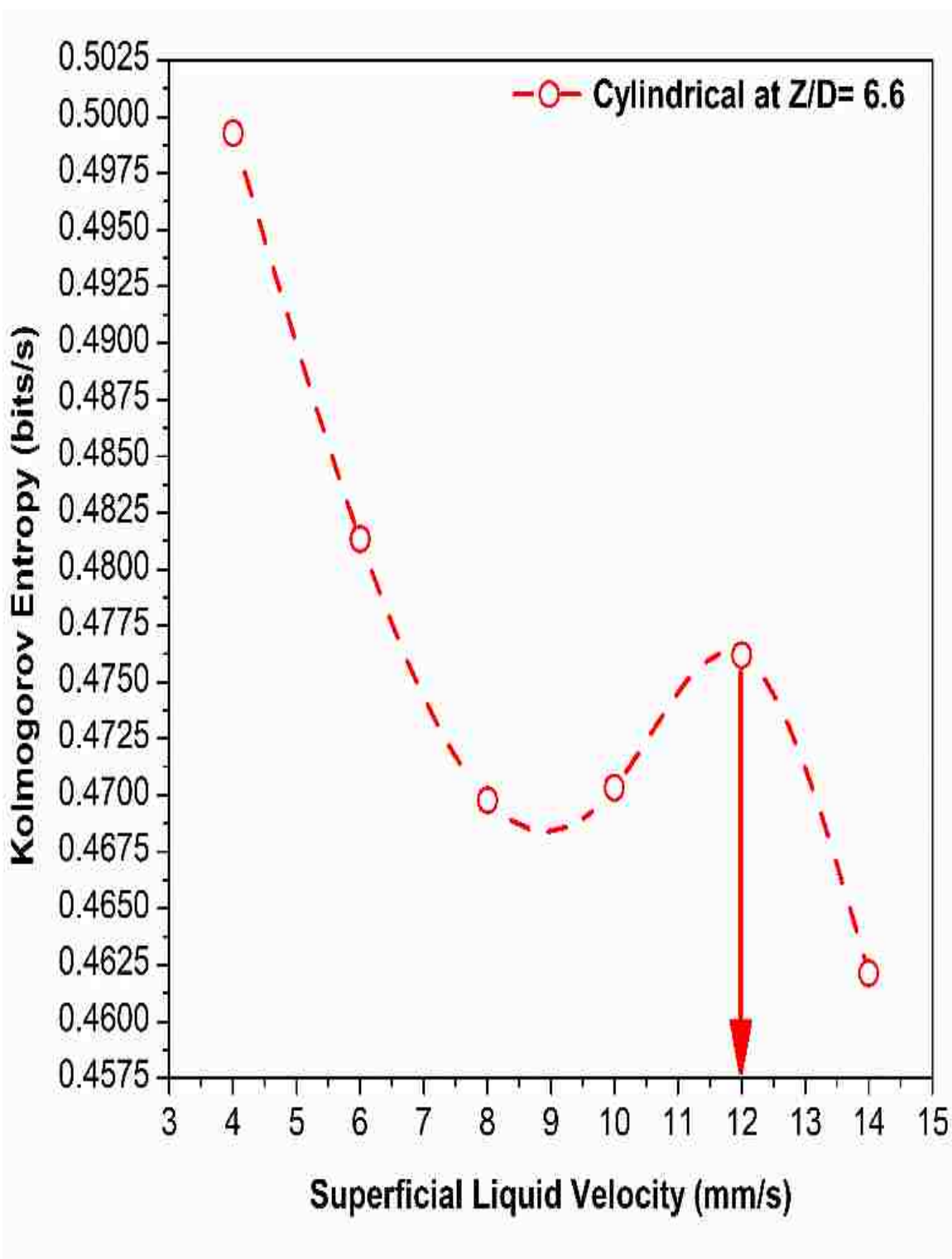


Figure 15. Kolmogorov Entropy (KE) of photon counts vs. superficial liquid velocity at the middle ($Z/D = 6.6$) and center of pilot plant reactor within cylindrical catalyst shape

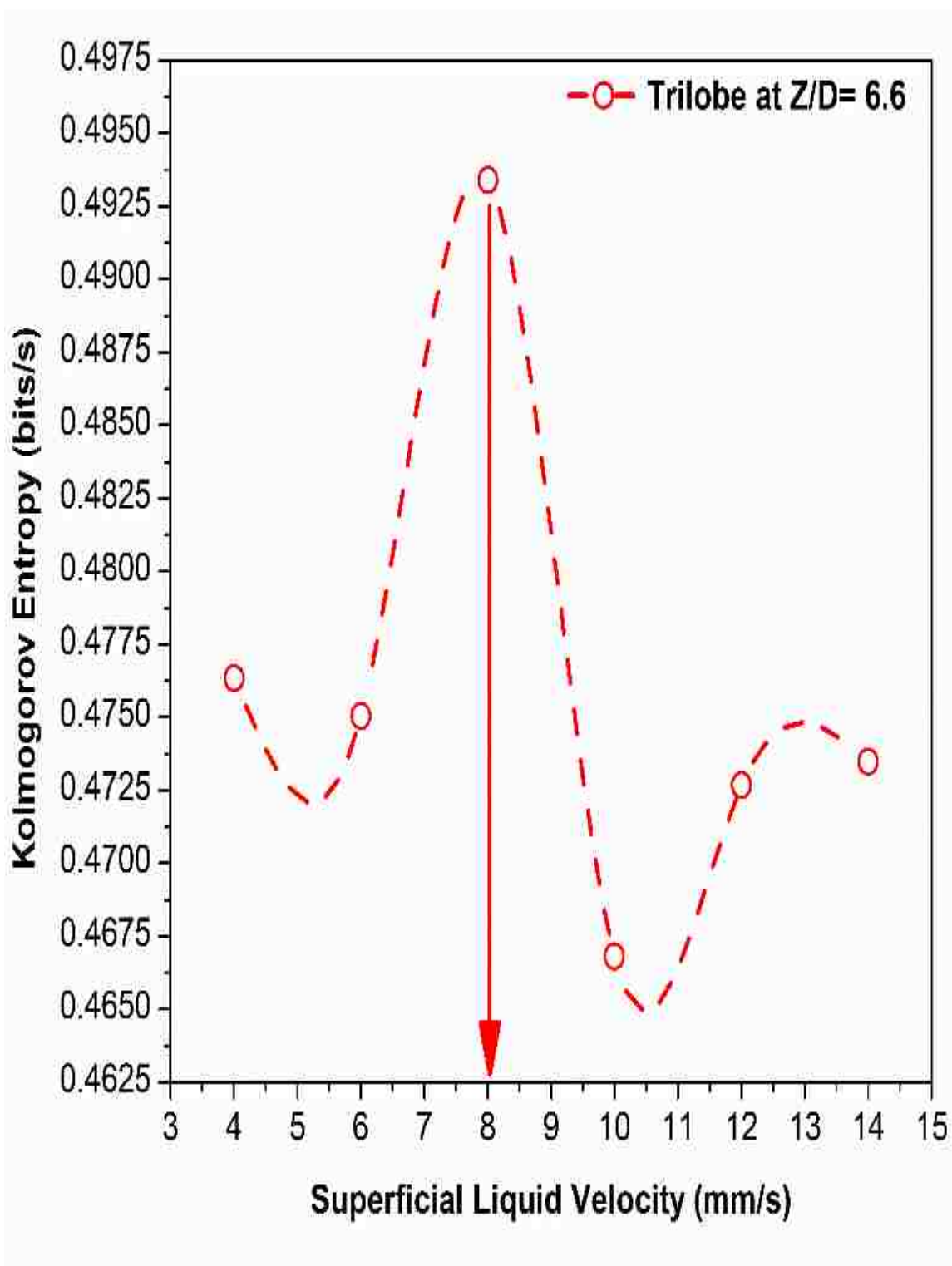


Figure 16. Kolmogorov Entropy (KE) of photon counts vs. superficial liquid velocity at the middle ($Z/D= 6.6$) and center of pilot plant reactor within trilobe catalyst shape

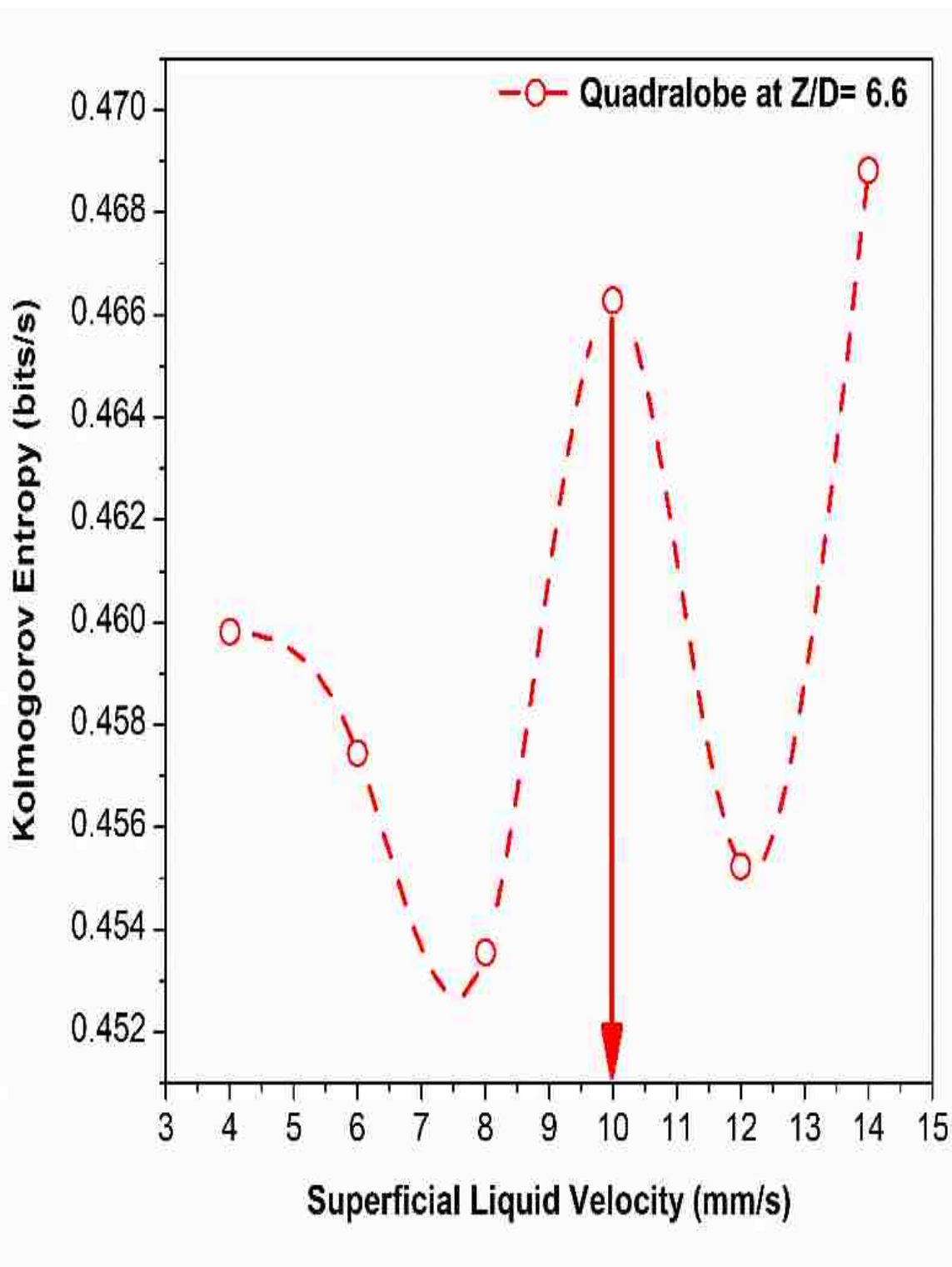


Figure 17. Kolmogorov Entropy (KE) of photon counts vs. superficial liquid velocity at the middle ($Z/D= 6.6$) and center of pilot plant reactor within quadrilobe catalyst shape

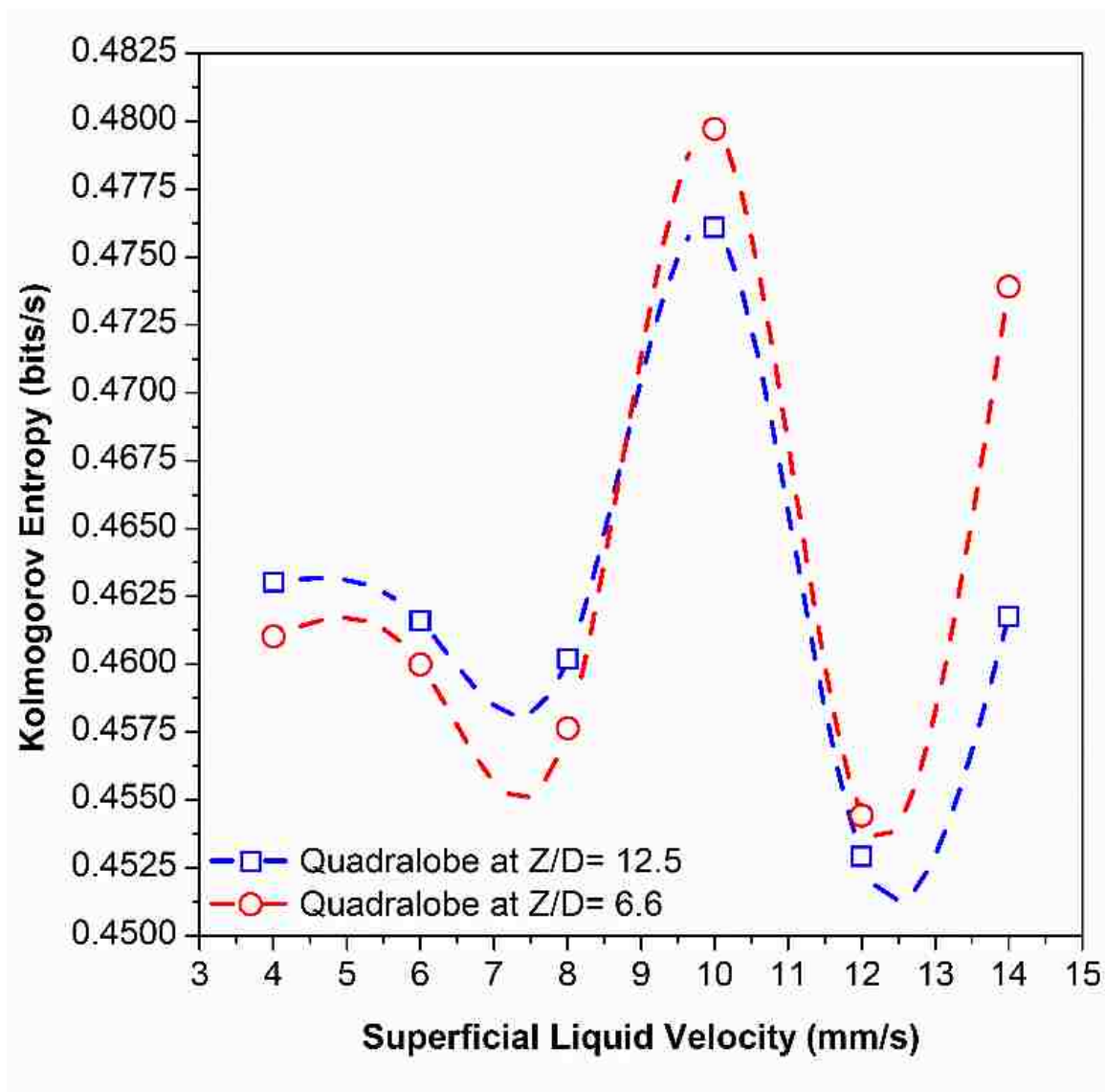


Figure 18. Kolmogorov Entropy of photon counts vs. superficial liquid velocity within quadralobe catalyst shape at center and different axial locations of pilot plant reactor.

Accordingly, a new coefficient flow transition identifier named variation coefficient from Poisson distribution (V_c) proposed to calculate the deviation of photon

counts from a Poisson distribution to specify the flow transition in TBR as defined in Eq. (7) below:

$$V_c = \frac{(\text{Variance})_i}{(\text{Variance})_p} \quad (7)$$

where:

$(\text{Variance})_i$: The variance of photon counts at specific superficial gas and liquid velocity

$(\text{Variance})_p$: The variance of photon counts at Poisson distribution conditions (empty, filled with water, melted catalyst)

Basically, the variation from Poisson distribution in two phase flow because gas and liquid flow rate, thus, the impacts of superficial gas and liquid velocities on photon counts deviation from Poisson distribution were studied to identify the flow regimes and their transition velocity in TBR. Gas variation coefficient $(V_c)_g$ from Poisson distribution was introduced as shown in Eq. (8).

$$(V_c)_g = \frac{(\text{Variance})_i}{(\text{Variance})_{pg}} \quad (8)$$

where

$(\text{Variance})_{pg}$: The variance of Poisson distribution at empty column.

In addition to, the liquid variation coefficient $(V_c)_l$ from Poisson distribution was detected as it is seen in Eq. (9).

$$(V_c)_l = \frac{(\text{Variance})_i}{(\text{Variance})_{Pl}} \quad (9)$$

where $(\text{Variance})_{Pl}$: the variance of Poisson distribution at column filled with water.

If it had been a Poisson distribution, i.e., the mean. This reduces Eq. (7) to Eq. (10)

$$V_c = \frac{(\text{Variance})_i}{(\text{Mean})_i} \quad (10)$$

$(\text{Mean})_i$: The mean of photon counts at specific superficial gas and liquid velocity

The value of V_c in Eq. (10) for empty column, column filled with water, and melted catalyst are equal to unity. While, the value of V_c changed from unity in case the gas and liquid flow due to the deviation from Poisson distribution as we can see in Figures 19-22.

It was detected that the transition velocity by variation coefficient from Poisson distribution (V_c) identical to STD and KE methods at different catalyst shapes as shown in Figures 19-22. Although the variation coefficient from Poisson distribution (V_c) has been demonstrated based on physics of gamma-ray, it is valuable for flow regime identification by purely empirical. The introduced variation coefficient from Poisson distribution (V_c) method as an identification method to be a powerful flow regime specifier in TBRs.

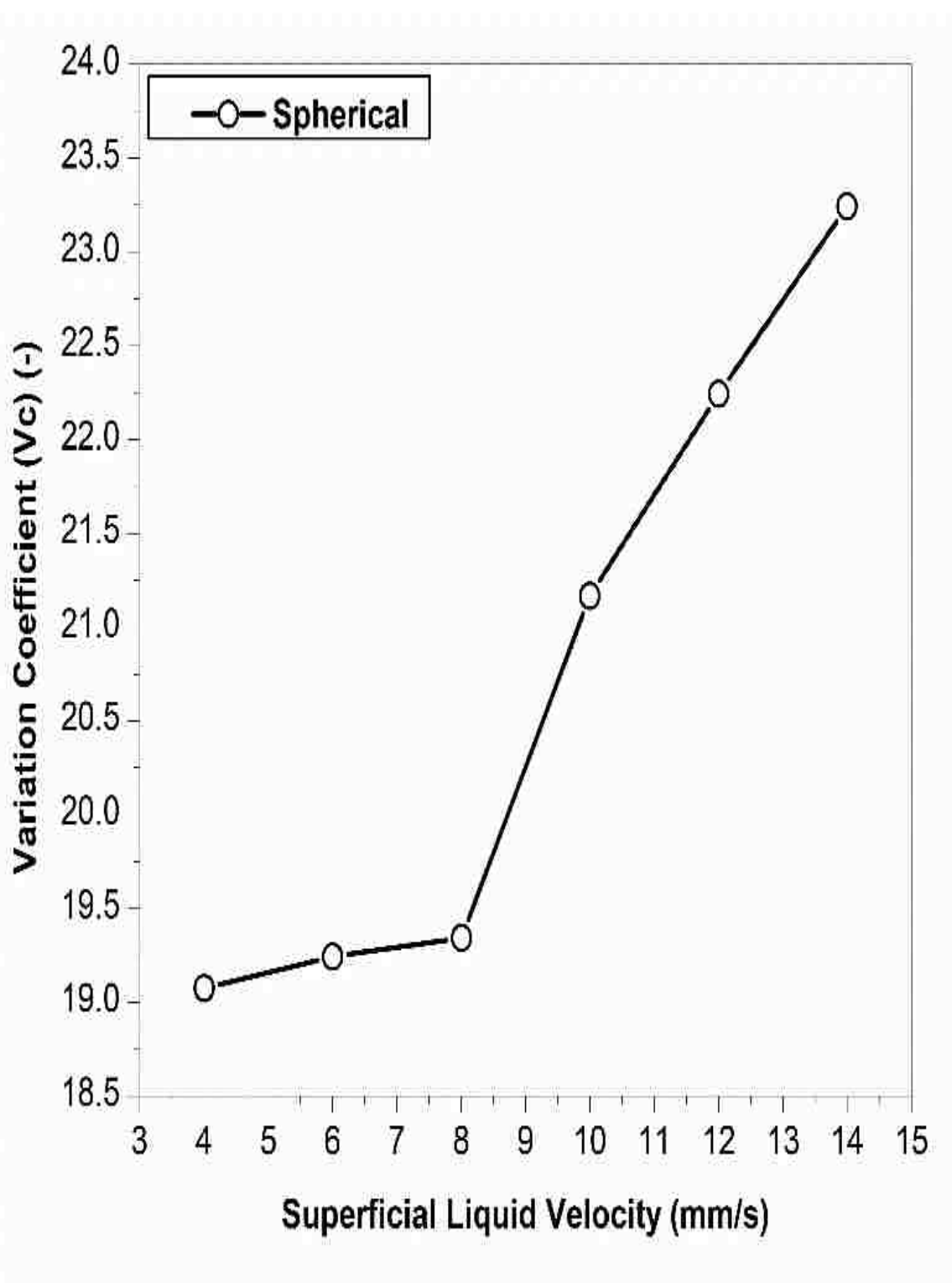


Figure 19. Variation coefficient from Poisson distribution vs. superficial liquid velocity at the middle ($Z/D= 6.6$) and center of pilot plant reactor within spherical catalyst shape

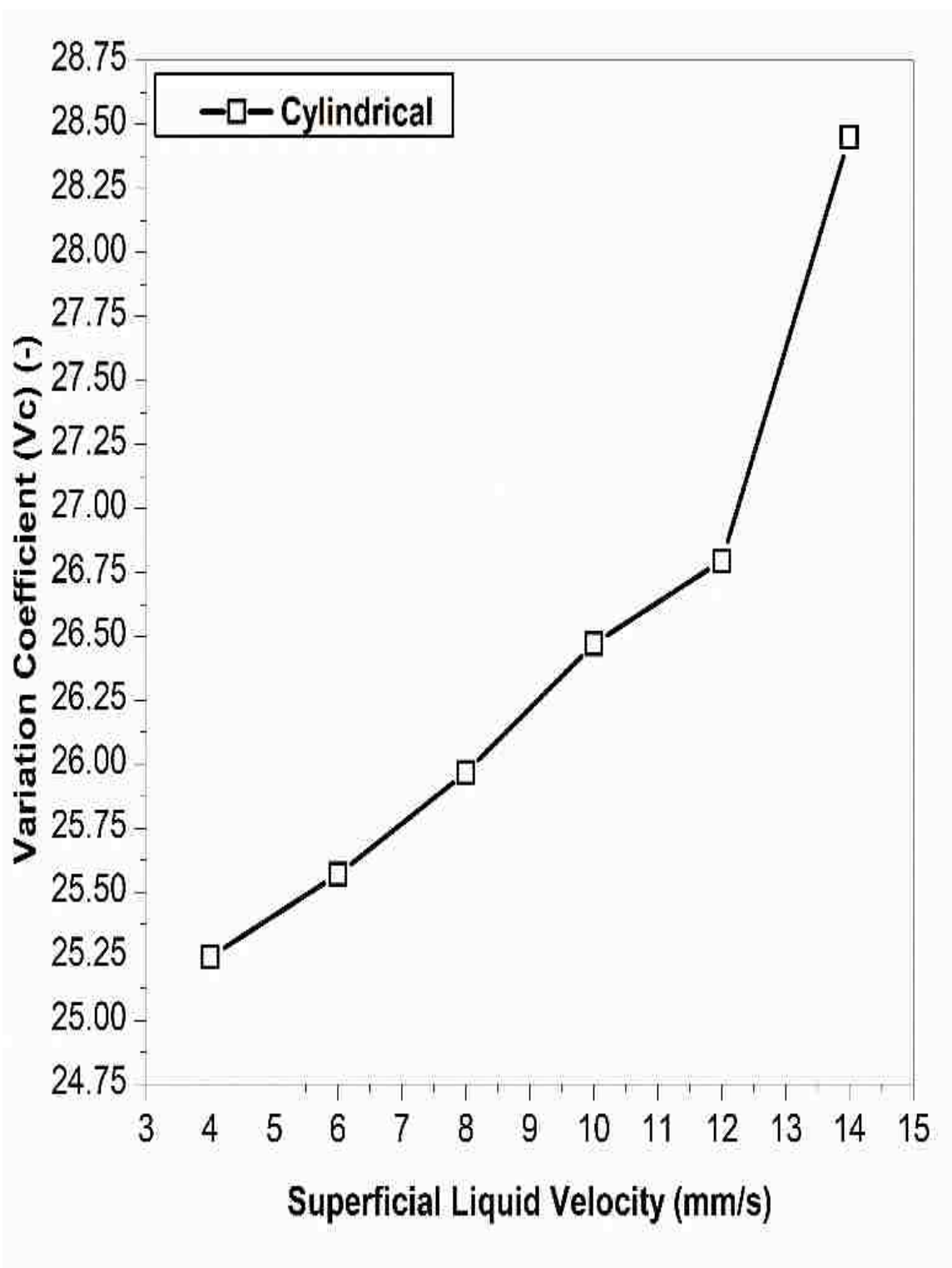


Figure 20. Variation coefficient from Poisson distribution vs. superficial liquid velocity at the middle ($Z/D= 6.6$) and center of pilot plant reactor within cylindrical catalyst shape

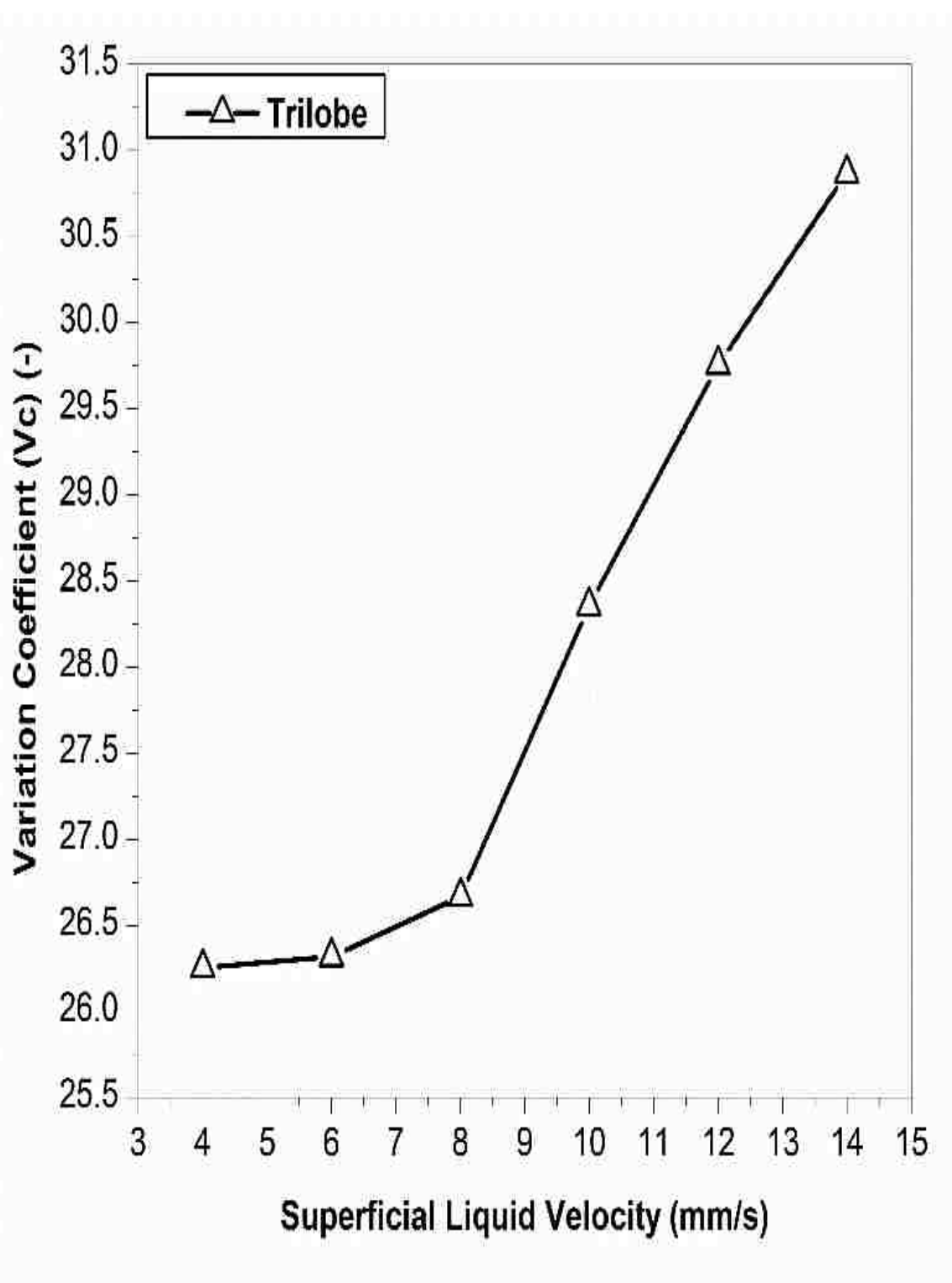


Figure 21. Variation coefficient from Poisson distribution vs. superficial liquid velocity at the middle ($Z/D= 6.6$) and center of pilot plant reactor within trilobe catalyst shape

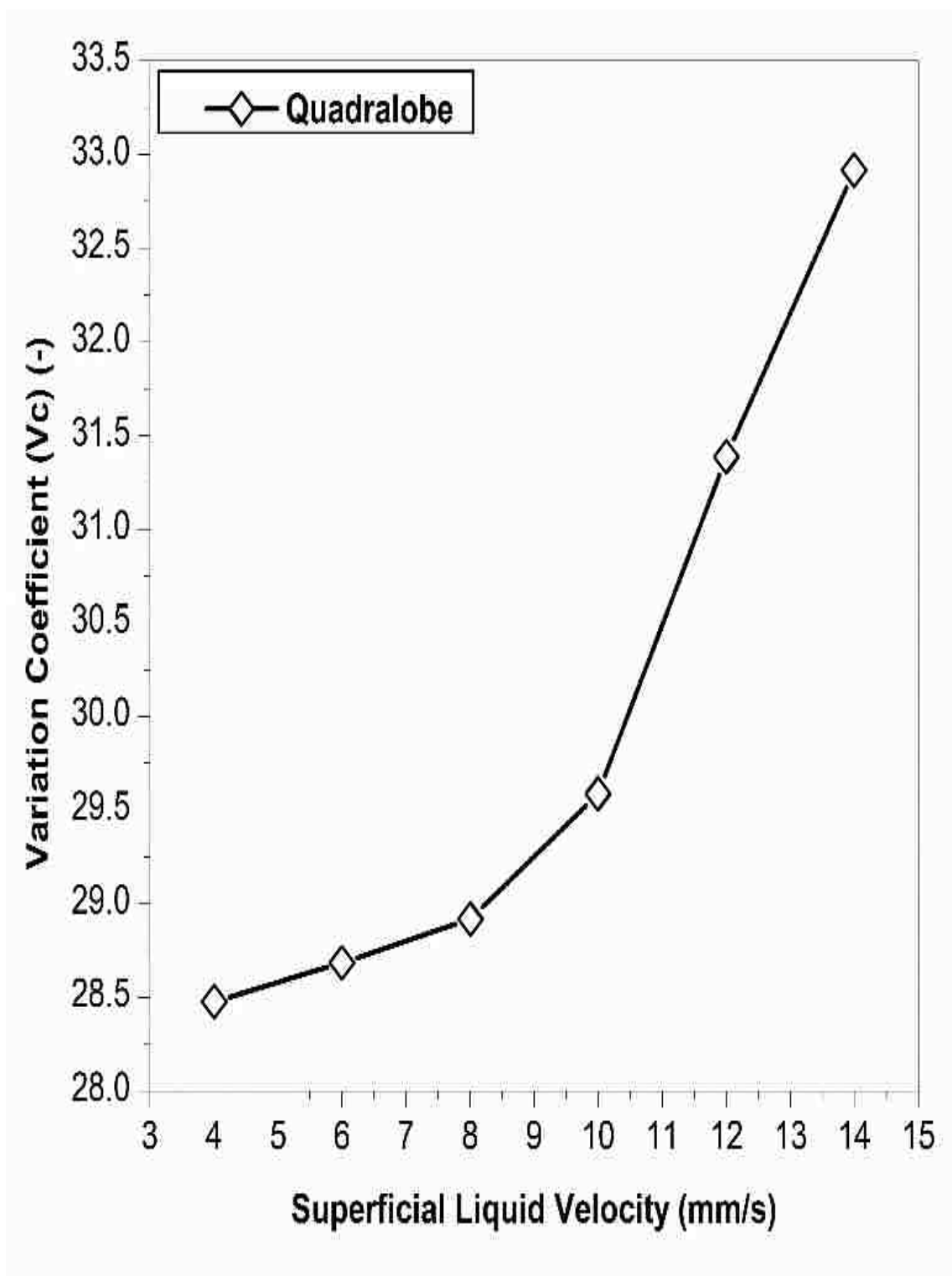


Figure 22. Variation coefficient from Poisson distribution vs. superficial liquid velocity at the middle ($Z/D= 6.6$) and center of pilot plant reactor within quadrilobe catalyst shape

5. REMARKS

Trickle to pulse flow regimes and their transition velocity have been determined within different commercial catalyst shapes using non-invasive industrial GRD technique in TBR. Plexiglas transparent column with 14 cm ID and 185 cm height bed. The range of gas and liquid velocities were used in different axial positions along the height bed and in the center ($r/R= 0$) of the reactor. The industrial non-invasive GRD technique was developed and constructed in multiphase reactor engineering and applications bench (mReal) in Missouri University of Science and Technology (S&T). Also, the GRD signals have been examined and validated in our bench (mReal through 3mm spherical glass beads catalyst particles to identify the flow regime in TBR (Fitri's work). In the present work, GRD signals have been used for first time to identify the flow regimes and their transition velocities within four different commercial catalyst shapes which the study has gone some way towards enhancing our understanding of effects of characteristics geometrical of catalyst particles on the gas-liquid interaction that important in scale up and reactor design by implementing a robust tool (KE) and new simple experimental analysis methods for TBRs and multiphase systems. The following points have found from the current investigation:

- A significant effect of the catalyst shape on the flow regimes and their transition velocity was indicated by using different catalyst shape within wide range of superficial gas and liquid velocities in TBRs. The void fraction distribution represents one of the important reasons that caused to change the transition velocity in the beds by changing the tortuosity and gas and liquid distribution in the void space as well.

- The results illustrated that the flow regime can be specified by GRD technique through analyzing the time series of photon count which can be useful for both the bench investigation and industrial development.
- KE one of a powerful analysis method that indicated clearly the flow transition between trickle to pulse flow regimes. While the flow transition identification based on the change in the slope by statistical analysis method (STD) is not enough to supply a clear transition velocity between low interaction and high interaction flow regimes.
- Further research is recommended to better understand and provide insights for future research of effects of the physical properties for gas and liquid within different catalyst shapes on the flow regimes in TBRs.

ACKNOWLEDGMENT

The author thankfully acknowledge the financial support in the form of scholarship provided by Ministry of Higher Education and Scientific Research-Iraq, and the funds provided by Missouri S&T and Professor Dr. Al-Dahhan to develop the experimental set-up and to perform the present study.

REFERENCES

- [1] V. V Ranade, R. Chaudhari, and P. R. Gunjal, *Trickle Bed Reactors: Reactor Engineering and Applications*. Elsevier Science, 2011.
- [2] S. A. Al-Naimi, F. T. J. Al-Sudani, and E. K. Halabia, "Hydrodynamics and flow regime transition study of trickle bed reactor at elevated temperature and pressure," *Chem. Eng. Res. Des.*, vol. 89, no. 7, pp. 930–939, 2011.

- [3] M. H. Al-Dahhan, F. Larachi, M. P. Dudukovic, and A. Laurent, "High-Pressure Trickle-Bed Reactors: A Review," *Ind. Eng. Chem. Res.*, vol. 36, no. 8, pp. 3292–3314, 1997.
- [4] M. and M. P. D. H. Al-Dahhan, "Pressure Drop and Liquid Holdup in High Pressure Trickle-Bed Reactors," *Chem. Eng. Sci.*, vol. 49, no. 24B, pp. 5681–5698, 1994.
- [5] R. A. Holub, M. P. Dudukovic, and P. A. Ramachandran, "A phenomenological model for pressure drop, liquid holdup, and flow regime transition in gas-liquid trickle flow," *Chem. Eng. Sci.*, vol. 47, no. 9–11, pp. 2343–2348, 1992.
- [6] K. D. P. Nigam and F. Larachi, "Process intensification in trickle-bed reactors," *Chem. Eng. Sci.*, vol. 60, no. 22, pp. 5880–5894, 2005.
- [7] S. A. Gheni and M. H. Al-Dahhan, "Assessing the Feasibility of Optical Probe in Phase Holdup Measurements and Flow Regime Identification," *Int. J. Chem. React. Eng.*, vol. 13, no. 3, pp. 369–379, 2015.
- [8] A. Atta, S. Roy, and K. D. P. Nigam, "Investigation of liquid maldistribution in trickle-bed reactors using porous media concept in CFD," *Chem. Eng. Sci.*, vol. 62, no. 24, pp. 7033–7044, 2007.
- [9] N. M. and A. S. M.A. Latifi, S. Rode, "The use of Microelectrodes for the Determination of Flow Regimes in a Trickle-Bed Reactor," *Chem. Eng. science*, vol. 47, no. 8, pp. 1955–1961, 1992.
- [10] P. S. T. SAI and Y. B. G. VARMA, "Flow pattern of the phases and liquid saturation in gas-liquid cocurrent downflow through packed beds," *Can. J. Chem. Eng.*, vol. 66, no. 3, pp. 353–360, 1988.
- [11] G. F. Attou, A., "A Two-Fluid Model for Flow Regime Transition in Gas-Liquid Trickle-Bed Reactors," *Chem. Eng. Sci.*, vol. 54, pp. 5031–5037, 1999.
- [12] C. Boyer and B. Fanget, "Measurement of liquid flow distribution in trickle bed reactor of large diameter with a new gamma-ray tomographic system," *Chem. Eng. Sci.*, vol. 57, pp. 1079–1089, 2002.
- [13] H. Nadeem, I. Ben Salem, and M. Sassi, "Experimental Visualization and Investigation of Multiphase Flow Regime Transitions in Two-Dimensional Trickle Bed Reactors," *Chem. Eng. Commun.*, vol. 204, no. 3, pp. 388–397, 2017.
- [14] P. R. Gunjal, M. N. Kashid, V. V. Ranade, and R. V. Chaudhuri, "Hydrodynamics of trickle bed reactors: experiments and CFD modeling," *Ind. Eng. Chem. Res.*, vol. 44, no. d, pp. 6278–6294, 2005.

- [15] M. E. Trivizadakis, D. Giakoumakis, and A. J. Karabelas, "A study of particle shape and size effects on hydrodynamic parameters of trickle beds," *Chem. Eng. Sci.*, vol. 61, no. 17, pp. 5534–5543, 2006.
- [16] G. S. Honda, J. H. Pazmiño, E. Lehmann, D. A. Hickman, and A. Varma, "The effects of particle properties, void fraction, and surface tension on the trickle-bubbly flow regime transition in trickle bed reactors," *Chem. Eng. J.*, vol. 285, pp. 402–408, 2016.
- [17] S. Afandizadeh and E. A. Foumeny, "Design of packed bed reactors: Guides to catalyst shape, size, and loading selection," *Appl. Therm. Eng.*, vol. 21, no. 6, pp. 669–682, 2001.
- [18] D. Nemeč and J. Levec, "Flow through packed bed reactors: 2. Two-phase concurrent downflow," *Chem. Eng. Sci.*, vol. 60, no. 24, pp. 6958–6970, 2005.
- [19] J. A. Helwick, P. O. Dillon, and M. J. McCready, "Time varying behavior of cocurrent gas-liquid flows in packed beds," *Chem. Eng. Sci.*, vol. 47, no. 13–14, pp. 3249–3256, 1992.
- [20] M. Schubert, H. Kryk, and U. Hampel, "Slow-mode gas/liquid-induced periodic hydrodynamics in trickling packed beds derived from direct measurement of cross-sectional distributed local capacitances," *Chem. Eng. Process. Process Intensif.*, vol. 49, no. 10, pp. 1107–1121, 2010.
- [21] M. C. Munteanu and F. Larachi, "Flow regimes in trickle beds using magnetic emulation of micro/macrogravity," *Chem. Eng. Sci.*, vol. 64, no. 2, pp. 391–402, 2009.
- [22] A. Muzen and M. C. Cassanello, "Flow regime transition in a trickle bed with structured packing examined with conductimetric probes," *Chem. Eng. Sci.*, vol. 62, no. 5, pp. 1494–1503, 2007.
- [23] E. A. Whitmarsh, D. R. Escudero, and T. J. Heindel, "Probe effects on the local gas holdup conditions in a fluidized bed," *Powder Technol.*, vol. 294, pp. 191–201, 2016.
- [24] T. R. Melli, J. M. de Santos, W. B. Kolb, and L. E. Scriven, "Cocurrent Downflow in Networks of Passages. Microscale Roots of Macroscale Flow Regimes," *Ind. Eng. Chem. Res.*, vol. 29, no. 12, pp. 2367–2379, 1990.
- [25] F. Takahashi, M. Toda, T. Hirose, and Y. Hashiguchi, "Flow pattern and pulsation properties of cocurrent gas-liquid downflow in packed beds*," *J. Chem. Eng. JAPAN*, vol. 6, no. 4, pp. 315–319, 1973.

- [26] G. I. Horowitz, A. L. Cukierman, and M. C. Cassanello, "Flow regime transition in trickle beds packed with particles of different wetting characteristics - Check-up on new tools," *Chem. Eng. Sci.*, vol. 52, no. 21–22, pp. 3747–3755, 1997.
- [27] J. R. Van Ommen, S. Sasic, J. Van der Schaaf, S. Gheorghiu, F. Johnsson, and M. O. Coppens, "Time-series analysis of pressure fluctuations in gas-solid fluidized beds - A review," *Int. J. Multiph. Flow*, vol. 37, no. 5, pp. 403–428, 2011.
- [28] J. Battista and A. Muzen, "Flow Regime Transitions in Trickle-bed Reactors with Structured Packings," *Can. J. ...*, vol. 81, no. August, pp. 802–807, 2003.
- [29] J. C. Schouten, F. Takens, and C. M. van den Bleek, "Estimation of the dimension of a noisy attractor," *Phys. Rev. E*, vol. 50, no. 3, pp. 1851–1861, Sep. 1994.
- [30] S. Nedeltchev, S. Aradhya, F. Zaid, and M. Al-Dahhan, "Flow regime identification in three multiphase reactors based on Kolmogorov entropies derived from gauge pressure fluctuations," *J. Chem. Eng. Japan*, vol. 45, no. 9, pp. 757–764, 2012.
- [31] S. Nedeltchev, "New methods for flow regime identification in bubble columns and fluidized beds," *Chem. Eng. Sci.*, vol. 137, pp. 436–446, 2015.
- [32] A. Toukan, V. Alexander, H. AlBazzaz, and M. H. Al-Dahhan, "Identification of flow regime in a cocurrent gas – Liquid upflow moving packed bed reactor using gamma ray densitometry," *Chem. Eng. Sci.*, vol. 168, pp. 380–390, 2017.
- [33] A. Shaikh and M. Al-Dahhan, "A new method for online flow regime monitoring in bubble column reactors via nuclear gauge densitometry," *Chem. Eng. Sci.*, vol. 89, pp. 120–132, 2013.
- [34] S. Nedeltchev, U. Hampel, and M. Schubert, "Experimental study on the radial distribution of the main transition velocities in bubble columns," no. October, pp. 127–138, 2015.
- [35] H. Taofeeq and M. Al-Dahhan, "Flow regimes in gas–solid fluidized bed with vertical internals," *Chem. Eng. Res. Des.*, vol. 138, pp. 87–104, 2018.
- [36] S. Nedeltchev, A. Shaikh, and M. Al-Dahhan, "Flow Regime Identification in a Bubble Column via Nuclear Gauge Densitometry and Chaos Analysis," *Chem. Eng. Technol.*, vol. 34, no. 2, pp. 225–233, 2011.
- [37] C. M. van den Bleek and J. C. Schouten, "Deterministic chaos: a new tool in fluidized bed design and operation," *Chem. Eng. J.*, vol. 53, pp. 75–87, 1993.
- [38] M. I. Urseanu, J. G. Boelhouwer, H. J. M. Bosman, J. C. Schroijen, and G. Kwant, "Estimation of trickle-to-pulse flow regime transition and pressure drop in high-pressure trickle bed reactors with organic liquids," *Chem. Eng. J.*, vol. 111, no. 1, pp. 5–11, 2005.

- [39] W. J. A. Wammes, S. J. Mechielsen, and K. R. Westerterp, "The transition between trickle flow and pulse flow in a cocurrent gas-liquid trickle-bed reactor at elevated pressures," *Chem. Eng. Sci.*, vol. 45, no. 10, pp. 3149–3158, 1990.
- [40] S. Nedeltchev, U. Jordan, O. Lorenz, and A. Schumpe, "Identification of various transition velocities in a bubble column based on Kolmogorov entropy," *Chem. Eng. Technol.*, vol. 30, no. 4, pp. 534–539, 2007.

II. EFFECT OF CATALYST SHAPE ON PRESSURE DROP AND OVERALL LIQUID HOLDUP IN A PILOT PLANT TRICKLE BED REACTOR

Mohammed Al-Ani, Muthanna Al-Dahhan*

Multiphase Reactors Engineering and Applications Bench (mReal), *Department of Chemical and Biochemical Engineering, Missouri University of Science and Technology, Rolla, MO 65409-1230. USA*

ABSTRACT

An atmospheric experimental study was carried out to measure hydrodynamics (pressure drop and liquid holdup) in TBR. The current work aimed to investigate the influence of catalyst shape, gas flow rate, and liquid flow rate on hydrodynamics through different industrial catalyst beds that comprised spherical, cylindrical, trilobe, and quadrilobe. Air was used as a gas phase with an extensive range from 0.03 to 0.27 m/s, while water was used with a range from 0.004 to 0.016 m/s, within 0.14 m inside diameter of a cylindrical column and 2 m bed length through various packing beds. The measured data were compared with two model approaches (phenomenological and empirical approaches) to investigate the effect of catalyst shape, gas flow rate, and liquid flow rate on the pressure drop and liquid holdup. The phenomenological model developed based on a physical picture with no two-phase fitted parameters. A single phase Ergun coefficients were implemented to represent the bed characteristics in the bed. Modified Ergun coefficients were determined for each bed and compared with universal Ergun coefficients ($E^*_1=150$ and $E^*_2=1.75$) and non-spherical universal coefficients ($E^*_1=180$ and $E^*_2=1.8$). The comparison for total data regardless the bed indicated a maximum deviation of $\pm 56\%$ with Ergun and non-spherical coefficients, while decreased to a negligible value of 7% with modified coefficients. The results revealed a significant impact for catalyst shape, gas

flow rate, and liquid flow rate on the hydrodynamics. Furthermore, the comparison between the data and models showed the phenomenological model exhibited a better agreement than the empirical model with a mean relative error for the pressure drop of 31.81% and the liquid holdup of 10.36%.

1. INTRODUCTION

A trickle bed reactors (TBRs) are packed bed reactors with static catalyst particles, in which gas and liquid reactants flow concurrently downward. TBRs are extensively used in petroleum, petrochemical, and chemical industries. The most common applications for TBR in the industry produce low sulfur fuel oils and middle-distillate fuels [1]–[3]. Due to a crucial role of TBR in various industrial fields, environmental, economic, and energetic constraints have been generated that required for environmental remediation, energy preservation and cost reduction. Reducing the amount of reactants waste in which gas, liquid, and solid and decreasing the amount of energy provided to produce products. Therefore, the research on TBRs has been pushed up to evaluate and develop the reactor performance and to optimize process conditions to achieve better performance [4]–[6].

The hydrodynamics have been played a central role in reactor performance, design, scale-up, and scale down. Pressure drop, liquid holdup, and flow regime are corresponding key hydrodynamic parameters for operation in the reactors. The hydrodynamics affected by essential factors such as bed characteristics (shape, size, and loading method), superficial gas and liquid velocities, and fluid properties. Although, a great deal of research has concentrated on hydrodynamics [7]–[10].

Bed characteristics (shape, size, and loading method) are actively impacted hydrodynamics thus the reactor performance by changing the void space and distribution in the bed that considered as a crucial factor due to it is involved in a relationship with process need and characteristics (Hydrodynamics and kinetics reaction). The primary aim of industrial and academic research was to develop a catalyst particle design. One of a quite important factor to optimize catalyst particle design is a geometric design of particle (catalyst shape) [11]. The geometric design can govern the amount of catalyst utilization by enhancing the ratio of surface area to volume and reduce the pressure drop. Selecting of particle shape will be impacted by several factors such as reactant fluids, bed aspect ratio (D_c/d_p), and fluids flow that specified based on the demand for a lowest acceptable reaction rate and highest allowable pressure drop.

Moreover, the catalyst shape has a considerable impact on bed voidage and thus hydrodynamics (flow regime, pressure drop, and liquid holdup) and performance [11], [12]. Recent improvements in the field of catalyst shape design conducted to an increased interest in study effects of catalyst shape on the hydrodynamics and renewed assess the performance of catalytic reactors with taking in the account influence the catalyst shape. In the past years, there have been a few studies in the literature reporting the effects of catalyst shape on the hydrodynamics in TBRs. Recently, Brunner et al., 2015 [13] developed model to understand effect of catalyst shape and size on different parameters (catalyst effectiveness, bed void fraction, and overall heat transfer coefficient) in fixed bed reactor with multitubular shell and tube heat exchanger. The authors stated that the catalyst shape significantly affected the bed void in the bed which this effect reflected sensitively on the hydrodynamic parameters [13].

The other study that investigated the effects of catalyst shape and size on the liquid distribution in TBR with five different catalyst shapes and sizes (spherical, tablet, holed tablet, cylindrical, and trilobe) was by Kundu et al. (2001) [14]. The results revealed a considerable impact of catalyst shape on the liquid distribution beside the liquid distributor in the packed bed reactors. However, this study was limited to the liquid distribution and more investigation to illustrate the effects of catalyst shape on the key hydrodynamic parameters such as pressure drop and liquid holdup [15].

Meanwhile, Trivizadakis et al. (2006) [16] studied the effect of catalyst shape and size on hydrodynamics and concluded the significant effect of shape and size on pressure drop, liquid holdup, and flow regime. The results displayed an increase in the pressure drop and holdup in the cylindrical bed than the spherical bed due to non-uniform distribution for voids in the cylindrical catalyst shape. However, the experiments were conducted at two catalyst shapes (spherical and cylindrical), whereas the industrial field (hydrotreating processes) still need more investigation on more different catalyst shapes that are more common in use in petroleum processes [16].

Also, Bazmi et al. (2013) [17] reported that the pressure drop and liquid holdup in the trilobe packed bed greater than the pressure drop and liquid holdup in the spherical packed bed due to increase the bed void and contact points between the catalyst particles which the results demonstrated the effect of catalyst shape on the hydrodynamics in the TBR [17].

Flow regime is one of the most important parameters that significantly impact the crucial hydrodynamics (Pressure drop and liquid holdup). Flow regime illustrates the interaction form between fluids in the bed. Different flow regimes exist in the TBRs which

categorized into two regimes low interaction regime (LIR) where shear of gas-liquid can be neglected and high interaction regime (HIR) where shear of gas-liquid noticeably impact the fluid flow in the bed. However, there are many studies to evaluate the hydrodynamics phenomena in different interaction regimes, but still need for a typical expression for drag forces. Flow regime in TBR depends on fluids flow rate and bed characteristics. Industrially, trickle flow regime, pulse flow regime and their transition are most interesting. Many researchers have argued a different methodologies to identify flow regimes and their transition in multiple powerful tools [16], [18], [19].

The correlations and models have been developed to predict pressure drop and liquid holdup in TBR which due to the complex interaction between gas and liquid reactants and catalyst particles as a solid phase no fundamental approaches exist to illustrate the hydrodynamic phenomena [1], [6], [18]. There is a very few information in the literature that paid attention for catalyst shape impact on the hydrodynamics and performance in the TBRs [16]. Various types of models and correlations have been developed to predict pressure drop and liquid holdup such as strictly empirical [20]–[23] and phenomenological (mechanistic) models [10], [18], [24], [25]. The strict empirical models represents theoretical method, whilst the phenomenological models developed based on physical picture that seems more reliable to apply at different operation conditions [26]. This study aims to measure pressure drop and liquid holdup and investigate the effects of different commercial catalyst shapes on the pressure drop and liquid holdup as a function of gas and liquid flow rate. Furthermore, modify Ergun single phase equation and re-estimate Ergun's universal coefficients for different beds (catalyst shape) and predict two-phase pressure drop and liquid holdup by using different models approaches

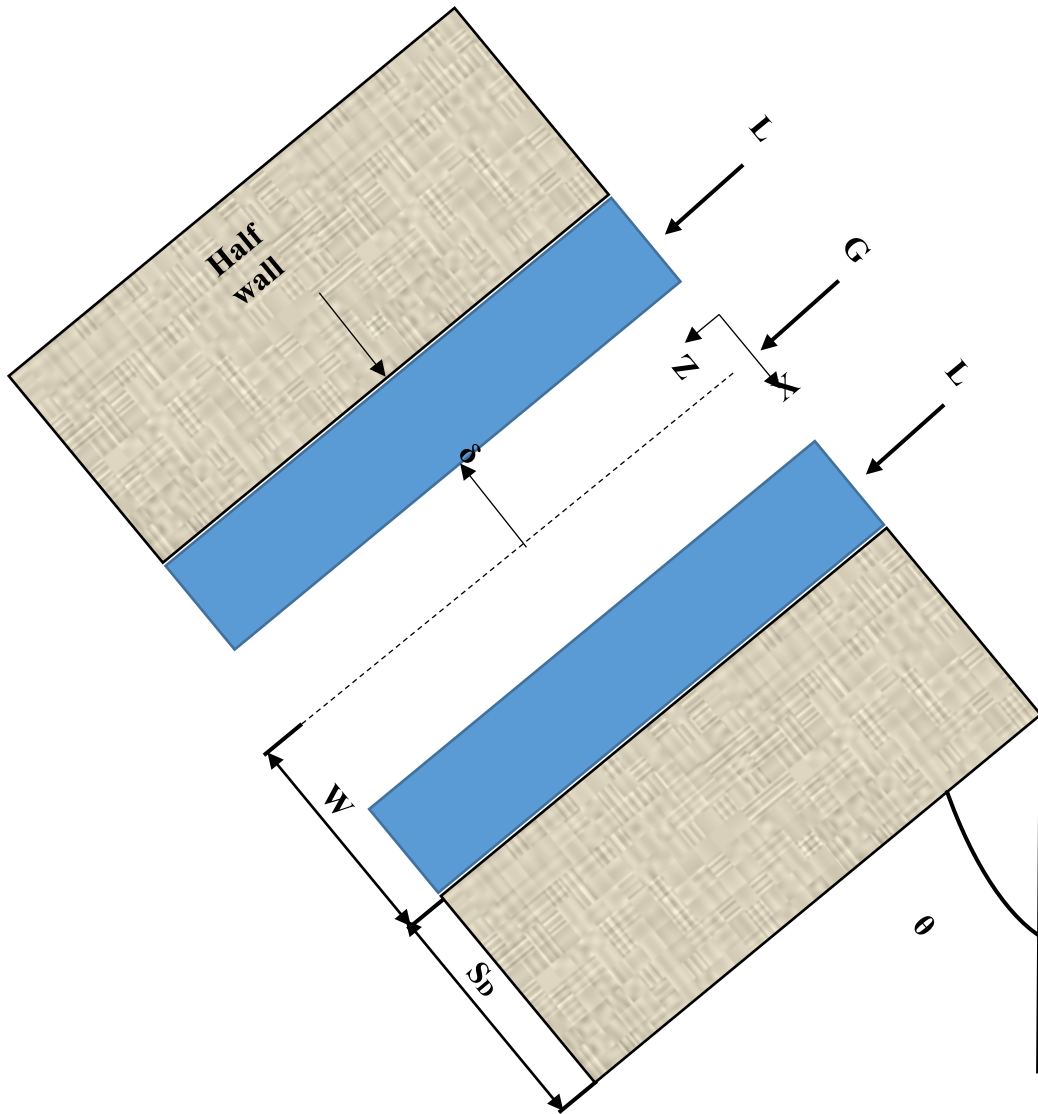
(phenomenological and empirical) to evaluate prediction accuracy for hydrodynamic parameters and illustrate the effects of catalyst shape on the hydrodynamics in TBR.

2. PHENOMENOLOGICAL MODEL

One of the most important factors in the multiphase reactors are void space volume and distribution that significantly impact the liquid distribution in the bed thus hydrodynamics. Liquid maldistribution is the main reason to create hot spots that effect to rapid deactivation for catalyst particles and decrease performance and may cause runaway for column [27]. Due to the complex geometry for void space in the bed it was so difficult to evaluate the hydrodynamic parameters. Holub et al., 1992 have developed a phenomenological or slit model based on represent the complex geometry of void space at microscale by inclined slit as shown in Figure 1.

The basis of the slit model, liquid flow over the solid phase as a film or rivulet in trickle flow regime, while the gas flow as a continuous flow through the rest of central void space of slit. In the current model liquid assumed to be thoroughly wetting (film flow) the surface of the slit wall (catalyst bed) with uniform thickness and gas flow in the central space for the slit. Gas and liquid momentum balance for slits formulated to final model as a dimensionless equations and modified Ergun' constants as displayed in Table 1 [24], [25].

E_1^* and E_2^* are modified Ergun's coefficients that estimated from single gas phase flow. Ergun's equation developed based on spherical shape of catalyst particles in the bed and considered as a universal coefficients [28].



$$\frac{W}{S_D} = \frac{\epsilon_B}{1 - \epsilon_B} ; \quad \frac{\delta}{S_D} = \frac{\epsilon_L}{1 - \epsilon_B} ; \quad S_D = \frac{d_p}{6}$$

$$\cos \theta = T ; \quad V_L = T \left[\frac{U_L}{\epsilon_L} \right] ; \quad V_G = T \left[\frac{U_G}{\epsilon_B} \right]$$

Figure1. Schematic diagram for single slit model.

Table 1. Slit Model (Phenomenological approach) of Holub et al., 1992, 1993 with single Phase Modified Ergun Coefficients.

	Equation	No
$\Psi_L = \frac{\Delta P/Z}{\rho_L g} + 1 = \left(\frac{\epsilon_B}{\epsilon_L}\right)^3 \left[\frac{E_1^* Re_L}{Ga_L} + \frac{E_2^* Re_L^2}{Ga_L} \right]$		(1)
$\Psi_G = \frac{\Delta P/Z}{\rho_G g} + 1 = \left(\frac{\epsilon_B}{\epsilon_B - \epsilon_L}\right)^3 \left[\frac{E_1^* Re_G}{Ga_G} + \frac{E_2^* Re_G^2}{Ga_G} \right]$		(2)
$\Psi_L = 1 + \frac{\rho_G}{\rho_L} (\Psi_G - 1)$		(3)

[29] demonstrate that there is a considerable deviation in Ergun's constant determination for interesting bed due to irregular shape of catalyst particles that impact the porosity of the bed. Modified Ergun's equation was used to formulate the relationship between equivalent diameters (d_{eq}) of catalyst particles and mesh size. Authors concluded for non-uniform shape of catalyst particles, it is necessary to estimate surface to volume ratio or sphericity to calculate d_{eq} and suggested 180 as a universal constant valued for the viscous flow region and 1.8-4 for the inertial flow region of non-uniform catalyst shape. Ergun's constants have been applied in different two phase model approaches. Sweeney, n.d. [30] reported model that compared the model to the pressure drop data. The authors assumed the solid particle size stay unchanged and the liquid was the ratio of solid to the gas. The authors used Ergun single phase coefficients in the developed model and recommended that it is necessary to measure single phase Ergun constants for packed bed of interest. Moreover, V. Specchia & G. Baldi, 1977 [31] developed a different model that modeling the gas phase pressure drop by decreasing the void space and increasing the particle size because of existence of liquid holdup. Meanwhile, in this study the authors

performed a single phase coefficients and suggested recalculate these coefficients in the bed of interest. Carbonell, 1985 [32] adopted relative permeabilities to predict hydrodynamics in the packed bed reactors. The concept of relative permeabilities uses parameter for the drag force for single phase flow, which defined as the ratio of drag force per unit volume (at single phase flow) to drag force per unit volume (at two phase flow) at same superficial velocity of given phase. Ergun constants implemented for pressure drop prediction under single phase and two phase flow conditions which the constants were taken 180 for the viscous flow region and 1.8-4 for the inertial flow region as recommended by Macdonald et al., 1979a [29] for non-uniform catalyst shape. The best representation for pressure drop determination in the single phase flow through packed bed proposed by Sabri Ergun, 1952 [28]. Ergun formulated the pressure drop as a function of various parameters such as fluid flow, shape and size of catalyst particles and physical properties of fluids as the following form:

$$\frac{\Delta P}{L} g_c = 150 \frac{(1-\epsilon)^2}{\epsilon^3} \frac{\mu U_m}{D_p^2} + 1.75 \frac{1-\epsilon}{\epsilon^3} \frac{G U_m}{D_p} \quad (4)$$

Where D_p is the diameter of spherical particles, which when we use equation 4 for non-spherical bed. Nevertheless, equivalent diameter calculation required to represent the catalyst shape impact in the non-spherical bed. Spherical diameter (D_p) in equation 4 have been modified and implemented for non-spherical catalyst shape by apply equivalent spherical diameter (d_{eq}) as defined below:

$$d_{eq} = \frac{6V_p}{\phi S_p} \quad (5)$$

Where

d_{eq} is the equivalent diameter (m)

V_p is the volume of non-spherical particle (m^3)

S_p is the surface area (m^2)

$S_{ep} = \varphi S_p$ Where S_{ep} is the surface area of equivalent volume sphere.

φ is the sphericity parameter that defined as

$$\varphi = \frac{\text{Surface area of the equivalent volume } (S_{ep})}{\text{surface area of non-spherical particle } (S_p)} \quad (6)$$

$$d_{eq} = \frac{6 V_p}{S_{ep}} \quad (7)$$

Modified Ergun coefficients (E1* and E2*) have been determined for different commercial catalyst shape to predict pressure drop and liquid holdup in pilot plant TBR. Pressure drop is the energy dissipated by fluid flow through the column bed. The energy dissipation can be occurred in TBRs due to the frictional losses at the surface of catalyst particles for the bed and driving force on the liquid flow through the reactor bed. The pressure drop essentially depends on superficial gas and liquid velocity which when increase the superficial gas and liquid velocity pressure drop will be increased considerably. The liquid holdup is one of the significant parameters for the reactor which it actively impacts several vital parameters in the reactor (pressure drop, a residence time of the liquid phase, axial dispersion coefficient and heat transfer coefficient, etc.). Superficial gas and liquid velocities significantly impacted liquid holdup which at increasing the superficial gas velocity the liquid holdup will be decreased, while at increasing the superficial liquid velocity the liquid holdup will be increased due to changing the thickness of liquid film over catalyst particles in the bed [18], [23], [33]–[35].

Table 2. Extended Slit Model (Phenomenological Approach) Equations for Pressure Drop and Liquid Holdup

Equation	No.
$\Psi_G = \left(\frac{\epsilon_B}{\epsilon_B - \epsilon_L} \right)^3 \left[\frac{E_1^*(Re_G - f_v \epsilon_G Re_i)}{Ga_G} + \frac{E_2^*(Re_G - f_v \epsilon_G Re_i)^2}{Ga_G} \right]$	(8)
$Re_i = \frac{V_{iL} D_p}{v_L (1 - \epsilon_B)}$	(9)
$\Psi_L = \left(\frac{\epsilon_B}{\epsilon_L} \right)^3 \left[\frac{E_1^* Re_L}{Ga_L} + \frac{E_2^* Re_L^2}{Ga_L} \right] + f_s \frac{\epsilon_G}{\epsilon_L} \left(1 - \frac{\rho_G}{\rho_L} - \Psi_L \right)$	(10)
$Re_i = \phi \eta_L$	$0 < \eta_L < 5$ (11)
$Re_i = \phi (-3.05 + 5 \ln(\eta_L))$	$5 < \eta_L < 30$ (12)
$Re_i = \phi (5.5 + 2.5 \ln(\eta_L))$	$\eta_L > 30$ (13)
Where	
$\phi_L = \frac{10}{(E_1)^{0.75}} \frac{v_L}{v_G} \sqrt{\Psi_L Ga_L \frac{\epsilon_L}{\epsilon_B^3} \left(1 + f_s \frac{\epsilon_G \rho_G \Psi_G}{\epsilon_L \rho_L \Psi_L} \right)}$	(14)
$\eta_L = \frac{1}{5(E_1)^{0.25}} \sqrt{\Psi_L Ga_L \left(\frac{\epsilon_L}{\epsilon_B} \right)^3 \left(1 + f_s \frac{\epsilon_G \rho_G \Psi_G}{\epsilon_L \rho_L \Psi_L} \right)}$	(15)
and	
$\Psi_L = 1 + \frac{\rho_G}{\rho_L} (\Psi_G - 1)$	(16)

In the TBRs the driving force contains gravitational force, gas-liquid interfacial drag force, and pressure gradient. The slit model revealed a better prediction for pressure drop and liquid holdup in the trickle flow regime (low interaction regime), which the drag force and pressure gradient negligible to the gravitational force. However, at high gas and liquid flow rate (high interaction regime) the status of operation will change from driving force controlled dominantly by gravity to driving force controlled by drag force and pressure gradient [6]. Therefore, M.H. Al-Dahhan et al., (1998) [1] extended the slit model and validated at high pressure and gas velocity (high interaction regime) by integrate the

velocity (f_v) and shear (f_s) slit coefficients based on two phase momentum balance for the slit. The velocity and shear coefficients exhibited in Table 2. Many theoretical models with strictly empirical reported by using different approaches [6], [20], [36]. However, the application of the strictly empirical models were restricted due to developed based on particular operation conditions and seems less reliable than the phenomenological models that developed based on physical phenomenal picture. Larachi et al., (1991) [37] developed empirical model that investigated the effects of gas and liquid flow rate, and particle size on pressure drop and liquid saturation. This model developed with absence of adjustable parameters related to catalyst shape effect. As a result comparison of phenomenological and empirical models and experimental data to study and evaluate the influences of packing shapes, gas flow rate, and liquid flow rate on pressure drop and liquid holdup in TBRs.

3. EXPERIMENTAL WORK

3.1. APPARATUS

A transparent acrylic cylindrical column was designed with the 2m length of bed (L) and 0.14m inside diameter (d_c) to conduct the experimental work in this study as given in Figure 2. Hydrodynamics were investigated at a trickle to pulse flow regime with a wide range of superficial gas velocity (U_g) from 0.03 to 0.27 m/s and air as a gas phase, while water as a liquid phase with a range of superficial liquid velocity (U_l) from 0.004 to 0.016 m/s Gas and liquid entered from the top of the reactor (head Section) in the concurrent downward flow. A transparent acrylic cylindrical column was designed with the 2m length of bed (L) and 0.14m inside diameter (d_c) to conduct the experimental work in this study

as given in Figure 2. Hydrodynamics were investigated at a trickle to pulse flow regime with a wide range of superficial gas velocity (U_g) from 0.03 to 0.27 m/s and air as a gas phase, while water as a liquid phase with a range of superficial liquid velocity (U_l) from 0.004 to 0.016 m/s. Gas and liquid entered from the top of the reactor (head section) in the concurrent downward flow. Shower distributor was used to distribute liquid and two holes with 12.7mm for gas over a perforated plate with 20 holes with 3mm diameter and five holes with 5mm diameter distributed within circular configuration (Figure1) to acquire uniform gas and liquid distribution. The inlet and outlet of gas and liquid have controlled by electronic solenoids valves to enable stopping fluids flow in and out of the column by On/Off switch see Figure 2. Different commercial catalyst shape and size (Trilobe, Quadrilobe, Cylindrical, and Spherical) loaded randomly to the reactor which the features of beds given in Table 3. The outlet water has collected in a plastic tank and circulated by a centrifugal pump through two flowmeters at different volumetric flow rate range

Table 3. Packed beds characteristics

Shape (-)	Porosity (-)	Size (L x d) (mm x mm)	Sphericity (-)	Volume (Vp) (mm ³)	Surface area (Ap) (mm ²)	Equivalent diameter (mm)	Equivalent area (mm ²)	dc/dp (-)
Spherical	0.36	4.7	1	55.287	70.18	4.7	55.28	29.8
Cylindrical	0.451	6 x 2.8	0.82	36.9	65.10	4.1	53.89	50
Trilobe	0.526	6 x 3	0.62	32.28	79.42	3.93	49.29	46.6
Quadrilobe	0.456	6 x 2.5	0.718	19.98	49.79	3.35	35.7	56

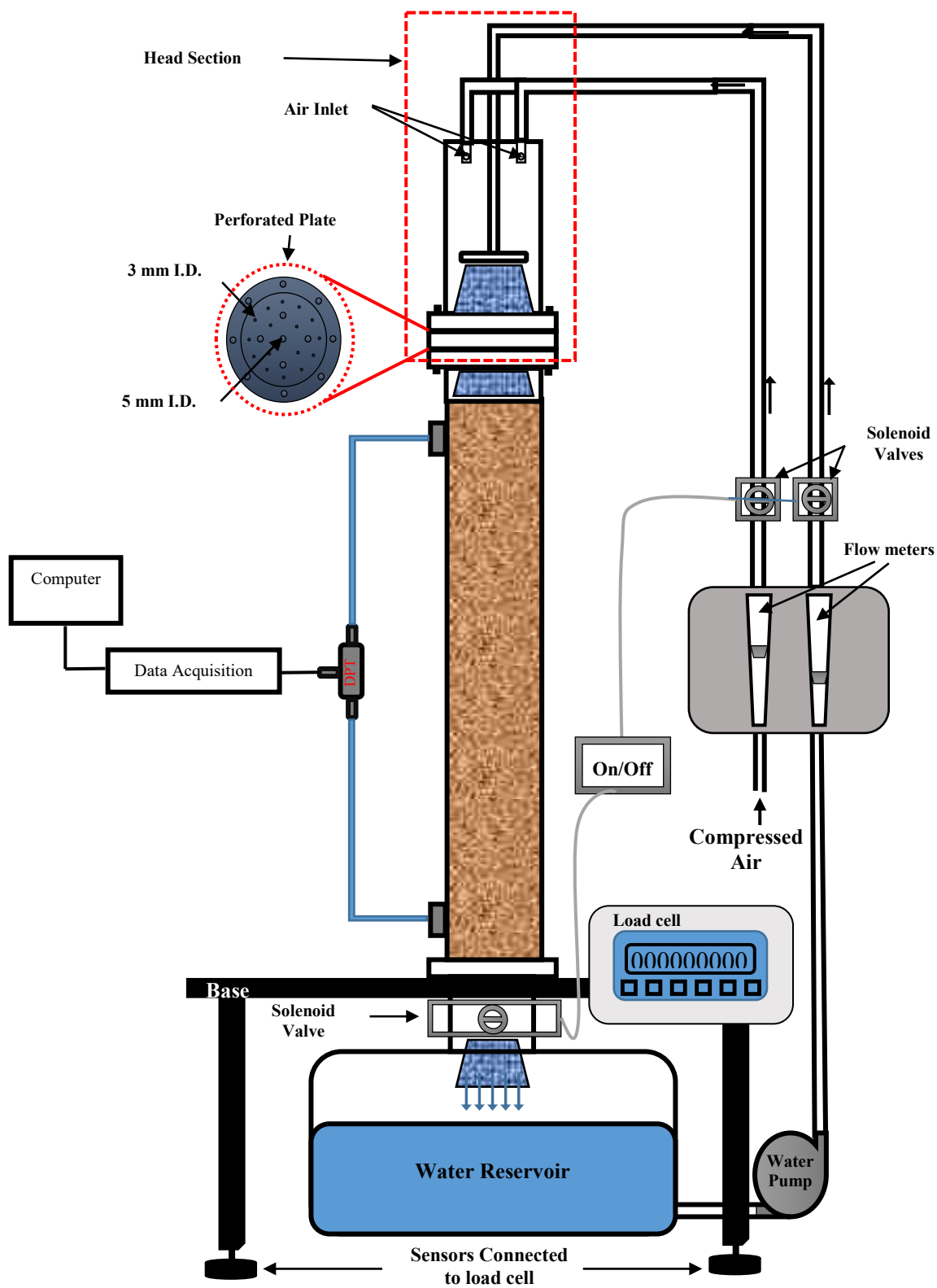


Figure 2. Schematic diagram of TBR.

3.2. OPERATION CONDITION

A randomly packed bed have pre-wetted by flooding the bed for 24 hours to ensure no hysteresis phenomena in the reactor. Gas and water have supplied to the reactor at particular superficial velocities and wait for 30-45 mins to reach a steady state flow rate. A high-frequency differential pressure transducer (HDPT) have been used to measure pressure drop between two points along the bed and connected to high-frequency data acquisition (0-1000 kHz) with high accuracy in the measurements see Figures 2 and 3. Additionally, a digital load cell has used to measure liquid holdup in the reactor by drainage method due to simplicity in the measuring and analyzing, reasonable accuracy as well. The apparatus legs have placed on four sensitive sensors (one sensor for each leg) that measure any slight change in the weight of the reactor see Figure 4. Two electronic solenoid valves used to control cut-off the inlet of gas and liquid flow rate to the reactor and one electronic solenoid valve to cut-off the outlet flow rate both linked together at the same time by one On/Off switch as shown in Figures 2 and 4. The liquid holdup of the bed was measured at steady state operating by drainage method by switching off the solenoid valves to stopping gas and liquid flow to inside and outside the reactor. The weight of liquid that captured divided by the liquid density to determine the volume of liquid (V_l) in the bed at particular operating. The ratio of liquid volume (V_l) at the bed to the bed volume (V_b) corresponding the liquid holdup in that bed. Meanwhile, by drain the liquid captured in the column and wait at least 45mins and then read the difference in the weight between the liquid captured and weight of liquid that remained (Static liquid between adjacent particles and inside the porosity of catalyst particles) represents the weight of liquid flow through the bed (dynamic

liquid). The steps of collecting and estimating global liquid holdup and dynamic liquid holdup exhibited as follow:

- 1) Weight of loaded bed dry (Wt_{dry}).
- 2) Flooding the bed for 24 hours and drain the liquid and waiting at least 45 mins to measure the weight of bed wet which represent the weight of static liquid and internal liquid in the porosity of catalyst particle (Wt_{wet}).
- 3) Weight the captured liquid at specific operating (Wt_{cap}).
- 4) Net weight of liquid in the bed (Wt_{total}) = (Wt_{cap}) - (Wt_{dry})
- 5) Net weight of liquid flow in the bed ($Wt_{dynamic}$) = (Wt_{cap}) - (Wt_{wet})
- 6) Volume of the bed (V_b) = $\frac{\pi}{4} d_c^2 L$

- 7) Volume of capture liquid in the bed (V_l) = $\frac{Wt_{total}}{\rho_l}$

Where: ρ_l is liquid density (kg/m³)

- 8) Volume of dynamic liquid ($V_{dynamic}$) = $\frac{Wt_{dynamic}}{\rho_l}$

- 9) Total liquid holdup (ϵ_l) = $\frac{V_l}{V_b}$

- 10) Dynamic liquid holdup ($\epsilon_{dynamic}$) = $\frac{V_{dynamic}}{V_b}$

- 11) Volume of static liquid and internal liquid ($V_{stat+Int}$) = $\frac{Wt_{wet}}{\rho_l}$

- 12) static liquid holdup by estimate Eötvös number (E_{δ}) as follow:

$$\text{Eötvös number } (E_{\delta}) = \frac{\rho_l g d_p^2 \epsilon_b^2}{\sigma_l (1 - \epsilon_b)^2}$$

$$\text{Static Liquid Holdup } (\epsilon_{stat}) = \frac{1}{20 + 0.9 E_{\delta}}$$



Figure 3. Physical picture for (a) differential pressure transducer (b) data acquisition.

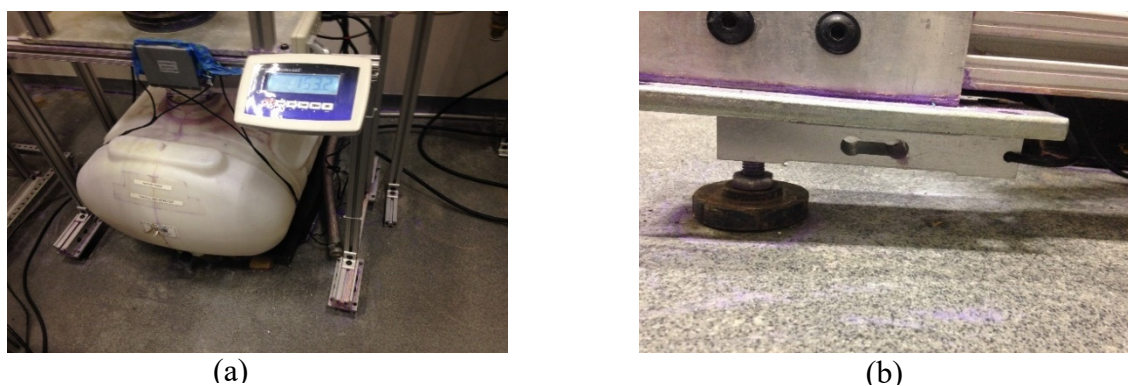


Figure 4. Physical picture for (a) digital load cell (b) sensor connected to load cell.

4. RESULTS AND DISCUSSION

4.1. ERGUN'S COEFFICIENTS CALCULATION

As we discussed in Section 3.2, high-frequency differential pressure transducer have been employed to measure the pressure drop within different commercial catalyst

shape at single phase flow (gas) and a wide range of superficial gas velocity. The findings of the present study suggest that need to calculate single phase coefficients to use in Ergun equation (equ. 1) for each interesting bed. Ergun's coefficients were recalculated by fitting data collected in each bed as presented in Table 4. All measured pressure drop data at different beds (experimentally) were compared with predicted pressure drop by using Ergun equation with universal Ergun coefficients (spherical), universal Macdonald coefficients (non-spherical), and modified coefficients (fitted).

Table 4. Modified Ergun Coefficients at Different industrial catalyst particles

	Spherical	Cylindrical	Trilobe	Quadrilobe
E_1^*	150	838.9	1421.34	629.44
E_2^*	1.75	3.04	2.32	0.89

Figure 5 exhibits the deviation range of each bed with compared coefficients. In Figure 5a shows the deviation range within a spherical bed, which the mean relative error (MRE) by using non-spherical universal coefficients ($E_1=180$ and $E_2=1.8$) is 13% and less than 1% deviation range at universal Ergun's coefficients ($E_1=150$ and $E_2=1.75$) and modified coefficients. However, the error of pressure drop prediction at a single phase flow

(gas flow) escalated with non-spherical beds due to different void space for each bed that impacted significantly by the geometry of catalyst particles as presented in Figure 5b, 5c, and 5d. The deviation range of MRE of pressure drop predicted by applying various coefficients within different beds displayed in Table 5. The parity plots for single-phase pressure drop prediction by using universal Ergun coefficients, universal non-spherical coefficients, and modified coefficients in the original Ergun correlation equation (eq. 5) are shown in Figure 6a, 6b, and 6c, respectively. The average deviation of MRE for all beds with modified coefficients was 7% while for non-spherical universal coefficients and universal Ergun coefficients were 56% and 55%, respectively.

Table 5. Average Mean Relative Error (MRE) with Different Catalyst Shapes and Total Data

	Spherical	Cylindrical	Trilobe	Quadrilobe	Total data
Ergun	0.83%	75%	83%	64%	55%
Non-spherical	13%	72%	80%	59%	56%
Modified	0.84%	9%	8.5%	9.5%	7%

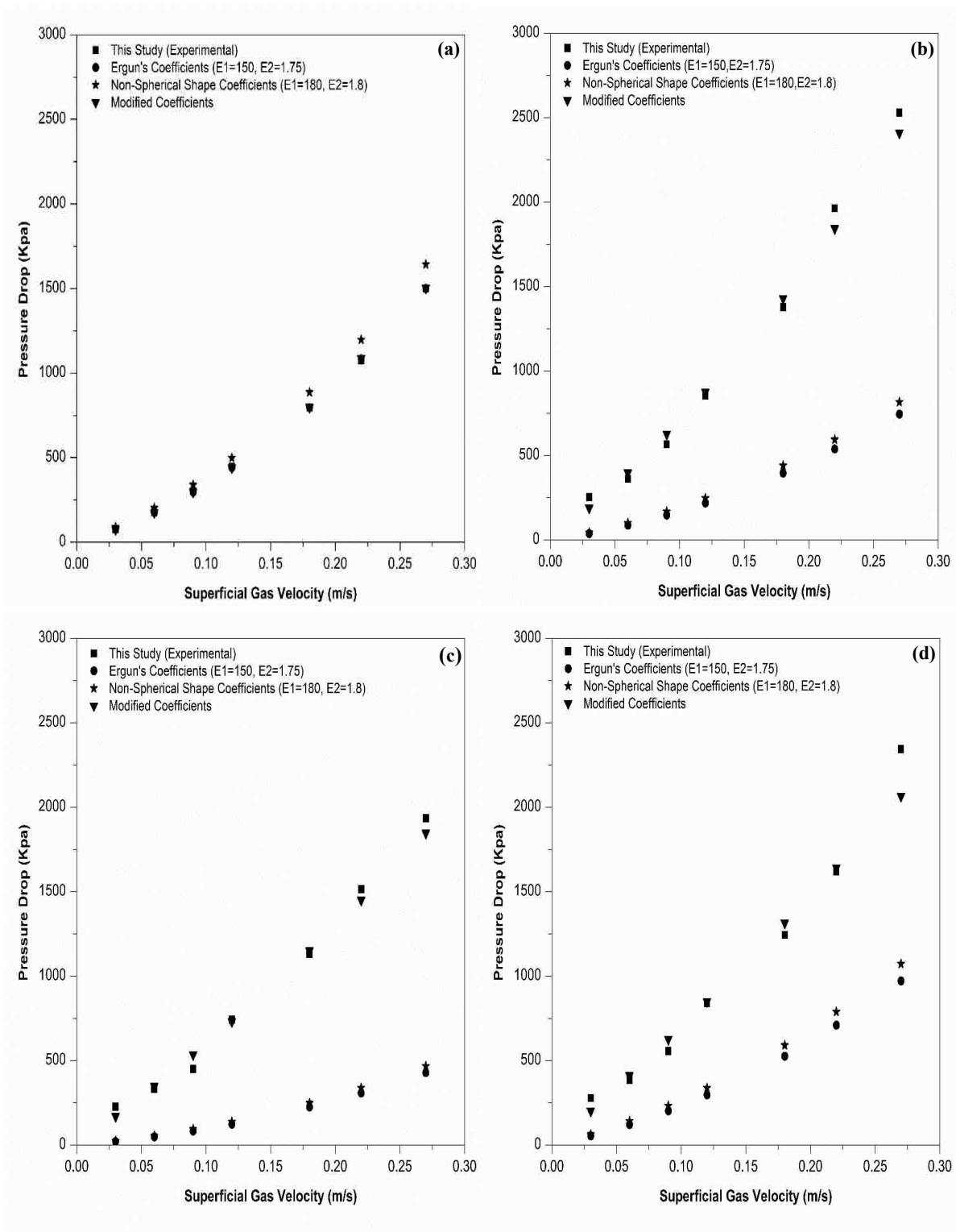


Figure 5. Pressure drop versus superficial gas velocity with single phase flow through (a) spherical (b) cylindrical (c) trilobe (d) quadri-lobe catalyst bed.

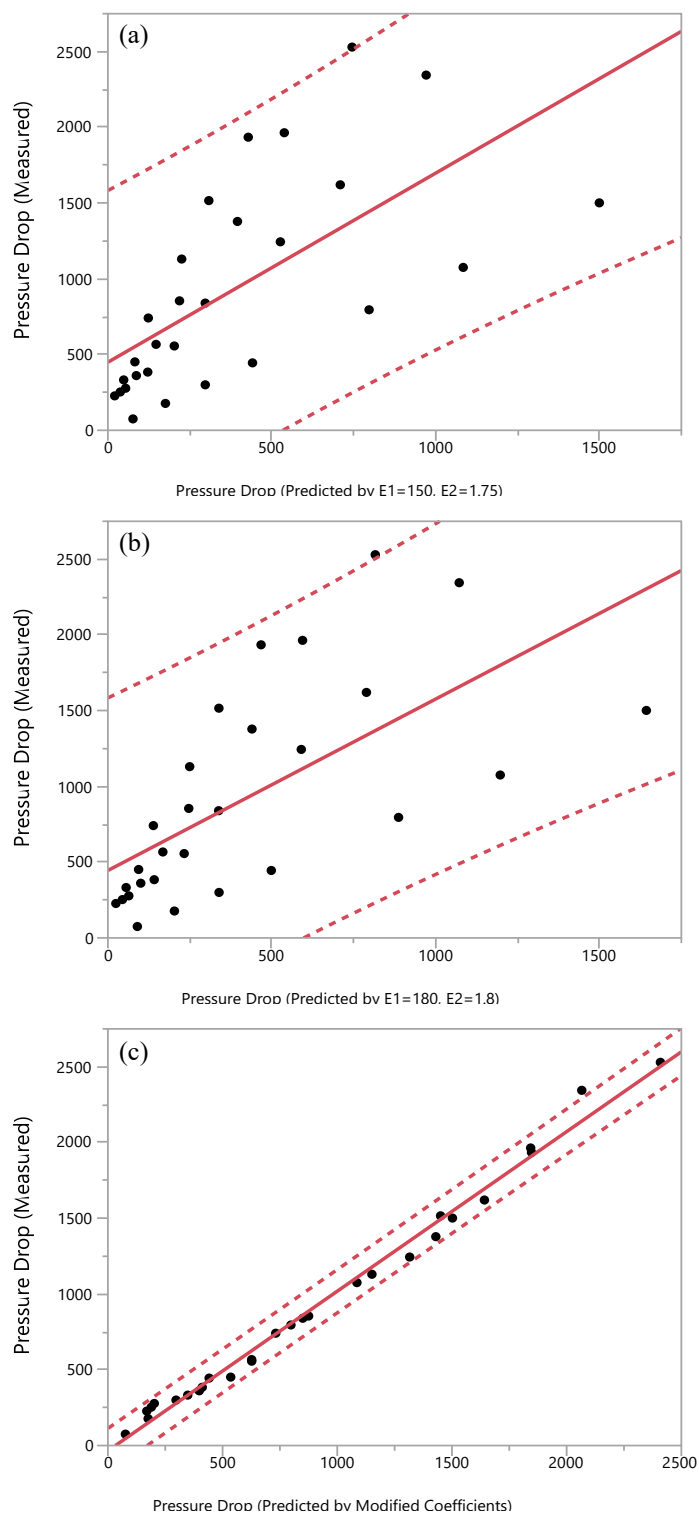


Figure 6. Parity plot for (a) using universal Ergun coefficients (b) using universal non-spherical coefficients (c) using modified coefficients by comparing the experimental observations with the predicted single phase pressure drop by original Ergun correlation.

4.2. LOW TO HIGH INTERACTION TRANSITION BOUNDARY

The flow pattern is crucial parameter of design in the reactor that significantly affects hydrodynamics (pressure drop and liquid holdup). Flow pattern have been categorized as a two pattern low and high interaction patterns. Low to high interaction transition boundaries diagnosed at various catalyst shapes. Figure 7 illustrates the map of transition boundaries in different beds. The transition flow for cylindrical and poly lobes (trilobe and quadrilobe) particles identified at lower liquid flow rate compared to spherical particles. At low gas flow rate, no change is recorded in the flow pattern between cylindrical and ploy lobes particles. The percentage of total data at low interaction flow regime is 30% and at high interaction flow regime is 70%. On other hands, at high gas flow rate, no differences in the gas and liquid interaction diagnosed between all catalyst shapes.

4.3. PRESSURE DROP

Pressure drop is crucial parameters for the design and performance of packed bed reactors. The pressure drop depends on gas and liquid velocities and bed characteristics such as catalyst shape and size. The effects of catalyst shape on the pressure drop were demonstrated in Figure 8. Comparison between spherical particles with those corresponding to cylindrical, poly lobes (trilobe and quadrilobe) particles. It is evident that the effects of catalyst shape on the pressure drop is noticed and need to be considered at operating conditions of industrial interests. It is noteworthy that the change in the dimensionless pressure drop at different catalyst shape is related to void space, void distribution, and contact points due to the effect of geometry design for catalyst particles.

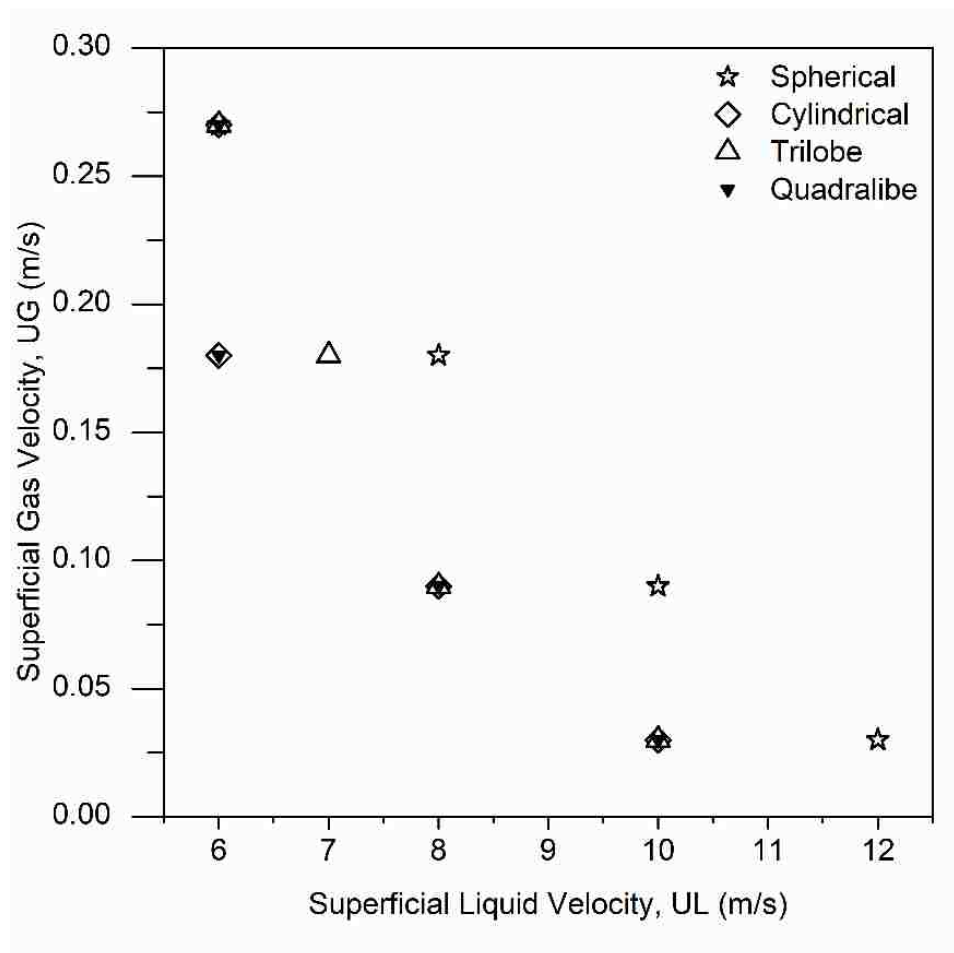


Figure 7. Transition boundary at different catalyst shape.

Additionally, the effects of catalyst shapes on dimensionless pressure drop are more noticeable at higher superficial liquid velocity (Figure 8). The results revealed a smaller dimensionless pressure drop for spherical particles than cylindrical, trilobe, and quadrilobe particles and a higher dimensionless pressure drop for cylindrical particles due to void space and contact points between solid particles in the beds. The slight difference in the bed void (volume and distribution) and contact points due to varying design for catalyst shape between the cylindrical and poly lobes particles was the reason for narrowing down

the gap in the dimensionless pressure drop among them. The measurements of dimensionless pressure drop are in good agreement with findings by Trivizadakis et al., (2006). It can be concluded that the new design for trilobe and quadralobe particles decreased the magnitude of dimensionless pressure drop compared to the cylindrical particles and enhanced the operation condition for the reactor.

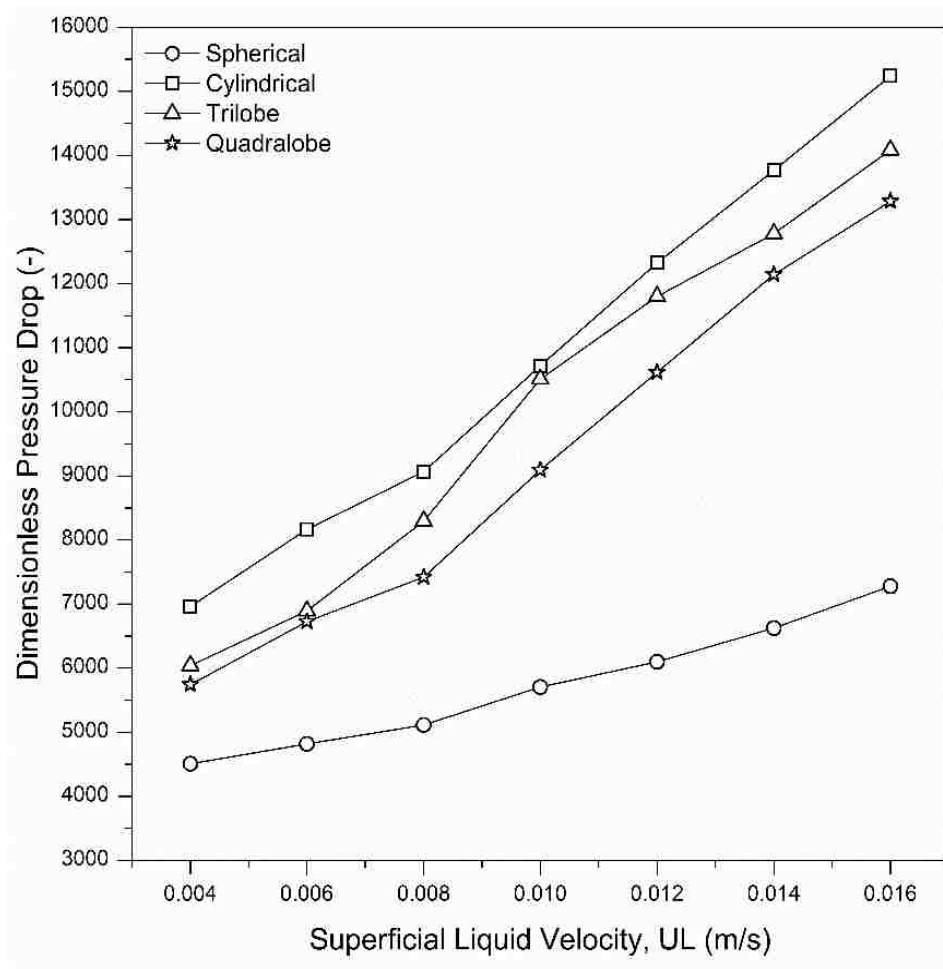


Figure 8. The effects of catalyst shape on the dimensionless pressure drop at different commercial beds.

Figure 9 exhibits the effects of gas and liquid velocities on the dimensionless pressure drop at different beds. An enhancement in the superficial gas or liquid velocities yields higher dimensionless pressure drop. The effects of increase superficial liquid velocity on the dimensionless pressure drop are more considerable than the effects of increasing the superficial gas velocity due to the superficial liquid velocity increases the gas –liquid interaction and liquid – solid shear stress in the bed void when the more liquid flow through bed voidage therefore resistance become significantly higher than driving force (Figure 9b, 9c, and 9d).

Consequently, the effects of superficial gas velocity on dimensionless pressure drop is noticeably significant at higher superficial liquid velocity due to at low interaction flow regime the drag force and pressure gradient negligible in comparison to the gravitational force in the driving force as shown in illustrated in Figure 10. Additionally, the relative high voidage in the cylindrical and poly lobes beds compared to the spherical bed increased the dimensionless pressure drop due to increase the amount of liquid flow through the void space and thus the resistance in the bed as depicted in Figure 10b, 10c, and 10d.

4.4. LIQUID HOLDUP

The average liquid holdup defined as a volumetric fraction of the total bed in the packed bed reactors. Liquid holdup considered as a critical parameter in reactor design and performance due to it is related to other hydrodynamics (degree of wetting, pressure drop, and thickness of liquid film).

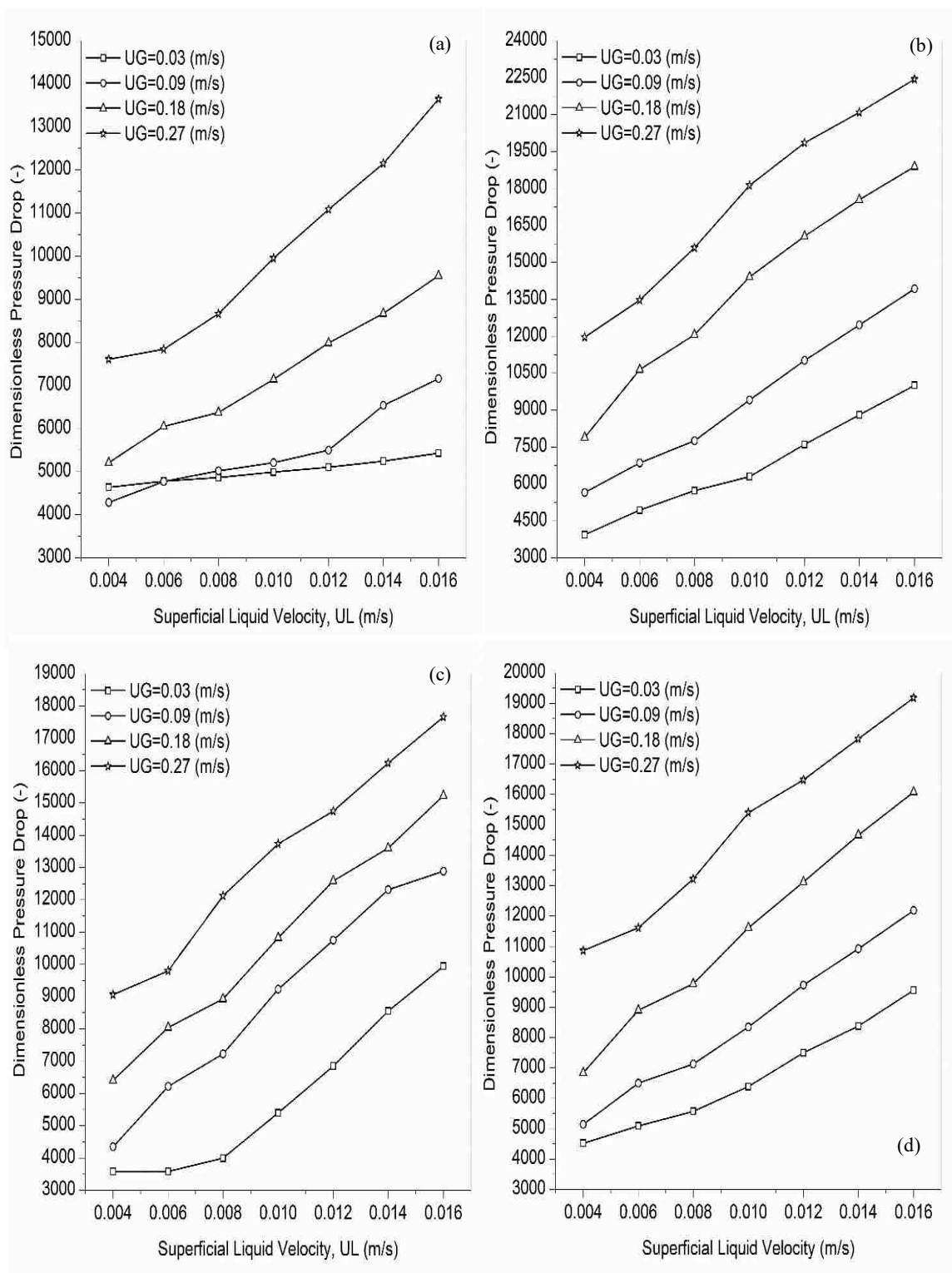


Figure 9. Dimensionless pressure drop vs superficial liquid velocity at different superficial gas velocity (a) spherical (b) cylindrical (c) trilobe (d) quadrilobe

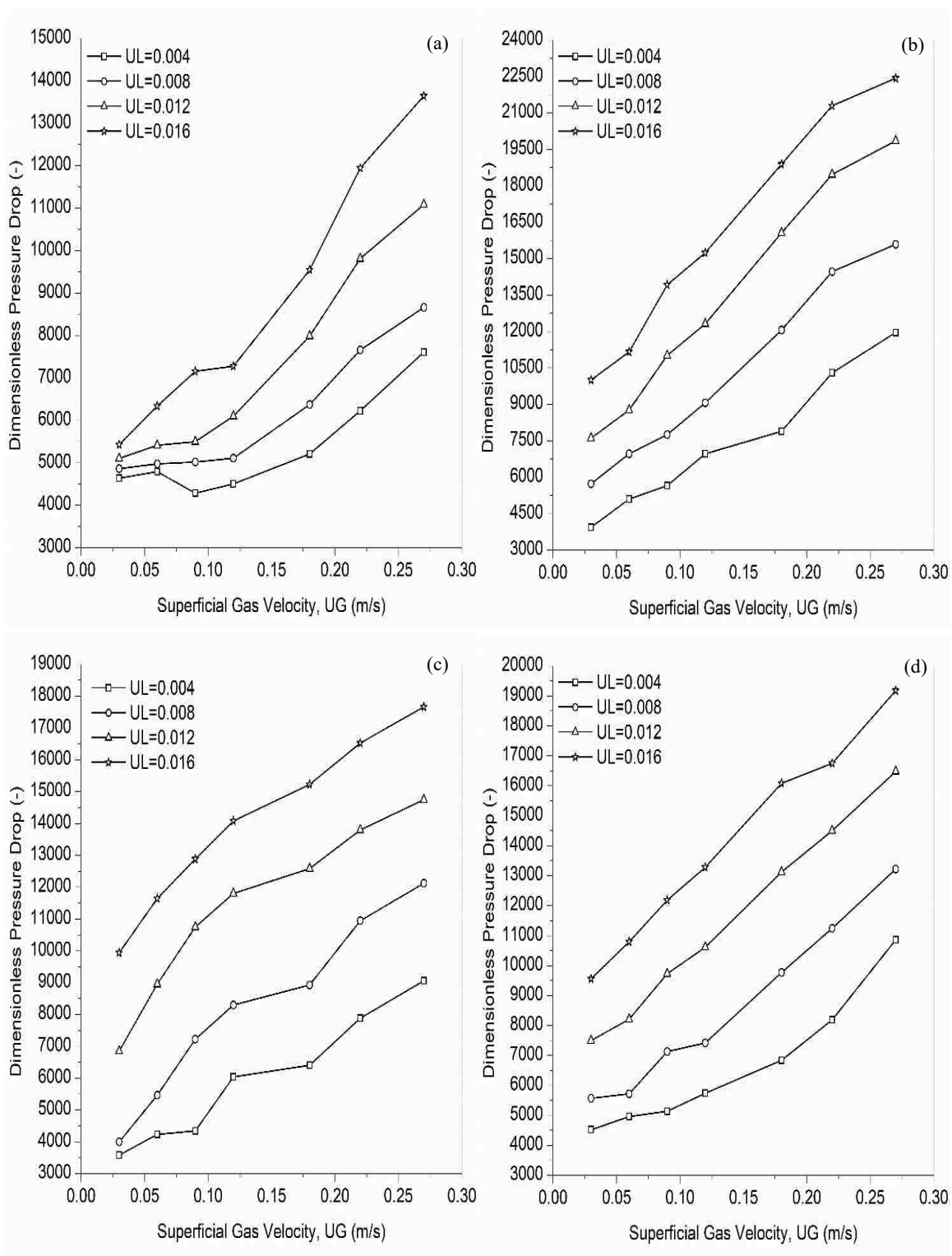


Figure 10. Dimensionless pressure drop vs superficial gas velocity at different superficial liquid velocity (a) spherical (b) cylindrical (c) trilobe (d) quadrilobe.

As displayed in Figure 11, the liquid holdup have significantly affected by catalyst shape which the liquid holdup considerably increased in the cylindrical and poly lobes particles than spherical particles due to increasing the void space in the beds that increased the amount of liquid pass through the bed. Meanwhile, increase the contact points between the particles in the bed increased the resistance compared to the driving force. The liquid holdup noticeably increased in the quadrilobe bed than cylindrical and trilobe particles due to increasing the contact points. It is evident that the liquid holdup increased with increase superficial liquid velocity due to increase the resistance compared to the driving force which increased the time residence and degree of wetting in the bed. It agrees with the findings of [14], [33]. The latter, the liquid holdup in the new catalyst shapes (trilobe and quadrilobe) leads to enhance the liquid holdup considerably compared.

The influence of superficial gas and liquid velocities on the liquid holdup is shown in Figures 12 and 13. The impact of superficial liquid velocity on the liquid holdup is more noticeable at high liquid velocity in all different beds due to increasing the amount of liquid flow through the bed voidage increased gas-liquid and liquid-solid interaction that increased the resistance compared to the driving force thus improving the degree of wetting and liquid holdup in the beds as illustrated in Figure 12a, 12b, 12c, and 12d.

A significant improvement for the liquid holdup at the cylindrical and poly lobes particles compared to the spherical particles was indicated due to increase the contact points and void volume in the beds. It is noteworthy that a considerable liquid holdup improvement with quadrilobe and trilobe beds compared to the cylindrical bed due to increasing the contact points between the adjacent particles in the bed.

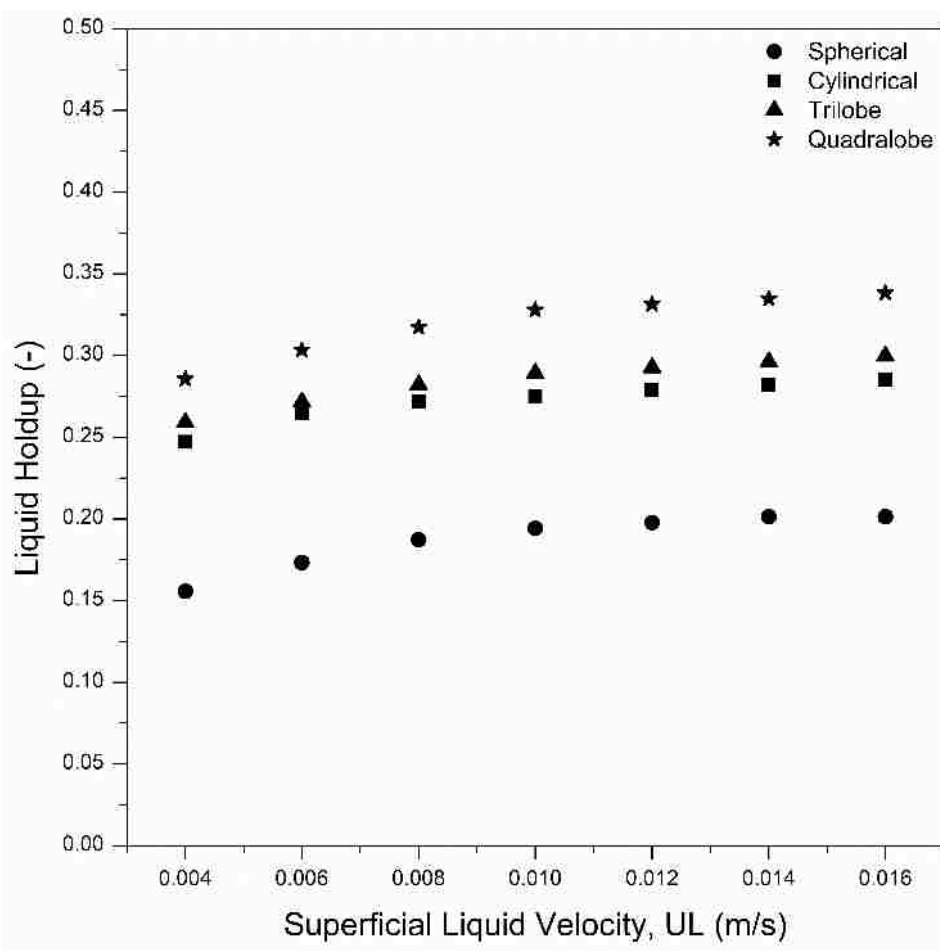


Figure 11. The effects of catalyst shape on the liquid holdup at different commercial catalyst particles (spherical, cylindrical, trilobe, and quadralobe).

It appears in Figure 12a-12d the impact of gas velocity on the liquid is lower than the impact of liquid velocity and agrees with findings presented in the literature (Schubert (Hydrodynamics) 2010, Saba).

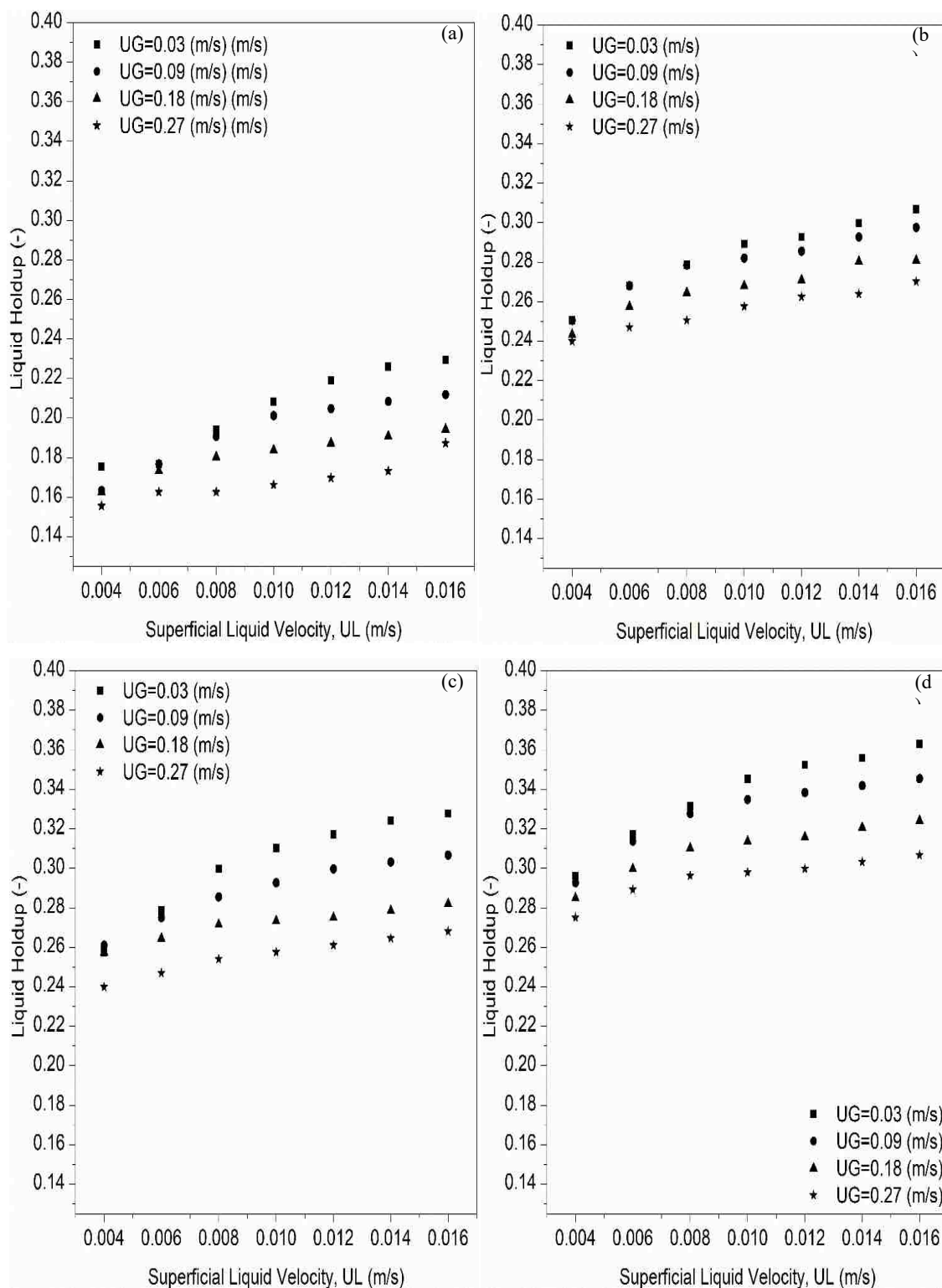


Figure 12. The effect of superficial gas and liquid velocities on the liquid holdup at different beds (a) spherical (b) cylindrical (c) trilobe (d) quadrilobe.

4.5. MODELS COMPARISON

4.5.1. Pressure Drop. Some correlations were developed for both pressure drop and liquid holdup as shown in Table 6. In the present work comparison between two correlation approaches one developed based on phenomenological approach at low interaction regime as shown in Table 1 [27] and at high interaction regime as presented in Table 2 [28] and the second one strictly empirical correlation as displayed in Table 6 [65]. Clearly, the phenomenological model more reliable than strict empirical models due to the phenomenological model developed based on a physical picture by representing the complex geometry of bed void in the packed bed reactors.

Meanwhile, the model does not require any fitted parameters by two-phase data which reduce the variation in the results by complex two-phase parameters such as liquid maldistribution, wall effect, and axial dispersion. Extensive range of gas and liquid flow rate (at low and high interaction regimes) have applied to measure both pressure drop and a liquid holdup at different industrial catalyst shapes. Comparison in terms means relative error (MRE) is presented in Table 7.

It is stated that slit model appropriately predicted the influences of superficial gas velocity, superficial liquid velocity, and bed characteristics (size and shape) at low interaction flow regime [69], while [58] extended slit model and validated with low and high interaction flow regimes data. [58] reported that slit model applicable at low and high interaction flow regimes and the results of the extended model revealed considerable improve in pressure drop and liquid holdup prediction compared to the slit model.

Table 6. Correlations for pressure drop and liquid holdup

Author	Shape	Size	ϵ_B	Pressure	approach
Larachi et al., 1991	Glass beads	0.14-0.2	-	Up to 12MPa	Empirical
					$\beta_t = 1 - 10^{-\Gamma} \quad (17)$
					$\Gamma = 1.22 \frac{We_L^{0.15}}{X_G^{0.15} Re_L^{0.2}} \quad (18)$
					$\frac{(\Delta P/Z)d_h \rho_G}{2G^2} = \frac{1}{\{(Re_L We_L)^{0.25} X_G\}^{1.5}} \left[31.3 + \frac{17.3}{\{(Re_L We_L)^{0.25} X_G\}^{0.5}} \right] \quad (19)$
					where
					$X_G = \frac{G}{L} \sqrt{\frac{\rho_L}{\rho_G}}, \quad Re_L = \frac{\rho_L U_L d_p}{\mu_L}, \quad We_L = \frac{L^2 d_p}{\rho_L \sigma_L}, \quad d_h = \left[\frac{16\epsilon_B^3}{9\pi(1-\epsilon_B)^2} \right]$
[68], [76]	Glass beads Cylindrical	0.3 0.32×0.33	0.39 0.41	Up to 7.5MPa	Empirical
					$\beta_d = 3.8 \left(\frac{\rho_L U_L d_p}{\mu_L} \right)^{0.55} \left[\frac{d_p^3 \rho_L^2 g}{\mu_L^2} \left(1 + \frac{\Delta P/Z}{\rho_L g} \right) \right]^{-0.42} \left(\frac{6(1-\epsilon_B)d_p}{\epsilon_B} \right)^{0.65} \quad (20)$
					$\frac{\Delta P}{0.5 \rho_G U_G^2} \left(\frac{d_p}{Z} \right) = 155 \left[\frac{\rho_G U_G d_p \epsilon_B}{\mu_G (1-\epsilon_B)} \right]^{-0.37} \left[\frac{1-\epsilon_B}{\epsilon_B (1-\beta_t)} \right] \quad (21)$
[66], [79]	Spherical Cylindrical	0.116-0.3	0.27-0.49	Up to 10MPa	Empirical
					$\beta_d = 10^k \quad (22)$
					$k = 0.001 - \frac{0.42}{\left[X_L^{0.5} Re_L^{-0.3} \left(\frac{a_s d_h}{1-\epsilon_B} \right)^{0.3} \right]^{0.48}}$
					$\frac{(\Delta P/Z)d_h \rho_G}{2G^2} = 200(X_G \delta_2)^{-1.2} + 85(X_G \delta_2)^{-0.5} \quad (23)$
					Where
					$\delta_2 = \frac{Re_L^2}{(0.001 + Re_L^{1.5})}, \quad X_G = \frac{G}{L} \sqrt{\frac{\rho_L}{\rho_G}}, \quad X_L = \frac{1}{X_G}, \quad Re_L = \frac{\rho_L U_L d_p}{\mu_L}$
					$a_s = \frac{6(1-\epsilon_B)}{d_p}, \quad We_L = \frac{L^2 d_p}{\rho_L \sigma_L}, \quad We_G = \frac{G^2 d_p}{\rho_G \sigma_L}, \quad d_h = \left[\frac{16\epsilon_B^3}{9\pi(1-\epsilon_B)^2} \right]^{0.33} d_p$

Table 7. Comparison of Models to Individual Beds in Terms of MRE

Model	Spherical		Cylindrical		Trilobe		Quadrilobe		Total data	
	ϵ_L	Ψ_L								
Slit	44.14	55.78	5.89	36.80	12.88	33.15	12.51	24.37	18.50	37.52
Extended Slit	12.5	55.90	3.8	31.06	10.20	25.51	14.95	14.78	10.36	31.81
Empirical	135.62	19.42	63.41	44.20	60.89	17.76	42.05	59.66	75.49	35.26

Consequently, both slit and extended slit model used to investigate the effects of gas and liquid velocities and particle shape on pressure drop and liquid holdup prediction. Additionally, a totally empirical model presented by [65] has investigated the impacts of superficial gas and liquid velocities, and particle size on the pressure drop and liquid saturation. Empirical model applied in the current work to assess the impact of packing shape on the pressure drop and liquid holdup due to the absence of adjustable parameters related to the catalyst shape impacts in the model. Regarding the pressure drop prediction, the differences in the average MRE regardless of the packing shape between slit, extended slit, and the empirical model for pressure drop is approximately 3-6%.

The extended slit model presented a lower relative error (31.81%) compare to slit model relative error (37.52%) due to 70% of total data in high interaction flow regime that improved predict pressure drop. Furthermore, Figure 13 compares the dimensionless pressure drop predicted and experimentally observed by phenomenological models (slit and extended slit), and the empirical model (Larachi model). The comparison illustrated a very good agreement between the extended slit model (Al-Dahhan) and the experimental observation.

The accuracy of pressure drop prediction for extended slit model is much better than the empirical model due to the absence of adjustable parameters for packing shape impact in the empirical model as depicted in Figure 13. Moreover, due to the slit model developed based on a low interaction flow regime, the extended slit model revealed better prediction with 70% of total data at high interaction flow regime. It is evident that the average of MRE is relatively changed in each packing shape, but the predictions for dimensionless pressure drop are usually better for extended slit model (Figure 14b, 14c, and 14d) except the trend by the empirical model revealed overprediction in the spherical bed due to the model developed based on strictly empirical with the spherical shape of catalyst particles (Figure 14a). Consequently, the phenomenological model in both faces slit and extended slit models demonstrated an excellent prediction for pressure drop in the packed bed due to comprehensive representing for the most parameters that impact the two-phase pressure drop and increase the accuracy by developing the model with no fitted parameters at two-phase flow. Additionally, confirm and evaluate the effects of the packing shape and gas and liquid velocities on the pressure drop within different industrial catalyst particles.

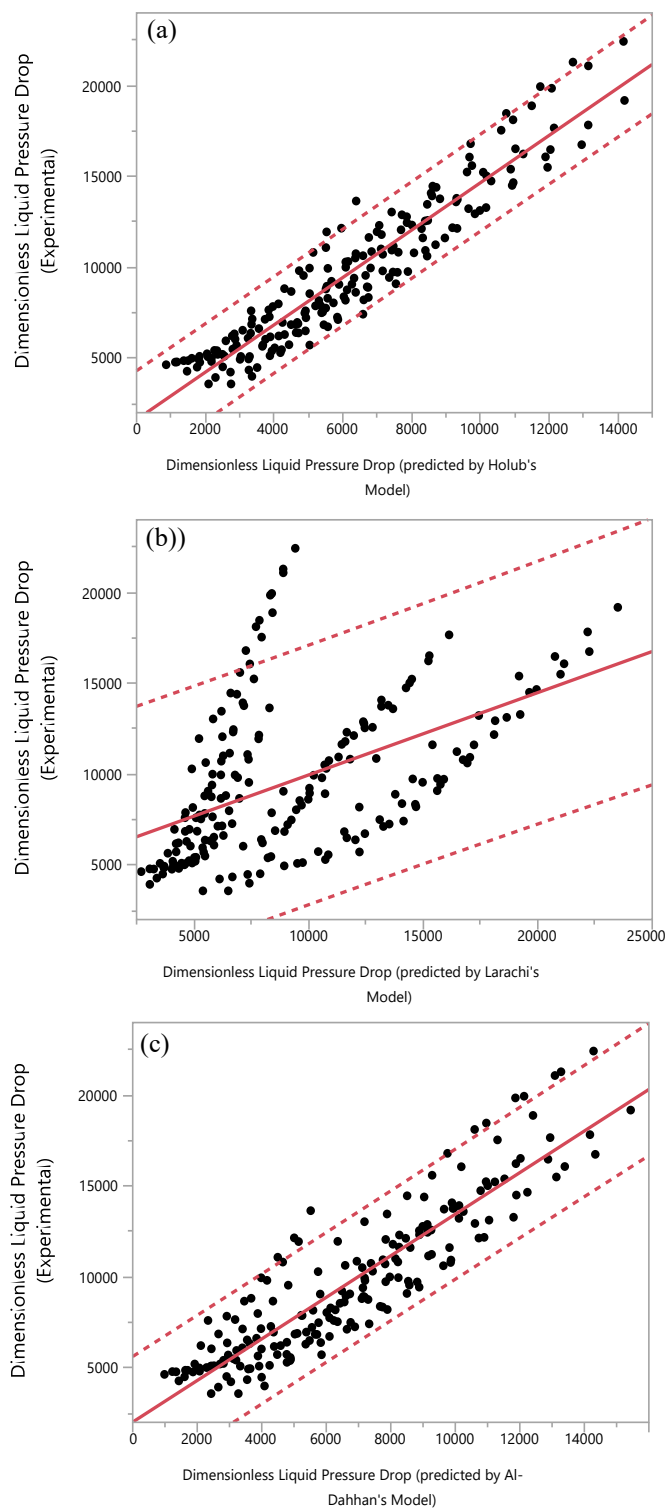


Figure 13. Comparison of predicted dimensionless pressure drop to experimental with 70% of total data at high interaction flow regime (a) slit model (by Holub) (b) empirical model (by Larachi) (c) extended model (by Al-Dahhan).

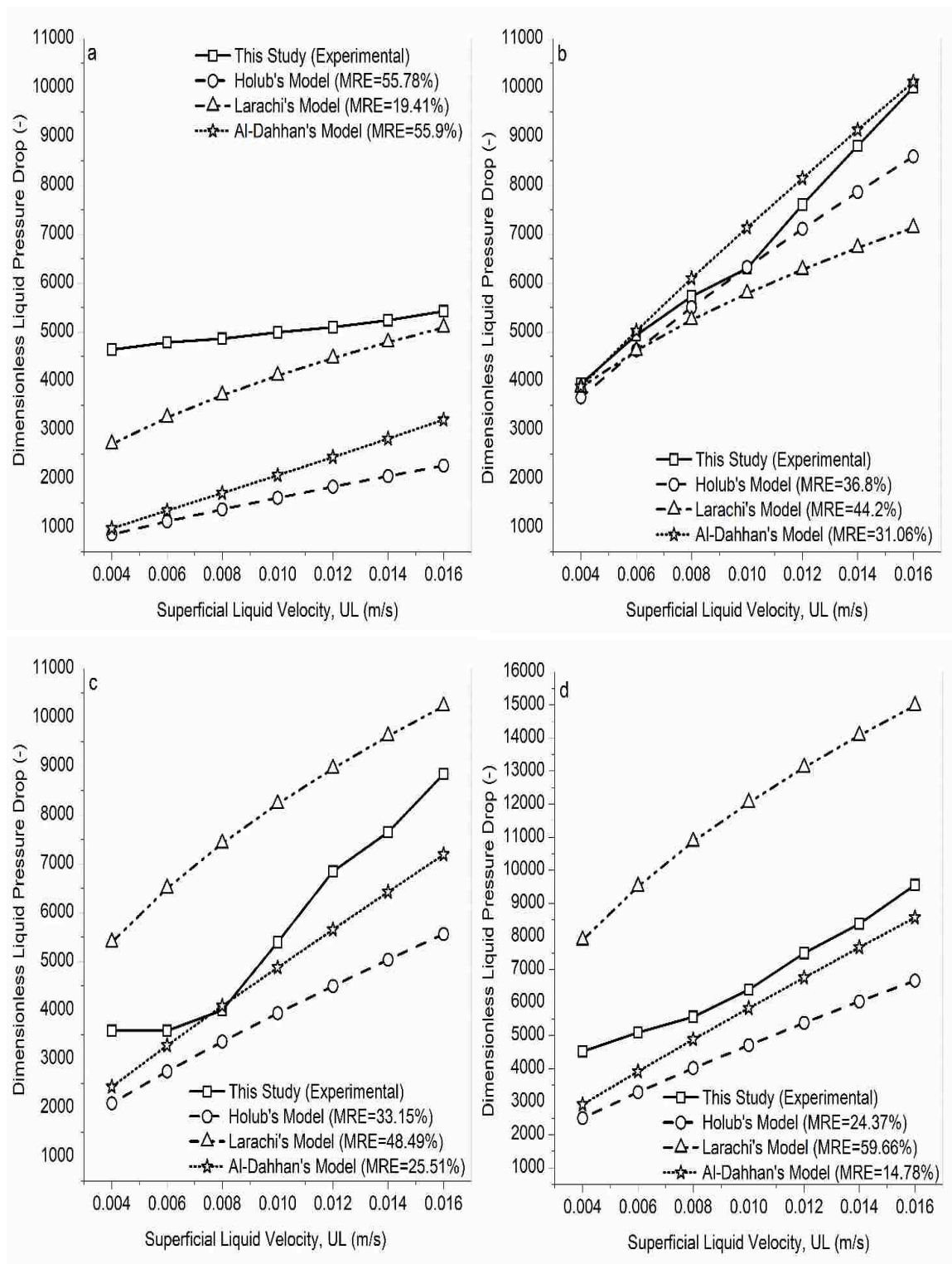


Figure 14. Comparison of dimensionless pressure drop data versus superficial liquid velocity for different model approaches, with (a) spherical (b) cylindrical (c) trilobe (d) quadrilobe catalyst particles.

4.5.2. Liquid Holdup. Regarding liquid holdup, widely efforts have been paid to develop a two-phase flow model to predict liquid holdup in TBRs. The liquid holdup is a crucial parameter for design due to it is significantly impacted the hydrodynamics in the reactors. In the present work, approximately 30% of the data is obtained at a low interaction flow regime. Phenomenological (slit model and extended slit model) and an empirical model [65] implemented compare the models to the data obtained at various bed geometry, gas flow rate, and liquid flow rate for the liquid holdup. The empirical model formulated correlation for liquid saturation which is the ratio of the liquid volume exist in the bed to the volume of void space of the bed. Figure 15 compares the predicted and experimental liquid holdup for the slit, extended slit, and empirical models. Table 5 shows the deviation of average MRE for liquid holdup with total data regardless of the bed shape and for each bed shape individually. The extended slit model by Al-Dahhan at 70% of total data at high interaction flow regime revealed overprediction with 10.36% for liquid holdup compared to 18.5% for slit model by Holub. Empirical model shows an underprediction trend with 75.49% MRE for the liquid holdup. Figure 15 compares the predicted and experimental liquid holdup at total data nevertheless to packing shape for the slit, extended slit, and empirical models. Comparison of the models to data at different catalyst shape of beds indicates that the empirical model by (Larachi 1991) is in underproduction for all beds, while the extended slit model showed better prediction with different beds as illustrated in Figure 16a, 16b, 16c, and 16d. The main reason for underprediction for the empirical model is the differences in the void space exist in the bed due to packing shape. Furthermore, the empirical model developed to predict liquid saturation that is why the MRE is higher than phenomenological models.

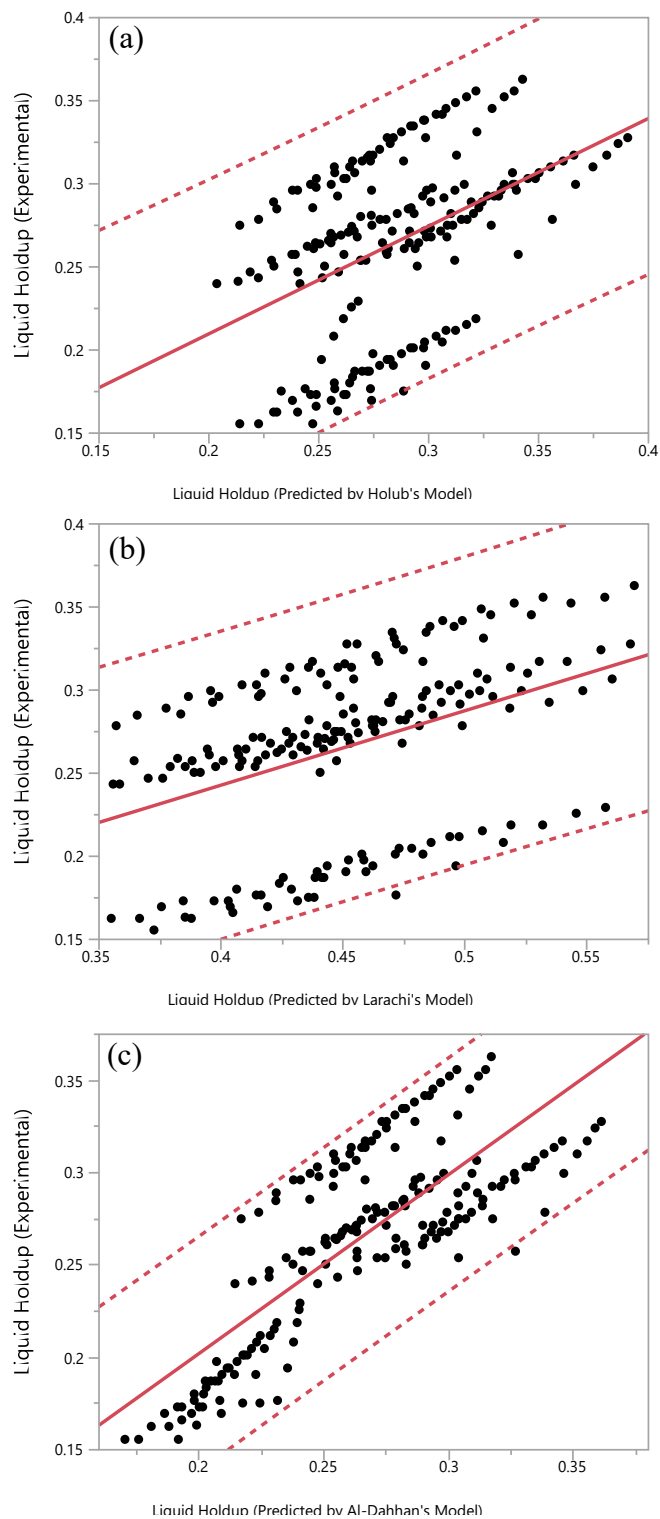


Figure 15. Comparison of predicted liquid holdup to experimental with 30% of total data at low interaction flow regime (a) slit model (by Holub) (b) empirical model (by Larachi) (c) extended model (by Al-Dahhan).

In the latter, the design of catalyst shape plays a central role on the liquid holdup in the packed bed reactors. Meanwhile, the phenomenological models showed a high accuracy to predict liquid holdup in different packing shapes in TBRs.

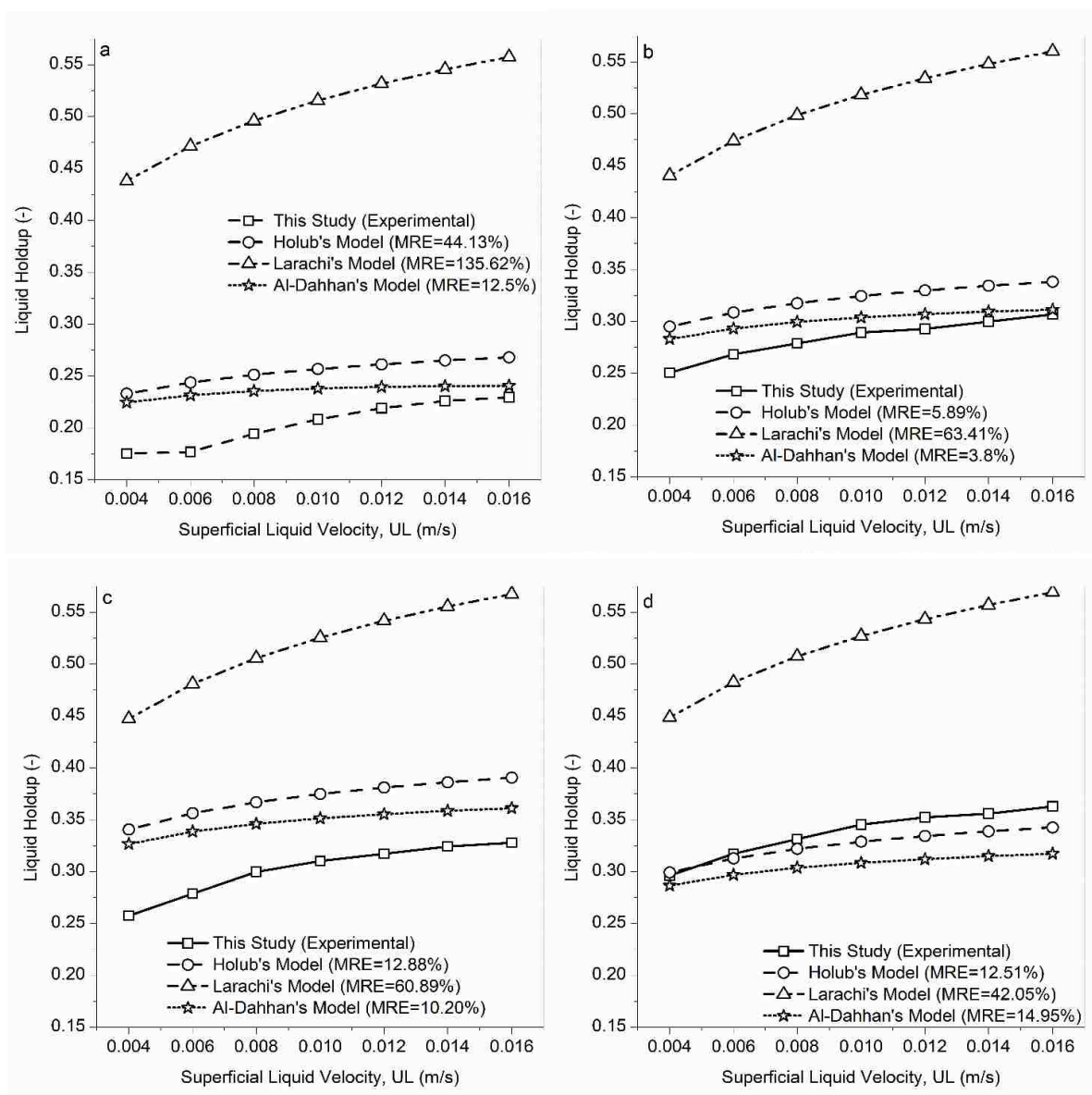


Figure 16. Comparison of liquid holdup data versus superficial liquid velocity for different model approaches, with (a) spherical (b) cylindrical (c) trilobe (d) quadrilobe catalyst particles.

5. REMARKS

Fluid dynamic parameters investigated in different industrial catalyst beds comprised of spherical, cylindrical, poly lobes (Trilobe and quadrilobe) particles. Additionally, the effects of gas flow rate and liquid flow rate on the hydrodynamics in different packing beds. The results revealed that the catalyst shape play a major role on the hydrodynamics in the TBRs. The catalyst shape in the packed bed reactors clearly impacted the void space, void distribution, and contact points between the adjacent particles in the bed and changed transport phenomena for gas and liquid in the reactor. Furthermore, a considerable effect for liquid flow rate on the hydrodynamic parameters is displayed in this study. The main finding can be concluded as follow:

1. The mapped transition boundaries illustrated the transition flow for cylindrical and poly lobes (trilobe and quadrilobe) particles identified at lower liquid flow rate compared to spherical particles. At low gas flow rate, no change is recorded in the flow pattern between cylindrical and ploy lobes particles. The percentage of total data at low interaction flow regime was 30% and at high interaction flow regime was 70%. On other hands, at high gas flow rate, no differences in the gas and liquid interaction diagnosed between all catalyst shapes.
2. A significant impact for catalyst shape, gas flow rate, and liquid flow rate on the pressure drop is illustrated in the different packing beds. A considerable increase in the magnitude in the cylindrical and ploy lobe particles compared to spherical particles, while a noticeable reduction in the pressure drop for poly lobes particles compared to the cylindrical particles.

3. The magnitude of the liquid holdup influenced significantly with the catalyst shape, gas flow rate, and liquid flow rate for in the column. The high magnitude for cylindrical and poly lobes particles compared to the spherical particles and the poly lobes beds displayed a considerable enhancement than the cylindrical bed in the TBR. Furthermore, increase liquid flow rate was increased the liquid holdup with different catalyst shapes.
4. Comparison between experimental observation and different models approaches using phenomenological (slit) and empirical approaches to investigate the effect of catalyst shape, gas flow rate, and liquid flow rate on the pressure drop and liquid holdup in TBR. The phenomenological approach developed based on the physical picture at low interaction flow regime (Holub) and developed to extend slit model at high interaction flow regime (Al-Dahhan). Additionally, empirical approach formulated based on strictly empirical (Larachi).
5. Phenomenological models indicated a high accuracy for pressure drop compared to the empirical model. The extended slit model was better than slit model within different operating conditions in the reactor. The average mean relative error (MRE) for total pressure drop regardless the shape of the bed for slit model was 37.52%, and for extended slit model was 31.81%, while for the empirical model was 35.26%.
6. The comparison between predicted values and experimental observations for liquid holdup showed an excellent agreement with the extended slit model compared to the slit and empirical models. The MRE was 10.36% for extended slit model and 18.5% and 75.49% for the slit and empirical models, respectively.

7. According to the findings of present work, additional investigation on the bed characteristics such as tortuosity in need to be developed which it will be so helpful for better understanding in the TBRs. Furthermore, study the effects of catalyst shape and other design parameters on the pressure drop and liquid holdup using advanced techniques is strongly recommended for extended the fundamental information.

ACKNOWLEDGMENT

The author thankfully acknowledge the financial support in the form of scholarship provided by Ministry of Higher Education and Scientific Research-Iraq, and the funds provided by Missouri S&T and Professor Dr. Al-Dahhan to develop the experimental set-up and to perform the present study.

REFERENCES

- [1] M. H. Al-Dahhan, M. R. Khadilkar, Y. Wu, and M. P. Dudukovic, "prediction of Pressure Drop and Liquid Holdup in High-Pressure Trickle-Bed Reactors," vol. 5885, no. 97, pp. 793–798, 1998.
- [2] C. N. Satterfield, "Trickle-bed reactors," *AIChE J.*, vol. 21, no. 2, pp. 209–228, 1975.
- [3] M. R. Khadilkar, P. L. Mills, and M. P. Dudukovic, "Trickle-bed reactor models for systems with a volatile liquid phase," *Chem. Eng. Sci.*, vol. 54, no. 13–14, pp. 2421–2431, 1999.
- [4] M. H. Al-Dahhan, "Trends in Minimizing and Treating Industrial Wastes for Sustainable Environment," *Procedia Eng.*, vol. 138, pp. 347–368, 2016.
- [5] K. Anuar Mohd Salleh, H. Koo Lee, and M. H. Al-Dahhan, "Studying local liquid velocity in liquid-solid packed bed using the newly developed X-ray DIR technique," *Flow Meas. Instrum.*, vol. 42, pp. 1–5, 2015.

- [6] J. Guo and M. Al-Dahhan, "Liquid holdup and pressure drop in the gas-liquid cocurrent downflow packed-bed reactor under elevated pressures," *Chem. Eng. Sci.*, vol. 59, no. 22–23, pp. 5387–5393, 2004.
- [7] A. Atta, S. Roy, and K. D. P. Nigam, "Prediction of pressure drop and liquid holdup in trickle bed reactor using relative permeability concept in CFD," *Chem. Eng. Sci.*, vol. 62, no. 21, pp. 5870–5879, 2007.
- [8] A. Attou, C. Boyer, and G. Ferschneider, "Modelling of the hydrodynamics of the cocurrent gas-liquid trickle flow through a trickle-bed reactor," *Chem. Eng. Sci.*, vol. 54, no. 6, pp. 785–802, 1999.
- [9] C. Boyer, C. Volpi, and G. Ferschneider, "Hydrodynamics of trickle bed reactors at high pressure: Two-phase flow model for pressure drop and liquid holdup, formulation and experimental validation," *Chem. Eng. Sci.*, vol. 62, no. 24, pp. 7026–7032, 2007.
- [10] M. H. Al-Dahhan, F. Larachi, M. P. Dudukovic, and A. Laurent, "High-Pressure Trickle-Bed Reactors: A Review," *Ind. Eng. Chem. Res.*, vol. 36, no. 8, pp. 3292–3314, 1997.
- [11] S. T. Sie and R. Krishna, "Process development and scale up: II. Catalyst Design Strategy," *Rev. Chem. Eng.*, vol. 14, no. 3, pp. 159–202, 1998.
- [12] S. Afandizadeh and E. A. Foumeny, "Design of packed bed reactors: Guides to catalyst shape, size, and loading selection," *Appl. Therm. Eng.*, vol. 21, no. 6, pp. 669–682, 2001.
- [13] K. M. Brunner *et al.*, "Effects of particle size and shape on the performance of a trickle fixed-bed recycle reactor for fischer-tropsch synthesis," *Ind. Eng. Chem. Res.*, vol. 54, no. 11, pp. 2902–2909, 2015.
- [14] K. D. P. Nigam, a K. Saroha, a Kundu, and H. J. Pant, "Radioisotope tracer study in trickle bed reactors," *Can. J. Chem. Eng.*, vol. 79, no. 6, pp. 860–865, 2001.
- [15] A. Chander, A. Kundu, S. K. Bej, A. K. Dalai, and D. K. Vohra, "Hydrodynamic characteristics of cocurrent upflow and downflow of gas and liquid in a fixed bed reactor," *Fuel*, vol. 80, no. 8, pp. 1043–1053, 2001.
- [16] M. E. Trivizadakis, D. Giakoumakis, and A. J. Karabelas, "A study of particle shape and size effects on hydrodynamic parameters of trickle beds," *Chem. Eng. Sci.*, vol. 61, no. 17, pp. 5534–5543, 2006.
- [17] M. Bazmi, S. H. Hashemabadi, and M. Bayat, "Extrudate Trilobe Catalysts and Loading Effects on Pressure Drop and Dynamic Liquid Holdup in Porous Media of Trickle Bed Reactors," *Transp. Porous Media*, vol. 99, no. 3, pp. 535–553, 2013.
- [18] M. and M. P. D. H. Al-Dahhan, "Pressure Drop and Liquid Holdup in High Pressure Trickle-Bed Reactors," *Chem. Eng. Sci.*, vol. 49, no. 24B, pp. 5681–5698, 1994.

- [19] A. Muzen and M. C. Cassanello, "Flow regime transition in a trickle bed with structured packing examined with conductimetric probes," *Chem. Eng. Sci.*, vol. 62, no. 5, pp. 1494–1503, 2007.
- [20] N. M. and G. W. Larachi, F., A. Laurent, "Experimental Study of A Trickle-Bed Reactor Operating at High Pressure: Two-Phase pressure Drop and Liquid Saturation," *Chem. Eng. Sci.*, vol. 46, no. 5/6, pp. 1233–1246, 1991.
- [21] M. J. Ellman, N. Midoux, G. Wild, A. Laurent, and J. C. Charpentier, "Anew, Improved liquid hold-up correlation for trickle bed reactors," *Chem. Eng. Sci.*, vol. 45, no. 7, pp. 1677–1684, 1990.
- [22] W. J. A. W. and K. R. Westerterp, "Hydrodynamics in a Pressurized Cocurrent Gas-Liquid Trickle-Bed Reactor," *Chem. Eng. Technol.*, vol. 14, pp. 406–413, 1991.
- [23] A. Wammes, S. J. Mechielsen, and R. Engineering, "The influence of pressure on the liquid hold-up in a co-current reactor operating at low gas velocities," *J. Hydrodyn.*, vol. 24, no. 1, pp. 39–49, 1991.
- [24] R. A. Holub, M. P. Dudukovic, and P. A. Ramachandran, "A phenomenological model for pressure drop, liquid holdup, and flow regime transition in gas-liquid trickle flow," *Chem. Eng. Sci.*, vol. 47, no. 9–11, pp. 2343–2348, 1992.
- [25] R. A. Holub, M. P. Duduković, and P. A. Ramachandran, "Pressure drop, liquid holdup, and flow regime transition in trickle flow," *AIChE J.*, vol. 39, no. 2, pp. 302–321, 1993.
- [26] M. P. Duduković, F. Larachi, and P. L. Mills, "Catalysis Reviews : Science and Engineering Multiphase catalytic reactors : a perspective on current knowledge and future trends," *Catal. Rev. Sci. Eng.*, vol. 44, no. February 2012, pp. 123–246, 2013.
- [27] V. V Ranade, R. Chaudhari, and P. R. Gunjal, *Trickle Bed Reactors: Reactor Engineering and Applications*. Elsevier Science, 2011.
- [28] Sabri Ergun, "Fluid Flow Through Packed Columns," *Chem. Eng. Prog.*, vol. 48, no. 2, pp. 89-, 1952.
- [29] I. F. Macdonald, M. S. El-Sayed, K. Mow, and F. A. L. Dullien, "Flow through Porous Media—the Ergun Equation Revisited," *Ind. Eng. Chem. Fundam.*, vol. 18, no. 3, pp. 199–208, 1979.
- [30] D. E. Sweeney, "Correlation for Pressure Drop in Flow in Packed Beds," vol. 13, no. 4, pp. 663–669.
- [31] V. Specchia and G. Baldi, "Pressure drop and liquid holdup for two phase concurrent flow in packed beds," *Chem. Eng. Sci.*, vol. 32, no. 5, pp. 515–523, 1977.
- [32] A. E. Saez and R. G. Carbonell, "Hydrodynamic Parameters for Gas-Liquid Cocurrent Flow in Packed Beds.," *AIChE J.*, vol. 31, no. 1, pp. 52–62, 1985.
- [33] R. a Holub, "Hydrodynamics of Trickle Bed Reactors," 1990.

- [34] W. J. a. Wammes, J. Middelkamp, W. J. Huisman, C. M. DeBass, and K. R. Westerterp, "Hydrodynamics in a cocurrent gas-liquid trickle bed at elevated pressures," *AIChE J.*, vol. 37, no. 12, pp. 1849–1862, 1991.
- [35] M. H. Al-Dahhan, "Effects of high pressure and fines on the hydrodynamics of trickle bed reactors.pdf," 1993.
- [36] I. Iliuta, F. Larachi, and B. P. A. Grandjean, "Pressure Drop and Liquid Holdup in Trickle Flow Reactors: Improved Ergun Constants and Slip Correlations for the Slit Model," *Ind. Eng. Chem. Res.*, vol. 37, no. 12, pp. 4542–4550, 1998.
- [37] F. Larachi, A. Laurent, G. Wild, and N. Midoux, "Some experimental liquid saturation results in fixed-bed reactors operated under elevated pressure in cocurrent upflow and downflow of the gas and the liquid," *Ind. Eng. Chem. Res.*, vol. 30, pp. 2404–2410, 1991.
- [38] M. J. Ellman, N. Midoux, A. Laurent, and J. C. Charpentier, "A new, improved pressure drop correlation for trickle-bed reactors," *Chem. Eng. Sci.*, vol. 43, no. 8, pp. 2201–2206, 1988.

III. PHASE DISTRIBUTION INVESTIGATIONS IN A MIMICKED BENCH SCALE HYDROTREATER REACTOR USING GAMMA-RAY DENSITOMETRY (GRD)

Mohammed Al-Ani^a, Hamza AlBazzaz^b, Muthanna Al-Dahhan^{a*}

^a Multiphase Reactors Engineering and Applications Bench (mReal), *Department of Chemical and Biochemical Engineering, Missouri University of Science and Technology, Rolla, MO 65409-1230. USA*

^b Kuwait Institute for Science Research, P.O. Box 24885, 13109, Kuwait

ABSTRACT

Bench-scale trickle bed reactors (TBRs) are difficult for researchers to use. Phase distribution and holdup are key parameters that significantly affect the performance in the reactor. In the real practice, bench-scale reactors have been used to testing catalyst particles, feedstock, and operation conditions. An advanced non-invasive gamma-ray densitometry (GRD) technique was implemented to investigate phase distribution and holdup in the bench-scale TBR. GRD has been used commonly in real practice at safe level. The results were validated by phantom results that revealed an ability to recognize the difference between substances and phases. A new methodology was followed to calculate the line averaged phase holdup in the bench-scale TBRs. A Plexiglas transparent column with a 1.18 cm inside diameter and a 72 cm length was conducted the experiments. Cold unit (air-water) was used to investigate the phase distribution and dynamic liquid holdup in the bench-scale reactor. However, the results is not applicable to the real practice, but to extrapolate it in the real hot unit. The study examined the effects of the distributor region, inlet configuration for mixed gas and liquid (side and top directions), and gas and liquid flow rates on the phase distribution and dynamic liquid holdup in diluted and non-diluted beds. The diluted bed results showed that significant improvement in the phase distribution

and dynamic liquid holdup.. Also, the exhibited inlet configuration for mixed gas and liquid has an impact on the phase distribution diameter profile and the magnitude of the dynamic liquid holdup in both diluted and non-diluted beds. Furthermore, the range of the dynamic liquid holdup diameter profile increased with increasing liquid flow rate, whereas the range was shown to decrease with increasing gas flow rate within diluted and non-diluted beds in the bench-scale fixed beds.

Keywords:

Scaled down, fixed bed reactor, dilution technique, commercial size of trilobe catalyst particles, radioactive Gamma-ray Densitometry, phase distribution and dynamic liquid holdup

Highlights:

- Wall effect and maldistribution in industrial size of trilobe catalyst particles in scaled down TBR.
- Wall effect and maldistribution reduced by dilution in bench-scale TBR.
- A significant effect of Inlet direction for fluids on performance in TBR.
- High capability and flexibility to recognize phase by GRD in TBR.

1. INTRODUCTION

Catalytic systems are one of the most important systems that are broadly used in the industry. Ordinarily, catalytic processes are carried out in the multiphase reactors using

heterogeneous solid catalysts. Among these reactors trickle bed reactors (TBRs) which have been extensively used for heterogeneous catalytic processes [1]–[4].

TBRs are conducted by concurrent downward flow of gas and liquid phases over a fixed-bed of catalyst particles. TBRs are widely applied in the petroleum industry in hydrotreating processes like hydrodesulphurization (HDS) and hydrodenitrogenation (HDN), petrochemical processes like hydrogenation and oxidation, chemical processes like reactive amination, waste treatment processes, electrochemical processes, and others [5]–[7].

Commercially, there is much interest in improvements and in development of sophisticated techniques that could monitor and measure performance hydrodynamic, transport, and reaction parameters with high efficiency for these kind of reactors. The performance of TBRs is a function not only of temperature and pressure, but also of hydrodynamics, reactor design, and catalyst design [8]–[12].

The commercial TBR design, scale-up, and catalyst testing and selection (scale-down) depend on the results of the bench-scale reactor. Thus, the bench-scale studies have been conducted for two different approaches. First approach is for scale-up that translates the bench-scale data to commercial-scale units. The second approach is for scale-down approach, which it is implemented to investigate the industrial units in operation and to examine the behavior of new catalysts, alternative feedstock, and/or operating conditions [8], [13], [14].

For the scale-up and scale-down studies of TBRs, the following have been used:

- Maintaining similar hourly space velocity with a reduction in residence time distribution (RTD) which is commonly used in industry.

- Using different hourly space velocity while maintaining similar RTD, which is used for conversion studies [14].

For bench-scale units the challenges are using low flow rates with commercial catalyst particles in small diameter reactor where the ratio of reactor diameter to particle diameter (D_c/d_p) is less than 20 [9]. This gives rise to wall effects, axial dispersion, liquid maldistribution, a low range of liquid holdup, incomplete wetting, and hence incomplete catalyst utilization. To reduce these effects catalyst bed dilution with fines has been used [8], [12], [14]–[17].

In the past few decades, extensive experimental works have been done to assess the capability of bed dilution with fines in overcoming the shortcomings mentioned above of bench-scale units. It has been found that the bed dilution with fine helps in Reducing the effect of the length of the reactor, decreasing the wall effects, and improved the catalyst wetting and utilization [8], [14], [18]–[24]. Most of the published works in the literature studied the effect of bed dilution on various parameters including reactor performance using spherical and cylindrical catalyst particles.

The shape of catalyst particles has been studied over the last few decades as it plays an essential role in significantly improving the performance of TBRs. Many researchers have argued that the shape of catalyst particles influences the active surface area per unit volume of solids, structure strength, simplicity in construction, manufacturing cost, bed void, pressure drop, and transport properties [25]–[28]. Therefore, for commercial applications trilobe and quadrilobe catalyst particles have been introduced particularly the trilobe catalyst particles for hydrotreating processes such as the hydrodesulphurization process [27], [29], [30]. However, in general studies related to trilobe catalyst particles

have been relatively sparse, but a few studies have examined the effects of trilobe catalyst particles on the hydrodynamic parameters in TBRs [28], [31]–[33].

Among these hydrodynamic parameters, the phase distribution is one of the most critical hydrodynamic parameters in packed bed reactors due to its significant effects on the performance. Many factors govern liquid distribution in TBRs, such as catalyst particle size and shape, gas and liquid flow rates, fluid properties, prewetting, packing method, inlet gas and liquid distributors, and flow pattern [34]–[36]. Liquid maldistribution is an essential reason for mal-contact between liquid-solid and gas-liquid, incomplete catalyst utilization, small ranges of liquid holdup, hot spots, and catalyst deactivation [10], [36]–[38]. It should also be mentioned that inlet distributor of gas and liquid represents the most crucial factor that impacts liquid distribution in the TBRs [16], [38], [39]. The following techniques have been used to measure and study the liquid distribution in various size of TBRs: flux collectors [40], [41]; electrical tomography [42], [43]; X-rays [44], [45]; magnetic resonance imaging (MRI) [46], [47]; and gamma-ray computed tomography (CT) [48], [49]. However, there have been no attempts to examine the phase distribution using trilobe catalyst particles with and without bed dilution with fine particles in the bench-scale TBRs. That is used in industry for catalyst testing feed stocks evaluation, and for studying operating conditions effects.

Furthermore, the liquid holdup is considered to be one of the crucial parameters in the TBRs. Hence, the investigation of liquid holdup in TBRs adds more understanding and knowledge to assess the reactor performance, design, physical and chemical interactions, and performance [18], [19], [50]. Low liquid holdup could indicate occurrence of low wetting efficiency that refers to an incomplete utilization of the pellet particles and non-

uniform heat distribution. thus, hotspots, bypassing, deactivation of catalyst particles, and dead zones will be a consequence for a low range of liquid holdup [9], [35], [51]. In the bench-scale reactors, the liquid holdup has been measured using a weight scale (also called a stop flow technique), residence time distribution, and tomography.

Accordingly, this work focuses on assessing the liquid distribution and holdup in a mimicked bench scale hydrotreater reactor packed with trilobe catalyst particles without and with fines using gamma-ray densitometry. The significance of this work is that while these commercial catalysts have been tested in bench scales TBRs at the industrial operation conditions there is no knowledge how uniform is the liquid distribution with and without fines and what is the range of the liquid holdup. Therefore, in this work such findings will be sought using room conditions and air-water system as a first step toward extending the application of gamma-ray densitometry to the real bench scale hydrotreated operated at industrial conditions. The work involves studying of the effects the flow rates of the gas and liquid and the inlet direction of gas and liquid distributors. The GRD technique, which developed in the Multiphase Flow and Reactors Engineering and Applications Laboratory (mFReal) at Missouri University of Science and Technology (S&T) for measuring instantaneous and time averaged line averaged hold up in multiphase flows, is vital for this study as it can measure holdups at several levels along the diameter, which offers new insights. However, to the best of the authors' knowledge, no work has been found that uses a non-invasive advanced GRD technique for such application. It should be also noted that most of the published liquid holdup data represent the total liquid holdup of the packed beds obtained by drainage or other similar techniques. However, in

this paper, we implement a single beam radioactive gamma rays, to measure the gas-liquid-solid phase distribution and holdups in trickling flow reactors.

2. EXPERIMENTAL WORK

2.1. EXPERIMENTAL SETUP

Bench-scale trickle bed reactors (TBRs) were developed to mimic the industrial hot bench-scale TBR hydrotreater unit as shown in Figure 1. Transparent Plexiglas reactor of internal diameter (I.D.) of 1.18 cm and a height of 72 cm was constructed with concurrent downward gas and liquid flow through the catalyst bed and 3 mm stainless steel pipe was fixed in the center of column as a thermowell as displayed in Figure 2. Air and water were used as the gas and liquid phases. The compressed air flow rate was controlled by two gas rotameters (Dwyer Instruments INC. RMC-106-SSV and RMC-102-SSV). The water was pumped from a water tank using a Weg Motor - HYPRO-00156OS1BJP56J, and the liquid flow rate was adjusted by one rotameter (Omega). Air and water were mixed and then fed to the reactor using two different inlet distributors on the top and side of the column as shown in Figure 3. No distributor was used in this work as mimicked for industrial hot bench-scale hydrotreater TBR. The effects of mixed of gas and liquid inlet direction investigated in this work on the phase distribution, range of liquid holdup, wettability, and catalyst utilization. The experiments were carried out at ambient temperature with a range of gas flow rate from 269.5 to 1796.5 cc/min and range of liquid flow rate from 0.39 to 2.46 cc/min. Different layers of particles employed in the reactor are shown in Figure 2 and the packed bed characteristics exhibited in Table 1.

Table 1. Characteristics of packed catalyst particles used in the reactor.

Reactor/ Packing	Characteristics
Reactor	inside diameter = 1.18 cm height = 72 cm
Packing	
COMMERCIAL TRILOBE CATALYST	length: 3 mm diameter: 1.5 mm
INERT BALL(ALUMINA)	Bed height: 60 cm diameter= 2mm Height = 2 cm in the top Height = 2cm in the bottom
NONPOROUS LAYER	Material: Medium Carborundum particles Bulk density = 1.67 (g/cc) Height = 4 cm over the trilobe Height = 4 cm under the trilobe
FINES PARTICLES	Material: Fine Carborundum particles Size: 350-500 μ m Bulk density = 1.76 (g/cc)

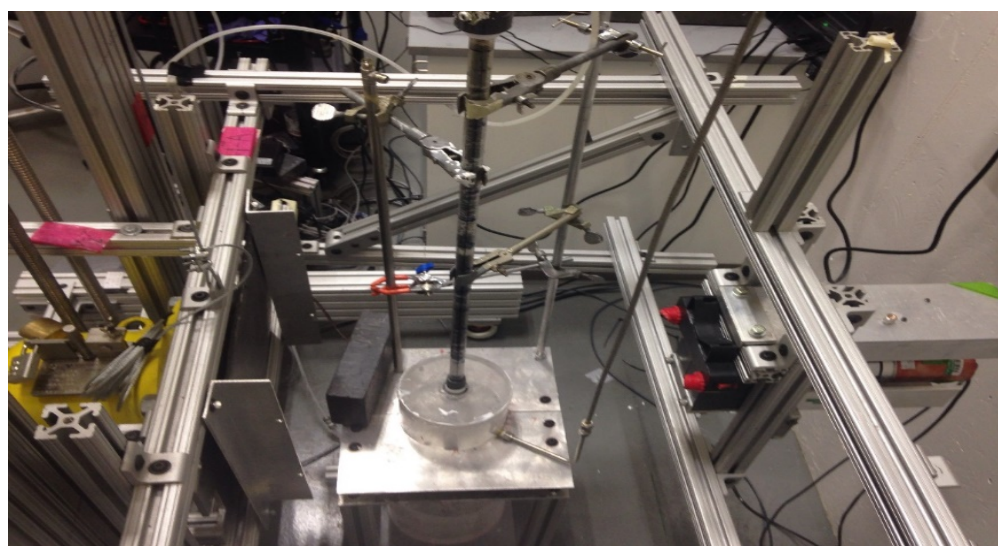


Figure 1. Physical picture for mimicked industrial hot bench-scale TBR hydrotreater unit.

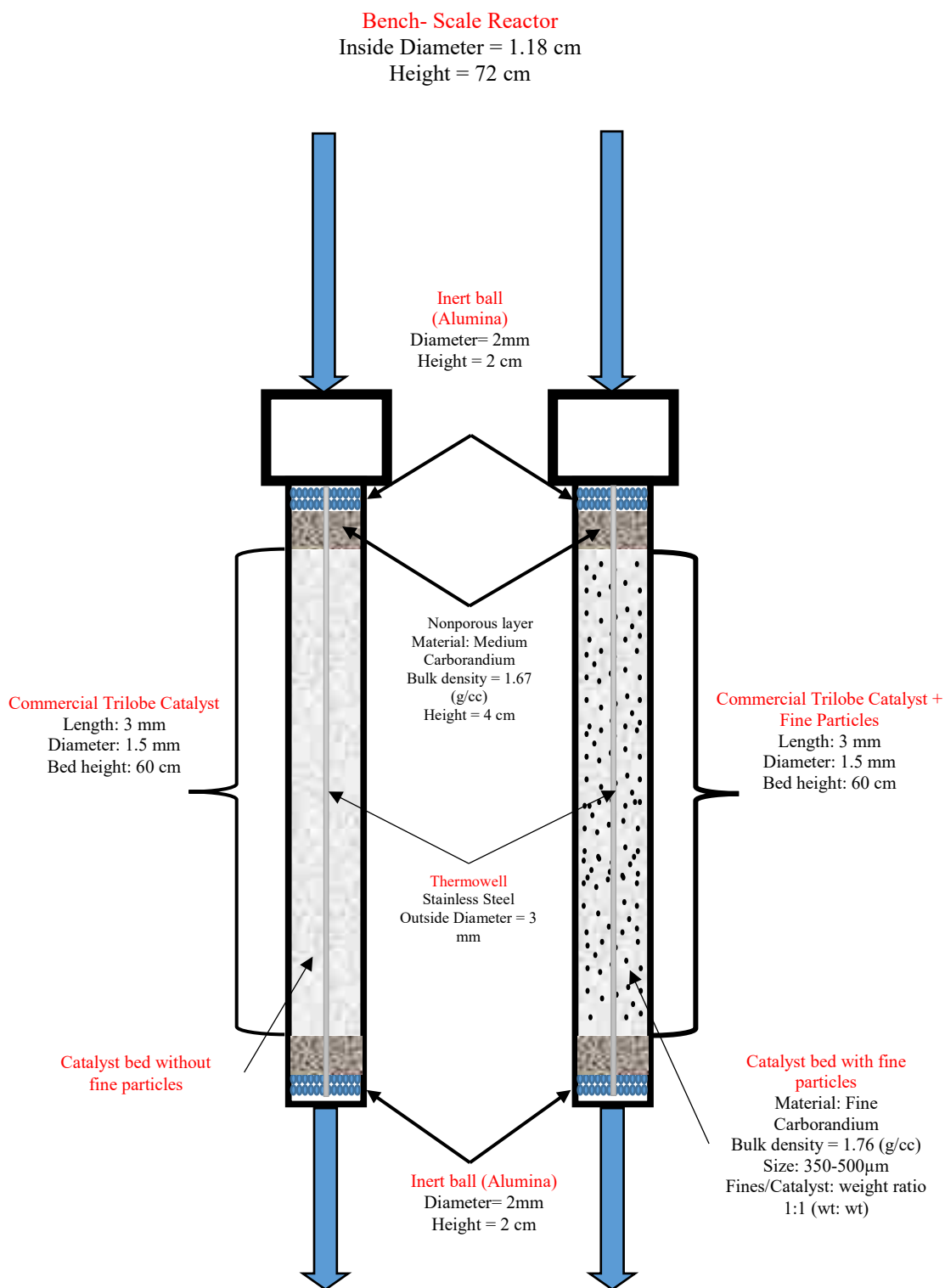


Figure 2. Bench-scale TBR design

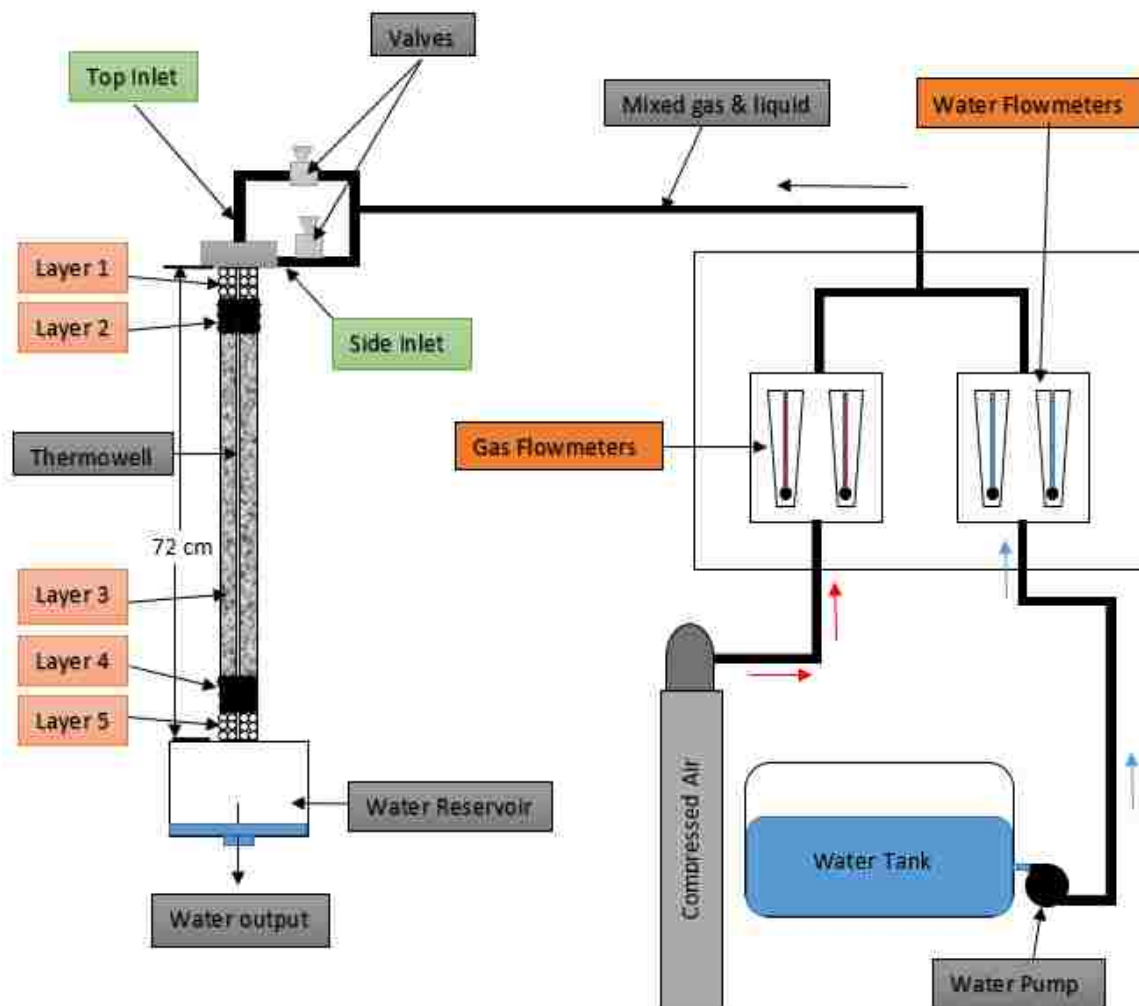


Figure 3. Schematic diagram for trickle bed reactor.

2.2. GAMMA-RAY DENSITOMETRY (GRD) TECHNIQUE

GRD is a non-invasive online single beam of gamma-ray that measures line averaged holdups, flow regime, and maldistribution. It consists of a collimated sealed source and a collimated NaI detector aligned with source opening mounted on the opposite side. The structure of the techniques was designed to allow horizontal and vertical

movement of the source-detector-set-up via the computer using stepper motor while the unit can be rotated manually around the column or the object.

For this experiment the GRD unit has moved multiple axial and radial positions; six levels along with the bed height (layer 3 of packing) in axial positions with equally spaced of 10 cm apart and 11 radial positions along the diameter with equally spaced of 0.18 cm apart for each axial level. One axial level is in the top layer for catalyst (layer 3 of packing) representing the distribution region of 5 cm above the catalyst bed as shown in Figure 4a and b.

The fundamental of the GRD measurement is based on number photon counts penetrate through substances. The number of photon counts changes by elements density which each element has a different density. Cs-137 has been used as a sealed collimated source with an initial activity of approximately 250 mCi from 2011. The source was housed inside a sealed chamber of lead as displayed in Figures 5a and b. A single beam with a beam angle about 10° that was directed straight towards a mounted detector collimated with 1 mm collimator opening. a collimated NaI scintillating detector was mounted on the opposite side of the sealed source as shown in Figure 6 that receives the radiation beam. The detector linked directly to data acquisition system that contained an Osprey unit (digital MCA tube base for gamma-ray spectrometry), a USB interface, and software to display and analyze of gamma-ray spectrometry data from the detector as shown in Figure 6a. The detector collimated and fixed inside the shielded chamber to ensure there was no detection for any scattering, as shown in Figure 6b. A total distance of 60 cm is between the source mounted on one side and the detector mounted on the other side.

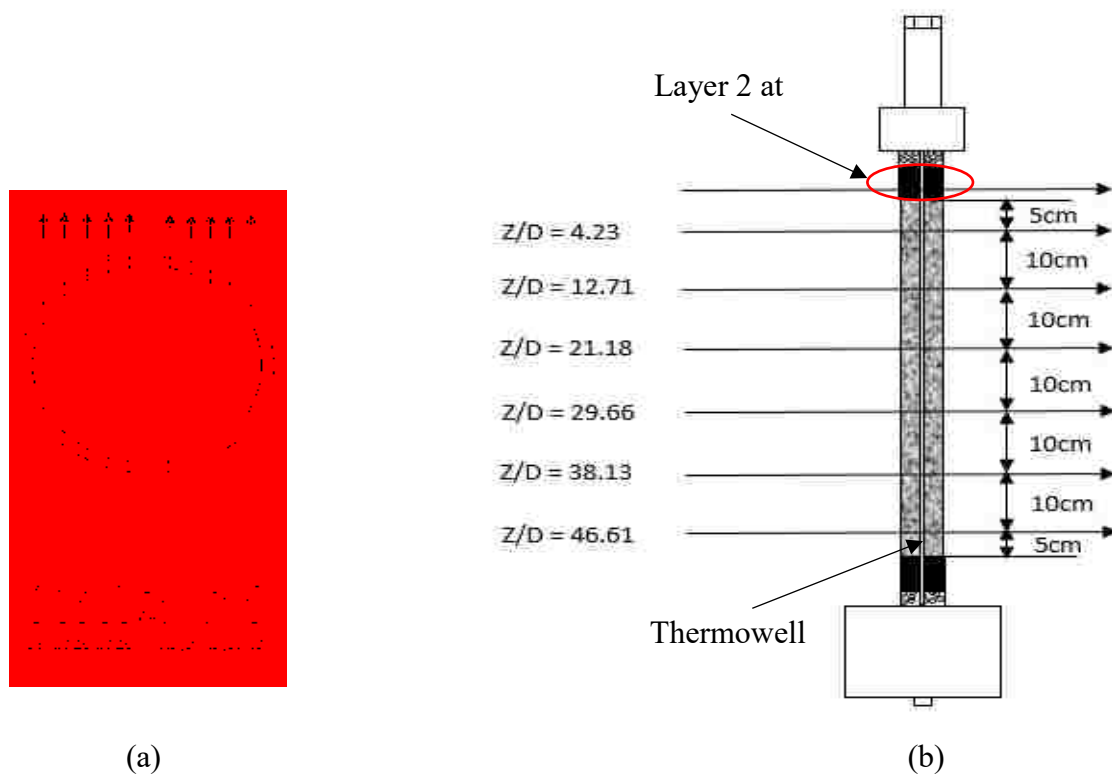


Figure 4. Online Single Beam of GRD at axial and radial positions.

The TBR was placed in the center between the source and the detector as revealed in Figure 7a and b. The GRD technique was designed to move with axial and radial directions with high flexibility by using multi-stepping motors controlled automatically by Ospry software. The GRD technique has been designed and developed to measure the line-averaged hold-up profile of three phases along the column diameter radially and along the bed height axially. The same technique is employed to detect the interstitial space profile between the catalyst particles.

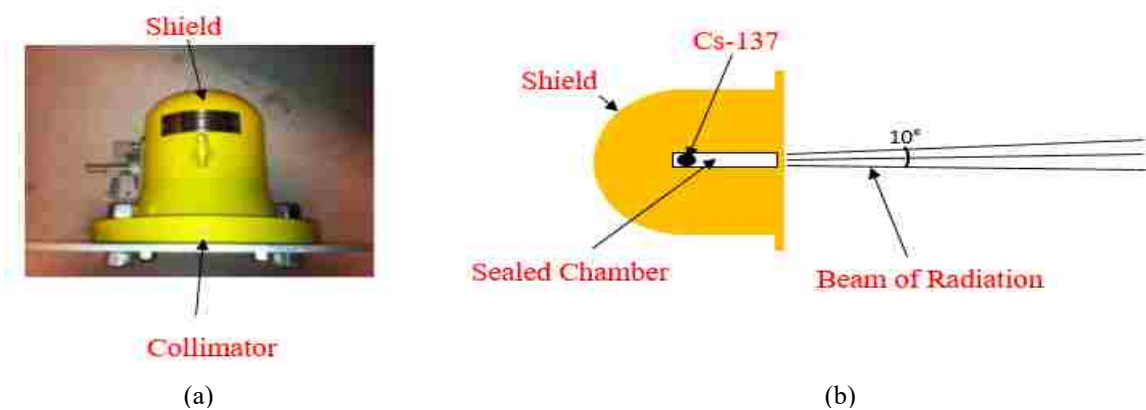


Figure 5. (a) Photo for Gamma-ray source (b) schematic diagram for Gamma-ray Source.

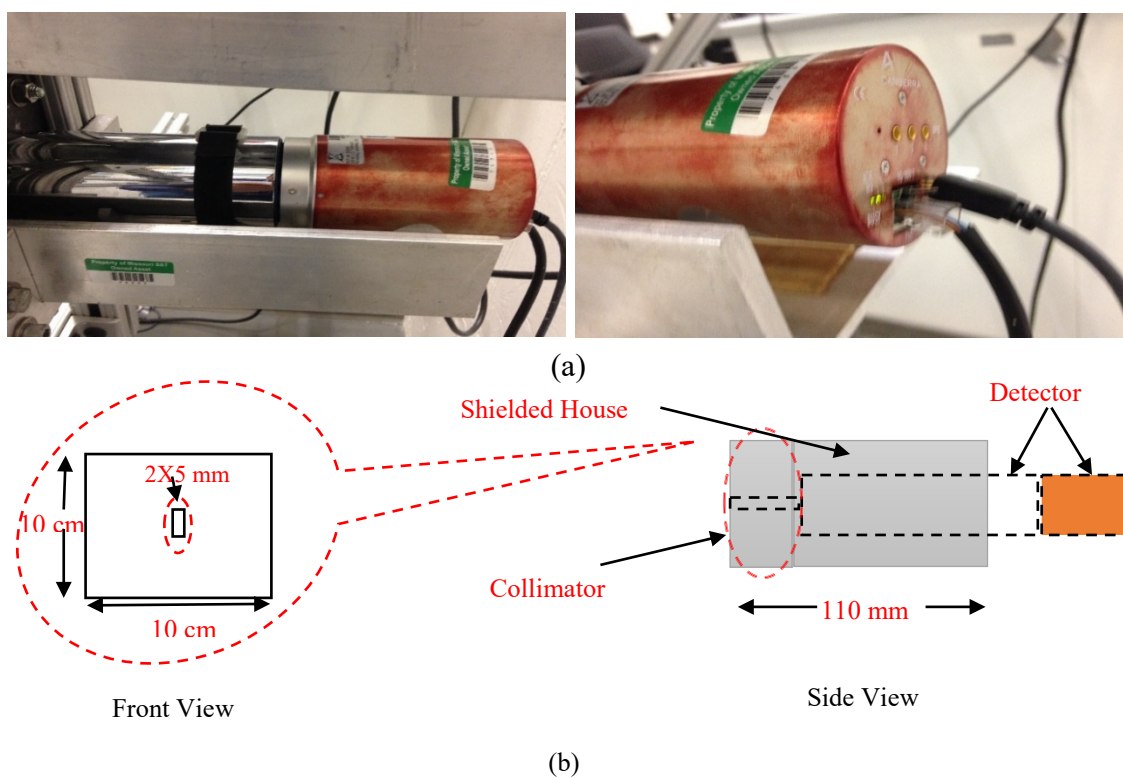


Figure 6. (a) Photo of NaI scintillating detector (b) Schematic diagram for NaI scintillating detector collimated and sited in shield house.

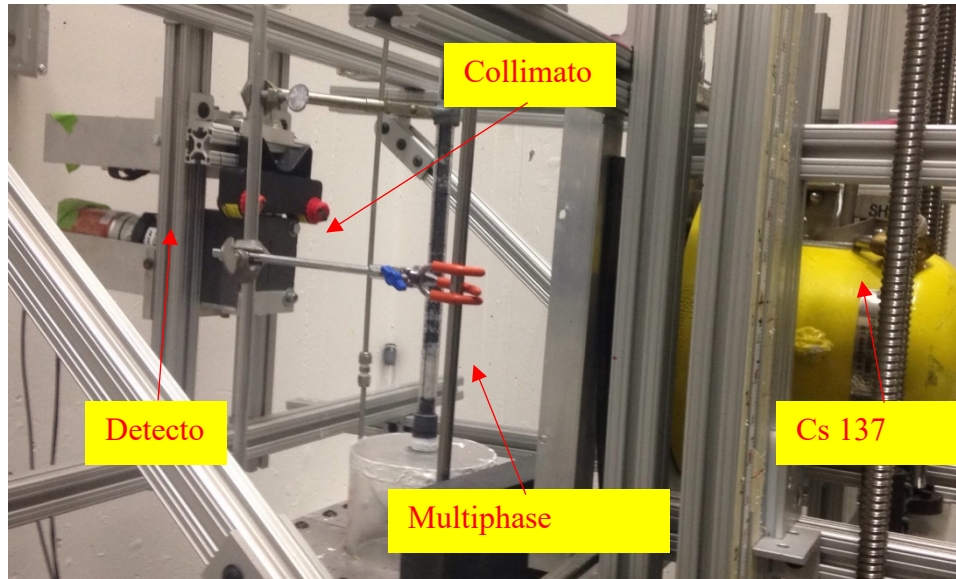
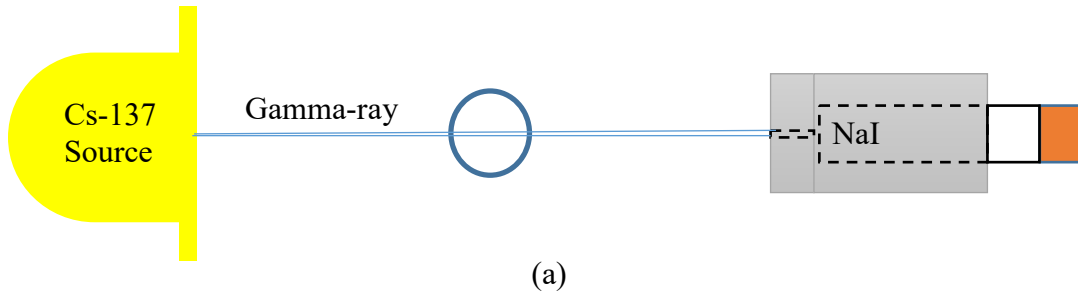


Figure 7. (a) Schematic diagram of GRD technique (b) GRD technique photo with TBR system.

2.3. PRINCIPAL OF MEASUREMENTS

The GRD measurement is based on Beer-Lambert's law which expresses the detected attenuated photon (I) from incident radiation (I_0) by the following equation:

$$I = I_0 e^{-\mu\rho L} \quad (1)$$

Equation 1 stated that the ratio of the detected radiation (I) to the incident radiation (I₀) varies exponentially with the length of absorbing medium (L), the density of absorbing medium (ρ), and mass absorption or attenuation coefficient (μ) of the medium, as follows:

$$\frac{I}{I_0} = e^{-\mu\rho L} \quad (2)$$

The measured $\ln(I_0/I)$ ratio represents the transmission ratio, and we will call it the attenuation ratio (A) for simplicity. The attenuation ratio is equal to the integral summation of the attenuation through the substances along the beam distance:

$$\ln \frac{I_0}{I} = \mu\rho l = A \quad (3)$$

For the GRD technique, the attenuation is estimated along the single beam path through TBR at different radial positions along the diameter. For a multiphase system, A will be the summation of line attenuation of the individual phase [52].

The attenuation ratio (A) for a single-phase system is as follows:

a) For a gas system (A_g)

$$\ln \frac{I_0}{I_g} = \mu_g \rho_g l_g = A_g \quad (4)$$

b) For a liquid system (A_l)

$$\ln \frac{I_0}{I_l} = \mu_l \rho_l l_l = A_l \quad (5)$$

c) For a solid system (A_s)

$$\ln \frac{I_0}{I_s} = \mu_s \rho_s l_s = A_s. \quad (6)$$

The attenuation ratio (A) for two phases is as follows:

$$\text{a) Gas-liquid system (A}_{gl}\text{): } \ln \frac{I_0}{I_{gl}} = \mu_g \rho_g l_g + \mu_l \rho_l l_l = A_{gl} \quad (7)$$

$$\text{b) Gas-solid system (A}_{gs}\text{): } \ln \frac{I_0}{I_{gs}} = \mu_g \rho_g l_g + \mu_s \rho_s l_s = A_{gs} \quad (8)$$

$$\text{c) Liquid-solid system (A}_{ls}\text{): } \ln \frac{I_0}{I_{ls}} = \mu_l \rho_l l_l + \mu_s \rho_s l_s = A_{ls} \quad (9)$$

The attenuation ratio (A) for a three-phase gas-liquid-solid system will be [120]

$$A_{gls} = \ln \frac{I_0}{I_{gls}} = \mu_g \rho_g l_g + \mu_l \rho_l l_l + \mu_s \rho_s l_s \quad (10)$$

where

I_0 : Incident radiation, I_g, I_l, I_s : Photon counts detected through single-phase gas, liquid, and solid system, respectively, I_{gl}, I_{gs}, I_{ls} : Photon counts detected through a two-phases gas-liquid, gas-solid-liquid, and liquid-solid systems, respectively, I_{slg} : Photon counts detected through a solid-liquid-gas system, μ_g, μ_l, μ_s : Mass attenuation coefficient of gas, liquid, and solid (catalyst) (cm²/g), respectively, ρ_g, ρ_l, ρ_s : Density of gas, liquid, solid (catalyst) (g/cm³), respectively, l_g, l_l, l_s : Length occupied by gas, liquid, solid (catalyst) among the total length (cm), respectively, A_g, A_l, A_s : Attenuation ratio for single-phase gas, liquid, solid, respectively, A_{gl}, A_{gs}, A_{ls} : Attenuation ratio for two-phases gas-liquid, gas-solid-

liquid, and liquid-solid systems respectively, and A_{slg} : Attenuation ratio for multiphase system (solid-liquid-gas).

The total length occupied by gas, liquid, and solid along the GRD's beam path (L) is the summation of length occupied by gas, liquid, and solid (cm):

$$L = l_s + l_l + l_g, \quad (11)$$

whereas:

$$l_s = \varepsilon_s L \quad (12)$$

$$l_l = \varepsilon_l L \quad (13)$$

$$l_g = \varepsilon_g L \quad (14)$$

where ε_s , ε_l , ε_g are solid holdup, dynamic liquid holdup, and gas holdup, respectively.

2.4. VALIDATION OF THE GRD MEASUREMENTS

A Plexiglas cylindrical column with inside diameter of 11.8 mm was used as a phantom to validate the GRD measurements. An aluminum column with inside diameter of 6 mm and outside diameter of 6.5 mm was fixed inside the Plexiglas column with 3 mm hollow stainless steel pipe in the center as displayed in Figure 8.

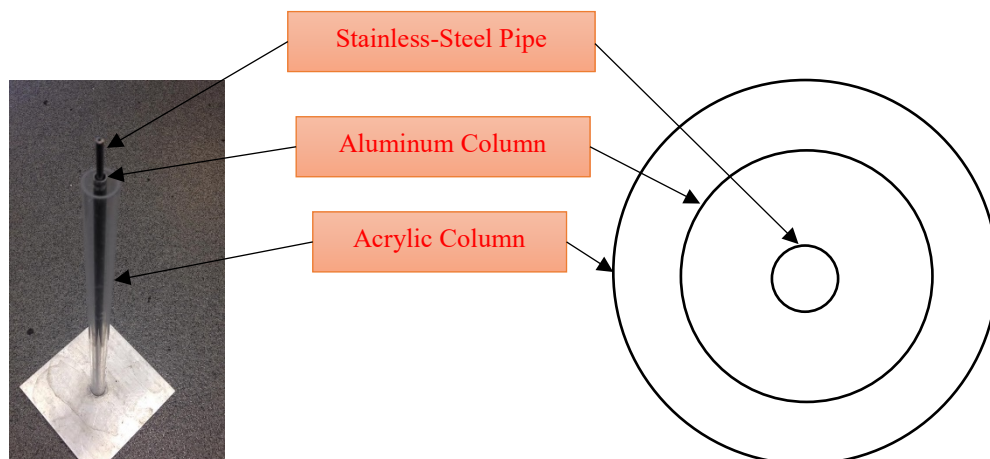


Figure 8. Picture and schematic diagram for phantom structure.

In present work, aluminum was used because its mass attenuation coefficient is very low, close to the mass attenuation coefficient of air. Separate scans were employed for the phantom with several cases to verify the extent of the capability of the GRD technique to recognize different multi-phases as shown below:

Case I: Empty column (air) between the Plexiglas and aluminum, and empty column (air) between the aluminum and stainless steel as shown in Figure 9a.

Case II: Empty column (air) between the Plexiglas and aluminum, and water filling the column between the aluminum and stainless steel, as shown in Figure 9b.

Case III: Dry catalyst (dry solid) between the Plexiglas and aluminum, and water filling the column between the aluminum and stainless steel, as presented in Figure 9c.

Case IV: Empty column (air) between the Plexiglas and aluminum, and water filling the column between the aluminum and stainless steel, as displayed in Figure 9d.

Figure 9 depicts the schematic diagram with a photon count profile for each case. Meanwhile, Figure 9 illustrates the validation of GRD data by scanning different cases of the phantom. Single beam radiation along beam paths measures the attenuations through TBR. The attenuations have been presented for each scan to determine the ingenuity in preliminary steps of experimental work.

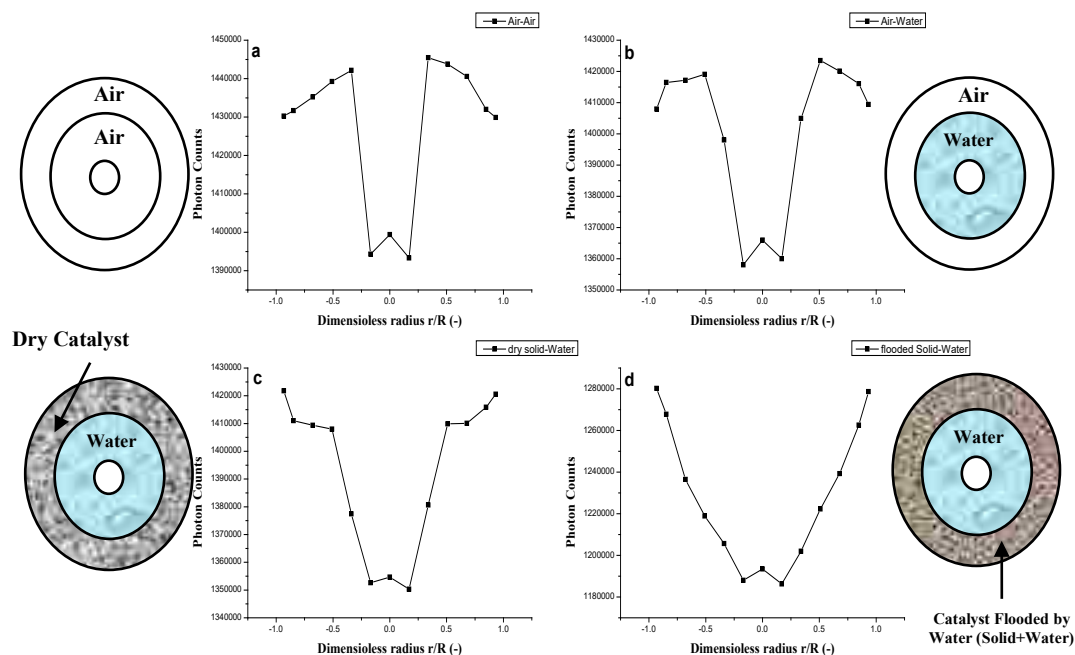


Figure 9. Photon counts profile at (a) case I (air-air) (b) case II (air-water) (c) case III (dry solid-water) (d) case IV (flooded solid-water).

The photon counts versus locations of the beam path through the reactor are plotted for each case of the scan. The average attenuation of photon counts was changed with changing the position due to escalation or reduction in the density of material, thereby changing the mass absorption coefficient. The GRD technique revealed a high capability of segregation the differences in the density of materials whether were solid, liquid or gas as seen Figure 10.

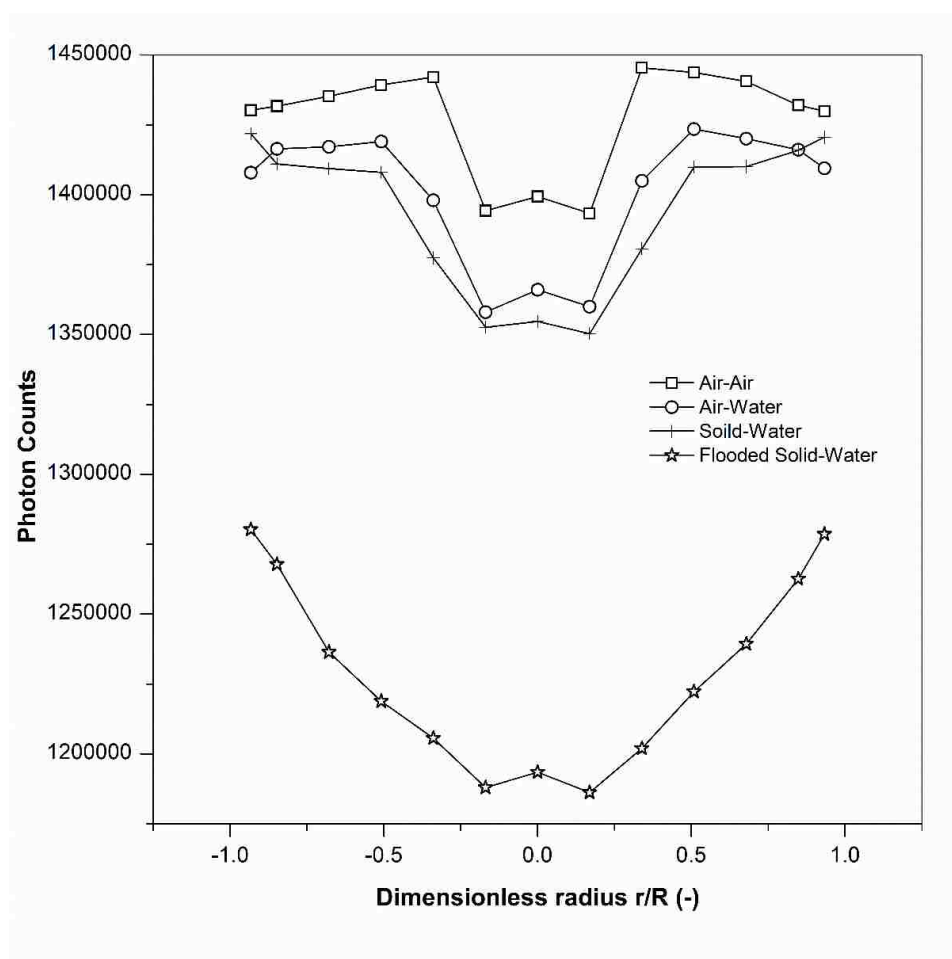


Figure 10. Comparison of photon counts profile for each case.

2.5. METHODOLOGY OF MEASUREMENTS

A new methodology is applied in our bench Multiphase Flow and Reactors Engineering and Applications Bench (mFReal) at Missouri University of Science and Technology (S&T) to estimate phase holdup in multiphase reactors. The scans are implemented with different constituting materials and flow rate conditions. The procedure and steps of scanning are as following:

1- Scanning without column (air only) that represents a reference (I_0), which approximates the incident radiation:

$$A_g = \ln \frac{I_0}{I_g} = \mu_g \rho_g l_g \quad (15)$$

since the attenuation due air and air density are small compared to the other phases, A_g can be neglected

$$A_g = \ln \frac{I_0}{I_0} = \mu_g \rho_g l_g \cong 0 \quad (16)$$

2- Scanning empty column, which contains air only. The attenuation in this scan is due to the wall of the column and air (A_c).

$$A_c = \ln \frac{I_0}{I_c} = \mu_c \rho_c l_c + \mu_g \rho_g l_g \quad (17)$$

Since, $A_g = \ln \frac{I_0}{I_0} = \mu_g \rho_g l_g \cong 0$

$$A_c = \ln \frac{I_0}{I_c} = \mu_c \rho_c l_c \quad (18)$$

Where,

I_c : Photon counts detected through column only due to $A_g \cong 0$, A_c : Attenuation ratio for the column wall.

3- Scanning column filled with water only. The attenuation in this scan is due to the column wall (A_c) and water (A_w).

$$A_{wc} = \ln \frac{I_0}{I_{wc}} = \mu_c \rho_c l_c + \mu_l \rho_l l_l \quad (19)$$

Where,

I_{wc} : photon counts detected through column filled with water, A_{wc} : Attenuation ratio for water and column wall.

By subtracting equation 19 from 18, we obtain gross attenuation for water (A_w) as follows:

$$A_w = A_{wc} - A_c \quad (20)$$

$$A_w = \mu_l \rho_l l_l + \mu_c \rho_c l_c - \mu_c \rho_c l_c \quad (21)$$

$$A_w = \mu_l \rho_l l_l \quad (22)$$

4- In this step, the reactor is packed with catalyst particles, then is flooded with the catalyst for 24 hours to ensure all the internal porosity of the catalyst is filled with water. The next step is draining the water and flow air and water at high gas and water superficial velocities relatively for 24 hours to guarantee that the packing is settled and there is no any movement for the catalyst particles during the normal operation of flow conditions. It has been showing that the bed packing get adjusted and packed dense when first we pack the bed loose due to the force imparted on the bed by the following gas and liquid drainage the operation. This cause errors in the final results of the scanning due to the change in the bed structure. After that, the bed is flooded again and then waiting for 6 hours before starting the scanning of the reactor under the flooded condition. The gathered photon counts are attenuated by the column wall, the catalyst particles that represents solid phases (the wall and catalyst), and water in external and internal voids (internal voids mean the porosity of the catalysts) (A_{cswf}).

$$A_{cswf} = \mu_c \rho_c l_c + \mu_s \rho_s l_s + (\mu_l \rho_l l_l)_{Int. Liquid} + (\mu_l \rho_l l_l)_{Ext. Liquid} \quad (23)$$

By subtracting equation 23 from 18, which we obtain the total attenuation for solid phase of catalyst only and water (A_{sw}) that is presence in both the external and internal voids.

$$A_{sw} = A_{cswf} - A_c \quad (24)$$

$$A_{sw} = \mu_c \rho_c l_c + \mu_s \rho_s l_s + (\mu_l \rho_l l_l)_{Int. Liquid} + (\mu_l \rho_l l_l)_{Ext. Liquid} - \mu_c \rho_c l_c \quad (25)$$

where, the A_{sw} here represents the solid of the catalyst

$$A_{sw} = \mu_s \rho_s l_s + (\mu_l \rho_l l_l)_{Int. Liquid} + (\mu_l \rho_l l_l)_{Ext. Liquid} \quad (26)$$

Since:

$$A_{l Ext. Liquid} = (\mu_l \rho_l l_l)_{Ext. Sta. Liquid} + (\mu_l \rho_l l_l)_{Dyn. Liquid} \quad (27)$$

where, $(\mu_l \rho_l l_l)_{Sta. void}$ is the attenuation ratio for static water between adjacent particles.

Substituting equation 27 in equation 26, yields

$$A_{sw} = \mu_s \rho_s l_s + (\mu_l \rho_l l_l)_{Int. Liquid} + (\mu_l \rho_l l_l)_{Ext. Sta. Liquid} + (\mu_l \rho_l l_l)_{Ext. without Sta. Liquid} \quad (28)$$

where,

$(l_l)_{Int. void}$: Length occupied by liquid in the internal voids for catalyst (cm), $(l_l)_{Sta. void}$:

Length occupied by stagnant liquid in the external voids for catalyst (cm), $(l_l)_{Dyn. void}$:

Length occupied by flowing liquid in the void space for catalyst (cm).

$$(l_l)_{Ext. without Sta. Liquid} = \varepsilon_{l Ext. without Sta. Liquid} L \quad (29)$$

$$(l_l)_{Int. void} + (l_l)_{Ext. Sta. Liquid} = \varepsilon_l' L \quad (30)$$

ε_l' is the line averaged liquid holdup in the internal void space and static liquid that completely occupied by water in this case.

$\varepsilon_{l\ void}$ is line averaged void holdup in external void space that occupied by the liquid.

Substitute equation 30 and equation 29 in equation 28

$$A_{sw} = \mu_s \rho_s l_s + \mu_l \rho_l \varepsilon_{l\ Ext. without Sta. Liquid} L + \mu_l \rho_l \varepsilon_l' L \quad (31)$$

It is worth to mention that

$$\varepsilon_{l\ Ext. without Sta. Liquid} = \varepsilon_{l\ Ext. dyn. Liquid} + \varepsilon_g \quad (32)$$

Where

$\varepsilon_{l\ dyn.}$: Line averaged liquid holdup in the void that occupied by liquid and represents the dynamic liquid holdup in the external void.

ε_g : Line averaged gas holdup in the void that occupied totally by liquid and represents the gas holdup in the external void.

5- Draining the water and waiting for 24 hours to guarantee that there is no any flow of water. Generally, liquid holdup in the porous catalyst particles bed is defined as an internal liquid holdup. Basically, the internal liquid holdup represents the volume fraction for the liquid inside the porosity of the catalyst particles with respect to the total bed volume. Whereas, the external liquid holdup in the porous media consists of static liquid holdup

and dynamic liquid holdup. Static liquid holdup is the volume fraction of liquid per total bed volume that being stagnant inside the reactor between the particles at the contact points, even after complete draining which it is approximated to be constant weather there is flow or there is no flow as long as there is no change in the bed structure. Dynamic liquid holdup (ϵ_{dl}) represents the volume fraction of the liquid flow through the void space per the total volume of the bed. In this scan, the photons intensity attenuation is affected by column wall, solid particles, internal and static liquid (inside the porosity of pellet particles and the pockets of liquid between adjacent particles), and air in void space (A_{csww}).

$$A_{csww} = \mu_c \rho_c l_c + \mu_s \rho_s l_s + (\mu_l \rho_l l_l)_{Int. Liquid} + (\mu_l \rho_l l_l)_{Ext. Sta. Liquid} + \mu_g \rho_g l_g \quad (33)$$

By subtracting equation 33 from equation 18, the net attenuation of wet catalyst (A_{sww}) is obtained.

$$A_{sww} = A_{csww} - A_c \quad (34)$$

$$A_{sww} = \mu_s \rho_s l_s + (\mu_l \rho_l l_l)_{Int. Liquid} + (\mu_l \rho_l l_l)_{Ext. Sta. Liquid} \quad (35)$$

$$A_{sww} = \mu_s \rho_s l_s + \mu_l \rho_l [(l_l)_{Int. Liquid} + (l_l)_{Sta. Liquid}] \quad (36)$$

Substituting equation 30 in 36

$$A_{sww} = \mu_s \rho_s l_s + \mu_l \rho_l \epsilon_l' L \quad (37)$$

6- Scanning the column under the desired flow rate condition which the acquired photons counts were attenuated by the column wall, solid particles, flow of water, and flow of gas (A_{csfw}). The attenuation by the flow of gas can be neglected.

$$A_{csfw} = \mu_c \rho_c l_c + \mu_s \rho_s l_s + (\mu_l \rho_l l_l)_{Int. Liquid} + (\mu_l \rho_l l_l)_{Ext. Sta. Liquid} + (\mu_l \rho_l l_l)_{Ext. dyn. Liquid} + \mu_g \rho_g l_g \quad (38)$$

By subtracting equation 38 from equation 18, to get the net attenuation of solid particles, internal liquid, static liquid, and dynamic liquid (A_{sfw}), can be obtained as follows:

$$A_{sfw} = A_{csfw} - A_c \quad (39)$$

$$A_{csfw} = \mu_c \rho_c l_c + \mu_s \rho_s l_s + (\mu_l \rho_l l_l)_{Int. Liquid} + (\mu_l \rho_l l_l)_{Ext. Sta. Liquid} + (\mu_l \rho_l l_l)_{Ext. dyn. Liquid} + \mu_g \rho_g l_g - \mu_c \rho_c l_c \quad (40)$$

$$A_{sfw} = \mu_s \rho_s l_s + (\mu_l \rho_l l_l)_{Int. Liquid} + (\mu_l \rho_l l_l)_{Ext. Sta. Liquid} + (\mu_l \rho_l l_l)_{Ext. dyn. Liquid} \quad (41)$$

Since

$$(l_l)_{Ext. dyn. Liquid} = \varepsilon_l Ext. dyn. Liquid L \quad (42)$$

Substituting equation 30 and 42 in equation 41, gives

$$A_{sfw} = \mu_s \rho_s l_s + \mu_l \rho_l \varepsilon_l' L + \mu_l \rho_l \varepsilon_l Ext. dyn. Liquid L \quad (43)$$

2.6. DYNAMIC LIQUID HOLDUP CALCULATIONS

By subtracting the attenuation ratio by flow condition (A_{sfw}) in equation 43 from attenuation ratio by wet catalyst in equation 37, we will obtain dynamic liquid holdup in the reactor as follow:

$$A_{sfw} - A_{sww} = \mu_s \rho_s l_s + \mu_l \rho_l \varepsilon_l' L + \mu_l \rho_l \varepsilon_{l \text{ Ext. dyn. Liquid}} L - \mu_s \rho_s l_s - \mu_l \rho_l \varepsilon_l' L \quad (44)$$

$$A_{sfw} - A_{sww} = \mu_l \rho_l \varepsilon_{l \text{ Ext. dyn. Liquid}} L \quad (45)$$

Which,

Due to subtracting the length of the path that crosses solid particles, dynamic liquid, and internal liquid as in equation 44, the rest of the length path is representing only liquid that occupied the void space. Based on that we can say

$$L = l_l \quad (46)$$

$$A_{sfw} - A_{sww} = \mu_l \rho_l \varepsilon_{l \text{ Ext. dyn. Liquid}} l_l \quad (47)$$

Since $A_w = \mu_l \rho_l l_l$ as in equation 22

Then,

$$\varepsilon_{l \text{ Ext. dyn. Liquid}} = \frac{A_{sfw} - A_{sww}}{A_w} \quad (48)$$

2.7. GAS HOLDUP CALCULATIONS

The line averaged gas holdup distribution is obtained by subtracting equation 43 from equation 31 as follows:

$$A_{sw} - A_{sfw} = \mu_s \rho_s l_s + \mu_l \rho_l \varepsilon_{l \text{ Ext. without Sta. Liquid}} L + \mu_l \rho_l \varepsilon_l' L - \mu_s \rho_s l_s - \mu_l \rho_l \varepsilon_l' L - \mu_l \rho_l \varepsilon_{l \text{ Ext. dyn. Liquid}} L \quad (49)$$

$$A_{sw} - A_{sfw} = \mu_l \rho_l \varepsilon_{l \text{ Ext. without Sta. Liquid}} L - \mu_l \rho_l \varepsilon_{l \text{ Ext. dyn. Liquid}} L \quad (50)$$

by, substituting equation 33 in equation 50

$$A_{sw} - A_{sfw} = \mu_l \rho_l \varepsilon_g L + \mu_l \rho_l \varepsilon_{l \text{ Ext. dyn. Liquid}} L - \mu_l \rho_l \varepsilon_{l \text{ Ext. dyn. Liquid}} L \quad (51)$$

$$A_{sw} - A_{sfw} = \mu_l \rho_l \varepsilon_g L \quad (52)$$

Where

ε_g : Line averaged gas holdup in void space.

Due to subtracting the length of the path that crosses solid particles, static liquid, and internal liquid equation 46 ($L = l_l$), the rest of the length path is representing only liquid that occupied the void space. Based on that we can say

Substituting equation 46 in equation 52

$$A_{sw} - A_{sfw} = \mu_l \rho_l \varepsilon_g l_l \quad (53)$$

Since in equation 23, $A_w = \mu_l \rho_l l_l$

then,

$$A_{sw} - A_{sfw} = A_w \varepsilon_g \quad (54)$$

$$\varepsilon_g = \frac{A_{sw} - A_{sfw}}{A_w} \quad (55)$$

2.8. EXTERNAL VOID SPACE CALCULATIONS

The distribution or the diameter profile of the volume void fraction with respect to the bed volume is a critical factor that effects the hydrodynamic parameters in the two phase flow packed bed reactors. The void holdup profile is estimated by subtracting the attenuation ratio of the drained condition (A_{sww}) of equation 37 from the attenuation ratio of the flooded condition (A_{sw}) of equation 31 where the external void is filled with water.

$$A_{sw} - A_{sww} = \mu_s \rho_s l_s + \mu_l \rho_l \varepsilon_l \text{ Ext. without Sta. Liquid } L + \mu_l \rho_l \varepsilon_l' L - \mu_s \rho_s l_s - \mu_l \rho_l \varepsilon_l' \quad (56)$$

$$A_{sw} - A_{sww} = \mu_l \rho_l \varepsilon_l \text{ Ext. without Sta. Liquid } L \quad (57)$$

$$A_{sw} - A_{sww} = \mu_l \rho_l \varepsilon_l \text{ Ext. without Sta. Liquid } l_l \quad (58)$$

$$\varepsilon_{l \text{ Ext. without Sta. Liquid}} = \frac{A_{sw} - A_{sww}}{A_w} \quad (59)$$

$\varepsilon_{l \text{ Ext. without Sta. Liquid}}$ is the volume fraction of external void without the volume fraction of external static holdup.

3. RESULTS AND DISCUSSIONS

3.1. EFFECT OF THE DISTRIBUTOR REGION ON THE LINE AVERAGED LIQUID HOLDUP DIAMETRICAL PROFILE IN BOTH DILUTED AND NON-DILUTED BEDS AT TWO DIFFERENT CONFIGURATIONS (SIDE AND TOP).

The scanning at 5 cm above to the surface of the packed bed (see Figure 4) was performed to identify the liquid distribution that is introduced to the surface of the bed. The layer above the surface of the packed bed could be important for the liquid distribution which is considered as a distributor to the packed bed in this case. The line averaged dynamic liquid holdup radial profiles at different gas and liquid flow rates are shown in Figures 11.

The obtained scanned diametrical profiles visualize qualitatively how the liquid phase is distributed prior feed to the surface of diluted packed bed. The results showed that good liquid distribution in case side or top inlet configuration for mixed gas and liquid within diluted and non-diluted beds. Figure 11 indicated low percentage of deviation from the mean value for all diametrical positions within both diluted and non-diluted beds at two different configurations (side and top).

The results revealed 2.4-16% within non-diluted bed, while 0.2-11 % within diluted bed. However, there is an obvious escalating in the magnitude for liquid holdup along the

diametrical profile in the diluted bed at both configuration inlet for mixed gas and liquid compared to the non-diluted bed due to decrease the wall effect and gas and liquid flow rate in the bed by decrease the voidage in the bed. The current results present the uniform distribution that represents as a one of a critical factor that leads to maldistribution and bypassing in the TBRs [54].

3.2. EFFECTS OF THE BED DILUTION ON THE LINE AVERAGED DIAMETRICAL PROFILES OF THE DYNAMIC LIQUID HOLDUP ALONG BED HEIGHT

Bed dilution has been applied in industry to decouple the hydrodynamics from the kinetics in trickle bed reactors for scale-down or scale up studies [9]. The challenge in the scale-down or scale up is the use of commercial sizes of catalyst particles in bench scale beds (1 inch diameter) where the ratio of the bed diameter to the particle diameter is below 20. This causes wall effects which yields liquid maldistribution and partial wettability of the catalysts that lead to incomplete catalyst utilization and hence decreasing the performance of the reactor. As shown in Figure 2. A 60cm bed height of a 1.18 cm diameter is loaded with commercial size of trilobe catalyst particles Six levels heights and 11 diametrical line scanning levels were performed to investigate the extent effects of implementing fine dilution particles on the line averaged diametrical profiles of the dynamic liquid holdup. Superficial gas velocity of 1796.5 cc/min and superficial liquid velocity of 0.39 cc/min for beds with and without fines were used. Figure 12 displays that the line averaged dynamic liquid holdup profiles for diluted catalyst bed is significantly higher 165-800 % along the bed height than that of the non-diluted catalyst bed due to a decrease in the bed void, an increase in the contact points between the adjacent particles

that give rise to higher pressure drop [9]. The findings in agreement [9], [19] findings which showed an increase in the liquid holdup with dilution catalyst bed. Also, the line averaged liquid holdup diametrical profiles indicated the liquid distribution along the diameter of the bed based on estimate the percentage value of deviation from the mean for each diametrical position along bed height in both diluted and non-diluted beds. Figure 12 indicated that there is liquid maldistribution in both diluted and non-diluted beds, however, the percentage of deviation decreased 64-85 % in the diluted bed than the non-diluted bed at low liquid and high gas flow rates.

3.3. EFFECTS OF THE BED DILUTION ON THE LINE AVERAGED DIAMETRICAL PROFILES OF THE VOID FRACTION OF THE BED

The external interstitial space represents crucial factors that significantly affects the hydrodynamics in the TBRs. In this work, the effects of bed dilution along bed height on the void fraction and void distribution were showed in Figure 13 A, B, C, D, E, and F.

The findings as shown in Figure 13 provides evidence that the line averaged diametrical profile of the void fraction profile for diluted catalyst bed significantly decreased 36-61% than that in the non-diluted catalyst particles. The external voids fraction diameter profile along the bed height for diluted catalyst bed are reflected more uniform distribution with 0.2-23 % deviation from the mean compared to 4-51% deviation from the mean in the non-diluted bed. However, the void fraction distribution is more uniform in the diluted bed, but the percentage of deviation from the mean still effective to lead to partial wetting and incomplete catalyst utilization for catalyst particles in the bed.

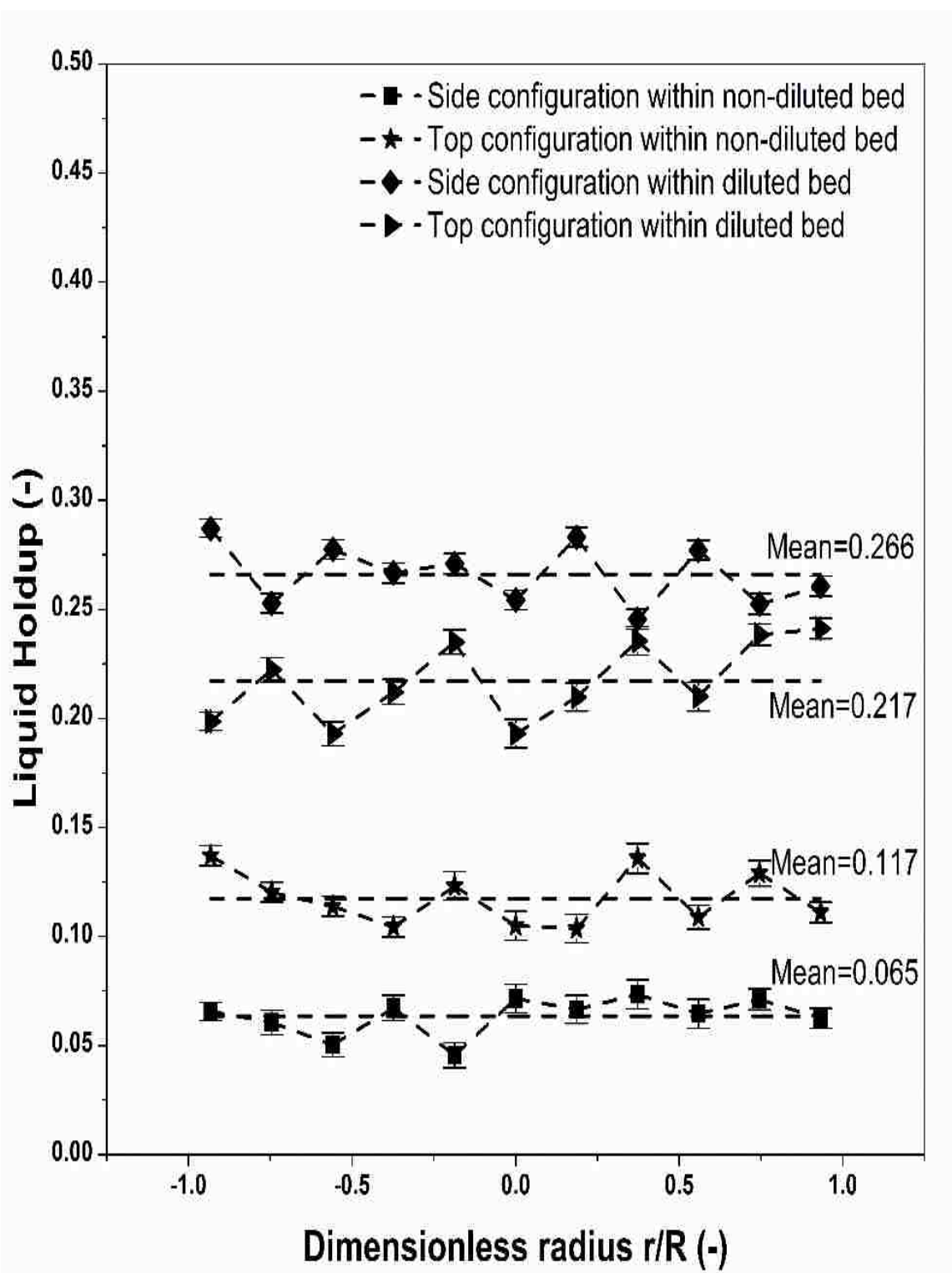


Figure 11. Liquid holdup diametrical profile at 5cm height above both diluted and non-diluted packed bed surface at two different inlet configuration (Side and Top configuration).

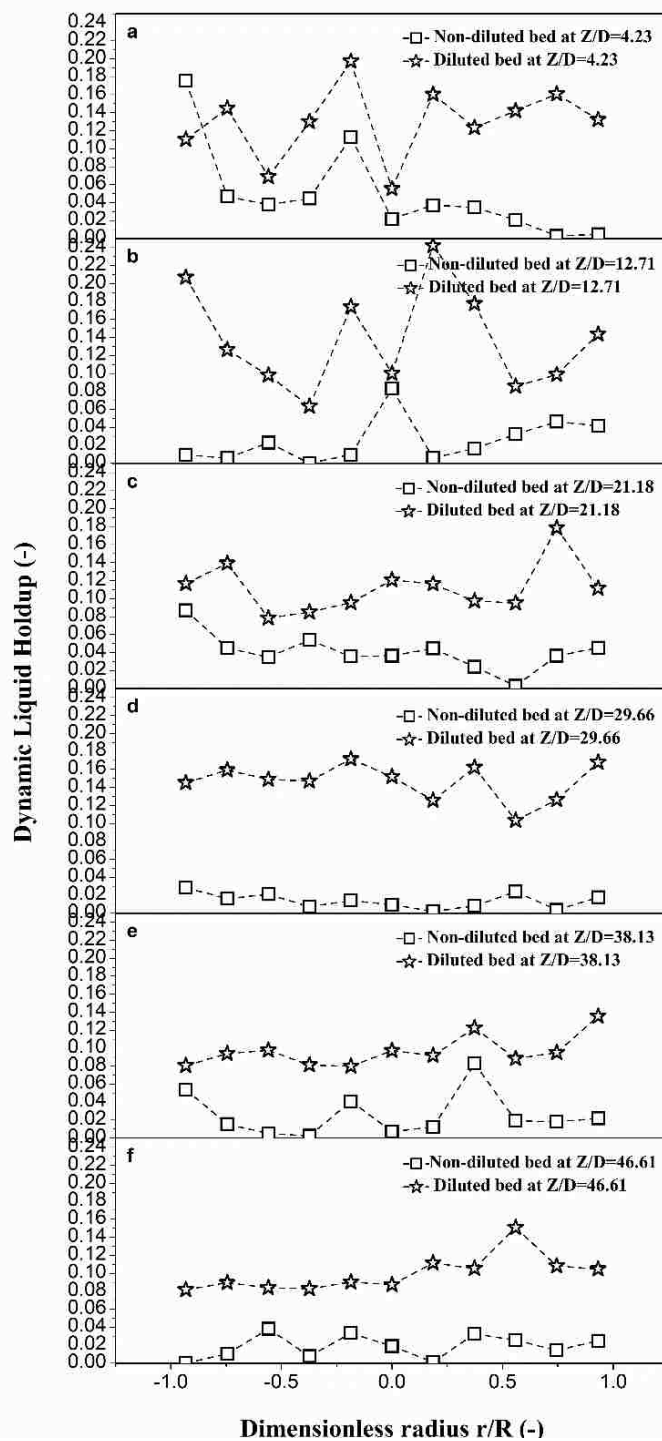


Figure 12. Dynamic liquid holdup profile with and without dilution particles at $UG=1796.5$, and $UL=0.39$ cc/min along the height bed.

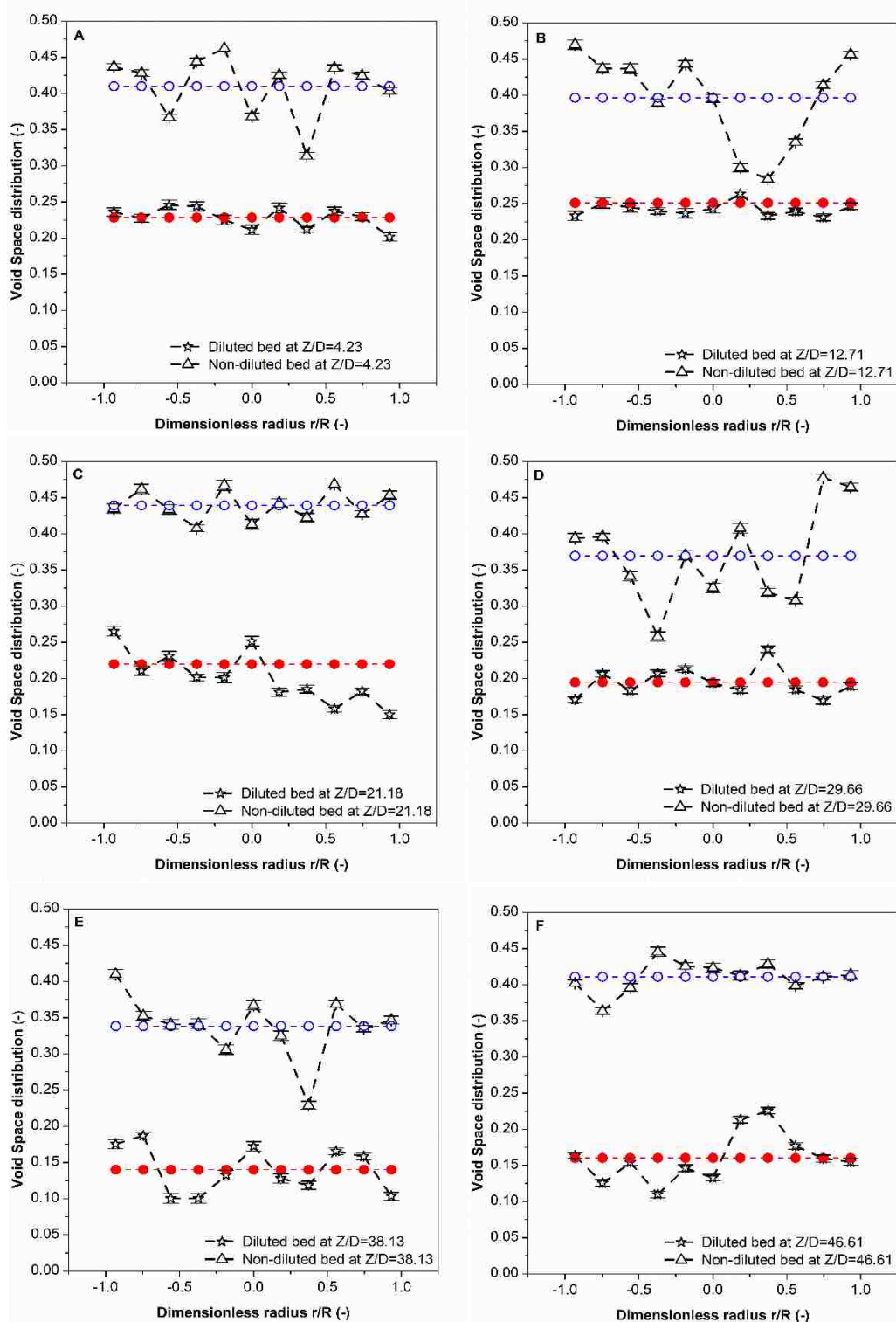


Figure 13. External void fraction diametrical profile within diluted and non-diluted at different axial levels along the bed height (A) at $Z/D=4.23$, (B) at $Z/D=12.29$, (C) at $Z/D=21.18$, (D) at $Z/D=29.66$, (E) at $Z/D=38.13$, (F) at $Z/D=46.61$.

3.4. EFFECTS OF INLET CONFIGURATION FOR THE MIXED GAS AND LIQUID ON THE LINE AVERAGED DIAMETRICAL PROFILES OF THE DYNAMIC LIQUID HOLDUP ALONG THE BED HEIGHT

The inlet configuration fluids are representing a most important factor that essentially effects on the phase distribution in the reactor by spreading the fluids in the catalyst bed. The inlet configuration for mixed gas and liquid at the head of the reactor were investigated in this study. In the real practice, the in the bench scale trickle bed reactor (hot unit) used two lines to feed the mixed gas and liquid by two lines. One line is fed the mixed gas and liquid to the reactor from the top and the other one from the side. Two Swagelok valves used to control the stream configuration in the mimicked bench-scale trickle bed reactor (cold unit) were used as exhibited in Figure 1.

Figures 14 a, b, c, d, e, f illustrate the effects of the side and top inlet configuration for mixed gas and liquid on the line averaged dynamic liquid holdup through the diluted bed at gas flow rates equal to 269.5 cc/min and liquid flow rate equal to 0.39 cc/min along bed height. Figures 14 a, b, c, d, e, f displayed that the magnitude for the dynamic liquid holdup within side inlet configuration significantly increased 46-90% than that in top inlet configuration of mixed gas and liquid.

Furthermore, Figures 14 a, b, c, d, e, f indicated the distribution for dynamic liquid in diametrical profile along bed height. The side inlet configuration for mixed gas and liquid showed an improvement in the dynamic liquid distribution with 1.5-78 % deviation from the mean, whereas the top inlet configuration for mixed gas and liquid displayed 3-99 % deviation from the mean.

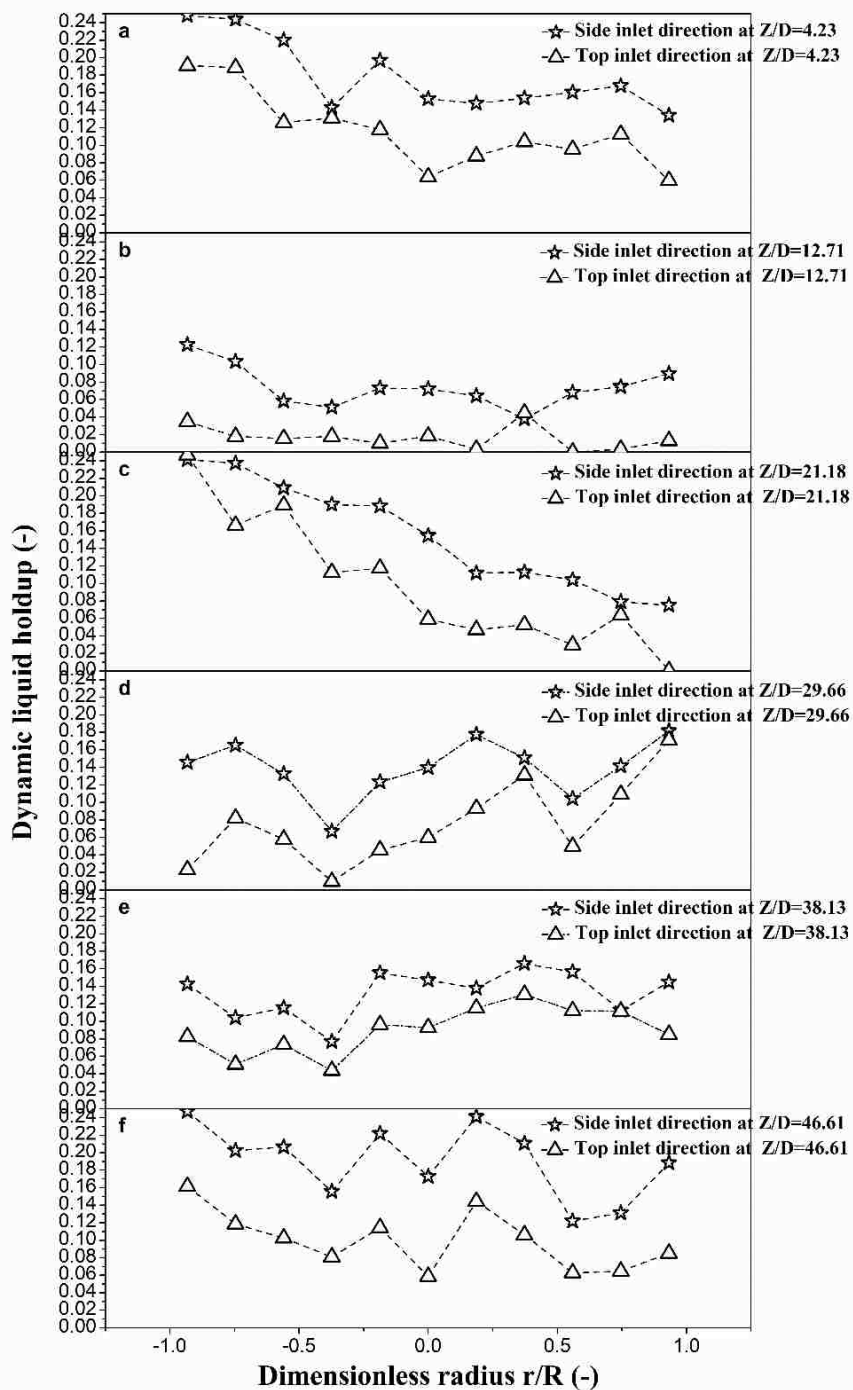


Figure 14. Line averaged dynamic liquid holdup diametrical profile within bed dilution at different inlet configuration of mixed gas and liquid with $UG=269.5$, and $UL=0.39$ cc/min along bed height (a) at $Z/D=4.23$, (b) at $Z/D=12.71$, (c) at $Z/D=21.18$, (d) at $Z/D=29.6$.

3.5. EFFECTS OF GAS AND LIQUID FLOW RATES ON THE LINE AVERAGED DIAMETRICAL PROFILES OF THE DYNAMIC LIQUID HOLDUP ALONG THE BED HEIGHT

Figure 15A displays influence the gas flow rate on the line averaged dynamic liquid holdup through bed dilution with top inlet configuration for mixed gas and liquid at different gas flow rate along bed height. The results showed that the dynamic liquid holdup significantly decreased 26-68 % with increase the gas flow rate in each level along bed height. There are similarities between the attitudes expressed by the gas flow rate in this study and those described by [9].

In addition to, the impact of liquid flow rate on the dynamic liquid holdup along diametrical profile was observed in Figure 15B. The results obtained through diluted catalyst bed with side inlet direction for gas and liquid at $U_G = 1796.5$ cc/min and different liquid flow rate. Figure 15B indicates that the magnitude of dynamic liquid holdup significantly increased 123-273 % with increase the liquid flow rate along the bed height. Obviously, the findings observed in this study mirror those of previous studies that have examined the effect of liquid flow rate [9], [13].

4. REMARKS

In the current project, GRD was used to indicate phase distribution and dynamic liquid holdup in cold system (air-water system) at ambient conditions. However, the air-water system data is not applicable in the real practice units, but the major benefit from this work to indicate the phase distribution and dynamic liquid holdup to extrapolate it in the real units. Fine particles mixed with the commercial size of trilobe catalyst particles at a

ratio (1:1) (wt:wt) as diluted particles for the bed. Line averaged of the dynamic liquid holdup at two different inlet configurations for mixed gas and liquid was quantified at different gas and liquid flow rates. The following points developed from the existing visualization:

- Good liquid distribution was existed in the distributor region (in 5cm above to the catalyst bed) with both diluted and non-diluted beds at the side and top inlet direction for mixed gas and liquid. The percentage of deviation from the mean revealed 2.4-16% within non-diluted bed, while 0.2-11 % within diluted bed.
- The void fraction and distribution significantly affected by bed dilution. The void fraction improved approximately 36-61% with diluted bed than non-diluted bed. Also, the void distribution improved in the diluted bed with 0.2-23% deviation from the mean compared to 4-51% in the non-diluted bed.
- The line averaged diametrical profiles of the dynamic liquid holdup and liquid distribution considerably affected by bed dilution. The magnitude of dynamic liquid holdup in the diluted bed was increased 165-800% than that in the non-diluted bed. Furthermore, the deviation from the mean was decreased 64-85 % than that in the non-diluted bed.
- The line averaged diametrical profiles of the dynamic liquid holdup and phase distribution changed significantly by changing the inlet configuration (side and top) for the mixed gas and liquid. The dynamic liquid holdup profile magnitude significantly increased 46-90% with the side inlet configuration than that in top inlet configuration for the mixed gas and liquid. Whereas, phase distribution improved from 3-99% to 1.5-78% deviation from the mean value with side inlet configuration compared to the top inlet configuration for mixed gas and liquid.

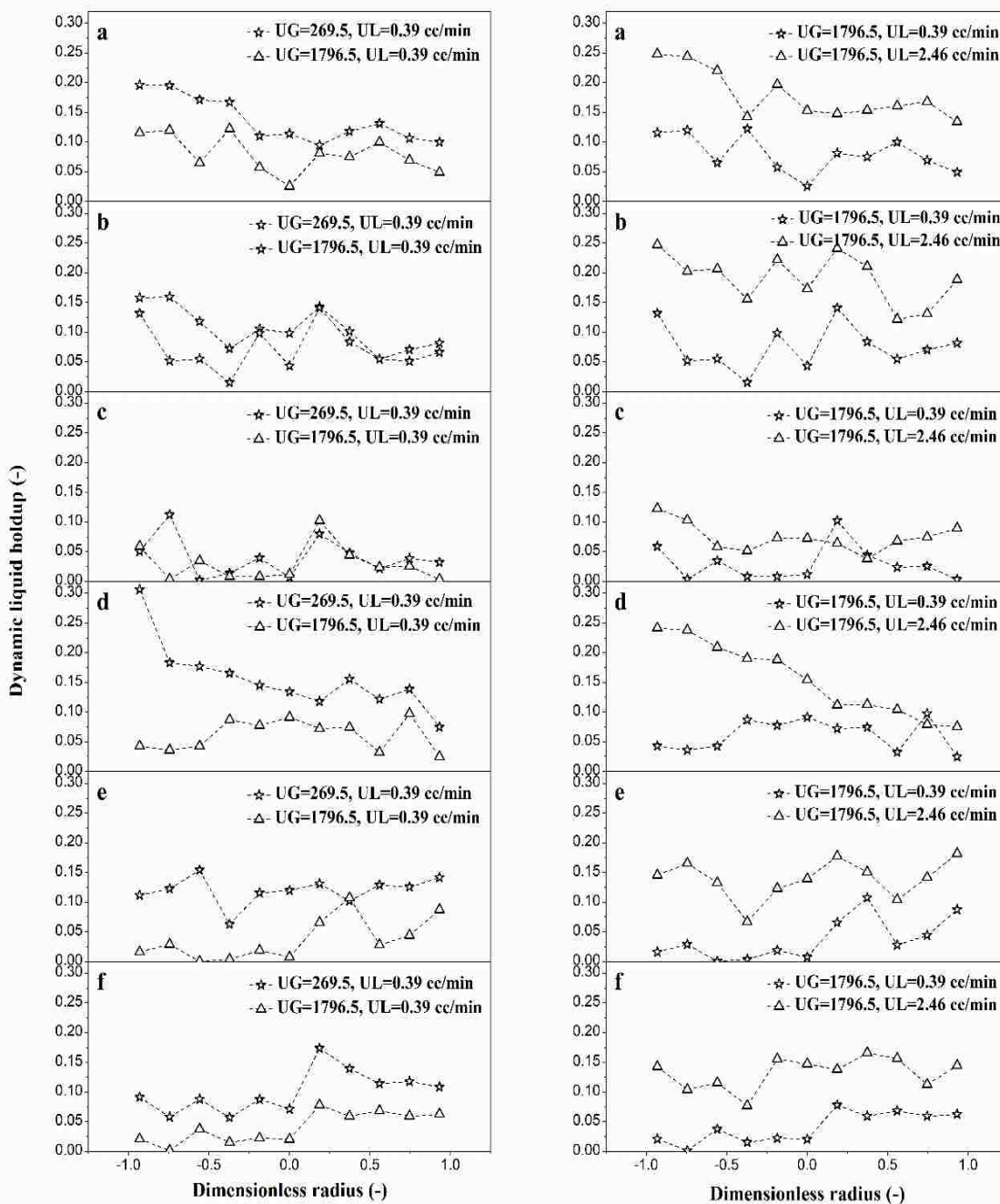


Figure 15. Line averaged dynamic liquid holdup Vs dimensionless radius r/R within diluted bed with side inlet configuration of mixed gas and liquid, (A) at $U_G=269.5$, $U_L=0.39$ cc/min and $U_G=1796.5$, $U_L=0.39$ cc/min (a) at $Z/D=4.23$, (b) at $Z/D=12.71$, (c) at $Z/D=21.18$, (d) at $Z/D=29.66$, (e) at $Z/D=38.13$, (f) at $Z/D=46.61$ (B) at $U_G=1796.5$, $U_L=0.39$ cc/min and $U_G=1796.5$, $U_L=2.46$ cc/min. (a) at $Z/D=4.23$, (b) at $Z/D=12.71$, (c) at $Z/D=21.18$, (d) at $Z/D=29.66$, (e) at $Z/D=38.13$, (f) at $Z/D=46.61$.

- A 26-68 % the dynamic liquid holdup magnitude was decreased with increasing the gas flow rate, 123-273 % was increased with increasing liquid flow rate within diluted bed.
- Further experimentation and investigation into hydrodynamics with the commercial size of trilobe catalyst particles to create a new methodology to predict and determine the amount of catalyst utilization that is one of the vital parameters that influence on the performance of TBR.
- More widely, research is needed further to examine the effect of the ratio of fine particles to the catalyst particles on the performance of the reactor using advanced techniques such as computed tomography (CT).

ACKNOWLEDGMENT

The authors gratefully acknowledge the financial support in the form of a scholarship provided by Ministry of Higher Education and Scientific Research-Iraq, and the funds provided by Missouri S&T and Professor Dr. Muthanna Al-Dahhan to develop the experimental set-up and to perform the present study. Also, the authors would like to thank, Dr. Premkumar Kamalanathan and Dr. Vineet Alexander for their help with the gamma-ray densitometry technique.

REFERENCES

- [1] A. Alvarez and J. Ancheyta, "Modeling residue hydroprocessing in a multi-fixed-bed reactor system," *Appl. Catal. A Gen.*, vol. 351, no. 2, pp. 148–158, 2008.
- [2] F. Augier, M. Fourati, and Y. Haroun, "Characterization and modelling of a maldistributed Trickle Bed Reactor," *Can. J. Chem. Eng.*, vol. 95, no. 2, pp. 222–230, 2017.

- [3] D. Beierlein, S. Schirrmeister, Y. Traa, and E. Klemm, "Experimental approach for identifying hotspots in lab- scale fixed-bed reactors exemplified by the Sabatier reaction," *React. Kinet. Mech. Catal.*, 2018.
- [4] J. Guo, Y. Jiang, and M. H. Al-Dahhan, "Modeling of trickle-bed reactors with exothermic reactions using cell network approach," *Chem. Eng. Sci.*, vol. 63, no. 3, pp. 751–764, 2008.
- [5] A. Atta, S. Roy, and K. D. P. Nigam, "A two-phase Eulerian approach using relative permeability concept for modeling of hydrodynamics in trickle-bed reactors at elevated pressure," *Chem. Eng. Res. Des.*, vol. 88, no. 3, pp. 369–378, 2010.
- [6] S. Lee, N. Zaborenko, and A. Varma, "Acetophenone hydrogenation on Rh/Al₂O₃ catalyst: Flow regime effect and trickle bed reactor modeling," *Chem. Eng. J.*, vol. 317, pp. 42–50, 2017.
- [7] P. Kawatra, S. Panyaram, and B. A. Wilhite, "Hydrodynamics in a pilot-scale cocurrent trickle-bed reactor at low gas velocities," *AIChE J.*, vol. 64, no. 7, 2018.
- [8] M. and M. P. D. H. Al-Dahhan, "Pressure Drop and Liquid Holdup in High Pressure Trickle-Bed Reactors," *Chem. Eng. Sci.*, vol. 49, no. 24B, pp. 5681–5698, 1994.
- [9] M. H. Al-Dahhan and M. P. Duduković, "Catalyst Bed Dilution for Improving Catalyst Wetting in Laboratory Trickle-Bed Reactors," *AIChE J.*, vol. 42, no. 9, pp. 2594–2606, 1996.
- [10] M. Bazmi, S. H. Hashemabadi, and M. Bayat, "Flow Maldistribution in Dense- and Sock-Loaded Trilobe Catalyst Trickle-Bed Reactors: Experimental Data and Modeling Using Neural Network," *Transp. Porous Media*, vol. 97, no. 1, pp. 119–132, 2013.
- [11] Y. Jiang, M. R. Khadilkar, M. H. Al-Dahhan, and M. P. Dudukovic, "CFD modeling of multiphase flow distribution in catalytic packed bed reactors: Scale down issues," *Catal. Today*, vol. 66, no. 2–4, pp. 209–218, 2001.
- [12] S. P. Maiti, R. and N. K., "TRICKLE-BED REACTORS: LIQUID DISTRIBUTION AND FLOW TEXTURE," *Rev. Chem. Eng.*, vol. 20, p. 57, 2004.
- [13] R. R. Kulkarni, J. Wood, J. M. Winterbottom, and E. H. Stitt, "Effect of fines and porous catalyst on hydrodynamics of trickle bed reactors," *Ind. Eng. Chem. Res.*, vol. 44, no. 25, pp. 9497–9501, 2005.
- [14] S. T. Sie and R. Krishna, "Process Development and Scale Up: III. Scale Up and Scale Down of trickle bed processes," *Rev. Chem. Eng.*, vol. 14, no. 3, pp. 203–252, 1998.

- [15] M. H. Al-Dahhan, F. Larachi, M. P. Dudukovic, and A. Laurent, "High-Pressure Trickle-Bed Reactors: A Review," *Ind. Eng. Chem. Res.*, vol. 36, no. 8, pp. 3292–3314, 1997.
- [16] A. Kundu, A. K. Saroha, and K. D. P. Nigam, "Liquid distribution studies in trickle-bed reactors," *Chem. Eng. Sci.*, vol. 56, no. 21–22, pp. 5963–5967, 2001.
- [17] D. A. Hickman, M. T. Holbrook, S. Mistretta, and S. J. Rozeveld, "Successful scale-up of an industrial trickle bed hydrogenation using laboratory reactor data," *Ind. Eng. Chem. Res.*, vol. 52, no. 44, pp. 15287–15292, 2013.
- [18] M. H. Al-Dahhan, Y. Wu, and M. P. Duduković, "Reproducible Technique for Packing Laboratory-Scale Trickle-Bed Reactors with a Mixture of Catalyst and Fines," *Ind. Eng. Chem. Res.*, vol. 34, no. 3, pp. 741–747, 1995.
- [19] J. V. K. and R. H. Van Dongen, "Catalyst Dilution for Improved Performance of Laboratory Trickle-Flow Reactors," *Chem. Eng. Sci.*, vol. 35, pp. 59–66, 1980.
- [20] G. H. Hong, Y. S. Noh, J. I. Park, S. A. Shin, and D. J. Moon, "Effect of catalytic reactor bed dilution on product distribution for Fischer-Tropsch synthesis over Ru/Co/Al₂O₃ catalyst," *Catal. Today*, vol. 303, no. August 2017, pp. 136–142, 2018.
- [21] K. M. Ng and C. F. Chu, "Trickle-bed reactors," 1987.
- [22] M. Tymchyshyn, Z. Yuan, and C. Xu, "Direct conversion of glycerol into bio-oil via hydrotreatment using supported metal catalysts," *Fuel*, vol. 112, no. 2013, pp. 193–202, 2013.
- [23] Y. Wu, M. R. Khadilkar, M. H. Al-Dahhan, and M. P. Duduković, "Comparison of upflow and downflow two-phase flow packed-bed reactors with and without fines: Experimental observations," *Ind. Eng. Chem. Res.*, vol. 35, no. 2, pp. 397–405, 1996.
- [24] M. E. Trivizadakis, D. Giakoumakis, and A. J. Karabelas, "A study of particle shape and size effects on hydrodynamic parameters of trickle beds," *Chem. Eng. Sci.*, vol. 61, no. 17, pp. 5534–5543, 2006.
- [25] S. Afandizadeh and E. A. Foumeny, "Design of packed bed reactors: Guides to catalyst shape, size, and loading selection," *Appl. Therm. Eng.*, vol. 21, no. 6, pp. 669–682, 2001.
- [26] K. M. Brunner *et al.*, "Effects of particle size and shape on the performance of a trickle fixed-bed recycle reactor for fischer-tropsch synthesis," *Ind. Eng. Chem. Res.*, vol. 54, no. 11, pp. 2902–2909, 2015.

- [27] J. Hanika and K. Sporka, "Catalyst Particle Shape and Dimension Effects on Gas Oil Hydrodesulphurization," *Chem. Eng. Sci.*, vol. 47, no. 9–11, pp. 2739–2744, 1992.
- [28] M. J. Taulamet, N. J. Mariani, G. F. Barreto, and O. M. Martínez, "Prediction of thermal behavior of trickle bed reactors : The effect of the pellet shape and size," vol. 202, pp. 631–640, 2017.
- [29] A. A. Montagna and Y. T. Shah, "The Role of Liquid Holdup, Effective Catalyst Wetting, and Backmixing on the Performance of a Trickle Bed Reactor for Residue Hydrodesulfurization," *Ind. Eng. Chem. Process Des. Dev.*, vol. 14, no. 4, pp. 479–483, 1975.
- [30] D. L. Xian Feng, C. Junghui, N. Menglong, L. Xu, and L. T. C. Lester, "Kinetic parameter estimation and simulation of trickle-bed reactor for hydrodesulfurization of crude oil," *Fuel*, vol. 230, pp. 113–125, 2018.
- [31] M. Bazmi, S. H. Hashemabadi, and M. Bayat, "Extrudate Trilobe Catalysts and Loading Effects on Pressure Drop and Dynamic Liquid Holdup in Porous Media of Trickle Bed Reactors," *Transp. Porous Media*, vol. 99, no. 3, pp. 535–553, 2013.
- [32] D. Nemeč and J. Levec, "Flow through packed bed reactors: 1. Single-phase flow," *Chem. Eng. Sci.*, vol. 60, no. 24, pp. 6947–6957, 2005.
- [33] D. Nemeč and J. Levec, "Flow through packed bed reactors: 2. Two-phase concurrent downflow," *Chem. Eng. Sci.*, vol. 60, no. 24, pp. 6958–6970, 2005.
- [34] J. Arpit and B. Vivek, V., "Droplet microfluidics on a planar surface," *AIChE J.*, vol. 63, no. 1, pp. 347–357, 2016.
- [35] S. P. Maiti, R. and N. K., "TRICKLE-BED REACTORS: LIQUID DISTRIBUTION AND FLOW TEXTURE," *Rev. Chem. Eng.*, vol. 20, p. 57, 2004.
- [36] N. A. Tsochatzidis, A. J. Karabelas, D. Giakoumakis, and G. A. Huff, "An investigation of liquid maldistribution in trickle beds," *Chem. Eng. Sci.*, vol. 57, no. 17, pp. 3543–3555, 2002.
- [37] A. Atta, S. Roy, and K. D. P. Nigam, "Investigation of liquid maldistribution in trickle-bed reactors using porous media concept in CFD," *Chem. Eng. Sci.*, vol. 62, no. 24, pp. 7033–7044, 2007
- [38] J. D. Llamas, C. Pérat, F. Lesage, M. Weber, U. D'Ortona, and G. Wild, "Wire mesh tomography applied to trickle beds: A new way to study liquid maldistribution," *Chem. Eng. Process. Process Intensif.*, vol. 47, no. 9–10, pp. 1765–1770, 2008.
- [39] R. N. Maiti and K. D. P. Nigam, "Gas–Liquid Distributors for Trickle-Bed Reactors: A Review," *Ind. Eng. Chem. Res.*, vol. 46, no. 19, pp. 6164–6182, 2007.

- [40] D. Borremans, S. Rode, and G. Wild, "Liquid flow distribution and particle-fluid heat transfer in trickle-bed reactors: The influence of periodic operation," *Chem. Eng. Process. Process Intensif.*, vol. 43, no. 11, pp. 1403–1410, 2004.
- [41] Z. Kuzeljevic, "Hydrodynamics of trickle bed reactor: Measurements and Modeling," no. May 2010, p. 217, 2010.
- [42] A. Atta, M. Hamidipour, S. Roy, K. D. P. Nigam, and F. Larachi, "Propagation of slow/fast-mode solitary liquid waves in trickle beds via electrical capacitance tomography and computational fluid dynamics," *Chem. Eng. Sci.*, vol. 65, no. 3, pp. 1144–1150, 2010.
- [43] A. Wongkia, F. Larachi, and S. Assabumrungrat, "Hydrodynamics of countercurrent gas-liquid flow in inclined packed beds - A prospect for stretching flooding capacity with small packings," *Chem. Eng. Sci.*, vol. 138, pp. 256–265, 2015.
- [44] M. G. Basavaraj, G. S. Gupta, K. Naveen, V. Rudolph, and R. Bali, "Local liquid holdups and hysteresis in a 2-D packed bed using X-ray radiography," *AIChE J.*, vol. 51, no. 8, pp. 2178–2189, 2005.
- [45] J. Zalucky, M. Wagner, M. Schubert, R. Lange, and U. Hampel, "Hydrodynamics of descending gas-liquid flows in solid foams: Liquid holdup, multiphase pressure drop and radial dispersion," *Chem. Eng. Sci.*, vol. 168, pp. 480–494, 2017.
- [46] L. D. Anadon, M. H. M. Lim, A. J. Sederman, and L. F. Gladden, "Hydrodynamics in two-phase flow within porous media," *Magn. Reson. Imaging*, vol. 23, no. 2 SPEC. ISS., pp. 291–294, 2005.
- [47] L. F. Gladden and A. J. Sederman, "Magnetic resonance imaging as a quantitative probe of gas-liquid distribution and wetting efficiency in trickle-bed reactors," *Chem. Eng. Sci.*, vol. 56, no. 8, pp. 2615–2628, 2001.
- [48] C. Boyer and B. Fanget, "Measurement of liquid flow distribution in trickle bed reactor of large diameter with a new gamma-ray tomographic system," *Chem. Eng. Sci.*, vol. 57, pp. 1079–1089, 2002.
- [49] A. F. Velo, D. V. S. Carvalho, and M. M. Hamada, "Liquid distribution and holdup in the random packed column," *Flow Meas. Instrum.*, 2017.
- [50] A. Gianetto and V. Specchia, "Trickle-Bed Reactors: State of Art and Perspectives," *Chem. Eng. Sci.*, vol. 47, no. 13/14, pp. 3197–3218, 1992.
- [51] H. C. Henry and J. B. Gilbert, "Scale Up of Pilot Plant Data for Catalytic Hydroprocessing," *Ind. Eng. Chem. Process Des. Dev.*, vol. 12, no. 3, pp. 328–334, 1973.

- [52] A. Rahman and M. Bin, "Investigation of local velocities and phase holdups, and flow regimes and maldistribution identification in a trickle bed reactor," 2017.
- [53] A. Toukan, "Hydrodynamic of a Co-Current Upflow Moving Packed Bed Reactor with a Porous catalyst," 2016.
- [54] P. R. Gunjal, V. V Ranade, and R. V Chaudhari, "Liquid Distribution and RTD in Trickle Bed Reactors: Experiments and CFD Simulations," *Can. J. Chem. Engineering*, vol. 81, no. June-August, pp. 821–830, 2003.

IV. NON-INVASIVE CATALYST UTILIZATION MEASUREMENT IN A MIMICKED BENCH SCALE HYDROTREATER REACTOR

Mohammed Al-Ani^a, Humayun Shariff^a, Hamza AlBazzaz^b, Muthanna Al-Dahhan^{a*}

^a Multiphase Reactors Engineering and Applications Bench (mReal), Department of Chemical and Biochemical Engineering, Missouri University of Science and Technology, Rolla, MO 65409-1230. USA

^b Kuwait Institute for Science Research, P.O. Box 24885, 13109, Kuwait

ABSTRACT

The volume of utilized catalyst was calculated by implementing new methodology based on the phase holdup, measured using advanced gamma-ray densitometry (GRD) technique in a mimicked bench scale hydrotreater reactor. The scaled down reactor design was designed with a 3mm diameter stainless steel pipe as a thermowell fixed in the center. A range of mixed gas and liquid velocities of 296.5-1796.5 cc/min and 0.39-2.46 cc/min respectively were investigated for a downward flow for a catalyst bed with commercial trilobe catalyst particles. The catalyst bed was packed with and without dilution to estimate the utilization with two inlet directions (top and side). The gas and liquid holdup values from the GRD experiments were evaluated at six different axial levels and a wettability factor was estimated based on the holdup values at the operating conditions. The effects of the top and side inlet direction for mixed gas and liquid flow indicated a significant impact on the volume of the utilized catalyst in the non-diluted bed which is dependent on the gas and liquid velocities, whereas there was no considerable influence on the volume of the utilized catalyst in the diluted bed. The diluted bed showed better-utilized catalyst volume compared to the non-diluted bed due to the increase in the liquid holdup values. The holdup

values were integrated into a multiscale model to approximate the catalyst utilization at different operating conditions to predict the actual reactor performance.

Keywords:

Catalyst Utilization, bench-scale hydrotreater reactor, diluted bed, commercial trilobe catalyst particles

Highlights:

- Volume of the utilized catalyst calculation by newly proposed methodology
- Fine particles (diluent particles) effects on Volume of the utilized catalyst in bench-scale trickle bed reactor.
- Top and side inlet configuration for fluids effects on Volume of the utilized catalyst
- Volume of the non-utilized catalyst
- Length required to substitute the non-utilized catalyst in the bed

1. INTRODUCTION

Trickle bed reactors (TBRs) are one of fixed bed reactors that the gas and liquid flow downward through the packed bed (catalyst particles) as a solid phase. TBRs extensively used in petroleum, chemical, and biochemical industries. Hydrotreating processes such as

hydrodesulfurization (HDS) process represent one of the most critical petroleum operations in multiphase phase processes [1]–[9].

The catalyst particles (solid phase) play a central role to improve performance in TBRs by providing a suitable surface area for reactants (gas and liquid), which considerably affect the conversion and selectivity for desirable products. Traditionally, incomplete wetting for catalyst bed especially with trickle flow regime due to liquid maldistribution and low wetting efficiency generate desirable (wetted) and undesirable (dry) surface area. The wetted area is highly required where both gas and liquid (reactants) co-exist to obtain high selectivity and desired products. The wetted surface area represents the amount of catalyst utilized in the bed which is a crucial parameter for assessing the reactor performance, catalyst life, cost, and in optimizing the operation conditions. The conventional way for conversion estimation in TBRs is by accounting the total amount of catalyst packed in the reactor as a utilized catalyst. But in fact, it does not represent the real amount of utilized catalyst in the reactor due to liquid maldistribution flow phenomena which leads to incomplete wetting for catalyst particles in the bed.

In exothermic reactions like hydrodesulfurization conducted in TBRs, liquid maldistribution and channeling occur due to improper distributor design, packing and operating conditions that can generate hot spots. This is considered as one of the main reasons to initiate coking and sintering of catalyst particles and reduces the life cycle of catalyst and the performance of the reactor. The shorter life of the catalyst and unsatisfactory reactor performance have significant impact on the operational cost and may increase the sulfur emissions to the atmosphere. Bench scale reactors have been employed to investigate the performance and efficiency to optimize the operation condition in the

TBRs. The major advantages to use a downsized reactor are decreasing the operation expense, less materials required, and safe handling [10]–[12]. On the other side, the low flow rate in the bench scale reactors significantly accounts for the liquid maldistribution due to packing commercial size catalyst particles, where the ratio of reactor diameter to particle diameter should be less than 20. [11], [13], [14]. This ratio plays a significant factor to increase the voidage in the bed especially near to the wall to cause wall effects on the hydrodynamic parameters in the bench scale reactors [11], [13], [14].

The bed height is considered as one of the parameters that significantly impacts the phase distribution due to non-uniform distribution of catalyst particles along the bed [15]. [15] employed a cylindrical column with 14 cm inside diameter and 100 cm height to conduct the experimental work to investigate bed height in the column. The authors reported that the bed height has an effective influence on the radial liquid distribution along the height bed axially at soak and dense packing. The results also showed that increasing the bed height improved the liquid distribution due to improving the uniformity of void fraction of the catalyst bed in the reactor.

The design of the distributor is another parameter that affects the liquid distribution and wetting efficiency of catalyst particles by affecting the flow of the reactants to the reactor. The distributor, placed on the top of the reactor, helps in providing a better mixing of gas and liquid as noted by [1].

Commercially, the effects of inlet direction is highly interesting to investigate its impact on the reactor performance at laboratory scale. The phase (gas and liquid) distribution are affected by several factors like reactor diameter to catalyst diameter ratio, distributor design, packing of the bed, capillary forces, spraying of gas, operating conditions etc.) [16].

One of the most important factors is inlet fluids distribution where the gas and liquid phases either are premixed or sent separately to the distributor [1]. However, the direction of the inlet (top, side, or inclined) can also have a significant effect on the liquid distribution. To our knowledge no work was available in open literature.

In the bench scale reactors, several authors recommended adding fine particles during operation at the same space velocity to the industrial processes to reduce the void fraction and achieve uniformity in the packing of the bed [13], [14], [17]. Al-Dahhan & Duduković 1996 demonstrated that adding fine particles as a diluent to the bed with two different catalyst shapes (Spherical and cylindrical) had a significant impact on the wetting efficiency and liquid holdup at high-pressure operation.

A comparative study was conducted using alpha-methyl styrene hydrogenation to cumene as a test reaction in a laboratory scale trickle bed reactor to understand the effect of fines on the reactor performance. (Wu et.al, 1996) It was observed that while using fines the conversion was up to 10% more than the reactor without dilution at different space times. To mention, higher spacetimes during high pressure operation yielded higher difference in the conversion. Recently, Mohammed Al-Ani et al. in paper III showed an a considerable effect of mixing the bed with fine particles on the performance by decrease the liquid maldistribution and increase the wetting for catalyst particles within commercial trilobe catalyst particles in the downsized reactors.

Over the past years, there has been a dramatic assessment of catalyst utilization by conversion measurements or by model prediction where the industry in high demand to develop a new methodology to evaluate the catalyst utilization based on reliable data by using advanced measurement technique which that will help to enhance the reactors

performance and the reactor efficiency. Hence, more investigation is recommended to enhance the accuracy of calculations and modify the conversion calculation in the TBRs by using the real calculated amount of utilized catalyst within operation condition that represents the precise value in conversion calculations. The aim of the present study is to estimate the holdup values using GRD technique and propose a methodology to approximate the catalyst utilization volume in bench scale hydrotreater reactors with and without dilution. Moreover, the effects of the gas and liquid flow rates on the reactants inlet direction (top and side) will be discussed for the first time.

2. EXPERIMENTAL WORK

2.1. EXPERIMENTAL SETUP

A bench-scale reactor was developed mimicking industrial hydrotreater reactors. A transparent acrylic reactor was used to conduct the experiments with concurrent downward gas and liquid flow through porous catalyst particles. Two different inlet direction streams of mixed gas and liquid (top and side) have been used and controlled by two valves. The column dimensions were 1.18 cm I.D. and 72cm length. A thermowell hollow stainless-steel pipe with 3mm O.D. was used in the system to replicate a thermowell design in the center of the reactor as shown in Figure 1. Air-water system was employed to investigate the hydrodynamic parameters (phase holdup) using advanced gamma-ray densitometry technique to estimate the catalyst utilization within diluted and non-diluted bed. The measurements are achieved at range of superficial gas velocity between 269.5-1796.5 cc/min and range of liquid velocity between 0.39-2.46 cc/min at six axial positions and

eleven diametrical locations as it shown in Figure 1. The reactor loaded with different layers of particles which the sequence of layers shown in Figure 1 and the packed bed characteristics displayed in Table 1.

2.2. MEASUREMENT TECHNIQUE

Gamma-ray densitometry (GRD) is a noninvasive technique based on the gamma-ray photon count measurement. The components of GRD sealed source of Cs-137 (the initial activity of 250 mCi) and a NaI detector mounted and aligned with the source on the opposite side as depicted in Figure 2.

The high flexibility for GRD technique enables it to provide diametrical profile as well as the bed height axially. The structure, principles, and measurements methods were discussed widely by [18] and Al-Ani (paper III). The results were confirmed and validated for with pilot plant scale TBRs loaded by glass beads particles [18] and by Mohammed Al-Ani (paper III) at bench scale.

The GRD methodology used in this work was structured and developed at Multiphase Flow Reactors Engineering and Applications (mFReal) in Missouri University of Science and Technology (S&T). The bench scale hydrotreater reactor is centered between the Gamma-ray of Cs-137 and the detector [18]. The reactor is fixed while the source and detector are mobile. The gamma-ray from the source penetrates through the reactor to the detector. The signals are processed to determine the holdup values at the operating conditions based on the previously validated methodology [18].

Table 1. Packed bed characteristics

REACTOR/ PACKING	CHARACTERISTICS
Reactor	<p>inside diameter = 1.18 cm</p> <p>height = 72 cm</p>
Packing	
Commercial Trilobe Catalyst	<p>length: 3 mm</p> <p>diameter: 1.5 mm</p> <p>Bed height: 60 cm</p>
Inert Ball(Alumina)	<p>diameter = 2mm</p> <p>Height = 2 cm in the top</p> <p>Height = 2cm in the bottom</p>
Nonporous Layer	<p>Material: Medium Carborundum particles</p> <p>Bulk density = 1.67 (g/cc)</p> <p>Height = 4 cm over the trilobe</p> <p>Height = 4 cm under the trilobe</p>
Fines Particles	<p>Material: Fine Carborundum particles</p> <p>Size: 350-500μm</p> <p>Bulk density = 1.76 (g/cc)</p>

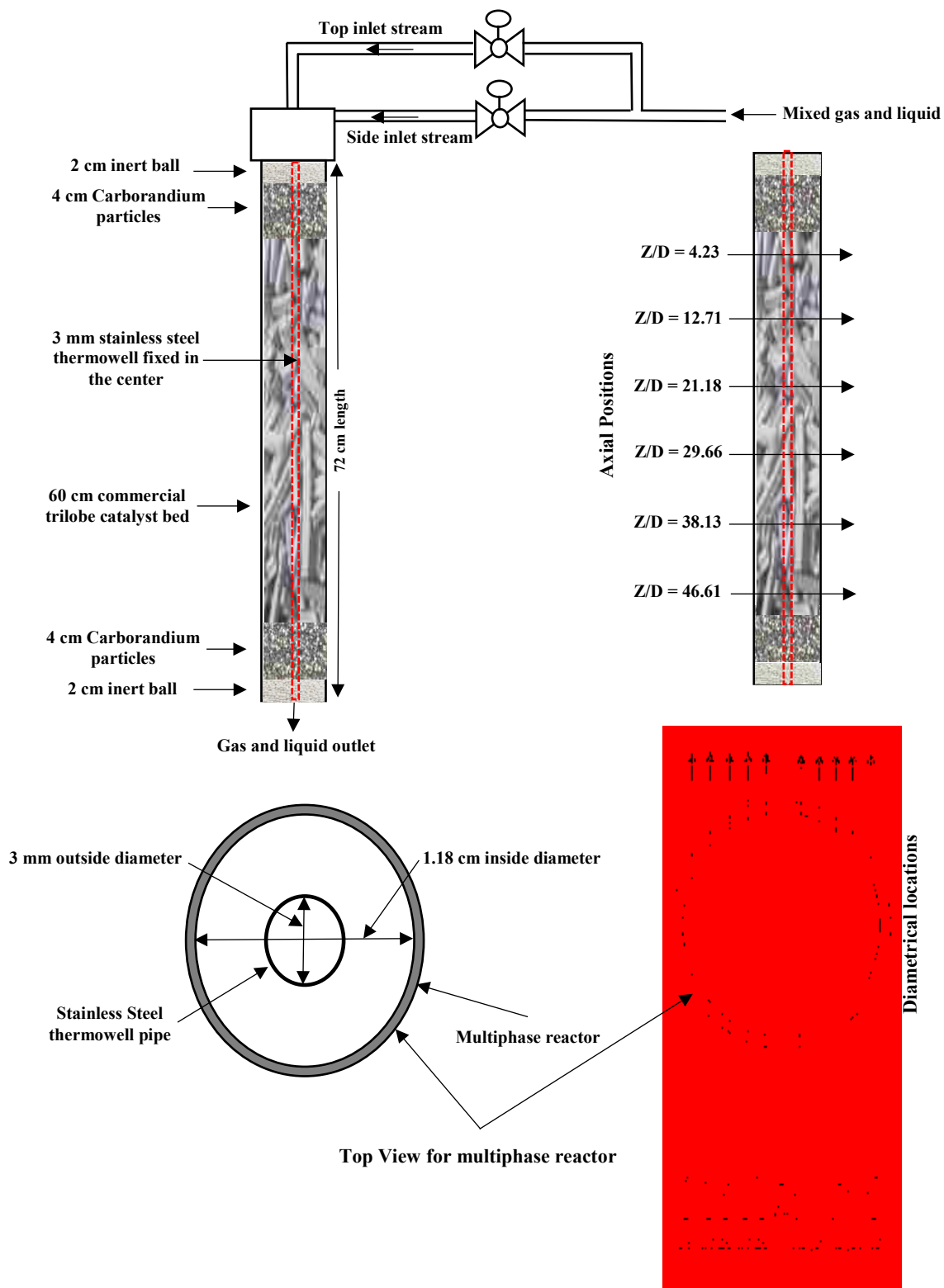


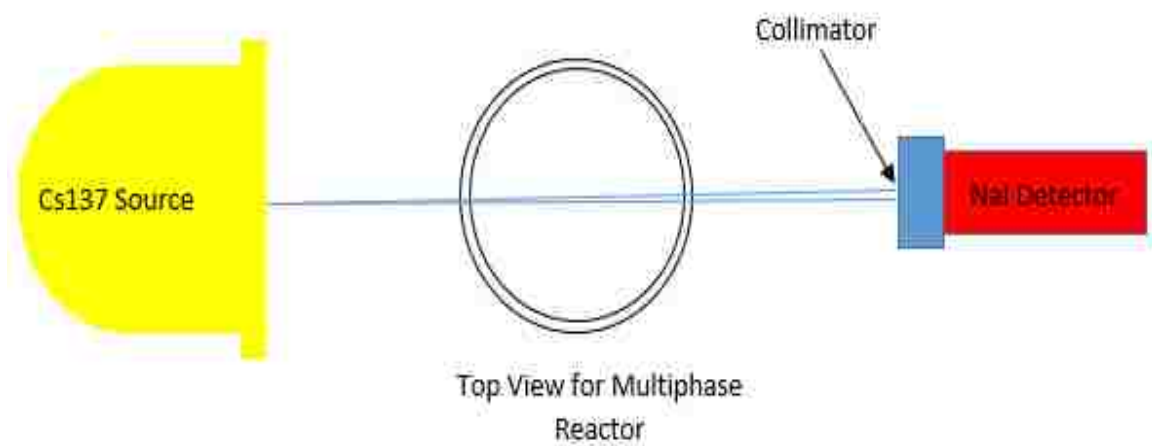
Figure 1. Schematic diagram of bench scale hydrotreater reactor

The high flexibility for GRD technique enables it to provide diametrical profile as well as the bed height axially. The structure, principles, and measurements methods were discussed widely by [18]. The results were confirmed and validated for with pilot plant scale TBRs loaded by glass beads particles [18] and by Mohammed Al-Ani (paper III) at bench scale. The GRD methodology used in this work was structured and developed at Multiphase Flow Reactors Engineering and Applications (mFReal) in Missouri University of Science and Technology (S&T). The bench scale hydrotreater reactor is centered between the Gamma-ray of Cs-137 and the detector [18]. The reactor is fixed while the source and detector are mobile. The gamma-ray from the source penetrates through the reactor to the detector. The signals are processed to determine the holdup values at the operating conditions based on the previously validated methodology [18] and Al-Ani (paper III).

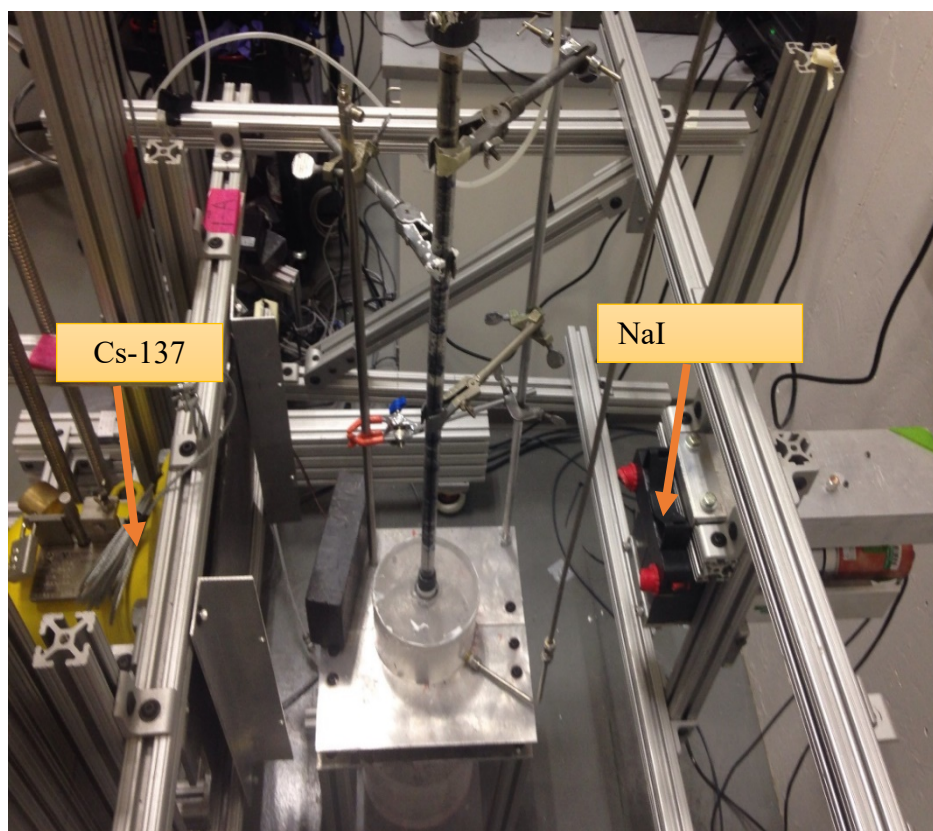
2.3. CATALYST UTILIZATION

The evaluation of performance for hydrotreater reactors essentially depends on the weight or volume of loaded catalyst in the reactor. Basically, the biggest challenge in the industry for fixed bed reactors is liquid maldistribution, so the full assessment for performance in fixed bed reactors should be built on the actual amount of utilized catalyst in the kinetic reaction. Industrial bench scale reactor dimensions and operating conditions were used in the current research to measure the percentage of catalyst utilized.

Based on the investigation from the GRD technique gas and liquid holdup will be estimated. These value will highly help to estimate the volume of utilized and non-utilized.



(a) Schematic representation of GRD



(b) GRD set-up at Missouri S&T

Figure 2. Photo and schematic diagram for Gamma-ray densitometry

catalyst in the reactor and determine the additional length to be added to the reactor to enhance the accuracy for performance evaluation.

In the previous study, the diametrical profile of line averaged at different axial levels (Z/D) of fluids holdup (gas, liquid, and solid holdup) were investigated using advanced non-invasive GRD technique in bench scale of hydrotreater reactor. Six axial levels were scanned along the bed height (60 cm) with same distance between each level (10 cm) and 11 diameter positions (Paper III). Consequently, ratio of liquid holdup (ε_l) to gas holdup (ε_g) is calculated at each axial level along diametrical location of the bed for different operating conditions. The ratio is called wettability factor ($\varepsilon_l/\varepsilon_g$). When the factor is equal to one it means we have 50% gas occupied the void space and 50% liquid occupying the void space. On other hand, if the ratio of ($\varepsilon_l/\varepsilon_g$) is more than one that is mean we have more of liquid than the percent of gas present in the void and vice versa. The steps to estimate the catalyst utilization are shown below:

- 1- The frequency distribution by Histogram for ($\varepsilon_l/\varepsilon_g$) for all diametrical profiles at each axial level (Z/D) at different operating conditions is plotted to identify the most frequent factor prevailing in range of operating condition as it seen in Figure 3. Three of the most frequent ratio out of 11 that are scanned along the diametrical profile are selected to be the dominant wettability factor for each level. According to, the range of dominant ratio, the maxima and minima of the factor of the three frequencies will for the wettability factor will be determined.

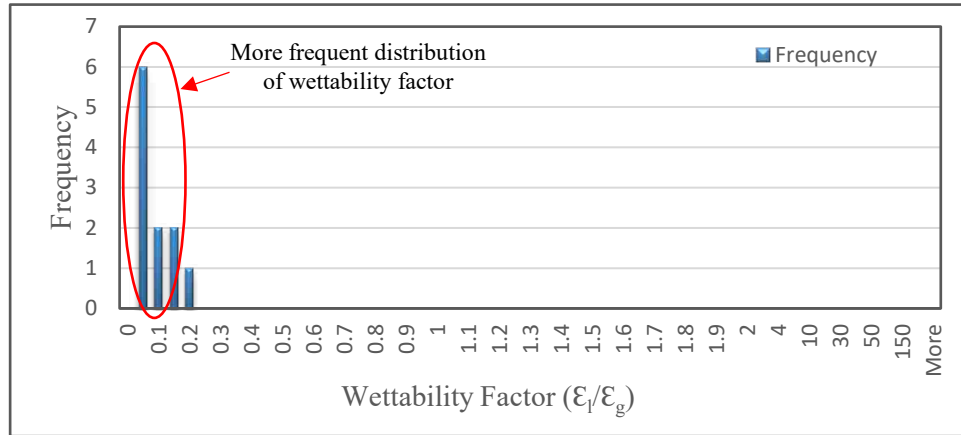


Figure 3. Histogram for wettability factor frequency distribution within $UG=1796.5$, $UI=2.64$ cc/min at axial level ($Z/D=12.71$)

- 2- By determining the range of dominant wettability factor, the corresponding range of liquid volume fraction (holdup) can be identified. These values are considered as the vital parameters as liquid holdup directly impacts the fraction and distribution of liquid in the hydrotreater reactors and hence the utilization as mentioned earlier. Furthermore, the range of gas and solid holdup are diagnosed based on the range of liquid holdup.
- 3- The catalyst bed height is divided to six similar Sections, each level considered as individual slice with the same volume of each slice (V_i) as seen in Eq. 1.

$$V_i = \frac{\pi}{4} d^2 L_i \quad (1)$$

- 4- The volume of each level is calculated with respect the solid volume fraction called volume of the actual catalyst utilized in the level (V_i^*) that is determined based on the

wettability factor as shown in equ. 2. The solid holdup ε_{si} values are determined based on the respective liquid and gas holdup values by the expression, $\varepsilon_g + \varepsilon_l + \varepsilon_s = 1$

$$V_i^* = \frac{\pi}{4} d^2 L_i \varepsilon_{si} \quad (2)$$

where:

d: Inside diameter for reactor

L: Length of bed

i: The axial level (1,2,3,4,5,6)

ε_{si} : Dominant solid holdup at i level

5- Summation of volume of the utilized catalyst in each level represents the total volume of the utilized catalyst ($\sum V_i^*$) for whole bed as Eq. 3

$$\sum V_i^* = V_1^* + V_2^* + V_3^* + V_4^* + V_5^* + V_6^* \quad (3)$$

6- Calculate the net volume of the catalyst bed (V_s) as it seen in Eq. 4.

$$V_s = \frac{\text{Weight of the catalyst bed}}{\text{Bulk density of the catalyst}} \quad (4)$$

where:

L: total length of bed (cm)

7- The percentage of the utilized catalyst in the bed ($\% V_u$) is the ratio of volume of utilized catalyst (V_i^*) to the total volume of the reactor (V_s) (Eq. 5).

$$\% V_u = \frac{V_i^*}{V_s} \times 100 \quad (5)$$

8- The total volume of the non-utilized catalyst in the reactor is equal to the difference between the total volume for the reactor and the total volume of the non-utilized catalyst (V_{non}) as shown in Eq. 4.

$$V_{non} = V_s - \sum V_i^* \quad (6)$$

3. RESULTS AN DISCUSSION

The volume of the utilized catalyst was calculated at 6 axial positions from top to bottom ($Z/D = 4.23, 12.71, 21.18, 29.66, 38.13, 46.61$) and 11 diametrical locations. The developed methodology explained in Section 2.3 was used to calculate the volume of catalyst utilized at different operating conditions. It was observed that the liquid distribution and wetting efficiency have a considerable impact on the utilized catalyst volume in the bed. Moreover, channeling and rivulet flow of liquid along the bed height due to nonuniformity void space distribution contribute to the deteriorating the wetting efficiency and thus reducing the volume of catalyst utilization. In the current reactor setup, no distributor has been used to distribute the fluids. On the other hand, layers of inert ball particles and medium Carborundum particles are used above and below the bed of trilobe catalyst particles to improve the distribution in the bed. Since no distributor was used in our work, both the liquid and gas were premixed and sent to the reactor but in two different

directions. The effect the of mixed gas and liquid inlet direction (top and side) on the volume of the utilized catalyst obtained in non-diluted and diluted bed are shown in Figure 4 and 5. In non-diluted bed, which has more voidage, the influence of mixed gas and liquid inlet direction (top and side) on the volume of catalyst utilization revealed oscillation in the results at low gas and high liquid flow rates as shown in Figure 4 a and b. The volume of the utilized catalyst improved approximately by 8-12 % with the inlet direction from the top (Figure 4a). Meanwhile, the local volume of the utilized catalyst enhanced noticeably with the inlet direction from the top in the non-diluted bed (Figure 4a) in the hydrotreater reactors. While using the side inlet fluctuation was noticed in the utilized catalyst volume especially towards the bottom of the reactor. This clearly explains the maldistribution of the liquid accounting for low catalyst utilization which may be due to the wall effects of the liquid flow. On the other hand, no considerable effect on the inlet direction on the volume of the utilized catalyst was detected for diluted bed at low gas and liquid flow rates (Figure 5 a and b). The overall catalyst utilization volume was observed to be in a closer range while using the top inlet as shown in Figure 5a. A similar trend was observed in both the cases where the catalyst utilization improved axially. This may be due to the fact that there was better liquid distribution due to the presence of fines in the bed. Additionally, Figure 6 a and b have illustrated the impact of using fine particles on the catalyst utilization. For this comparison, the top inlet direction was chosen as it showed better utilization in both types of beds. It can be observed that the volume of catalyst utilization in the diluted bed is larger than non-diluted bed due to increasing the liquid holdup by improving the contacting efficiency in the bed, eventually enhancing the wetting efficiency.

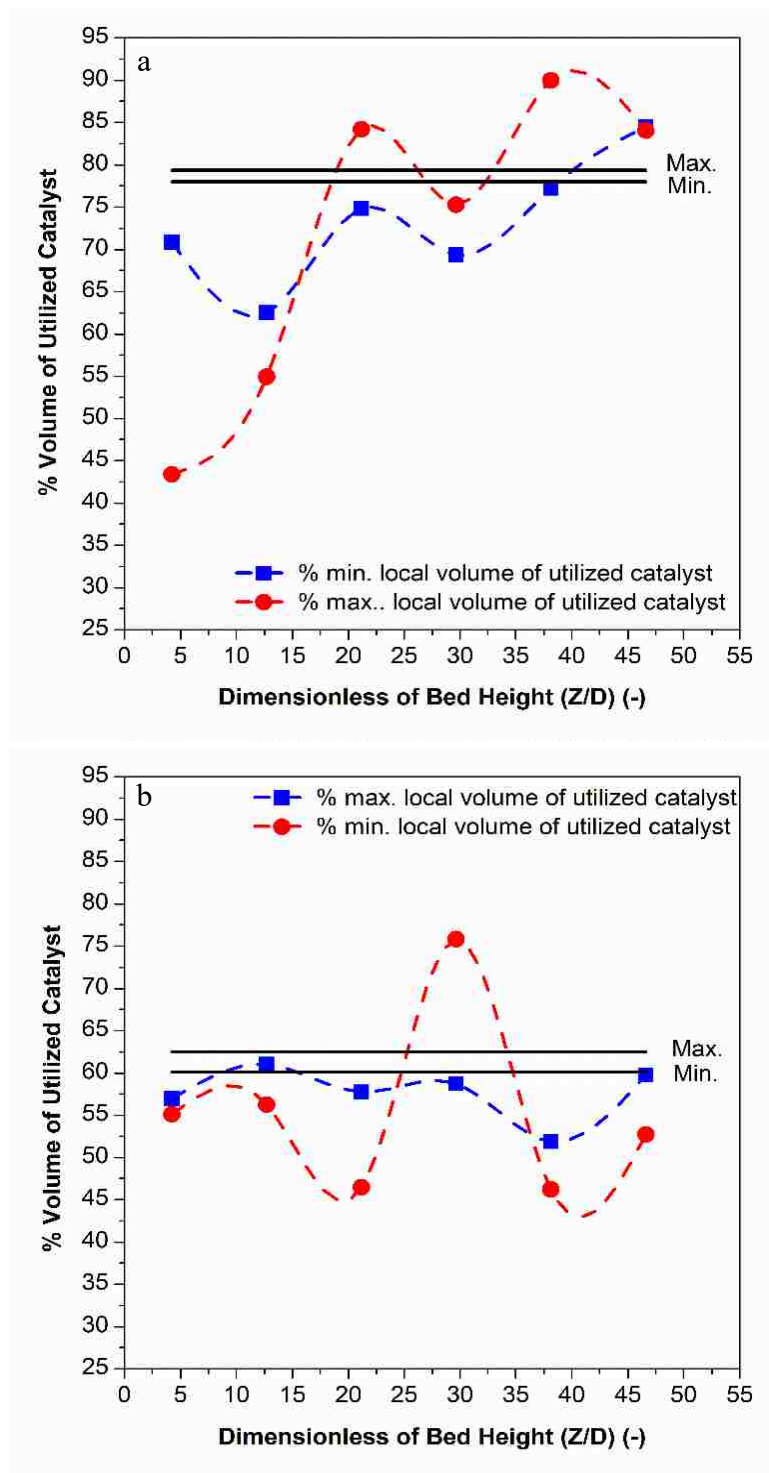


Figure 4. Volume of catalyst utilization vs bed height at $U_g = 1796.5$ and $U_l = 0.39$ cc/min from top direction (a) non-diluted bed (b) diluted bed

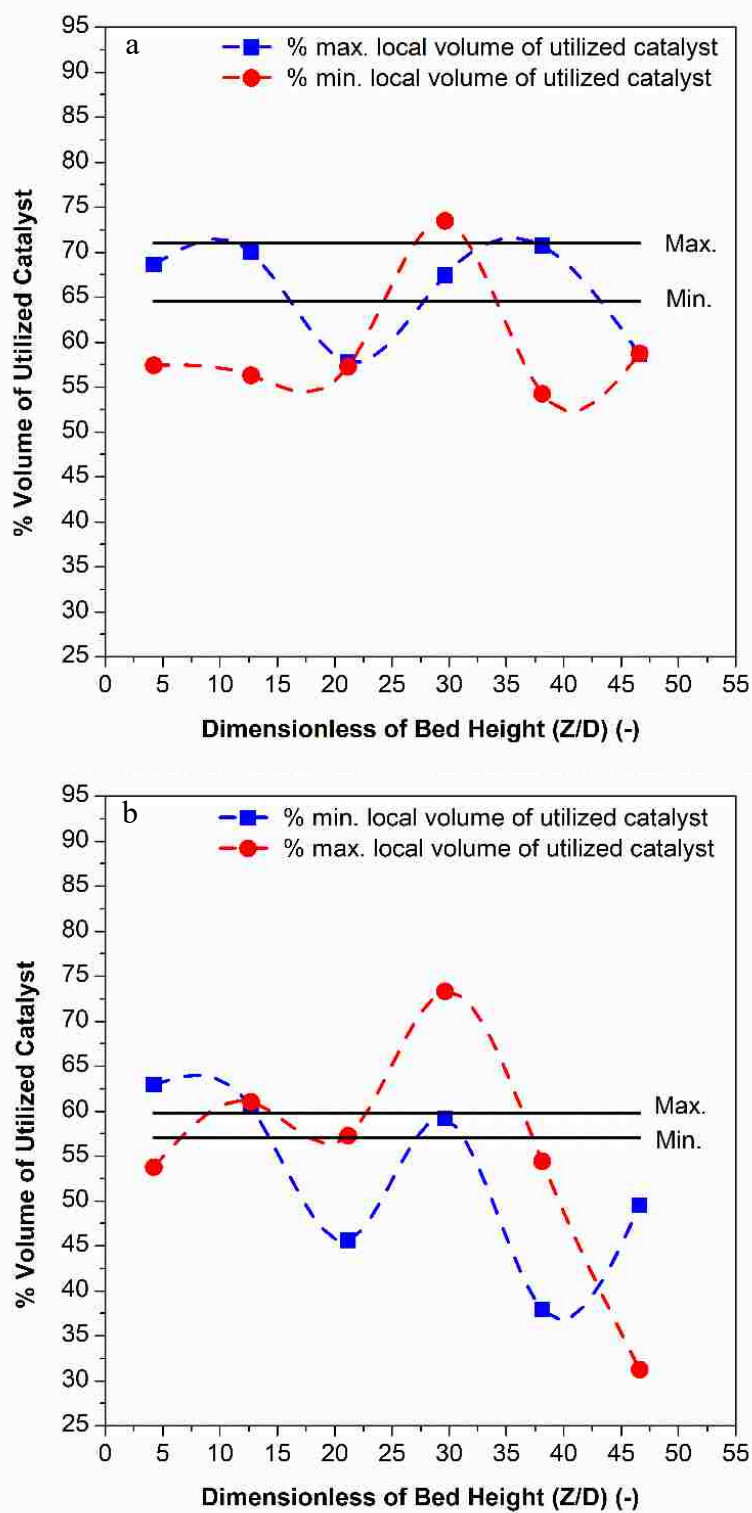


Figure 5. Volume of catalyst utilization vs bed height at $U_g = 269.5$ and $U_l = 2.46$ cc/min within non-diluted bed (a) top inlet direction (b) side inlet direction

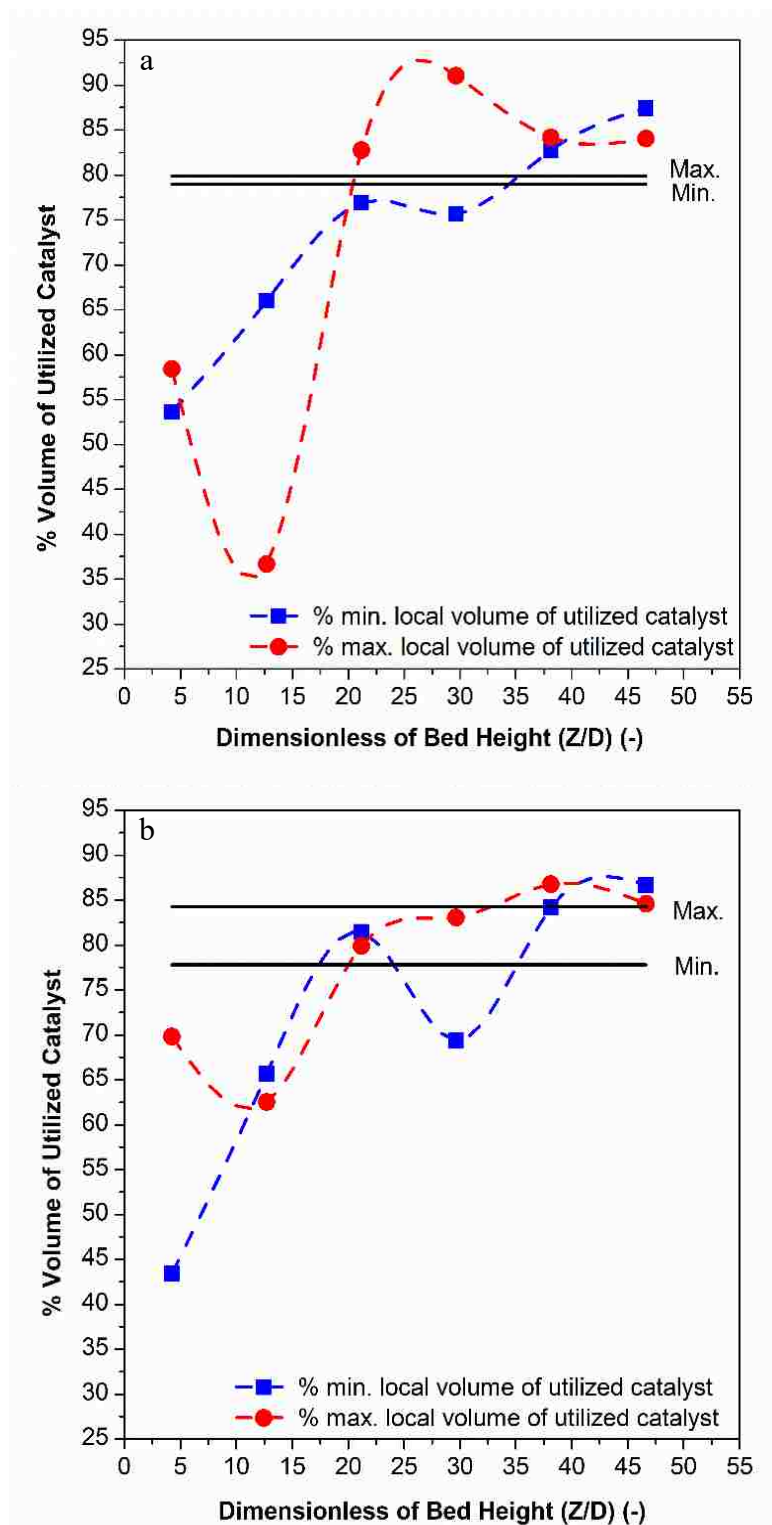


Figure 6. Volume of catalyst utilization vs bed height at $U_g = 269.5$ and $U_l = 0.39$ cc/min within diluted bed (a) top inlet direction (b) side inlet direction

Obviously, the whole volume of the utilized catalyst (global maximum line and global minimum line) increased 18-20 % in the diluted bed than the non-diluted bed at low liquid and high gas flow rates (Figure 6 a and b). The results showed a good agreement with several researchers who studied the effect of fines in bench scale TBRs [14], [17], and Al-Ani (paper III).

4. MODELING SIMULATION TO IDENTIFY CATALYST UNDER UTILIZATION USING EXPERIMENTAL DATA

From the GRD experiments, the holdup (liquid, gas and solid) values were determined for the similar operating conditions and reactor configuration. The experimental results from the hydrotreating reactions involving removal of asphaltene, sulfur, metals, microcarbon residue (MCR) conducted in an industrial scaled down scale hydrotreating unit were obtained in terms of conversion against Liquid Hourly Space Velocity (LHSV). The overall conversion value obtained from the reaction experiments was used in the modeling strategy to evaluate the new rate constant. At steady state, the mole balance of the species for a second order reaction will be

$$v \frac{dC_A}{dV} = r_A = k C_A^2$$

$$\frac{dC_A}{k C_A^2} = \frac{dV}{v}$$

The actual volume of the catalyst dV utilized needs to account the holdup term, ε_e . V - catalyst volume (mL) and v – flow rate (mL/hr). Then the above expression becomes

$$\frac{dC_A}{C_A^2} = k \varepsilon_u \frac{dV}{v}$$

where,

$$\varepsilon_u = \frac{\varepsilon_s}{\varepsilon_{void}} \varepsilon_L$$

This utilized holdup ε_u term defines the actual amount of catalyst being utilized with ε_s – solid holdup and ε_{void} – bed voidage.

Integrating the above equation with inlet and outlet concentration and limits for V as 0 to total catalyst volume we get

$$\left(\frac{1}{C_{out}} - \frac{1}{C_{in}} \right) = \frac{k V \varepsilon_u}{v}$$

The catalyst volume should be multiplied by the ε_u term to get the actual catalyst volume being utilized in the reactor. For the chosen operating condition, the experimental ε_s , ε_L and ε_{void} values were 0.082885, 0.755 and 0.245 respectively. The ε_u value was 0.2554 for 60 mL/hr feed flow rate condition. Using the experimental conversion value,

the rate constant is estimated. The new rate constant is integrated in a simple reactor scale model (Shariff and Al-Dahhan, 2019) and fitted to get the experimental conversion. It can be seen from the Figure 7, at the actual conditions the catalyst bed length needs to be increased by 24% in order to achieve the experimental conversion estimated from the rate constant calculated using the actual catalyst utilized. This clearly indicates that experimental changes need to be made in order exactly account for the complete catalyst utilization by increasing the length of the catalyst bed during modeling. This way modeling driven experimental investigation and vice versa become very essential in predicting the reactor performance, design and scale up.

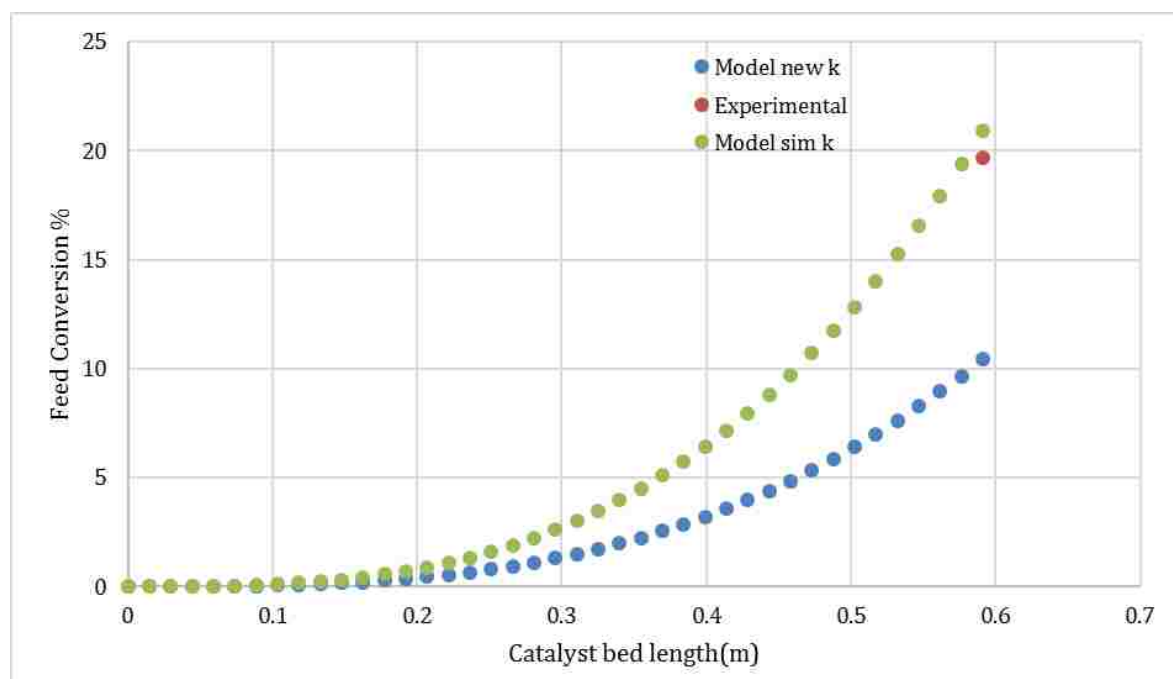


Figure 7. Reactor Performance Comparison of the experimental and model accounting for the catalyst under-utilization. ($T=370^{\circ}\text{C}$, LHSV 2 hr⁻¹, Feed S = 4.644 wt%)

The conversion determined by the model using the rate constant incorporating the liquid holdup was less than the experimental conversion. The new rate constants estimated differed by an order of magnitude. This is mainly due to the calculation of the rate constant directly using the total catalyst volume while the actual catalyst volume being not completely utilized. Also, twice the value of the rate constant (simulated k) was used to fit the curve to the obtained experimental conversion as shown in Figure 7. A better way to calculate rate constant can be from basket reactor studies or modifying the equation used to calculate it.

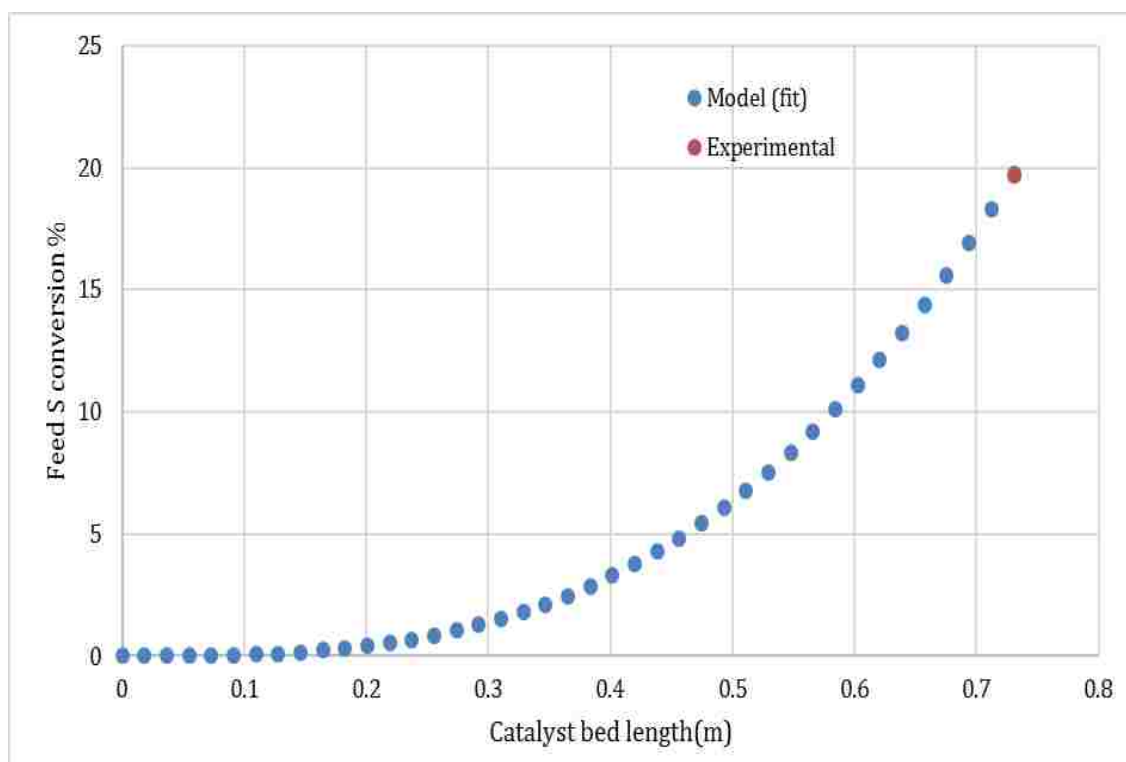


Figure 8. Reactor Performance Comparison of the experimental and model accounting for the catalyst under-utilization. ($T= 370^{\circ}\text{C}$, LHSV 2 hr⁻¹, Feed S = 4.644 wt%)

5. REMARKS

The volume of the utilized catalyst is measured in diluted bench scale hydrotreater reactor by implementing the new methodology. The line averaged of gas, liquid, and solid holdup that obtained by advanced Gamma-ray densitometry technique have used to calculate the volume of catalyst utilized in the reactor. Transparent Plexiglas column with 1.18 cm inside diameter and 72 cm length of reactor employed to govern the experimental work in the present work. The experiments conducted at a range of gas and liquid superficial velocities 296.5-1796.5 and 0.39-2.46 cc/min, respectively. The mixed gas and liquid have fed by two directions (top and side) though diluted and non-diluted of 1.5 mm diameter of commercial trilobe catalyst particles bed. The current work makes many noteworthy contributions to enhance the commercial understanding and enrich the literature with valuable information. The main finding can be summarized as follow:

- The newly proposed methodology based on the phase holdup obtained by photon counts of advanced gamma-ray densitometry technique is successfully calculated for the first time the volume of the utilized catalyst in diluted bed for bench scale hydrotreater reactor.
- A significant effect of dilution bed was observed on the volume of the utilized catalyst due to improve the contacting efficiency (solid-solid) induced to increase liquid holdup and wetting efficiency, thus increase the volume of catalyst utilization.
- The inlet direction for mixed gas and liquid flow (top and side) have an oscillation impact on the volume of catalyst utilization depend on the gas and liquid superficial velocities, void fraction and distribution that play a significant role on liquid distribution and flow pattern in the bed.

- The mixed gas and liquid inlet direction indicated an effective influence on the volume of the utilized catalyst in the non-diluted bed, while negligible effect for fluids flows inlet direction in the diluted bed due to reduce the void fraction and improve the contacting efficiency (solid-solid) in the reactor.
- More experimentation complemented with modeling efforts are needed in the catalyst utilization calculations and performance assessment for hydrotreater reactors.

ACKNOWLEDGMENT

The authors gratefully acknowledge the financial support in the form of a scholarship provided by Ministry of Higher Education and Scientific Research-Iraq, and the funds provided by Missouri S&T and Professor Dr. Muthanna Al-Dahhan to develop the experimental set-up and to perform the present study. Also, the authors would like appreciatively to thank, Kuwait Institute Scientific Research (KISR)-Kuwait for financial and technical support.

REFERENCES

- [1] R. N. Maiti and K. D. P. Nigam, "Gas-liquid distributors for trickle-bed reactors: A review," *Ind. Eng. Chem. Res.*, vol. 46, no. 19, pp. 6164–6182, 2007.
- [2] S. A. Ghenni and M. H. Al-Dahhan, "Assessing the Feasibility of Optical Probe in Phase Holdup Measurements and Flow Regime Identification," *Int. J. Chem. React. Eng.*, vol. 13, no. 3, pp. 369–379, 2015.
- [3] Y. Wang, J. Chen, and F. Larachi, "Modelling and simulation of trickle-bed reactors using computational fluid dynamics: A state-of-the-art review," *Can. J. Chem. Eng.*, vol. 91, no. 1, pp. 136–180, 2012.

- [4] P. R. Gunjal, V. V. Ranade, and R. V. Chaudhari, "Liquid Distribution and RTD in Trickle Bed Reactors: Experiments and CFD Simulations," *Can. J. Chem. Engineering*, vol. 81, no. June-August, pp. 821–830, 2003.
- [5] S. A. Al-Naimi, F. T. J. Al-Sudani, and E. K. Halabia, "Hydrodynamics and flow regime transition study of trickle bed reactor at elevated temperature and pressure," *Chem. Eng. Res. Des.*, vol. 89, no. 7, pp. 930–939, 2011.
- [6] J. Martínez, J., & Ancheyta, "Modeling the kinetics of parallel thermal and catalytic hydrotreating of heavy oil," *Fuel*, vol. 138, pp. 27–36., 2014.
- [7] S. Sundaresan, "Role of hydrodynamics on chemical reactor performance," *Curr. Opin. Chem. Eng.*, vol. 2, no. 3, pp. 325–330, 2013.
- [8] A. Atta, S. Roy, and K. D. P. Nigam, "Investigation of liquid maldistribution in trickle-bed reactors using porous media concept in CFD," *Chem. Eng. Sci.*, vol. 62, no. 24, pp. 7033–7044, 2007.
- [9] A. Kundu, K. D. P. Nigam, and R. P. Verma, "Catalyst wetting characteristics in trickle-bed reactors," *AIChE J.*, vol. 49, no. 9, pp. 2253–2263, 2003.
- [10] R. Moonen, J. Alles, E. J. Ras, C. Harvey, and J. A. Moulijn, "Performance Testing of Hydrodesulfurization Catalysts Using a Single-Pellet-String Reactor," *Chem. Eng. Technol.*, vol. 40, no. 11, pp. 2025–2034, 2017.
- [11] S. T. Sie and R. Krishna, "Process Development and Scale Up: III. Scale Up and Scale Down of trickle bed processes," *Rev. Chem. Eng.*, vol. 14, no. 3, pp. 203–252, 1998.
- [12] D. A. Hickman, M. T. Holbrook, S. Mistretta, and S. J. Rozeveld, "Successful scale-up of an industrial trickle bed hydrogenation using laboratory reactor data," *Ind. Eng. Chem. Res.*, vol. 52, no. 44, pp. 15287–15292, 2013.
- [13] J. V. K. and R. H. Van Dongen, "Catalyst Dilution for Improved Performance of Laboratory Trickle-Flow Reactors," *Chem. Eng. Sci.*, vol. 35, pp. 59–66, 1980.
- [14] M. H. Al-Dahhan and M. P. Duduković, "Catalyst Bed Dilution for Improving Catalyst Wetting in Laboratory Trickle-Bed Reactors," *AIChE J.*, vol. 42, no. 9, pp. 2594–2606, 1996.
- [15] M. Bazmi, S. H. Hashemabadi, and M. Bayat, "Flow Maldistribution in Dense- and Sock-Loaded Trilobe Catalyst Trickle-Bed Reactors: Experimental Data and Modeling Using Neural Network," *Transp. Porous Media*, vol. 97, no. 1, pp. 119–132, 2013.
- [16] S. T. Sie and R. Krishna, "Process development and scale up: II. Catalyst Design Strategy," *Rev. Chem. Eng.*, vol. 14, no. 3, pp. 159–202, 1998.

- [17] R. R. Kulkarni, J. Wood, J. M. Winterbottom, and E. H. Stitt, "Effect of fines and porous catalyst on hydrodynamics of trickle bed reactors," *Ind. Eng. Chem. Res.*, vol. 44, no. 25, pp. 9497–9501, 2005.
- [18] A. Rahman and M. Bin, "Investigation of local velocities and phase holdups, and flow regimes and maldistribution identification in a trickle bed reactor," 2017

**V. LOCAL GAS AND LIQUID SATURATIONS AND VELOCITIES STUDY
OF VARIOUS HYDROTREATING CATALYST SHAPES USING
ADVANCED OPTICAL FIBER PROBE IN A PILOT PLANT
TRICKLE BED REACTOR**

Mohammed Al-Ani, Muthanna Al-Dahhan*

Multiphase Reactors Engineering and Applications Bench (mReal), Department of
Chemical and Biochemical Engineering, Missouri University of Science and Technology,
Rolla, MO 65409-1230. USA

ABSTRACT

Experimental study to investigate hydrodynamics in a pilot plant-scale trickle bed reactor using advanced Two-Tips Optical Probe (TTOP) technique. Local flow dynamic parameters such as local gas and liquid saturation and velocities were investigated within different hydrotreating catalyst shapes along bed height of packed bed. The TBR used in this study is made up of Plexiglas column of diameter 0.14m and filled with different hydrotreating shapes such as trilobe, quadrilobe, cylindrical, and spherical packing. Water and air are the phases with the superficial velocity of liquid from 0.004 m/sec to 0.016 m/sec and range of superficial gas velocity of the gas at 0.09-0.27 m/sec. Local hydrodynamic parameters are evaluated using TTOP at these conditions. The results showed a significant effect of catalyst shape and bed height on the local gas and liquid saturation and velocities.

1. INTRODUCTION

Trickle bed reactors one of crucial processes in the industrial fields which the gas and liquid flow concurrently downward within a fixed bed as a solid phase (catalyst

particles). TBRs have been used extensively in different industrial fields such as chemical and biochemical industries [1], [2]

Numerous studies have been investigated the hydrodynamics in TBRs [3]–[5]. Most previous studies have used an averaged data obtained using invasive and non-invasive techniques, however, it is essential to provide local data that beneficial for benchmarking data.

In TBRs, the local gas and liquid saturation and velocities information are still lacking. However, there have been relatively few recent studies on local gas and liquid saturation and velocities. There are different techniques used to provide local data in the packed bed reactors which can be classified invasive and non-invasive techniques. The invasive techniques are needle probes (optical/conductivity), heat transfer probes, ultrasound probes [6]. The noninvasive techniques can be classified as photographic, particle tracking (PIV), radiography (X-Ray), resonance based (MRI, NMR) [6]. The major disadvantages are its implementation is limited by the size of the column, operating condition and high operating cost.

Alexander et al. [7] studied the local gas and liquid saturation and velocities in TBR. The author performed experimental investigations on local gas and liquid saturation and velocities using advanced invasive two tips optical fiber probe technique within spherical glass beads particles. Although, this investigation presented interesting results, nobody has examined the local gas and liquid saturation and velocities in different industrial catalyst shapes. [7].

Alexander et al. [8] investigated local gas and liquid saturation and velocities in upflow packed bed reactors using two tips optical probe (TTOP). The authors implemented TTOP within spherical catalyst particles with 11 inch bed diameter [8].

The objective of this study is to implement TTOP at various axial levels and radial positions inside the bed part of the pilot-scale TBR and to investigate the performance of the catalyst bed in terms of measured parameters at these conditions. Also, study the effects of different industrial catalyst shapes such as trilobe, quadrilobe, spherical, and cylindrical shapes on local gas and liquid saturation and velocities.

2. EXPERIMENTAL WORK

2.1. SETUP

A Plexiglas pilot plant-scale trickle bed reactor with 0.14 m inside diameter and 1.85 m height carried out the experiments in the current work as shown in Figure 1. Air-water system used as gas and liquid phase, respectively. Shower distributor with industrial design used to distribute the liquid in the reactor. Also, perforated plate with 16 holes of 3 mm diameter and 5 holes with of 5 mm applied in the experiments to improve the gas and liquid distribution in the reactor as seen in Figure 1.

2.2. OPERATION CONDITIONS

Table 1 shows the operating conditions that implemented to obtain the results in the present work. Also, Table 2 present the bed characteristics loaded to the reactor.

2.3. ADVANCED TWO TIP OPTICAL PROBES (TTOP) TECHNIQUE

2.3.1. Measurement Technique Two-Tip Optical Probe (TTOP). The optical probes are commonly used to identify gas-liquid phase. Based on light propagation behavior inside the probes follow's snell's law.

Table 1. Operation conditions characteristics

CONDITIONS	CHARACTERISTICS
Flow Rates	
Gas Flow Rate	0.09-0.27 m/s
Liquid Flow Rate	
Liquid Flow Rate	0.004-0.016 m/s
Locations	
Axial Levels	At the Top ($Z/D = 0.715$)
	At the Middle ($Z/D = 6.6$)
	At the Bottom ($Z/D = 12.5$)
Diametrical Positions	9 diametrical positions along bed diameter

Table 2. Packed beds characteristics

Shape (-)	Porosity (-)	Size (L x d) (mm x mm)	Sphericity (-)	Volume (V _p) (mm ³)	Surface area (A _p) (mm ²)	Equivalent diameter (mm)	Equivalent area (mm ²)	dc/dp (-)
Spherical	0.36	4.7	1	55.287	70.18	4.7	55.28	29.8
Cylindrical	0.451	6 x 2.8	0.82	36.9	65.10	4.1	53.89	50
Trilobe	0.526	6 x 3	0.62	32.28	79.42	3.93	49.29	46.6
Quadrilobe	0.456	6 x 2.5	0.718	19.98	49.79	3.35	35.7	56

Snell's law stated that when the light travels from the optically dense medium to lesser dense medium, the light will be entirely scattering back to the dense medium when the light fall at angle greater than the critical angle at the plane of the interface. The overall back scattering phenomena of optical probe used as basis to distinguish gas-liquid phase [9].

The optical cable that used in the experiments manufactured by thor labs. The optical cable consist on 200 μm quartz glass that represent the core for the optical cable and 400 μm of silicon cladding and Teflon to protect the core part of cable. Regarding to all details and fabricating procedure of optical fiber probe can be found [10], [11].

2.3.2. Raw Signal of Two Tip Optical Fiber Probes. Figure 2 present the time series of two tip optical fiber probe. The larger voltage peaks illustrate the time frame of gas phase on the probe tip and the base voltage slots show the time of liquid phase on the probe tip. Butterworth filter applied on the raw signals to remove any electronic noises.

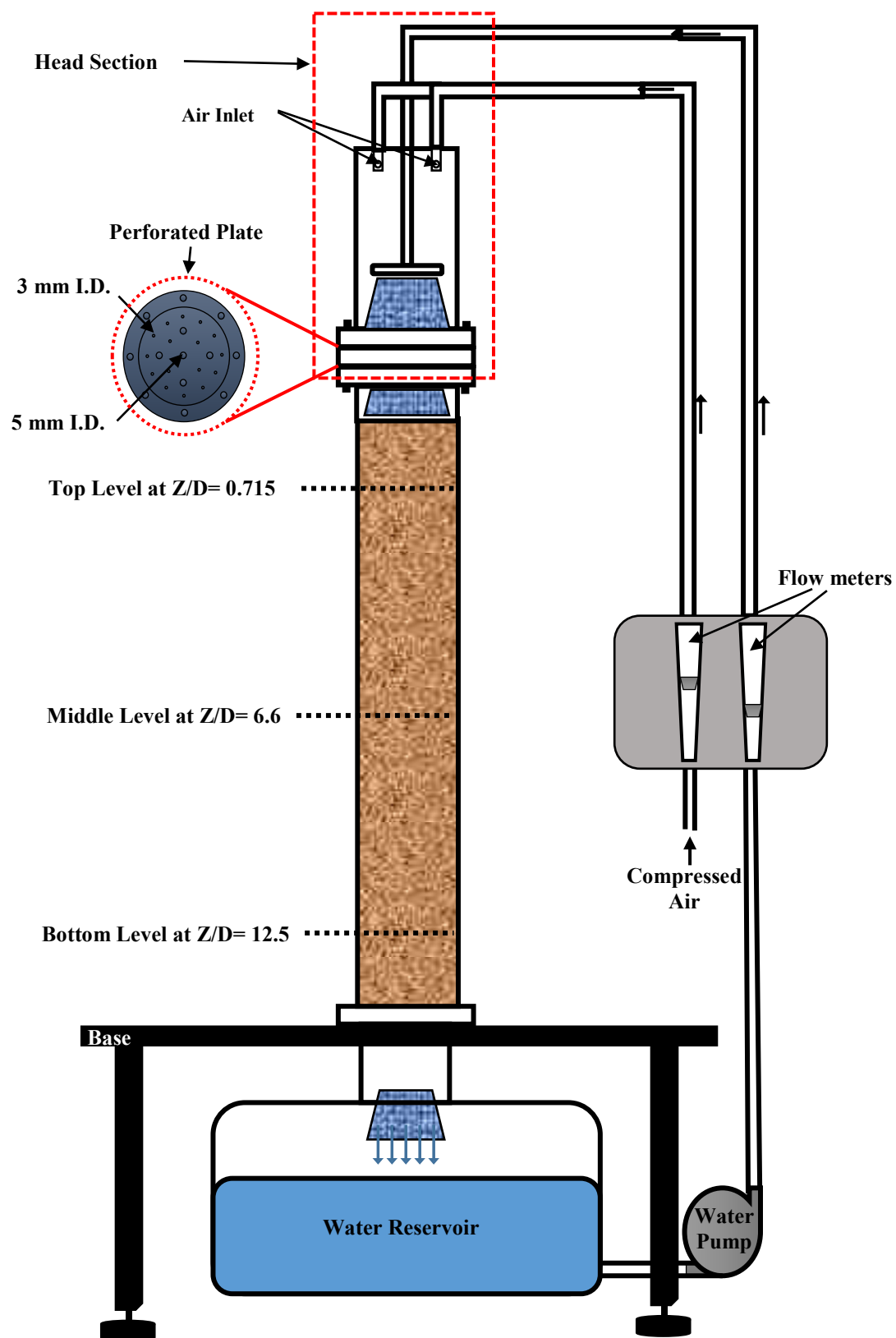


Figure 1. Schematic diagram for Trickle Bed Reactor.

2.3.3. Local Phase Saturations Measurements. The phase saturation definition is the amount of volume occupied by particular phase to the amount of volume of void. The basis of phase saturation in this work based on ergodic hypothesis that volume average is equivalent to time average for the flowing system. Hence, the local gas saturation is the ratio of time used by the gas phase on the probe tip to the total time of measurement (equ. 1). Whereas, the local liquid saturation is one minus the local gas saturation calculated in the probe (equ. 2).

$$\beta_{g,local} = \frac{t_{g,local}}{t_{g,local}+t_{l,local}} \quad (1)$$

where,

$t_{g,local}$ is the time used by gas phase in the probe tips, and $t_{l,local}$ is the time used by liquid phase in the probe tips.

$$\beta_{l,local} = 1 - \beta_{g,local} \quad (2)$$

2.3.4. Local Phase Velocities Measurement. The foundation of local phase based on calculate the time delay and the distance between tips then the local phase velocity will be obtained. The time delay calculation will be applied on matched signals as shown in Figure 3. The details of match the signal, the bubble tracking and matching algorithm we can find it in [132].

The local gas and liquid calculation shown in equ. 3 and 4 below

$$V_{g,local} = \frac{\text{distance between tips}}{t_{2a}-t_{1a}} \quad (3)$$

$$V_{l,local} = \frac{\text{distance between tips}}{t_{2d}-t_{1d}} \quad (4)$$

where,

t_{1a} time used to arrive the upper tip (tip1), t_{1d} time used to depart the upper tip (tip1),
 t_{2a} time used to arrive the lower tip (tip2), and t_{2d} time used to depart lower tip (tip2).

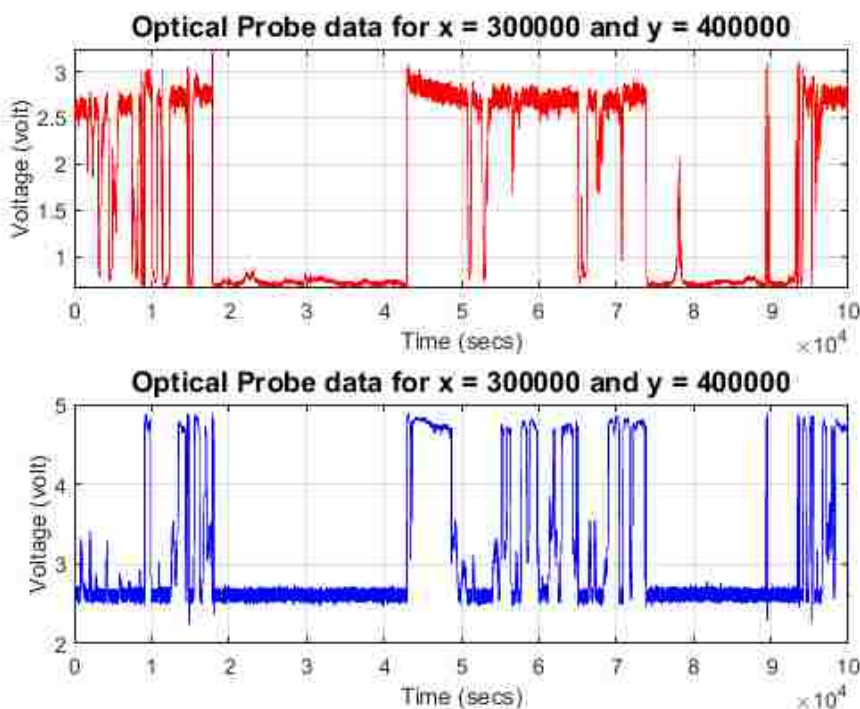


Figure 2. Time series of two tip optical fiber probe technique.

3. SAMPLE OF RESULTS

In this work, the effects of catalyst shapes, bed height (axial level), gas flow rate, and liquid flow rate on the local gas and liquid saturation diametrical profiles, and local gas and liquid velocities were investigated using two tip optical fiber prober technique.

Sample of results were displayed in this Section and more details will be showed in my manuscript Figure 4 shows the magnitude of local liquid saturation within trilobe and quadrilobe particles increased relatively that that in spherical and cylindrical particles. Also, the local liquid distribution revealed a high fluctuation for all catalyst shapes in the bed as shown in Figure 4.

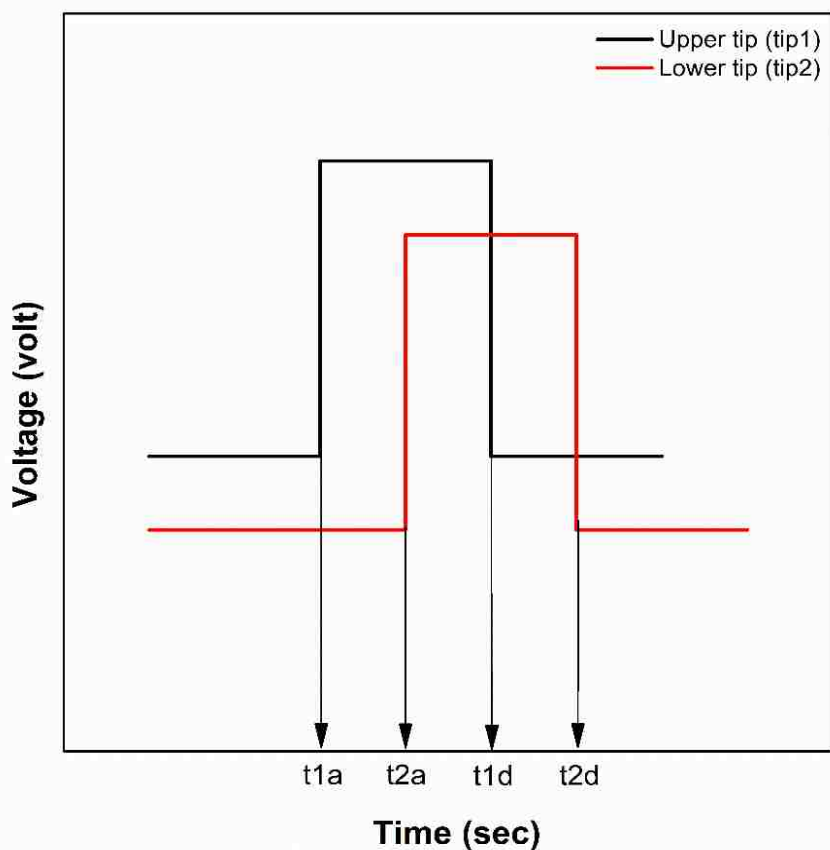


Figure 3. Schematic of matched bubble signals used for velocity measurement.

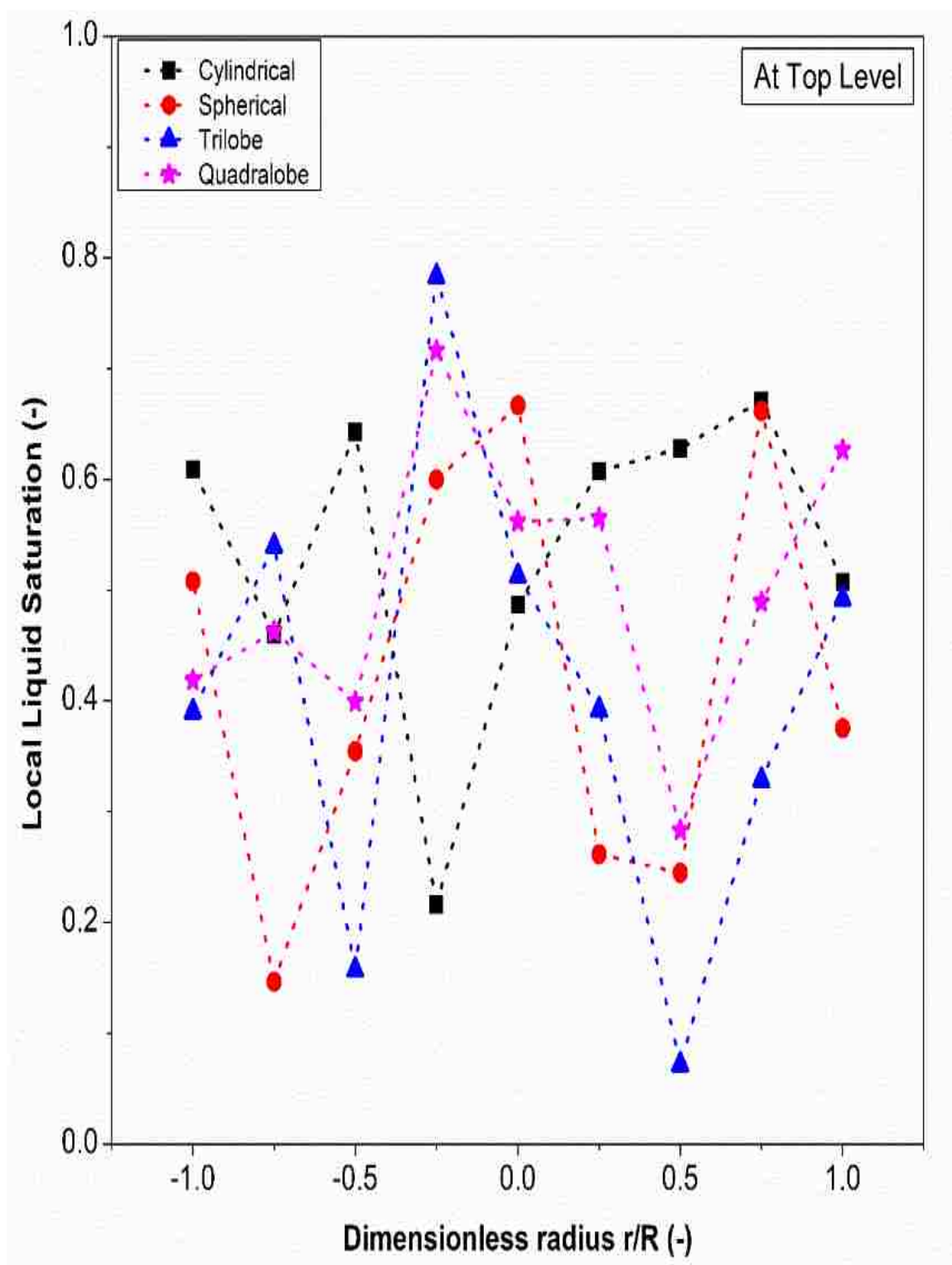


Figure 4. Local liquid saturation diametrical profiles Vs dimensionless radius (r/R) within different industrial catalyst shapes at the top level of the bed.

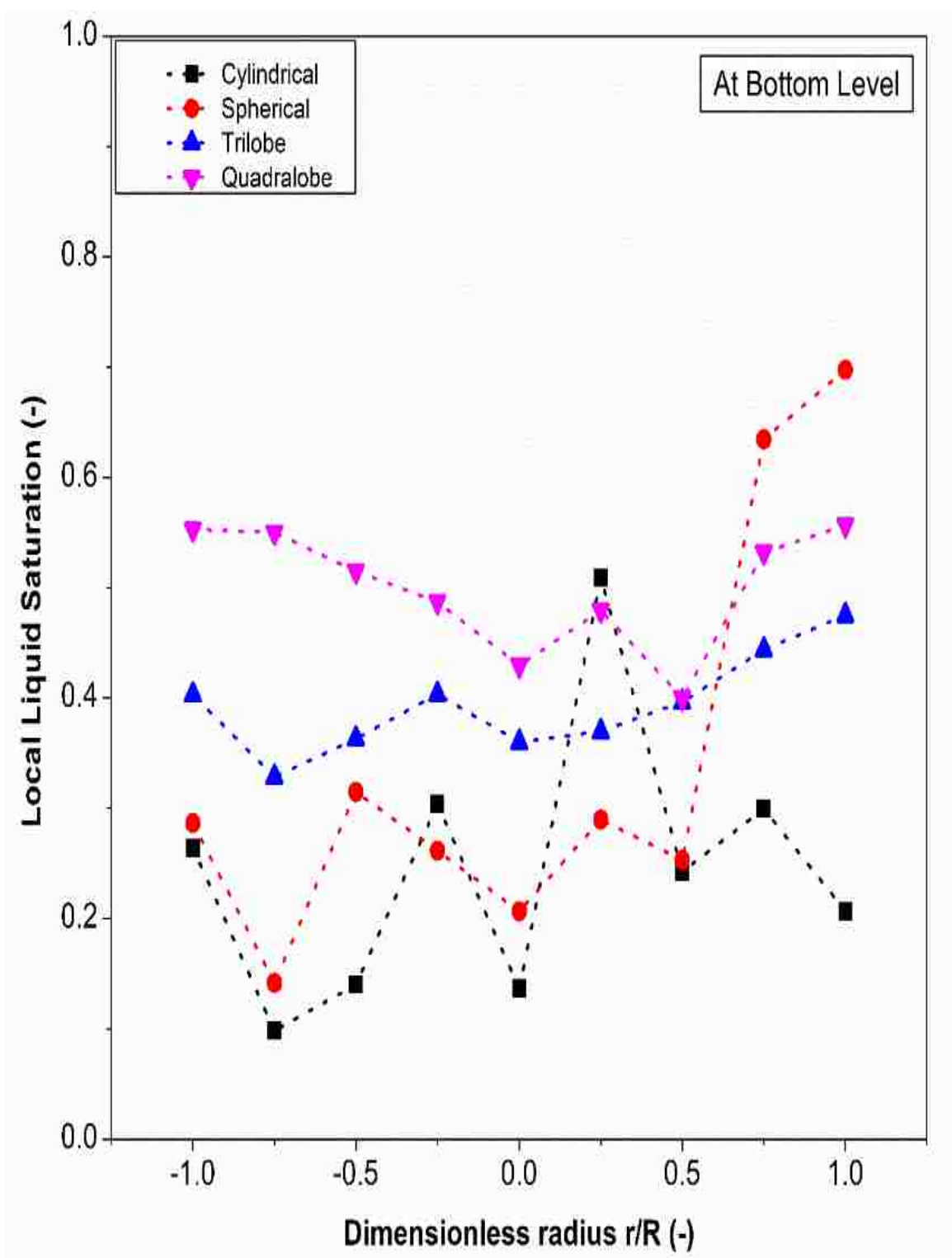


Figure 5. Local liquid saturation diametrical profiles Vs dimensionless radius (r/R) within different industrial catalyst shapes at the bottom level of the bed.

4. REMARKS

Most of studies presented to the literature using averaged data for entire bed, so the required for local data in high demand to enhance the fundamental knowledge in TBRs. Also, most the investigations have been examined the hydrodynamics within spherical and cylindrical shapes and nobody paid attention to provide local data within trilobe and quadrilobe that applied extensively in the refineries. Local gas and liquid saturation diametrical profiles and local gas and liquid velocities were studied within different catalyst shapes along bed height with range of gas and liquid flow rates. The following points developed from the existing visualization:

- 1- There is a significant effect of catalyst shape on the hydrodynamics in TBRs.
- 2- A significant effect of bed height on the local liquid saturation and local liquid distribution along bed diameter.
- 3- More details and information will be provided in my manuscript.

ACKNOWLEDGMENT

The authors gratefully acknowledge the financial support in the form of a scholarship provided by Ministry of Higher Education and Scientific Research-Iraq, and the funds provided by Missouri S&T and Professor Dr. Muthanna Al-Dahhan to develop the experimental set-up and to perform the present study.

REFERENCE

- [1] M. H. Al-Dahhan, M. R. Khadilkar, Y. Wu, and M. P. Dudukovic, "prediction of Pressure Drop and Liquid Holdup in High-Pressure Trickle-Bed Reactors," vol. 5885, no. 97, pp. 793–798, 1998.
- [2] J. Martínez, J., & Ancheyta, "Modeling the kinetics of parallel thermal and catalytic hydrotreating of heavy oil," *Fuel*, vol. 138, pp. 27-36., 2014.
- [3] A. Atta, S. Roy, F. Larachi, and K. D. P. Nigam, "Cyclic operation of trickle bed reactors: A review," *Chem. Eng. Sci.*, vol. 115, pp. 205–214, 2014.
- [4] P. R. Gunjal, M. N. Kashid, V. V. Ranade, and R. V. Chaudhuri, "Hydrodynamics of trickle bed reactors: experiments and CFD modeling," *Ind. Eng. Chem. Res.*, vol. 44, no. d, pp. 6278–6294, 2005.
- [5] M. H. Al-dahhan, F. Larachi, M. P. Dudukovic, and A. Laurent, "High-Pressure Trickle-Bed Reactors : A Review," *Ind. Eng. Chem.*, vol. 36, pp. 3292–3314, 1997.
- [6] C. Boyer, A. M. Duquenne, and G. Wild, "Measuring techniques in gas-liquid and gas-liquid-solid reactors," *Chem. Eng. Sci.*, vol. 57, no. 16, pp. 3185–3215, 2002.
- [7] V. Alexander, M. Fitri, A. Rahman, and H. Albazzaz, "Novel Measurement Technique Based on Optical Probe to Measure Local Flow Dynamics in Packed Bed Reactors."
- [8] V. Alexander, "Hydrodynamics related performance evaluation of Upflow Moving Bed Hydrotreater reactor (MBR) using developed experimental methods and CFD simulation Presented to the Graduate Faculty of the In Partial Fulfillment of the Requirements for the Degree," 2018.
- [9] X. Li, C. Yang, S. Yang, and G. Li, "Fiber-optical sensors: Basics and applications in multiphase reactors," *Sensors (Switzerland)*, vol. 12, no. 9, pp. 12519–12544, 2012.
- [10] A. Rahman and M. Bin, "Investigation of local velocities and phase holdups, and flow regimes and maldistribution identification in a trickle bed reactor," 2017.
- [11] J. Xue, "Bubble Velocity , Size and Interfacial Area Measurements in Bubble Columns," no. December, pp. 1–210, 2004.

SECTION

2. CONCLUSION

The general outcomes of the present study can be concluded as follows:

- 1- For the flow regime and their transition velocities, it has been found that the catalyst shape has a considerable impact on the flow regimes and transition velocities by using different catalyst shapes at a wide range of superficial gas and liquid velocities in TBRs. The results illustrated that the flow regime could be identified by GRD technique through analyzing the time series of photon count, which can be useful for both the bench investigation and industrial implementation. KE as one of a robust analysis methods and statistical parameter have been used to indicate the flow transition between trickle to pulse flow regimes
- 2- Pressure drop have shown that the spherical particles give reduced pressure drop inside the bed with about 42%, 24%, and 32% compared with cylindrical, trilobe, and quadrilobe, respectively due to higher equivalent diameter. The cylindrical particles can increase the pressure drop with about 31% and 20% comparing with trilobe and quadrilobe, respectively even though with larger equivalent diameter. Also, it has been demonstrated that the liquid holdup improved with quadrilobe with about 75%, 18%, and 15% comparing with spherical, cylindrical, and trilobe, respectively.
- 3- A significant effect was indicated when using bed dilution on the phase distribution, and line averaged diametrical profiles of the dynamic liquid holdup at different superficial gas and liquid velocities in bench-scale trickle bed reactor. Furthermore, the inlet configuration for the mixed gas and liquid considerably affects the phase

- distribution and dynamic liquid holdup. Although, the phase distribution was enhanced with diluting the bed with fines, the liquid maldistribution still exists in the bed.
- 4- A new methodology to calculate the volume of catalyst utilized in the bed based on the phase distribution obtained using GRD has been suggested. The results indicated that increasing the gas flow rate decreased the volume of catalyst utilized. Also, it has been indicated that the liquid flow rate has a remarkable effects on the volume of catalyst utilization in the bed.
 - 5- Local gas and liquid saturation and velocities are critical parameters in the TBRs. Local data using different industrial catalyst shapes that are rarely found in the literature which has been addressed for the first time in this study. The liquid saturation increased significantly with increase liquid flow rate and decreased with increasing the gas flow rate.

3. RECOMMENDATIONS

This research has thrown up several questions in need of more investigation. Further investigations are strongly recommended for better understanding in both pilot plant and bench scale TBRs. The following is a summary of future recommendations:

1. More information on a mixture of different industrial catalyst shape (Trilobe and Quadrilobe) and fine particles in the bench scale TBR is highly suggested using advanced measurements techniques.
2. Further investigation into the impacts of gas and liquid physical properties with different commercial catalyst shapes on the hydrodynamics in the bench scale TBR using advanced Gamma-ray densitometry (GRD) and computed tomography (CT).
3. More broadly, a study is necessary to measure local gas and liquid velocities at different commercial catalyst shapes using advanced optical fiber probe that is benefited to validate models in the bench scale TBR.
4. It is recommended to use fine particles with different commercial catalyst shapes packed according to Al-Dahhan et al. method and examine the reproducibility and examining the effects of different gas and liquid physical properties to introduce comprehensive insights.
5. Quantifying radial profile for the effects of different industrial catalyst shapes with different gas and liquid velocities using various physical properties (gas density, liquid density, liquid viscosity, and liquid surface tension) on the hydrodynamics using advanced Gamma-ray densitometry (GRD) in pilot plant scale TBR.

6. Developing optical fiber probe technique to measure not only local gas and liquid velocities, and gas and liquid saturation but also bubble characteristics that is highly important to increase the fundamental understanding and provide new insights.
7. Considerably more investigation will be desired to identify flow regime and their velocities with using various catalyst shapes and different gas and liquid flow with different physical properties. Meanwhile, using simple and powerful tools for identify flow regime while the reactor in operation.

REFERENCES

- [1] BP Energy Economics, "2018 BP Energy Outlook 2018 BP Energy Outlook," 2018.
- [2] J. Meurig and K. D. M. Harris, "Environmental Science Some of tomorrow ' s catalysts for processing increasing the production of energy," *Energy Environ. Sci.*, pp. 687–708, 2016.
- [3] M. J. Taulamet, N. J. Mariani, G. F. Barreto, and O. M. Martínez, "A critical review on heat transfer in trickle bed reactors," *Rev. Chem. Eng.*, vol. 31, no. 2, pp. 97–118, 2015.
- [4] P. V. Ravindra, D. P. Rao, and M. S. Rao, "Liquid Flow Texture in Trickle-Bed Reactors: An Experimental Study," *Ind. Eng. Chem. Res.*, vol. 36, no. 12, pp. 5133–5145, 1997.
- [5] M. E. Trivizadakis and A. J. Karabelas, "A study of local liquid/solid mass transfer in packed beds under trickling and induced pulsing flow," *Chem. Eng. Sci.*, vol. 61, no. 23, pp. 7684–7696, 2006.
- [6] D. L. Xian Feng, C. Junghui, N. Menglong, L. Xu, and L. T. C. Lester, "Kinetic parameter estimation and simulation of trickle-bed reactor for hydrodesulfurization of crude oil," *Fuel*, vol. 230, pp. 113–125, 2018.
- [7] A. Atta, S. Roy, F. Larachi, and K. D. P. Nigam, "Cyclic operation of trickle bed reactors: A review," *Chem. Eng. Sci.*, vol. 115, pp. 205–214, 2014.
- [8] A. Burghardt, "Eulerian three-phase flow model applied to trickle-bed reactors," *Chem. Process Eng. - Inz. Chem. i Proces.*, vol. 35, no. 1, pp. 75–96, 2014.
- [9] M. F. Abid, "Hydrodynamics and Kinetics of Phenols Removal from Industrial Wastewater in a Trickle Bed Reactor (Part I: Hydrodynamic Study)," *Chem. Biochem. Eng. Q. J.*, vol. 28, no. 3, pp. 319–327, 2014.
- [10] J. Guo and M. Al-dahhan, "Kinetics of Wet Air Oxidation of Phenol over a Novel Catalyst," *Ind. Eng. Chem. Res.*, vol. 42, pp. 5473–5481, 2003.
- [11] V. V. Ranade, R. Chaudhari, and P. R. Gunjal, *Trickle Bed Reactors: Reactor Engineering and Applications*. Elsevier Science, 2011.
- [12] Q. Xiao, A. M. Anter, Z. M. Cheng, and W. K. Yuan, "Experimental investigation of dynamic liquid holdup under pulse flow in trickle-bed reactor," *Huagong Xuebao/Journal Chem. Ind. Eng.*, vol. 52, no. 4, pp. 327–332, 2001.
- [13] R. J. G. Lopes and R. M. Quinta-Ferreira, "CFD modelling of multiphase flow distribution in trickle beds," *Chem. Eng. J.*, vol. 147, no. 2–3, pp. 342–355, 2009.

- [14] R. N. Maiti and K. D. P. Nigam, "Gas-liquid distributors for trickle-bed reactors: A review," *Ind. Eng. Chem. Res.*, vol. 46, no. 19, pp. 6164–6182, 2007.
- [15] M. E. Trivizadakis, D. Giakoumakis, and A. J. Karabelas, "A study of particle shape and size effects on hydrodynamic parameters of trickle beds," *Chem. Eng. Sci.*, vol. 61, no. 17, pp. 5534–5543, 2006.
- [16] V. Sodhi and a Bansal, "Analysis of foaming flow instabilities for dynamic liquid saturation in trickle bed reactor," *World Acad. Sci. Eng. Technol.*, vol. 80, no. 8, pp. 1382–1388, 2011.
- [17] A. K. Saroha and I. Nandi, "Pressure drop hysteresis in trickle bed reactors," *Chem. Eng. Sci.*, vol. 63, no. 12, pp. 3114–3119, 2008.
- [18] S. Sharma, M. D. Mantle, L. F. Gladden, and J. M. Winterbottom, "Determination of bed voidage using water substitution and 3D magnetic resonance imaging, bed density and pressure drop in packed-bed reactors," *Chem. Eng. Sci.*, vol. 56, no. 2, pp. 587–595, 2001.
- [19] C. Boyer and B. Fanget, "Measurement of liquid flow distribution in trickle bed reactor of large diameter with a new gamma-ray tomographic system," *Chem. Eng. Sci.*, vol. 57, pp. 1079–1089, 2002.
- [20] J. Zalucky, M. Wagner, M. Schubert, R. Lange, and U. Hampel, "Hydrodynamics of descending gas-liquid flows in solid foams: Liquid holdup, multiphase pressure drop and radial dispersion," *Chem. Eng. Sci.*, vol. 168, pp. 480–494, 2017.
- [21] H. Nadeem, I. Ben Salem, and M. Sassi, "Experimental Visualization and Investigation of Multiphase Flow Regime Transitions in Two-Dimensional Trickle Bed Reactors," *Chem. Eng. Commun.*, vol. 204, no. 3, pp. 388–397, 2017.
- [22] S. A. Al-Naimi, F. T. J. Al-Sudani, and E. K. Halabia, "Hydrodynamics and flow regime transition study of trickle bed reactor at elevated temperature and pressure," *Chem. Eng. Res. Des.*, vol. 89, no. 7, pp. 930–939, 2011.
- [23] P. Niegodajew and D. Asendrych, "An interfacial heat transfer in a countercurrent gas-liquid flow in a trickle bed reactor," *Int. J. Heat Mass Transf.*, vol. 108, pp. 703–711, 2017.
- [24] K. Anuar Mohd Salleh, H. Koo Lee, and M. H. Al-Dahhan, "Studying local liquid velocity in liquid-solid packed bed using the newly developed X-ray DIR technique," *Flow Meas. Instrum.*, vol. 42, pp. 1–5, 2015.
- [25] A. Kundu, A. K. Saroha, and K. D. P. Nigam, "Liquid distribution studies in trickle-bed reactors," *Chem. Eng. Sci.*, vol. 56, no. 21–22, pp. 5963–5967, 2001.

- [26] A. K. Saroha, K. D. P. Nigam, A. K. Saxena, and V. K. Kapoor, "Liquid distribution in trickle-bed reactors," *AIChE J.*, vol. 44, no. 9, pp. 2044–2052, 1998.
- [27] R. A. Holub, M. P. Dudukovic, and P. A. Ramachandran, "A phenomenological model for pressure drop, liquid holdup, and flow regime transition in gas-liquid trickle flow," *Chem. Eng. Sci.*, vol. 47, no. 9–11, pp. 2343–2348, 1992.
- [28] M. H. Al-Dahhan, M. R. Khadilkar, Y. Wu, and M. P. Dudukovic, "prediction of Pressure Drop and Liquid Holdup in High-Pressure Trickle-Bed Reactors," vol. 5885, no. 97, pp. 793–798, 1998.
- [29] A. Atta, S. Roy, and K. D. P. Nigam, "Investigation of liquid maldistribution in trickle-bed reactors using porous media concept in CFD," *Chem. Eng. Sci.*, vol. 62, no. 24, pp. 7033–7044, 2007.
- [30] A. E. SAEZ and R. G. CARBONELL, "Hydrodynamic Parameters for Gas-Liquid Cocurrent Flow in Packed Beds.," *AIChE J.*, vol. 31, no. 1, pp. 52–62, 1985.
- [31] A. Attou, C. Boyer, and G. Ferschneider, "Modelling of the hydrodynamics of the cocurrent gas-liquid trickle flow through a trickle-bed reactor," *Chem. Eng. Sci.*, vol. 54, no. 6, pp. 785–802, 1999.
- [32] A. Lakota, J. Levec, and R. G. Carbonell, "Hydrodynamics of trickling flow in packed beds: Relative permeability concept," *AIChE J.*, vol. 48, no. 4, pp. 731–738, 2002.
- [33] M. Bazmi, S. H. Hashemabadi, and M. Bayat, "Extrudate Trilobe Catalysts and Loading Effects on Pressure Drop and Dynamic Liquid Holdup in Porous Media of Trickle Bed Reactors," *Transp. Porous Media*, vol. 99, no. 3, pp. 535–553, 2013.
- [34] A. Bansal, R. K. Wanchoo, and S. K. Sharma, "Flow Regime Transition in a Trickle Bed Reactor," *Chem. Eng. Commun.*, vol. 192, no. 8, pp. 1046–1066, 2005.
- [35] M. H. Al-Dahhan and M. P. Duduković, "Catalyst Bed Dilution for Improving Catalyst Wetting in Laboratory Trickle-Bed Reactors," *AIChE J.*, vol. 42, no. 9, pp. 2594–2606, 1996.

VITA

Mohammed Jaber Al-Ani was born in Baghdad, Iraq. He received his B.S. in chemical engineering from the University of Technology Baghdad, Iraq in 2002. He joined the Research and Industry Development Center, Ministry of Industry and Minerals, Iraq in 2003. He participated and led different projects in various industrial fields (infrastructure projects, petroleum, petrochemicals, biochemical, and renewable energy projects). He awarded the first scholarship by Research and Industry Development Center, Ministry of Industry and Minerals, Iraq in 2005. He received his first M.S. in chemical engineering from the University of Baghdad, Iraq in 2008. During his M.S. study, he received a grant to fund the research by Ministry of Oil – Petroleum Research Centre, Iraq. He continued his career in Research and Industry Development Center, Iraq in 2008. In 2010, He worked as a lecturer in Dijlah University College in the Department of Cooling and Air Conditioning Technologies. During this period, He proposed and received a grant to establish the Nanotechnology Department as a part of the Research and Industry Development Center, Iraq. In 2011, he promoted as a Head of Nanotechnology Department in the Research and Industry Development Center, Iraq. He received a second scholarship by University of Baghdad / Chemical Engineering Department, Ministry of Higher education and Scientific Research, Iraq in 2013. He joined Missouri University of Science and Technology (S&T) in fall 2014. He received his second M.S. in Chemical Engineering from Missouri S&T in fall 2015. He contributed by oral and poster articles in several conferences. Mohammed has many peer review papers and under submitting. Al-Ani received his Ph.D. degree in Chemical Engineering from Missouri S&T in July 2019.